UNIVERSITI TEKNOLOGI MARA

COMPUTATIONAL INTELLIGENCE BASED POWER SYSTEM SECURITY ASSESSMENT AND IMPROVEMENT UNDER MULTI-CONTINGENCIES CONDITIONS

NOR RUL HASMA ABDULLAH

Thesis submitted in fulfillment of the requirements
for the degree of
Doctor of Philosophy

Faculty of Electrical Engineering

June 2012

AUTHOR'S DECLARATION

I declare the work in this thesis was carried out in accordance with the regulations of Universiti Teknologi MARA. It is original and is the result of my own work, unless otherwise indicated or acknowledged as referenced word. This thesis has not been submitted to any other academic institution or non-academic institution for any other degree or qualification.

I, hereby, acknowledge that I have been supplied with the Academic Rules and Regulations for Post Graduate, Universiti Teknologi MARA, regulating the conduct of my study and research.

Name of Student	:	Nor Rul Hasma Abdullah
Student I.D. No.	:	2008264876
Programme	:	Doctor of Philosophy (Electrical Engineering)
Faculty	:	Electrical Engineering
Thesis Title	:	Computational Intelligence Based Power System Security Assessment and Improvement under Multi-Contingencies Conditions.
Signature of Student	:	…………………………………………
Date	:	June 2012

ABSTRACT

This thesis presents new techniques for voltage stability assessment and improvement in power system under multi-contingencies. A line-based voltage stability index termed as Static Voltage Stability Index (*SVSI*) was used to evaluate the voltage stability condition on a line. The value of *SVSI* was computed to identify the most sensitive line and corresponding weak bus in the system. The results obtained from the voltage stability analysis using *SVSI* were utilized to identify most sensitive line corresponds to a load bus and estimate the maximum loadability and operating margin in the system. The *SVSI* was consequently used as the line outage severity indicator in the implementation of contingency analysis and ranking. The application of *SVSI* was extended for the evaluation of the constrained power planning (CPP) and Flexible AC Transmission Systems (FACTS) devices installation using Evolutionary Programming (EP) by considering multi-contingencies occurrence in the system. The minimizations of *SVSI* and transmission loss are used as two separate objective functions for the development of optimization technique. The effect of reactive power load variation on transmission loss in the system is also investigated. Consequently, the EP optimization technique is extended for the evaluation of the operating generator scheduling (OGS) to be applied on reactive power control in power system. The results obtained from the study can be used by the power system operators to make a decision either to achieve minimal *SVSI*, minimal transmission loss or minimal installation cost. This has also avoided all generators to dispatch power at the same time. Finally, a novel multi-objective Constrained Reactive Power Control (CRPC) algorithm using the state-of-the-art of EP for voltage stability improvement has been developed. A performance comparison with Artificial Immune System (AIS) in terms of *SVSI* and loss minimization was made and it is found that the proposed algorithm has been able to produce better results as compared to AIS. The contributions of the studies among the others are the development EP and AIS engine for CPP considered multi-contingencies *(N-m)*, the development of EP and AIS engine for FACTS installation considered multi-contingencies *(N-m)* for the determination of FACTS placement using *SVSI* and optimal sizing of FACTS using EP and AIS, the development of new technique for OGS based on EP optimization technique and the development of multi-objective EP and AIS engines for CRPC considered multi-contingencies *(N-m)*.

ACKNOWLEDGEMENTS

Bismillahirrahmaanirrahiim
In the name of Allah, the Most Merciful and the Most Compassionate

Praise to Allah S.W.T for the blessing and everything given to me to complete this project. I would like to take this opportunity to express my sincere gratitude and appreciation to my supervisor, Assoc. Prof. Dr. Ismail Musirin for his continuous guidance and assistance towards the accomplishment of this research work and in the preparation of the thesis. I am also indebted to The Faculty of Electrical Engineering, Universiti Teknologi MARA (UiTM), Malaysia for allowing me to fully utilise the necessary facilities during my studies. I would also like to thank to Ministry of Higher Education (MOHE) for the Skim Latihan Akademik IPTA (SLAI) scholarship.

I would also like to record my gratitude to my co-supervisor Dr. Muhammad Murtadha and to all the people who have given me their support, advices and encouragement either directly or indirectly throughout my course in UiTM and also in Universiti Malaysia Pahang (UMP).

Special appreciation, love and gratitude to my parents, my beloved husband, my son and my daughter for all their love, prayers and support.

TABLE OF CONTENTS

CHAPTER THREE: MULTI-CONTINGENCY COMPONENT IDENTIFICATION FOR POWER SCHEDULING

CHAPTER FOUR: COMPUTATIONAL INTELLIGENCE REACTIVE POWER PLANNING TECHNIQUE FOR LOSS MINIMIZATION AND VOLTAGE STABILITY IMPROVEMENT CONSIDERING INSTALLATION COST

CHAPTER SIX: OPERATING GENERATOR SELECTION FOR INTELLIGENT REACTIVE POWER CONTROL

CHAPTER SEVEN: CONSTRAINED REACTIVE POWER CONTROL BASED MULTI-OBJECTIVE OPTIMIZATION UNDER MULTI-CONTINGENCIES *(N-m)*

CHAPTER EIGHT: OVERALL CONCLUSION AND RECOMMENDATION

LIST OF TABLES

LIST OF FIGURES

NOMENCLATURE

AIS	:	Artificial Immune System
ANN	:	Artificial Neural Network
BCS	:	Best Compromise Solution
CAPS	:	Constrained Active Power Scheduling
CHPS	:	Constrained Hybrid Power Scheduling
CPP	:	Constrained Power Planning
CRPC	:	Constrained Reactive Power Control
EP	:	Evolutionary Programming
FACTS	:	Flexible AC Transmission Systems
GA	:	Genetic Algorithm
MOEP	:	Multi-Objective EP
MOAIS	:	Multi-Objective AIS
PI	:	Performance Index
PQ	:	Load bus
PV	:	Voltage Control Bus
RPD	:	Reactive Power Dispatch
RPP	:	Reactive Power Planning
RTS	:	Reliability Test System
SA	:	Simulated Annealing
STATCOM	:	Static Synchronous Compensator
SVC	:	Static VAR Compensator
SVSI	:	Static Voltage Stability Index
TCSC	:	Thyristor-controlled Series Capacitor
TS	:	Tabu Search
UPFC	:	Unified Power Flow Controller
VSA	:	Voltage Stability Assessment
VSI	:	Voltage Stability Improvement

β	:	Mutation scale
C_{ci}	:	Per unit reactive power source purchase cost at bus i
δ_i, δ_j	:	Voltage angles at bus i and bus j
δ_{ji}	:	Angle difference
e_i	:	Fixed reactive power source installation cost
f_i	:	Fitness for the i^{th} random number
f_{max}	:	Maximum fitness
G_{ij} and B_{ij}	:	Mutual conductance and subceptance between bus i and bus j
g_k	:	Conductance of branch k
h	:	Per unit energy cost
N	:	Gaussian random variable with mean μ and variance γ^2
N-1	:	Single Contingency
N_B	:	Number of buses
N_{B-1}	:	Total buses excluding slack bus
N_c	:	Possible reactive power source installation buses number
N_E	:	Branch number
N_i	:	Numbers of buses adjacent to bus i including bus i
N-m	:	Multi-Contingencies
N_{PQ}	:	PQ bus number
N_{PV}	:	PV bus number
n_s	:	Slack (reference) bus number
Q_{ci}	:	Amount of reactive power either positive (reactance) or negative (capacitance) installation
Q_d	:	Reactive power loading (reactive load)
Q_{gn}	:	Reactive power to be injected to generator n
S_i, P_i and Q_i	:	Apparent, active and reactive powers at bus i
S_j, P_j and Q_j	:	Apparent, active and reactive powers at bus j
$SVSI\_avg$	:	Average fitness (with $SVSI$ as fitness)
$SVSI\_max$	:	Maximum fitness (with $SVSI$ as fitness)

SVSI_min	:	Minimum fitness (with *SVSI* as fitness)
SVSI_set	:	*SVSI* value before optimised CPP
SVSI_sum	:	Sum of fitness (with *SVSI* as fitness)
V_set	:	Bus voltage before optimised CPP
V_i , V_j	:	Voltages at bus i and bus j respectively
$x_{i+m,j}$	:	Mutated parents (offsprings)
x_{ij}	:	Parents
$x_{j\ max}$	:	Maximum random number for every variable
$x_{j\ min}$	:	Minimum random number for every variable
Z_{ji}, R_{ji} , X_{ji}	:	Line impedance, resistance and reactance
θ_i	:	Voltage angle different between bus i and bus j(rad),

CHAPTER ONE
INTRODUCTION

Nowadays, the power transmission systems have been changed a lot. The voltage deviation due to load variation and power transfer limitation was experienced due to reactive power unbalance which has drawn attention to better utilize the existing transmission line. The shortage of reactive power can cause the generator and transmission line failure leading to blackout or collapse in a system [1]. It also causes a higher impact on power system security and reliability [6]. Hence, the electrical energy demand increases continuously from time to time. This increase is due to the fact that few problems could appear with the power flows through the existing electric transmission networks. If this situation is uncontrollable, some lines located on the particular paths might become overloaded [2]. Due to the overloaded conditions; the transmission lines will have to be driven close to or even beyond their transfer capacities. Consequently, the transmission line outage in a power system was reported to be the main issue towards voltage instability as well as generator outage contingency [3-4]. The line outage may cause violations on bus limit, transmission line overloads and lead to system instability [5]. While, the generator outage can be caused by failure of generator; this may interrupt system delivery and lead to system instability [6].

1.1 PROBLEM STATEMENT

Voltage stability has become a concern in power system operation when it involves heavy load and contingencies. It is highly dependent upon the system limits, which leads to the restriction of loading capability of a network. Therefore voltage stability study becomes an important issue in power system planning and operation since it was reported in [7-12] that this problem is a progressive issue which receives major concern. The increment in load demands will decrease the reactive power and voltage, which leads to voltage collapse in the system. Therefore, the system consumes more reactive power to raise the voltage level and improve the voltage stability condition in the system. Voltage instability phenomenon could also be resulted from the contingencies caused by either line or generator outages apart from the stressed conditions of a power system network [13]. During contingency, the operating generators fail to operate and cause the reactive power supply by the generators suddenly drop in the system. Therefore, the system also has to improve the reactive power level to prevent voltage collapse in the system. Furthermore, power scheduling has also resulted in the change in power flow in the network and hence affects the system voltage profiles. Therefore, voltage stability in the system will be affected. Voltage stability is important to maintain a secure power system operation. Therefore, an efficient voltage stability analysis technique is required in order to perform the voltage stability study accurately with less computational burden. Studies have shown that voltage stability can be improved by means of real and reactive power rescheduling in a power system [14 – 17]. Basically, real and reactive power planning could be controlled by reactive power dispatch, compensating capacitor placement, transformer tap changer setting and installation of FACTS devices. Hence, this research proposed a new technique for rescheduling the real and reactive power at voltage controlled buses and also identifying suitable location and sizing of compensating capacitors in order to improve voltage stability in power system and at the same time minimizing the total losses in the system under multi-contingencies.

This research also proposes a new approach for operating generator scheduling to be applied on reactive power control based on Evolutionary Programming optimization technique in power system. The proposed technique will determine the best combination of generator which should be dispatched with reactive power in the system based on *SVSI*, transmission loss and installation cost in order to improve voltage stability condition of a system. Two objective functions were considered separately for the OGS namely improving voltage stability condition indicated by reduction in *SVSI* and transmission loss minimization (TLM) in the system. The information obtained from this analysis allows the power system operators to schedule generator units in an economic way as required by the utility company.

In reactive power control (RPC) problem, many of the proposed methods for optimization focus on the constraints related to the steady state operations. Numerous optimization problems have more than one objective function in conflict with each other. It is very difficult to decide which section is most suitable for the objective function. Therefore, instead of single-objective function, this research has implemented the multi-objective into the system in order to solve the optimal RPC problem where trade-off between the different components of the objective function is fixed. It is important to develop a multi-objective optimization algorithm which take both voltage stability index and transmission loss into account, to provide users a set of options with flexibility to solve the problem. The presence of reactive power control into power system brings many benefits. If the goals of the research need more than one objective function to be optimized, then it is called multi-objective optimization problems. The genuine way of solving multi-objective problem is to consider all objective functions applied simultaneously. That is why this research has been implemented in multi-objective optimization in order to take all the objective functions into account.

1.2 OBJECTIVES OF STUDY

The objectives of this research are:-

(i) To develop an algorithm for the identification of sensitive lines and generators, weak bus and secure in power system for constrained power planning analysis.

(ii) To develop a new and superior technique of power scheduling to improve voltage stability, minimize total transmission losses; and enhance of voltage profile for the system under stress and contingencies.

(iii) To develop a new and superior technique of FACTS devices installation in order to minimize total transmission losses and enhancement of voltage profile in the system under contingency (*N-m*) such as line outages and generator outages.

(iv) To develop an algorithm for operating generator scheduling identification in order to avoid hundred percent generator operations.

(v) To develop a multi-objective Evolutionary Programming algorithm to improve voltage stability, minimize total transmission losses for the system under stress and contingencies.

1.3 SCOPE OF WORK

Figure 1.1 shows the block diagram of overall activities conducted in this research. Initially, this work involved the implementation of *SVSI* for evaluating the voltage stability condition and optimization in power system for a system under stress and multi-contingencies. *SVSI* is used to evaluate contingency analysis and ranking for the line and generator outages. The results obtained from the line and generator outage contingency analysis and ranking were sorted in descending order to identify the line and generator outage severity in the system. Results from the contingency analysis and ranking are utilized in order to form the multi-contingencies selection to be applied in constrained power planning, constrained FACTS and multi-objective constrained reactive power control. In OGS, system with only stress condition is considered to be applied and tested. A stochastic optimization technique in the Evolutionary Computation hierarchy called the EP is applied in determining optimum CPP and FACTS to improve the voltage stability condition in the power system. Multi-objective optimizations namely MOEP and MOAIS are also considered for the combination of two objective functions namely VSI and TLM. *SVSI* is utilized as the fitness when VSI is taken as the objective function, while transmission loss is taken as the fitness when objective function is to minimize the transmission loss. The process was conducted at various loading condition in order to investigate the effects of loading condition and also to monitor the consistency of the process. For the purpose of validation, the propose techniques are tested on most IEEE Reliability Test System (RTS) namely IEEE 30-bus RTS and IEEE 118-bus RTS.

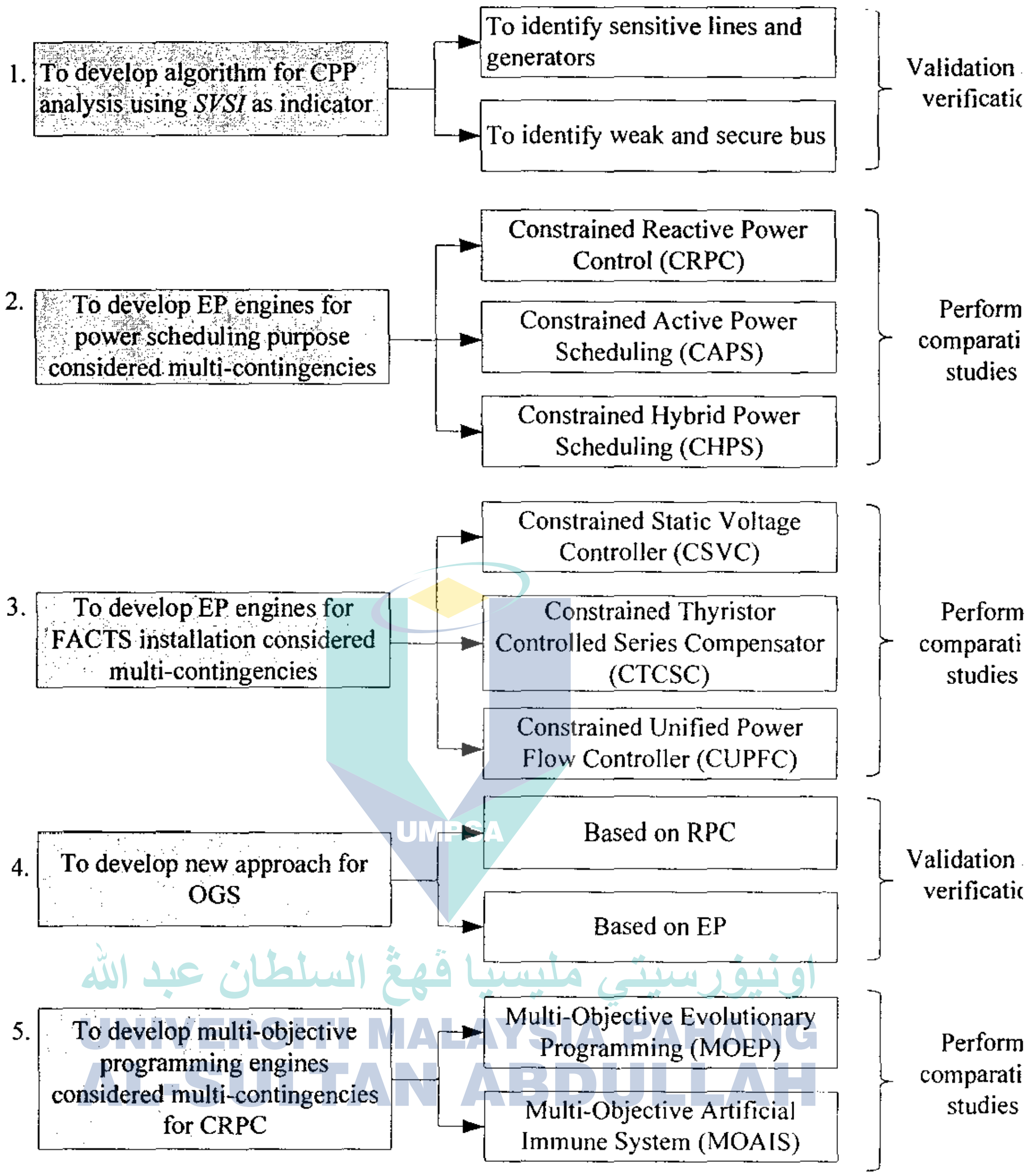

Figure 1.1: Scope of Work diagram

1.4 SIGNIFICANCE OF THE STUDY

The significance of this study are:-

(i) The power scheduling research explored a new approach in optimizing the power control which will result in the improvement of voltage stability condition in a power system.

(ii) The proposed technique can be utilized by the power system engineers and operators in order to alleviate the problems related to voltage instability and hence reduce the incidence of voltage collapse especially in the event of contingencies

(iii) In operating generator scheduling, the proposed technique able to economize the usage of capacitor bank or of the reactive power support devices. This will help power system utility to get ideas in managing the reactive power support. In addition, the implementation of the technique can be utilized by the power system engineers and operators in order to identify the correct combination of generators operation and the power schedule in the power scheduling system hence will minimize the system operation cost.

1.5 ORGANIZATION OF THESIS

This thesis begins with some preliminary studies on the current scenarios of voltage stability analysis, contingencies analysis, power planning, FACTS, operating generator scheduling and multi-objective. Literature review on the work that has been carried related to voltage stability studies are presented in Chapter 2. This chapter describes several important terminologies related to voltage stability studies including voltage stability analysis techniques, voltage stability index, maximum loadability and contingency studies, power scheduling, FACTS devices as compensation tools, operating generators scheduling and multi-objective optimization techniques.

Chapter 3 presents the multi-contingency component identification for power scheduling in power system. The study involves weak and secure buses identification so that the correct buses can be chosen to perform the power support scheme for the next chapters.

In Chapter 4, CPP procedures utilizing the EP optimization techniques are presented. In this study, three CPP techniques are proposed namely Constrained Reactive Power Control (CRPC), Constrained Active Power Reschedule (CAPR) and Constrained Hybrid Power Scheduling (CHPS). Two separate objective functions are used in the optimization procedures namely the VSI and TLM. *SVSI* is employed as the fitness when VSI is taken to be the objective function in the optimization process. While, the transmission loss in the system is utilized as the fitness when TLM is implemented as the objective function. Comparative studies are performed between the developed CPP procedures with both objective functions implemented separately in terms of voltage stability improvement, transmission loss minimization and constraint violation.

Chapter 5 presents a new approach for FACTS based on EP optimization technique considering multi-contingencies *(N-m)* which occurs in the system. The proposed technique determine the optimum sizing of Static Voltage Controller (SVC), Thyristor Controlled Series Compensator (TCSC) and Unified Power Flow Controller (UPFC) in order to improve the total transmission loss condition of a system. The *SVSI* is used as the tool to indicate the FACTS location to be installed into the power system network. Comparative studies are performed between AIS in terms of transmission loss minimization and constraint violation.

The development of a new approach for operating generator scheduling reactive power control based on EP optimization technique is described in Chapter 6. The proposed technique determines the best combination of generator that should be dispatched with reactive power in the system based on *SVSI*, transmission loss and installation cost in order to improve voltage stability condition of a system. Two objective functions were considered separately for the operating generator scheduling namely improving voltage stability condition indicated by reduction in *SVSI* and TLM in the system. In the beginning, *SVSI* was taken as the fitness for determining the optimum values of RPC and then the optimization was repeated for transmission loss minimization as the fitness function. The operating generator scheduling is developed to assist the system operator in scheduling generator units in an economic way as required by the utility company.

Chapter 7 describes a new approach for CPP based on MOEP optimization technique considering multi-contingencies *(N-m)* that may occur in a power system. The proposed technique will determine the optimum CRPC, by the generators in order to improve voltage stability condition of a system. The multi objective of constrained reactive power control problems has been implemented by considering two combinations of objective functions namely VSI and TLM. *SVSI* and transmission loss were taken as the fitness for determining the optimum values of CRPC. Comparative studies are performed between AIS with both objective functions implemented simultaneously in terms of voltage stability improvement, transmission loss minimization and constraint violation.

Finally, Chapter 8 provides the overall conclusion of the studies followed by the recommendations for future research work.

CHAPTER TWO
LITERATURE REVIEW

2.1 INTRODUCTION

Almost all aspects of daily life in modern society depend on the use of electricity. The basic function of an electric power system is to satisfy the system load requirement as economically as possible and with a reasonable assurance of continuity and quality of power supply [18]. In power system, the average duration of interruption that customers suffer is a total of two to three hours per year, but increasing load makes the power grid more stressed leading to blackouts more often [19].

Voltage instability was found to be responsible for several major network collapses in many countries [6]. Voltage stability analysis is considered as either static or dynamic which reflects to different fields of concentrations. This thesis puts forward the voltage stability analysis in static mode which can assist the power system engineers in understanding the mechanism of voltage collapse due to voltage instability in power transmission system [6]. The outcome obtained from the voltage stability assessment would be beneficial to power system researchers and engineers towards the development of control strategies for avoiding the voltage collapse incidence.

This chapter presents a survey on the published literature related to voltage stability studies in order to investigate the trend of evolution in voltage stability studies from the early stages to the current situation. Other literature on the impact of voltage collapse as a result of voltage instability condition and various approaches for improving voltage stability condition are also investigated.

Over the past decades, utility companies have confronted a serious problem in maintaining their network which has led to major concerns in power system operation and planning. Therefore, power control procedures are required in order to enhance the voltage stability in power system network. Voltage control in an electrical power system is important for proper operation for electrical power equipment to prevent damage such as overheating of generators and motors, to reduce transmission losses and to maintain the ability of the system to withstand and prevent voltage collapse. Decreasing in reactive power can cause voltage to drop; while increasing it caused voltage rise. A voltage collapse occurs when the system tries to serve much more load than the voltage can support. When reactive power is supply at lower voltage, current must increase to maintain power being supplied, causing the system to consume more reactive power and the voltage drops further. If the voltage drops too low, some generators will disconnect automatically to protect themselves.

Voltage collapse occurs when load increases or due to less generation or transmission facilities causes dropping in voltage, which causes a further reduction in reactive power from capacitor and line charging, and later will cause further voltage reductions. If voltage reduction continues, these will cause additional elements to trip, leading to further reduction in voltage and loss of load. Insufficient reactive power support has been identified as one of the factors for power blackout. There was a blackout occurred in the United States and Canada on August 14, 2003. The report [20] shows that the blackout was due to insufficient amount of reactive power. Due to difficulties in modeling the dynamic generators output, the amount of dynamic reactive output from generators has been less than expected, worsening voltage problems and resulting in power outages.

The role of reactive power in power system is to maintain the voltage profile as the active power delivered through transmission lines. When the reactive power supplied by generator is inadequate, voltage sags down and power demanded by loads become critical. The shortage of reactive power can cause the generator and transmission line failure leading to blackout or collapse in the power system [21]. Therefore in order to resolve the reactive power problem, synchronous generators, STATCOM, SVC and various types of other reactive power controller devices are injected into the system [22]. By adjusting the reactive power controllers, the output voltage can be improved; thus the power system become stable. There are various methods to determine the voltage stability in a system. One of them is the use of voltage stability index on transmission line [23]. This index gives a scalar number to each transmission line and it is in the range of zero to one to indicate no-load and voltage instability.

2.2 DEFINITIONS

Voltage instability condition is recognized as a progressing issue mostly in the power transmission system resulted from the stressed condition on the power system network. Therefore, several terminologies related to voltage stability studies should be clearly defined in order to reduce the ignorance discovered in this field. The three main terms are voltage stability, voltage collapse and voltage security. The definitions are given by The System Dynamic Performance Subcommittee of the IEEE Power System Engineering Committee in [24].

Voltage stability is defined in terms of the loadability of a system to maintain voltage s that when load is increased, load flow will increase, and so that both the power and voltage are controllable.

Voltage collapse is defined as the process by which voltage instability leads to a very low voltage profile in a significant part of the system.

Voltage security is defined as the ability of a system not only to operate stably but also to remain stable following any reasonably credible contingency or adverse system change, as far as the system voltages are within tolerable limits.

2.3 VOLTAGE STABILITY ANALYSIS (VSA) TECHNIQUES IN ELECTRIC POWER SYSTEMS

Voltage collapse due to voltage instability condition have been attracted much attention among the power engineering community as to ensure secure and economic operation of power transmission system. This phenomenon is a progressing issue, which requires a voltage stability analysis to be properly conducted especially at the planning stage. Therefore, it has a motivation in the development of power system optimization solution for enhancement and maintaining system security thus increasing quality of supply to customers. The static voltage stability analysis was widely accepted in the foregoing papers although the dynamic voltage instability has been the one that cause many interruptions. This is because the dynamic voltage stability analysis deals with the non-linear load that is rather difficult to model. Static voltage stability analysis is conducted by assuming the system operates in the steady state [25 – 30].

The increment of reactive power demand in existing power transmission systems can cause a lacking in reactive power support. Consequently, it makes the power system to be in stress condition and therefore responsible for several voltage collapse incidents [18]. Utility companies have experienced serious problem in maintaining their network which has led to major concerns in power system operation and planning. Thus, it is important for power system planning and operating engineers to be capable in performing comprehensive voltage stability analysis of the systems by maintaining the load bus voltages within their permissible limits. Generally, power losses in the transmission of electrical energy cause a loss of revenue. So, even a small percentage of savings in losses are acceptable since the total generated power is in the order of thousands in megawatts.

2.4 VOLTAGE STABILITY INDEX (VSI)

Several methods have been proposed in conducting the voltage stability analysis such as the use of P-V and Q-V curves, modal analysis [31], artificial neural networks [7], and sensitivity analysis [8]. In the modal analysis technique, a specified number of the smallest eigenvalues and the associated eigenvectors of a reduced Jacobian matrix were calculated using a steady state system model. Each eigenvalue was associated with a mode of voltage or reactive power variation whereby it provides a relative measure of proximity to voltage collapse [9–10].The P-V and Q-V curve have been used to determine proximity to voltage collapse while the other methods used voltage stability indices as indicators. These indices are derived by referring to either a bus or a line. Line stability indices can be used to evaluate the online voltage stability condition since they can be evaluated without having to turn off the generators [11–12, 32–33].

Voltage stability indices or proximities that are developed based on bus are observed to be time consuming since two procedures need to be conducted to satisfy the essence of Thevenin's theorem adopted in the method [18, 20]. In this method, an ac load flow is conducted for the no-load and loaded cases, which do not allow direct computation of bus indices. This takes a long process until bus indices are calculated. In the line-based voltage stability index, the load flow solutions are directly used to compute the line stability indices and it is feasible to be implemented on-line. When a particular load bus is subject to reactive power variation, this index is able to identify the sensitive lines with respect to the load bus [3, 25-27, 32-33, 34] along with identifying the voltage stability limit of a particular bus in the system. The voltage stability index that is derived based on bus has been used to identify the voltage collapse point and weak bus in the system. The bus evaluated with the highest voltage stability index which implies the weakest bus in the system [33].

In [35], voltage collapse proximity indicator is developed based on the optimal impedance solution of a two-bus system. This technique is reported to be able to investigate the stable and unstable regions with respect to the reactive load variation at a particular load bus. Many techniques are reported in avoiding voltage collapse occurrence in power system. The application of fast active power rescheduling proposed in [36] provided an insight of the voltage collapse avoidance technique. In this work, active power production is rescheduled automatically in order to increase the loadability of the power system during a voltage instability occurrence. Another method for avoiding the steady-state voltage instability is the application of load shedding as described in [37]. The application of voltage stability index referred to a bus in the approach of determining the location and quantity of load to be shed indicated the flexibility of bus index. Similarly, a proximity index could also be used to monitor and enhance voltage stability as reported by Tare *et al.* [38]; at which, an index based on the angle between the real (P) and reactive power (Q) gradient vectors of load buses is proposed. In this work, the voltage stability improvement is achieved by the application of optimization technique; at which the control mechanisms are the bus voltage settings, capacitor shunts and transformer taps.

Jasmon *et al.* [39] derived a line-based voltage stability index for assessing the voltage instability condition in a radial distribution system addressed as overall system stability at which collapse point was determined. The work was also concerned on the comparisons in performance of various load flow techniques in terms of speed of convergence, accuracy of solution and storage requirement. On the other hand, Yogendra *et al.* [40] developed a line-based index for assessing the voltage stability in a radial system as an equivalent single line diagram. The criteria chosen to characterise the voltage instability condition was similar to the approach adopted in [34, 41] in which the discriminant of quadratic equation set greater than zero to maintain stability in the system. The merit recognised from this work was its capability to select and discriminate the critical and non-critical contingencies in a system. In order to improve voltage stability condition, there are various techniques which can be adopted. One of them is power scheduling. The role of power scheduling in power system is to maintain the voltage profile while the active power is delivered through transmission lines. Managing rescheduling is one of the important control activities in a power system. Visakha *et al.* [14] used voltage stability index as the basis to develop an approach for real power scheduling in order to improve system stability margins under normal and network contingencies. On the other hand, reference [23] proposed the static voltage stability index of the load bus as one of the possible methods. The static voltage stability index (*SVSI*) is used as the basis for evaluating the most real-power generation scheduling. This index gives a scalar number to each load line and it is in the range of zero to one.

From the cited references, it was found that voltage stability study has gained numerous concerns from the power systems researchers because voltage collapse occurrences led by the voltage instability are still a progressing issue. Various techniques reported in the literature in addressing, monitoring and assessing voltage instability phenomena revealed the importance of voltage stability situation.

2.5 MAXIMUM LOADABILITY AND CONTINGENCY ANALYSIS IN ELECTRIC POWER SYSTEMS

Maximum loadability has also become a crucial factor in addressing capital investment optimization while meeting demand and security requirements in terms of steady-state and dynamic constraints [42]. Traditionally, determining the maximum loadability in power system involves highly mathematical formulation making the analysis complicated. Voltage stability analysis can be a tool for estimating maximum loadability for a power system during off-line. In this process, maximum loadability wa estimated when the system reaches a pre-determined limit before system started to lose its stability. Most literature agreed that maximum loadability depends on the solvability margin of load flow [43-46] i.e., when the Jacobian matrix becomes singular. Sauer *et al.* [43] determined maximum loadability of a power system based on the equality and inequality constraints. The equality constraint dealt with the Kirchoff's circuit laws while the inequality constraints reflect physical limits such as thermal overload, critical voltage drop and steady-state stability. Maximum loadability can also be determined using the direct interior point algorithm as reported in [47-49]. Maximum loadability could also be addressed concerning the voltage stability and thermal limit at the distribution feeders as described in [50]. Nevertheless, it was reported that the maximum loadability might be limited by the voltage stability rather than the thermal limit. In this work, nodal voltage stability index was incorporated to assess the voltage stability condition in the distribution feeders. The voltage stability margin was also an important feature in the maximum loadability issue. The enhancement of voltage stability margin could be done by improving the maximum loadability point particularly at the weak bus in a system. This issue was addressed in [51] at which; voltage stability margins were investigated under normal operating conditions and contingencies. The application of modal analysis in assessing the voltage stability condition was able to identify the weakest bus in which it was identified as the best location for performing any remedial action. Maximum loadability was a crucial issue in voltage stability studies as it determined the capacity of a particular load bus leading to the determination of voltage point collapse. Various techniques reported in the literature to identify and estimate maximum loadability [25, 43, 50-63] indicated the importance of them in power system studies.

Contingency analyses have also been regarded to voltage stability analysis in power systems as reported in [6, 19, 20, 22, 64]. Contingency analysis evaluates the whole system security [65]. This is because contingencies caused by line, generator or transformer outages would normally lead to voltage instability condition resulting in cascading blackout to the system especially at a heavily loaded situation. The occurrence of voltage collapse and blackout that could occur in an electric power system when load powers vary so that the system lost stability in a saddle node bifurcation was further described in [66-68]. In this work, new iterative and direct methods to compute load powers at which bifurcation occurred closest to the current operating load powers were proposed. Voltage instability analysis involves both static and dynamic factors. The static voltage instability analysis involves determination of an index known as voltage collapse proximity indicator [23]. This index is an approximate measure of closeness of the system operating point to voltage collapse. On the other hand, contingencies are ranked based on the value of scalar performance index (PI) which measures the system stress in some manner as reported in [69-73]. The occurrence of line outages that was normally called as disturbances could be caused by single or multiple outages. Throughout the years offline simulation studies were progressively carried out in order to investigate further impact of contingencies caused by line or generator outages. Line outage contingency analysis could be conducted by evaluating local load flow as suggested in [69]. In this work, contingency study was conducted to screen and select the credible contingencies that could cause system violations.

In [74], it was reported that power outage could also be caused by storm leading to power lines and towers damage. Consumers in most industrialized world could not tolerate with power outage even in a significant duration. The occurrence of generator outage could lead to other contingencies such as line or transformer outages. Therefore, the analysis is normally incorporated together with state estimation, short-term load forecasting, external network, security assessment and correction, automatic contingency selection and optimal power flow as reported in [75]. Another study was also conducted in [76] to evaluate the contingency problems using the Fast Decoupled Load Flow (FDLP). In this study, contingency problems were addressed as distributed analysis concerning the practical issue of it. Linear contingency analysis could be conducted by efficient bounding method as proposed in [77]. In this method, contingency analysis was conducted to detect branch flow violations. The bounding criterion was introduced to reduce the number of branch flow computations and limit checking while sparse matrix/vector method was also adopted to run the contingency analysis. Contingency was also regarded to be the triggering mechanism to voltage instability in power system as reported in [78], in which sensitivity analysis on generated reactive powers with respect to load requirements was adopted. In [70] automatic contingency selection was proposed using the reactive type performance index, which involved optimization process. One of the most common optimization processes was the Tabu search based approach to *(N-k)* static contingency selection as described in [79]. In this technique, tabu search was utilized to identify the most severe *(N-k)* contingencies. Bijwe *et al.* [80] described an efficient iterative method for ranking the line outage contingencies in an AC-DC system based on overload and voltage performance indices. The development of line outage distribution factors extended from the proposed method was capable to reduce the computation burden experienced in the study.

Contingency analysis could be conducted in other power system environment as reported in [81]; in which analysis was done in the presence of FACTS devices. In this work, PI was assigned to each contingency case followed by the determination of the correctability of overloaded lines and the worst and the noncorrectable contingencies were analyzed together. This technique resulted to the determination of generation shifts and load shedding to alleviate overloading. Contingency was also known as unpredictable even that might occur in power transmission system, thus it could also be considered as a probabilistic problem. The effect of probabilistic line outages on small disturbance stability analysis was reported in [39]. In this work, a model for power systems has been presented incorporating small magnitude load and transmission line fluctuations and configuration changes resulted from the probabilistic transmission line outages. On the other hand, new contingency ranking technique incorporating a voltage stability criterion was proposed by Jasmon *et al.* [82]. A line-based voltage stability index was utilized as a measure to voltage stability condition while the critical contingencies that led to voltage instability was revealed. Contingency studies have also been regarded to voltage stability analysis in power systems as reported in [83-96]. This is because contingencies caused by line, generator or transformer outages would normally lead to voltage instability condition resulting in cascading blackout to the system especially at a heavily loaded situation. On the other hand, a fuzzy logic and probability based real time contingency ranking technique proposed in [97] revealed another option in contingency studies. In this work, the probability of occurrence, the severity of violations of system voltage and thermal limit and the amount of curtailed loads were considered in ranking the contingencies. In [98-99] two performance indices (PI) were proposed for evaluating the contingencies based on the real power transmission losses. These indices were utilized to evaluate line overloading and bus voltage limit violation. The beauty of the proposed indices was that; the indices depended on the system variables making them an efficient technique for contingency evaluation and bus voltage limit violation.

Prada *et al.* [88] proposed contingency analysis to be included in the nodal assessment of static voltage stability. The proposed method was based on the straightforward physical characterization of the voltage stability phenomena while emphasis was given on the computational efficiency. A fuzzy-set based technique could also be used as a technique for contingency ranking studies [5]. In this study, the linguistic description of system operators' experience and heuristic rules were represented in the form of fuzzy reasoning rules. The post contingency quantities were expressed in fuzzy set notation prior to the formation of fuzzy reasoning rules. Contingency evaluation technique in [100] was reported as fast and efficient accurate method in addressing the contingency problems. It employed the complete Taylor series expansion of the nodal equations while the non-linearity of the load flow equations was retained. In [101-102], the contingency problems were addressed in the viewpoint of dynamic stability. The work looked into the dynamic stability analysis in performing the contingency screening and ranking processes. A new model for transmission line outage in large electric networks was reported in [4]. In this study, a new method for calculating the multiple line outages was presented at extremely high computation speed.

Contingency analysis was normally conducted on the transmission system for the sake of monitoring the whole system security. However, contingency analysis was also considered important as reported in [103]. In this study, a structured method was proposed in the form of flow diagram for simulating the contingencies in distribution system. A corrective action procedure was formulated considering the voltage profiles and power flows leading to the smoothness of electric supply to the utilities. If a contingency occurs in an already stressed system, stability may be lost, leading to the most critical outcome of a voltage instability process: the so-called voltage collapse. Voltage collapse occurs when a system is heavily loaded and unable to maintain its generation and transmission schedule, observed by a sudden decline in system-wide voltages. There are various methods in determining the voltage collapse proximity indicator. Kessel *et al.* [104] suggests an indicator L method for the on line testing of a power system, which is aimed at the detection of voltage instabilities. An indicator L varies in the range between 0 (no load of system) and 1 (voltage collapse). In [14], a VSI was proposed for improving system stability margins under normal and network contingencies. This index was utilized to evaluate the power generation scheduling. A new index of the load bus for evaluated voltage stability analysis in power system was proposed in [23]. In this study, an index termed as static voltage stability index (*SVSI*) is used as the basis for evaluating the real power generation scheduling. This index was utilized to measure a closeness of the system operating point to voltage collapse. The bus evaluated with the highest voltage stability index implies the weakest bus in the system [8].

Contingency could also be caused by generator outages. Although generator outage occurrence is seldom in most power system networks in the world, however once it happens the impact is disastrous, involves monetary losses and failure in utility operation [105]. The occurrence of generator outage could lead to other contingencies such as line or transformer outages. Therefore, the analysis is normally incorporated together with state estimation, short-term load forecasting, external network, security assessment and correction, automatic contingency selection and optimal power flow as reported in [75].

2.6 POWER SCHEDULING FOR VOLTAGE STABILITY IMPROVEMENT IN POWER SYSTEMS

Voltage stability condition is a crucial aspect in the power system operation and planning. The stressed condition in a power system caused by reactive power loading has made the system operating close to its stability limit while reducing the voltage on a particular load bus. Hence, some measures should be taken in order to improve the voltage stability condition in the electrical power system. The lack of reactive power support was known to be the voltage instability phenomena in power system. Therefore Reactive Power Planning (RPP) procedures are required in order to enhance the voltage stability in power system network. Most of the popular techniques are the reactive power dispatch, capacitor placement, transformer tap changer setting, FACTS devices and other reactive power compensation techniques [106-123]. Voltage stability improvement could also be implemented by reactive power dispatch.

The attempt of RPP procedures was widely addressed as regards to VAR planning for voltage stability improvement as reported in [87, 124-134]. Chattopadhyay *et al.* [106] described the statistical approximation procedure to simplify the voltage stability constrained VAR planning optimization model. In this study, optimization models were simplified using statistical approximation, which has proven reduced computation time. Thukaram *et al.* [21] proposed a reactive power dispatch technique for monitoring and improving voltage stability in power system at base case and credible contingency conditions. In this work, index of load buses (L-index) was employed as the proximity of stability condition in which the sum of the squares of L-indices for a given loading condition have to be minimized in the attempt of control against voltage collapse. The generator excitation, switchable VAR compensators and OLTC transformers were chosen as the control variables towards the optimization process of the sum of L-indices.

The proposed technique has demonstrated encouraging results in improving the voltage stability at the base case and credible contingency conditions. Similar approach was implemented by Thukaram *et al.* [29] resulting a good agreement between them. The work conducted in [134] in developing the optimal reactive planning revealed the importance and concern of voltage instability problem. The work duly emphasized on the reactive power compensation installation in economical way without jeopardizing the security. Reactive power planning was not only implemented in a normal power system environment but rather possible to be implemented in the deregulation power utilities. This issue has been emphasized in reference [107]. This work has highlighted the necessity of the distribution companies for the compensation reactive power loads while the transmission companies responsible for the reactive power compensation in ensuring a smooth power delivery to the consumers.

The implementation of RPP involved optimization process. There are numerous optimization techniques such as Tabu Search, linear programming, non-linear programming, Simulated Annealing (SA), Genetic Algorithm (GA), Evolutionary Programming (EP), Evolutionary Strategy (ES) and Genetic Programming (GP). GA, EP, ES and GP are the optimization methods based on natural evolution called the Evolutionary Computation (EC) in the Artificial Intelligence (AI) hierarchy. In references [117-118, 135-141], described the GA based optimization technique in the RPP procedures. In [141] the GA based optimization for reactive power dispatch that aimed to control the voltage in power system was proposed. The capability of the proposed technique to outperform the conventional gradient-based optimization was highlighted. Lee *et al.* [135] proposed an improved method of operational and investment-planning utilizing a Simple Genetic Algorithm (SGA) combined with the successive linear programming method. The flexibility, robustness and easy modification of SGA were highlighted which implied that the proposed technique was a promising approach for RPP. Similarly, in [136-138]; the GA optimization technique for the reactive power optimization was utilized to solve the problem. In these studies, the GA-based method utilizing the unique intentional operations involved with "interbreeding"; which was done on a kind of crossover using decomposed subsystems.

The capability of the proposed technique in searching for a global solution using multiple paths was highlighted and it was reported that the integer problem was treated naturally. Further work could be observed through study conducted in [142], where GA was utilized for the reactive power dispatch. In this study, the GA was applied for optimizing the transformer tap settings and value of shunt capacitors in the attempt of improving voltage stability conditions in power systems. The capability of proposed technique in obtaining the optimized transformer tap setting values and shunt capacitors were reported with the additional merit of minimizing total loss in the system.

The application of EP in the RPP optimization was reported as a reliable technique in improving the voltage stability condition and voltage profile in power systems as reported in [113-114, 143-146]. In [114, 143-144], the EP based technique for RPP taking total cost of energy loss and total cost of VAR source as two objective functions were proposed. It was reported that EP performed better than the non-linear programming especially in the case of non-smooth and non-continuous functions. EP was found better than the Broyden's method in terms of convergence and search the global optimum capability. EP based optimization technique was also conducted for optimal reactive power dispatch [141]. The proposed technique was compared to the conventional gradient-based optimization method resulted a better performance in determining the global optimum, fast convergence rate, robust computation and possessed an inherent capability for parallel processing. The capability of EP in solving the RPP was further enhanced by making a rigorous study with other EC techniques and other optimization method. Lee *et al*. [147] performed a comparative study for the three EC techniques namely the EP, ES and GA with the linear programming method in solving the RPP. In this study, operation cost minimization (*i.e*., operation cost and investment cost) was applied as the objective function since the conventional total cost minimization did not guarantee the optimal operation with minimum fuel. Results obtained from the proposed ECs techniques indicated better performance over the linear programming method in terms of total cost, power loss with hard limits satisfied. The work conducted by Cao *et al*. [120] indicated the capability of GA in adaptive form for solving optimal reactive power dispatch. Adaptive GA (AGA) was proposed to solve the reactive power dispatch along with voltage control of power systems.

There were also efforts in applying fuzzy logic techniques for solving the reactive power problems as described in [148-150]. In [48] the integration of AI techniques with sensitivity analysis for the RPP formulation was proposed. In this study, the objectives and constraints were translated into fuzzy sets and the problem was solved using the fuzzy goal programming. This allowed the optimization process with multi-objective functions. The fuzzy sets techniques were also utilized for solving the RPP problems considering the security constraints [116, 118, 135-138]. In this study, the overall objective was to minimize the real power losses under various loading conditions, minimizing of allocation cost of a new reactive power sources while satisfying the static system security by controlling the final solution of bus voltages. The application of expert system was another alternative for solving the reactive power planning problems as reported in [151-153]. Bansilal *et al.* [1] developed an expert system for monitoring and improving steady state voltage stability utilizing a bus based index as the monitoring indicator. In this work, VAR compensators, OLTC transformers and generation excitation were considered as the control variables. The proposed expert system was reported capable the on-line application in Energy Control Centre for monitoring and improving the voltage stability. Capacitor placement has been identified as another RPP technique, which was meant to improve the voltage profile at a local bus. This could be implemented either on the transmission or distribution system as reported in [109, 116, 154-155]. Baran *et al.* [154] proposed the application of non-linear programming technique for optimizing the capacitor sizing placed on a radial distribution system taking total loss minimization as the objective function. In this work, a new formulation of the ac power flow equation called the Dist-Flow for the radial distribution system was introduced. The application of Tabu Search (TS) optimizations technique was another option capacitor placement in radial distribution system [55].

The implementation of optimization process using an Immune-Based Algorithm (IA) was identified as a new approach in solving the capacitor placement in recent years as proposed by Huang [118]. In this method, the optimizing parameters were the load profiles, feeder capacities and allowable voltage limits; while the objective functions were the minimization of investment cost and energy loss. The work conducted in [128] took into consideration the presence of harmonics distortion in shunt capacitor allocation process. Optimization process was solved using non-linear programming in determining the optimal locations and sizes of the shunt capacitors. It was reported that the application of non-linear programming for RPP process considering the harmonics distortion has shown a good result while the merits of this technique were highlighted. In [156-157], Affonso *et al.* proposed a procedure for active and reactive power re-dispatch under normal operation condition. The study also looked into active and reactive power re-dispatch plus minimal load shedding for operation under severe contingency. In this work, reactive power rescheduling method was first implemented to the system to maximize the voltage stability margin. If the margin is still less than the minimum criterion, the real and reactive power rescheduling would be applied to the system and if the margin is still less than the minimum criteria, load shedding technique was also applied in order to increase the voltage stability margin. In reference [16], Dopazo *et al.* presented the economic allocation of real and reactive power by applying the method of Lagrangian multipliers and gradient method. In this work, the Lagrangian multipliers method was employed to obtain real power generation schedule whereas the gradient method was used for allocating reactive power generation in order to reduce transmission loss. Kumar *et al.* [17] propose a zonal congestion management approach based on the real and reactive power flow sensitivity indices to reschedule the generators on practical power systems.

2.7 FACTS COMPENSATION FOR VOLTAGE STABILITY IMPROVEMENT IN POWER SYSTEMS

Building a new transmission line will not be an efficient way to solve the problems since it is quite complicated which can be due to the environmental and political reasons [158]. Therefore the only way to overcome this major problem is by developing a new way of transmitting more efficient and economical supply using the existing transmission lines. There are few other methods available in solving the problems. In couple of years, the electromechanical equipments were used. Those equipments were switched inductors or capacitors banks and phase-shifting transformer. However all this equipments are not reliable or not efficient enough due to the certain problems related to this equipments. They are not only relatively slow but they also cannot be switched frequently because they tend to wear out quickly [2]. In this context, one possible solution to improve the system operation was the use of FACTS technologies. It opens up new opportunities for controlling the power, decreasing the losses and enhancing the unstable capacity of existing transmission lines [2]. However not all can be provided by FACTS devices and it is important to select the type of devices in order to achieve the purpose.

The use of FACTS devices could extend the voltage stability margin as reported in [159]. In this work, three FACTS technologies were investigated; static VAR compensator (SVC), unified power flow controller (UPFC) and the thyristor-controlled series capacitor (TCSC). This technique dealt with small-signal voltage stability, singular value decomposition (SVD) and modification of power system, representation in order to comprehend the remedial measures for voltage stability improvement. It was also reported that several FACTS technologies have the potential for voltage stability improvement particularly under the high stress conditions. The placement of UPFC at the weakest transmission line and SVC on the critical bus has shown similar performance in the voltage stability improvement techniques. Moghavvemi *et al.* [110] also suggested the application of FACTS devices for improving the static voltage stability conditions. In this study, the merits of using the FACTS devices were highlighted such as increase in power limit, line power and loading capability, improvement in voltage regulation, damping of oscillation and transient stability. On the other hand, in [111] proposed a new formulation for FACTS allocation for security enhancement against voltage collapse. It involved optimization process for formulating the problem utilizing the non-linear programming methods. The merits of using FACTS technologies in voltage stability improvement have been further analyzed in [112]. In this work, the steady state models for SVC and TCSC were presented in order to study their effects of voltage collapse phenomena. Design strategies were proposed from the study for identifying the optimal location, dimensions and controls in order to increase the system loadability. In [119], the FACTS devices is used as additional control parameters in the optimal reactive power dispatch (ORPD) formulation. In this work, three FACTS technologies namely the SVC, TCSC and Thyristor Controlled Phase Angle Regulator (TCPAR) were considered for the ORPD formulation. Sensitivity based method was applied to determine the optimal placement of FACTS devices for voltage stability improvement. The proposed technique revealed the effectiveness of using sensitivity-based method for the FACTS devices placement in solving RPP problems.

In last few years, some papers have been published on solving the problem related to FACTS devices with respect to different purpose and methods [160-161]. Various optimization techniques have been applied for the optimal placement of multi-type FACTS devices such as TS, GAs, SA [162-163] and Bee algorithm [164]. An evolutionary programming approach to determine the optimal allocation of multi-type FACTS devices [165-66, 208], a GA technique which was proposed for solving the optimal location of FACTS [167-168] and a particle swarm technique for optimal location of FACTS devices [169-170]. Further implementations of FACTS devices for power system security enhancement were reported in [122-123, 142, 171-172]. In [121] the optimal location of shunt FACTS devices in long transmission line for investigating the power transfer capability and stability was reported. It was also revealed that the placement of shunt FACTS device slightly off-centre has shown the highest possible benefit when the power flew in a particular direction. Sensitivity-based method incorporated with FACTS devices was also conducted by Singh [123]. The modeling of FACTS devices for power flow studies was conducted by Gotham *et al.* [171]; at which FACTS devices several scenarios were simulated. The developed models were based on the following scenarios; prevention of loop flows, implementation of an electronics fence, increase in power transfer capability, unloading a selected line and direct power flows between regions. In some models, more than FACTS technologies were exemplified. Galiana *et al.* [142] proposed a technique to systematically evaluate the impact of FACTS devices on the steady-state behavior of power system through the concept of generalized security regions and scalar measures of these regions obtained from optimal power flow simulation. In this study, such regions were defined by the operational equality and inequality constraints that the system variables must satisfy. Hybrid optimization technique, which incorporated TS and SA for optimal power flow (OPF) with multi-type FACTS devices was proposed in [163]. In this work, TS and SA were 'hybridly' utilized for minimizing the generator fuel cost in OPF control with multi-type FACTS devices. It was reported that the proposed technique has effectively and successfully implemented while proven relatively fast computation time. In [119] proposed a loss sensitivity approach for location of phase shifters, series capacitors, and static VAR compensators. In this study, EP technique was used as one of the optimization technique. By using EP technique to optimize the size of UPFCs, the loss can be minimized and voltage profile can be improved. Therefore, the recovered supply can be used to support the increasing electrical energy demand in the system.

Other works utilizing FACTS technologies were reported in [155,173-178]. The application of TCSC as a compensation technique for stability control in power system is a good proposal that needs to be appreciated [174]. The effects of TCSC phase and amplitude were investigated while the capability of TCSC in performing better compensation process over the traditional series compensation and parallel lines were highlighted. Mahseredjian *et al.* [175] investigated currently available solution methods for the simulation of power electronics circuits used in most FACTS devices. In these works, the limitations of the current and future research were outlined in the attempt of finding solutions related to power electronics network. However, this study is slightly deviated as far as voltage stability is concerned. Optimal allocation of transmission rights in system with FACTS devices [155] and application of structure preserving energy margin sensitivity to determine the effectiveness of shunt and series FACTS devices [176] were two important areas that could be further explored in related to voltage stability studies. The steady-state optimization in power systems to identify the key location of FACTS devices in the ac network for increasing the maximum megawatt power transfer was reported in [177]. The study proved that the installation of a single device (TCSC and UPFC) have achieved a more uniform loading of the available parallel paths with higher transferred flows. In [178], a novel versatile power flow control approach based on a power injection model of FACTS devices and optimal power flow model was put forward. In this work, FACTS devices were incorporated into the existing power system analysis and control programs efficiently, while the physical limits were considered in the modeling process. The performance of the proposed technique was realized by implementing it on a practical system while its vigorousness for the control process in power systems was highlighted. The analysis of non-linear modal interaction in stressed power systems with SVCs inclusion in power system network was reported in [173]. In this study, a comprehensive analytical technique based on normal form theory and symbolic computer algebra was proposed for the analysis of non-linear oscillations in of stressed power systems with SVCs.

The application of UPFC as the main instrument to improve voltage profile has also been addressed in various researches [165, 167, 169, 179]. UPFC can effectively control both the active and reactive flows on the lines and voltage magnitudes at the buses to which they are connected [165]. The application of SVC [127] considering a voltage constraint in the attempt of improving voltage stability condition was reported. In this work, the availability of reactive power alone was reported inadequate in the voltage stability improvement scheme, but rather considering the control of voltage violation as the constraint. TCSC offer smooth and flexible control of the line impedance with much faster response compared to any other control devices [180]. These devices have been commonly used in electric power systems for voltage stability enhancement. A proper use of TCSC can eliminate line overloads and hence increases the system security margin [2]. The application of TCSC as a compensation technique for stability control in power system was reported in [174]. The effects of TCSC phase and amplitude were investigated while the capability of TCSC in performing better compensation process over the traditional series compensation and parallel lines were highlighted.

2.8 OPERATING GENERATOR SCHEDULING (OGS) IN ELECTRIC POWER SYSTEMS

In the worldwide trend towards restructuring electricity industry, there is an interest in developments and studies that can minimize energy cost in operations cost and reducing in transmission loss. A scheduling of generators resources to meet system demand can provide extensive annual savings in fuel cost and a suitable decision making tool is needed. Information of the minimum cost or minimum loss for a day would provide a measure of the performance of the selection of dispatching power generators and suggest ways to improve future schedules thus reduce the cost of electricity. An effort has been made in this work to incorporate a several algorithms and scheme in order to solve the generator scheduling problem. The scheduling problem is difficult to be solves by conventional programming methods. Solving the scheduling problems is important for the economic operation of facilities.

A variety of different techniques and methods have been employed to solve the generation scheduling problem with varying degrees of success. These included; GA method [181-184], fuzzy [185], integer programming [186], simulated annealing [187], augmented Hopfield network [186] and artificial neural network (ANN) [188]. A lot of researches have been carried out in the area of scheduling generator because better synchronization of schedules can result in substantial savings for utilities [189]. One of the approach, involves scheduling of thermal generators by determining the optimum combination of the available units to supply a given load profile at minimum cost, subjected to a number of system and unit constraints. GA method has been widely used to solve generation scheduling problems in different formulation. In [181] the GA integrated with the fast priority list heuristic has shown a great potential for large scale system by speed up the genetic algorithm search mechanism process although these heuristic methods do not always guarantee the globally optimal solution. Another paper in [182] presented a hybrid GA where a GA based approached incorporate a sequential decomposition logic was applied shows a great potential by providing a faster search mechanism to the scheduling of generator. In this work, the performance on the test system demonstrates that it is able to provide a good unit scheduled for a medium sized power system as long as there are enough generators available to meet the load demand. Lora *et al.* [183] used genetic algorithm technique to determine which generator units should be online and generation scheduling period in order to minimize the total cost of the system. Optimal scheduling of generation is a nonlinear, non-convex, combinatorial, mixed-integer and very large problem. Therefore, this technique has been applied to this particular problem and depends on the knowledge of power plan operators. A method based on real coded genetic algorithm for finding the most economical hydrothermal generation schedule under practical constraint is reported in [184]. The search technique is simple and has very fast computation and convergence speed. Nevertheless, the algorithm is very sensitive to the initial feasible values selected to start the search. The application of genetic algorithm proposed in this paper provided an insight of the evolutionary computation technique.

Another approach utilizing the fuzzy set application was proposed in [185]; at which a novel multi-objective fuzzy set index was developed to analyze the generation scheduling and integrated with pattern recognition technique optimize the reserve requirements of individual systems in an interconnected system. Mohatram *et al.* [188] solved the generation scheduling problem with an ANN method, a type of artificial intelligent technique performed in different central load dispatch centers. It is observed that, results showed a better performance in accuracy and time compare to a conventional method, Classical Kirchmayer method. Conventional method requires excessive calculation time and computer storage. Wong *et al.* [187] have integrated a genetic algorithm with a simulated annealing approach called GAA2 hybrid algorithm for solving the thermal generator scheduling problem. In this paper, it has determined the most economical and the fastest way on scheduling the generator and the approach has the ability to find the global optimum value of generator schedules. However, the control parameters setting for simulated annealing algorithm become complex and cause the speed of the algorithms slow when applied to a practical sized power system. The augmented Hopfield network proposed in [186] has been successfully applied to the scheduling problem by considering all the physical constraints in addition to the common constraints namely ramp rate, transmission and fuel constraints. This method can solve problems including thermal, hydro and pumped-storage units. Garver [190] proposed the solutions for generator scheduling problem using integer programming technique by providing the formulations of the discontinuous input-output characteristics and start-up cost of the generators. This technique was reported to be able to develop standard scheduling patterns which could be applied quickly in accordance with changing conditions. In [191], evolutionary hybrid approached was utilized in order to determine the solution for generation scheduling. In this work, a variety of metaheuristic, heuristic and mathematical programming technique was introduced in order to identify the optimum solution for generation scheduling within a realistic timeframe. It also requires less computation time compared with linear programming (LP) methods.

2.9 MULTI-OBJECTIVE OPTIMIZATION FOR VOLTAGE STABILITY IMPROVEMENT IN POWER SYSTEM

In recent years there has been attention in applying multi-objective optimization for solving power system problems. Multi-objective optimization can be considered as optimizing more than one objective function and satisfy some constraints violations namely equality constraints and inequality constraint. There is no single global optimum when implementing multi-objective optimization because of tradeoffs between each objectives function. The optimal solution of multi-objective optimization has a set of solutions rather than a single solution. The solution set can provide users the choice of diversification. As for reactive power control or dispatch applications, the objective functions can be a combination of voltage stability index, transmission line, cost, voltage deviation and etc. Many techniques have been applied and implemented in order to solve multi-objective optimization problems. For reactive power control, it is important to develop a multi-objective optimization algorithm which take both voltage stability index and transmission loss into account, to provide users a set of options with flexibility to solve the problem. The presence of reactive power control into power system brings many benefits. The goal of a study can be single objective, where only one objective need to be minimized or maximized. If the goals of the research need more than one objective to be optimized, then it is called multi-objective optimization problems. The genuine way of solving multi-objective problem is to consider all objective functions applied simultaneously.

In power systems applications, many of the proposed methods for multi-objective optimization focus on the constraints related to the steady state operation. Numerous optimization problems have more than one objective in conflict with each other. Since there is no single solution for these problems, the aim is to find the Pareto optimal trade-off solutions that represent the best possible compromises among the objectives. Therefore, the multi-objective is implemented into the system in order to solve the optimal RPD problem where trade-off between the different components of the objective function is fixed. Many studies have been made on the reactive power control or dispatch for multi-objective optimization. A number of multi-objective evolutionary computation techniques like GA, Evolutionary Algorithms (EA), and Swarm intelligence have been applied [192-206]. Multi-Objective Genetic Algorithms (MOGA) was proposed by P. A. Jeyanthy *et al.* in [192] is applied to optimize the reactive power dispatch by minimizing the losses and maximizing the voltage stability margin. The proposed method emphasizes non-dominated solutions and simultaneously maintains diversity in the non-dominated solutions. Subsequently, various multi-objective evolutionary algorithms (MOEAs) have been developed to solve these problems [193-194]. Multi-objective evolutionary programming (MOEP) applied in this thesis is one of the MOEAs to solve the multi-objective optimization problems. MOEP is an extended version of single objective EP. Hsaio *et al.* [195] introduced the Evolutionary Algorithms (EAs) technique where they developed a program for reactive power dispatch that results in the minimizing of voltage difference in addition to loss minimization. K. Deb *et al.* [196-197] proposed the NSGA-II for RPD and this been demonstrated to be the most efficient algorithm for multi-objective optimization where it outperforms two other multi-objective algorithms namely Strength-Pareto Evolutionary Algorithm (SPEA) [198] and Pareto-archived evolution strategy (PAES) [199] in term of finding a diversity among the solutions in the pareto-front. Marouani *et al.* [200] presented MOEA method for reactive power dispatch with FACTS devices and the NSGA-II approach is applied to solve this nonlinear multi-objective problems. A. A. A. El-Ela *et al.* [201] proposed the application of multi-objective fuzzy based procedure for optimal reactive power dispatch problem. The work was concerned on solving ORPD problem by controlling the control variables such as the generator voltages, transformer tap ratios and switchable reactive power sources. In addition, this work also considered the dependent variables as the controlling methods and able to improve the ORPD solution by minimizing the total transmission power losses. Evolutionary Algorithms (EAs) also have been applied effectively to solve the optimal reactive power dispatch problem in [202-203]. This method requires multiple runs to find the Pareto-optimal solutions and cannot be used for a non-convex pareto-optimal front. In order to solve the problem, Chen [204] introduces a Bacterial Swarming Algorithm (BSA) method that capable to search a multiple pareto-optimal solutions in a single run. The work reported in [205] presented the implementation of Multi-Objective Particle Swarm Algorithm (MOPSO) for power system reactive power dispatch. In this work the active power loss and voltage deviation were taken as the objective functions for this optimization.

2.10 OPTIMIZATION TECHNIQUE USING EVOLUTIONARY PROGRAMMING

The application of Artificial Intelligence (AI) in solving power system problem was profoundly well known. AI is subdivided into three components namely the ANN, Fuzzy Logic and EC. EC has four subordinates under its hierarchy namely the EP, ES, GA and GP. One of the optimization techniques implemented solving power optimization problems in this research is EP. EP is a stochastic optimization technique based on the natural generation. It was first invented by D. Fogel in 1962 and further extended for the optimization process Burgin [75]. It has been widely used and applied in a range of problems related to unit commitment [40], optimal reactive power dispatch [34], reactive power planning [14, 41], and optimal power flow problems

[65]. The process involves random number generation as the initialization, followed by statistical evolution, fitness calculation, mutation and finally the new generation created as a result of selection [98,104]. The generated random numbers represent the parameters responsible for the optimization of the fitness value.

2.11 SUMMARY

This chapter has highlighted the concept of voltage stability assessment implemented in power system networks. Based on previous researches, the use of line stability indices as a tool for assessing the voltage instability condition has been proved to be useful in power system network. They have produced reliable results and have provided a good indicator in addressing and assessing voltage instability phenomenon. Other methods have also been discussed.

The reviews also show that maximum loadability plays an important role in the determination of status of the particular buses in the power system networks. Various techniques are reported in the literature to identify and estimate maximum loadability indicated of it in power system studied.

On the other hand, the power system network these days does not face single contingency but multi-contingencies. Identification of multi-contingencies in this research is crucial so that remedial action can be planned and implemented in the power system. Contingency analysis evaluates the whole system security and it discovers that the most crucial outages were caused by line outage and generator outage. There were various methods in analyzing the contingencies and the analysis is normally incorporated together with state estimation, optimal power flow, reactive power dispatch, power planning and other methods which are appropriate to be implemented.

In addition, the stress condition and outage condition occurred in a power system operation and planning caused by reactive power loading has been highlighted in this chapter. The reactive power planning for voltage stability improvement was not only implemented in a normal power system but should also be possible to be implemented in the system under-contingencies.

CHAPTER THREE
MULTI-CONTINGENCY COMPONENT IDENTIFICATION FOR POWER SCHEDULING

3.1 INTRODUCTION

Multi-contingency events have been reported to be the practical disturbances experienced in power system network [206]. Today, power system network these days does not face single contingencies i.e. *(N-1)*, rather *(N-m),* which implies that several components will involve which result in a voltage instability. Identification of multi-contingency is crucial during the off-line study so that remedial actions that are planned to be implemented in the system such as reactive power support or congestion management schemes will tolerate these scenarios.

This chapter presents multi-contingency component identification for power scheduling in power system. The study involves weak and secure buses identification so that the correct buses can be chosen to perform the power support scheme. As shown in Figure 3.1, this chapter presents the weak and secure bus identification and multi-contingencies component identifications techniques. In the VSA technique, the *SVSI* is applied as an indicator to the all components identifications applied in this chapter. The load bus which has the smallest value of maximum loadability is recognized as the weak bus in the system. On the other hand, the secure bus is identified when the load bus has the largest amount of maximum loadability in the system. Furthermore, this chapter also presents a technique applied for contingency analysis and ranking caused by line and generator outages in a system. Two separate algorithms were implemented in order to simulate the contingencies caused by line or generator outages. Again, *SVSI* was used as a tool in determining the severity of the contingencies. All the techniques were tested on two IEEE Reliability Test System (RTS) i.e., 30-bus and 118-bus as shown in Figures 3.2 and 3.3. The efficiency of the VSA shows that *SVSI* is reliable tool for VSA for identifying all components applied in any similar power system.

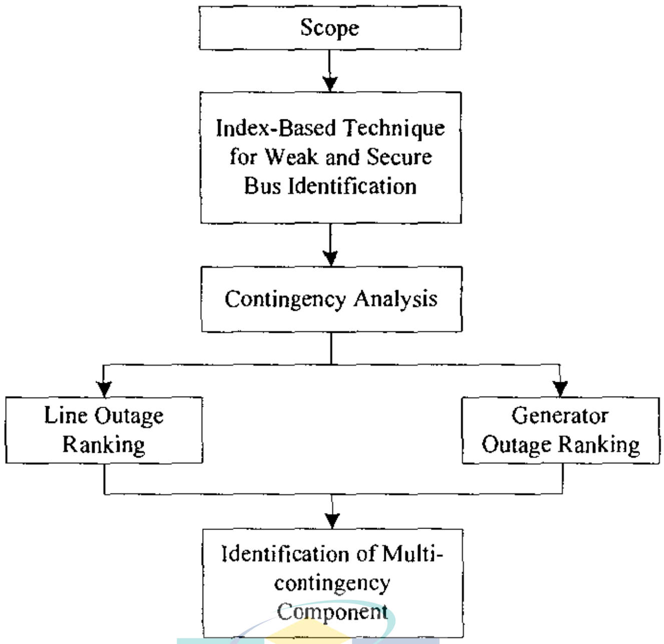

Figure 3.1: Algorithm for Severity Studies

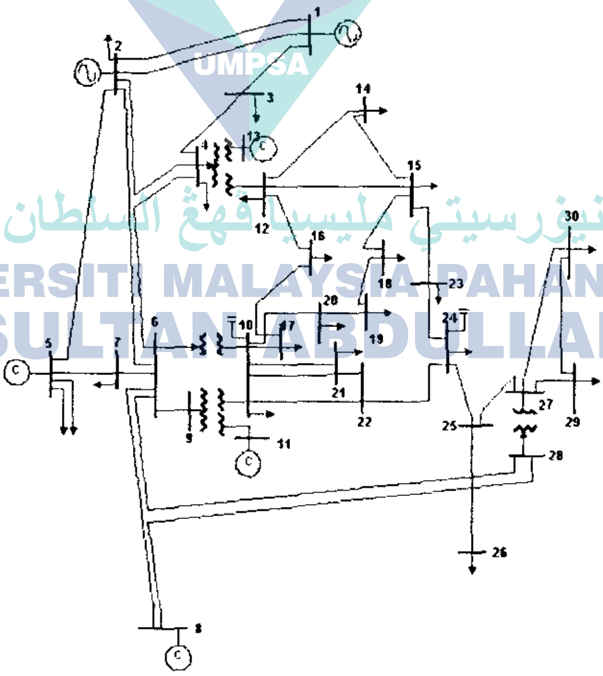

Figure 3.2: Single line diagram for IEEE 30-bus RTS

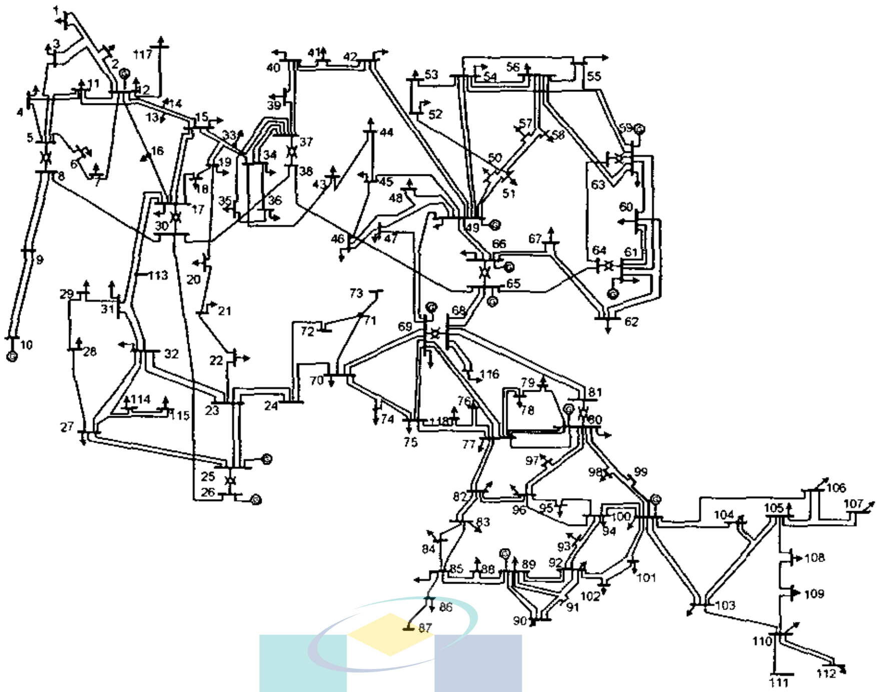

Figure 3.3: Single line diagram for IEEE 118-bus RTS

3.2 STATIC VOLTAGE STABILITY INDEX

SVSI which is a line-based voltage stability index was developed by L. Qi [23]. This index used in the voltage stability analysis as an indicator of the voltage stability condition of a system. The voltage stability condition of all lines in power system could be assessed using this index which could predict the occurrence of voltage collapse in a system. *SVSI* was formulated by deriving the voltage quadratic equation for a general two-bus system at the receiving end. Figure 3.4 shows a two-bus power system. Sending end bus i is connected to a source and receiving end bus j is connected to a load. The two buses, sending end bus i and receiving end bus j, are connected by a line, L_{ji} with impedance Z_{ji}. The power flow on the connecting line at the receiving end bus j is S_{ji}. The current flowing from bus i to bus j is I_{ji}.

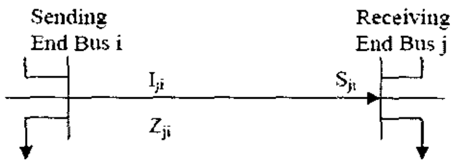

Figure 3.4: General two-bus system

The power flow on the connecting line S_{ji}, the voltage on sending end bus V_i and receiving end bus V_j, and the line impedance Z_{ji} are define as (3.1)-(3.4).

$$S_{ji} = P_{ji} + jQ_{ji} \tag{3.1}$$

$$V_j=|V_j| \cos \delta_j + j|V_j| \sin \delta_j \tag{3.2}$$

$$V_i=|V_i| \cos \delta_i + j|V_i| \sin \delta_i \tag{3.3}$$

$$Z_{ji} = R_{ji} + jX_{ji} \tag{3.4}$$

The active power and reactive power are P_{ji} and Q_{ji}. The line resistance and reactance are R_{ji} and X_{ji}. The voltage magnitude and angle are $|V|$ and δ. The subscript i and j denote variables associated with bus i and bus j.

According to the power flow concept in the line, the power flow into the receiving end bus j and from the sending end bus i, S_{ji} is derived as equation (3.5).

$$\begin{aligned} S_{ji} &= V_j I_{ji}^* \\ &= V_j\left(\frac{V_i - V_j}{Z_{ij}}\right)^* = V_j\left(\frac{V_i^* - V_j^*}{R_{ji} - jX_{ji}}\right) = \frac{V_j V_i^* - |V_j|^2}{R_{ji} - jX_{ji}} \\ &= \frac{|V_i||V_j|(\cos\delta_{ji} + j\sin\delta_{ji}) - |V_j|^2}{R_{ji} - jX_{ji}} \end{aligned} \tag{3.5}$$

where $\delta_{ij} = \delta_j - \delta_i$, and $\delta_{ji} = \delta_i - \delta_j$. The sign "*" indicates the conjugate of the associated current variable.

Separating equation (3.5) into real and imaginary parts, we have a real power balance equation (3.6) and a reactive power balance equation (3.7).

$$P_{ji} = \frac{|V_j||V_i|R_{21}\cos\delta_{ji} - |V_j||V_i|X_{21}\sin\delta_{ji} - |V_j|^2 R_{ji}}{R_{ji}^2 + X_{ji}^2} \tag{3.6}$$

$$Q_{ji} = \frac{|V_j||V_i|X_{21}\cos\delta_{ji} + |V_j||V_i|R_{ji}\sin\delta_{ji} - |V_j|^2 X_{ji}}{R_{ji}^2 + X_{ji}^2} \tag{3.7}$$

Taking the magnitude of sending end bus voltage as the unknown variable, rearranging equations (3.6) and (3.7) into two quadratic equations (3.8) and (3.9), we have:

$$|V_j|^2 - |V_j||V_i|\left(\cos\delta_{ji} - \frac{X_{ji}}{R_{ji}}\sin\delta_{ji}\right) + \left(R_{ji} + \frac{{X_{ji}}^2}{R_{ji}}\right)P_{ji} = 0 \tag{3.8}$$

$$|V_j|^2 - |V_j||V_i|\left(\cos\delta_{ji} + \frac{R_{ji}}{X_{ji}}\sin\delta_{ji}\right) + \left(X_{ji} + \frac{{R_{ji}}^2}{X_{ji}}\right)Q_{ji} = 0 \tag{3.9}$$

Subtracting equation (3.8) from equation (3.9), we have:

$$|V_j||V_i|\left(-\frac{R_{ji}}{X_{ji}}\sin\delta_{ji} - \frac{X_{ji}}{R_{ji}}\sin\delta_{ji}\right) + \left(X_{ji} + \frac{{R_{ji}}^2}{X_{ji}}\right)Q_{ji} - \left(R_{ji} + \frac{{X_{ji}}^2}{R_{ji}}\right)P_{ji} = 0 \tag{3.10}$$

Multiplying equation (3.10) by $R_{ji}X_{ji}$ and making simplifications, in the form of the sine of the angle difference δ_{ji}, we have:

$$\sin\delta_{ji} = \frac{-X_{ji}P_{ji} + R_{ji}X_{ji}}{|V_i||V_j|} \tag{3.11}$$

Adding the results of the multiplication equation (3.8) by $\frac{X_{ji}}{R_{ji}}$ and the multiplication of equation (3.9) by $\frac{R_{ji}}{X_{ji}}$,

$$
\begin{aligned}
&|V_j|^2\left(\frac{X_{ji}}{R_{ji}}+\frac{R_{ji}}{X_{ji}}\right)-|V_j||V_i|\left(\frac{R_{ji}}{X_{ji}}\cos\delta_{ji}+\frac{X_{ji}}{R_{ji}}\cos\delta_{ji}\right)\\
&+\left(X_{ji}+\frac{R_{ji}}{X_{ji}}\right)\frac{X_{ji}}{R_{ji}}Q_{ji}+\left(R_{ji}+\frac{X_{ji}}{R_{ji}}\right)\frac{R_{ji}}{X_{ji}}P_{ji}=0
\end{aligned}
\tag{3.12}
$$

Multiplying equation (3.12) by $R_{ji}X_{ji}$, and making simplification, in the form of the cosine of the angle difference δ_{ji},

$$
\cos\delta_{ji}=\frac{|V_2|^2+X_{ji}Q_{ji}+R_{ji}P_{ji}}{|V_i||V_j|}
\tag{3.13}
$$

Applying the trigonometric identity on equations (3.11) and (3.13),

$$
\left(\frac{-X_{ji}P_j+R_{ji}Q_{ji}}{|V_i||V_j|}\right)^2+\left(\frac{|V_j|^2+X_{ji}Q_j+R_{ji}P_{ji}}{\|V_i\|V_j\|}\right)^2=1
\tag{3.14}
$$

With $|V_2|$ as the unknown variable, equation (3.14) can be written as a quadratic equation (3.15),

$$
|V_j|^4+|V_j|^2\left(2X_{ij}Q_j+2R_{ij}P_j-|V_i|^2\right)+X_{ij}{}^2P_j{}^2+R_{ij}{}^2Q_j{}^2+X_{ij}{}^2Q_j{}^2+R_{ij}{}^2P_j{}^2=0
\tag{3.15}
$$

There are four solutions for the quadratic equation (3.15). The four solution are shown as equation (3.16),

$$
|V_j|=\pm\frac{\sqrt{|V_i|^2-2X_{ji}Q_{ji}-2R_{ji}P_{ji}\pm\sqrt{\left(2X_{ji}Q_{ji}+2R_{ji}P_{ji}-|V_i|^2\right)^2-4\left(X_{ji}{}^2+R_{ji}{}^2\right)\left(P_{ji}{}^2+Q_{ji}{}^2\right)}}}{2}
\tag{3.16}
$$

Two variables a and b are defined as equations (3.17) and (3.18). Equation (3.15) thus can be written in the form of a and b as equation (3.19). a and b are two real numbers and b must be positive.

$$a = |V_i|^2 - 2X_{ji}Q_{ji} - 2R_{ji}P_{ji} \tag{3.17}$$

$$b = \left(X_{ji}^{\ 2} + R_{ji}^{\ 2}\right)\left(P_{ji}^{\ 2} + Q_{ji}^{\ 2}\right) \tag{3.18}$$

$$|V_j| = \frac{\pm\sqrt{a \pm \sqrt{a^2 - 4b}}}{2} \tag{3.19}$$

Among the four solutions of $|V_2|$, two are positive, the other two are negative. Because voltage magnitude must be a non-negative number, the two negative solutions are not true solutions. Among the two positive solutions, one has a high value and the other has a low value. In power systems, voltages must be maintained close to system voltage, which is the base voltage in a per unit system. Voltage magnitude in per unit thus should be high and close to one. The low positive solution is thus not a feasible solution for a real power system. To derive a positive feasible solution for a real system, the expression under square root sign of equation (3.19) should be positive. Hence, two inequality equations (3.20) and (3.21) must be satisfied to obtain a real and positive solution for equation (3.15).

$$a \pm \sqrt{a^2 - 4b} \geq 0 \tag{3.20}$$

$$a^2 - 4b \geq 0 \tag{3.21}$$

As defined earlier, b is larger than zero. If a is negative or zero, equation (3.20) can not be satisfied. Thus, a must be positive. One inequality equation (3.22) is derived as the solution for the inequalities equations (3.20) and (3.21).

$$0 < \frac{2\sqrt{b}}{a} \leq 1 \tag{3.22}$$

From the deduction earlier there exists a feasible solution for a real power system if equation (3.22) is satisfied. If equation (3.22) is not satisfied or the inequality equation (3.23) is satisfied, there is no feasible solution for a real system.

$$\frac{2\sqrt{b}}{a} > 1 \tag{3.23}$$

Substituting equations (3.17) and (3.18) into $\frac{2\sqrt{b}}{a}$, a new voltage static stability index $SVSI_{ji}$ can be defined as equation (3.24) for the two-bus system in Figure 3.4.

$$SVSI_{ji} = \frac{2\sqrt{\left(X_{ji}^2 + R_{ji}^2\right)\left(P_{ji}^2 + Q_{ji}^2\right)}}{\left| |V_i|^2 - 2X_{ji}Q_{ji} - 2R_{ji}P_{ji} \right|} \tag{3.24}$$

SVSI indicated the steady state voltage stability of the line. If the *SVSI* is less than one, there are solutions for equation (3.15) and the system is stable. If the SVSI is larger than one, there is no solution for equation (3.15) and the system becomes unstable or steady state voltage collapse occurs in the system.

3.3 WEAK AND SECURE BUS IDENTIFICATION

Determination of load bus capacity is an important criterion so that the strength of a system can be determined. This phenomenon is much related to the buses strength; whether a bus will be categorized as a weak or secure bus. The classification process for weak or secure buses is normally based on voltage stability analysis. Previous research conducted by Musirin *et al.* in [28] proved that this technique is acceptable as a benchmark in identifying a weak or secure bus in a system. In this study pre-developed *SVSI* by L. Qi in [23] is utilized as an indicator for voltage stability condition. The profile of *SVSI* variation with respect to the reactive power loading gradual increment is able to demonstrate the maximum loadability of a chosen load bus. The reactive power loading, Q_d is defined as

$$Q_d = \lambda \times r \tag{3.25}$$

where λ is the loading factor and r is equal to 10 MVAr.

As the reactive power loading increases, *SVSI* values for the corresponding lines connected to the bus increase accordingly. The minimum value of maximum loadability referring to a bus will determine the weakest bus in the system and vice versa for the secure bus in the system. The *SVSI* value of 1.0 is taken to be the voltage stability limit. At this point the load flow will normally fail to converge and the system is said to have reached its instability point. This phenomenon can be demonstrated in Figure 3.5, which describes the effect of reactive power loading at a particular load bus on *SVSI* values at the corresponding connected lines. This scenario can be demonstrated for both system conditions; pre-contingencies or post-contingencies. From the figure, consider line X_1 is connected to a common load bus for a system without contingencies. As the reactive power loading at the bus increases, the *SVSI* profile for the respective line increases accordingly and line X_1 is observed to approach 0.9 value. The reactive load at this point $Q_{d_{\max 1}}$ is identified as the estimated maximum loadability of the respective bus. On the other hand, by considering contingencies occur in the system, the decrement in *SVSI* value is observed at line X_2 therefore the maximum loadability, $Q_{d_{\max 2}}$ is lower than the system without contingency.

3.3.1 Algorithm for Weak and Secure Bus Identification

Identifying maximum loadability of a particular load bus in a system involves the load flow analysis followed by the calculation of *SVSI* values using the load flow solution. This process is performed repeatedly for various loading conditions at all the participating buses. The procedures implemented to identify the maximum loadability in a system are represented in the flowchart of Figure 3.6.

The identification of maximum loadability begins with the selection of load bus to be assessed in order to initiate the initial loading condition. Load flow is performed to the system at this loading condition. Results from the load flow solution are extracted to calculate *SVSI* values for all the lines in the system. The highest *SVSI* value is extracted to indicate the voltage stability for the whole system. This value is normally the value on

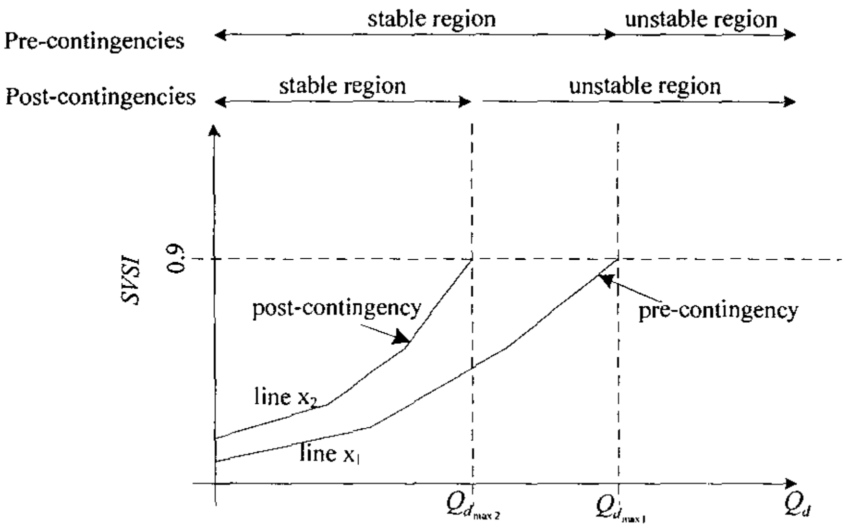

Figure 3.5: *SVSI* profiles with respect to Q_d variation during pre and post-contingency

of the corrected lines to the assessed bus. This *SVSI* value is recorded in an array to monitor its values of each load variation. The process repeats until the highest *SVSI* value is close to 0.9. The value of loading condition which gives *SVSI* close to 0.9 is termed as the maximum loadability of the load bus. At this point, the maximum loadability is denoted as Q_{max} or the maximum permissible load that can be connected to that particular bus. In order to determine the Q_{max}, or maximum loadability for the load buses, similar processes have to be performed. To rank the bus from the weak bus to secure bus, the Q_{max} for all load buses are ranked in ascending order. The bus which gives the lowest Q_{max} value is called as the weakest bus. The bus with the highest Q_{max} value is called as the most secure bus.

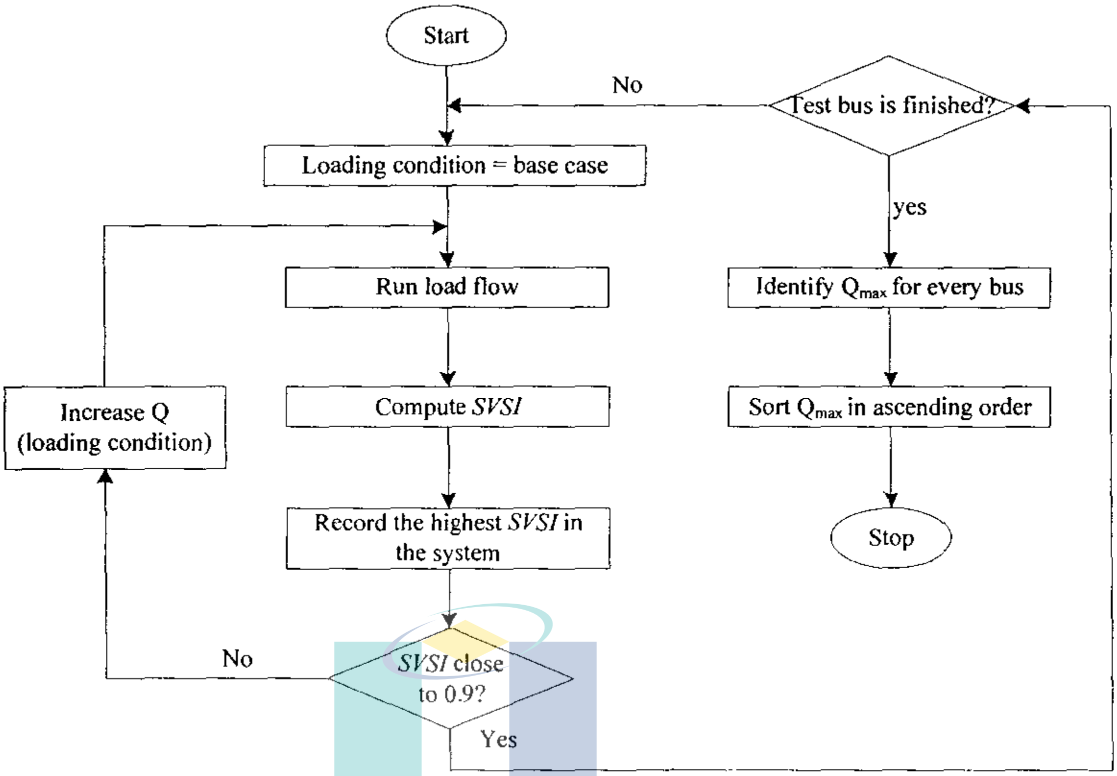

Figure 3.6: Flowchart for maximum loadability identification in power system

3.4 CONTINGENCY ANALYSIS

A power system operates in normal operating conditions if there is equilibrium between power generation and demand. In addition, the magnitude of the bus voltage in the system must be within the prescribed limit and the power system required satisfying the load flow condition. Contingencies occur in a power system due to planned or unplanned line and generator outages may lead the system to experience overloads. Under a normal circumstances, a power system may face contingency condition such as generator outage, line outage or transformer loss. These conditions would reduce the security level and cause a sudden depreciation of the power demand on the system. Contingencies caused by line and generator outages have been identified as unpredictable events that can cause failure of electric supply to the utilities. If the system is found to be insecure, then the system engineer determines the preventive controls to be applied to bring the system back into the secure zone. Preventive controls such as rescheduling of active and reactive power, re-synchronization and automatic installation of FACTS devices in the system may bring the system from this state to the normal conditions. A system operator has to analyze the effect of such contingencies so that the operator may take preventive and corrective actions in the event of the occurrences.

This contingency analysis can help in enhancing system security of the power system. By considering the line outage occurs in the system after the line between the buses is opened, this outage could bring on changes in line flows where the flow on adjacent line with the outage line will be increased as well as most of other line flows. It is also being noted that bus voltage magnitudes will also get affected after the outage occurs by reduction in voltage magnitude. In addition, other contingency such as the generator outage is also affect the line flow and bus voltages as well as line outage. All the generator loss from the generator bus outage is provided by the other generator. For that reason, to find the effects of outages, contingency analysis techniques are implemented in the system.

The generation shift factor can be used to verify the overloads when the generator is outage in the system. The generation shift factors, α_{li} is defined as [76]:

$$\alpha_{li} = \frac{\Delta f_l}{\Delta P_{Gi}} \tag{3.26}$$

where Δf_l is the change of power flow on line l when a change in generation, ΔP_{Gi} take place at the i^{th} bus in MW.

Considering an outage occurrance at the generation unit and all loss at generation (P_{Gi}^0) is assumed to be supplied by the slack bus generation. In that case, ΔP_{Gi} can be written by

$$\Delta P_{Gi} = -P_{Gi}^0 \tag{3.27}$$

The new power flow on each line is given as:

$$\hat{f}_l = f_l^0 + \alpha_{li} \Delta P_{Gi}, \qquad \text{for all lines } \forall l \tag{3.28}$$

where, $\hat{f}_l$ is the power flow on l^{th} line after the failure of ith generator and f_l^0 is the power flow on l^{th} line before the failure of pre-contingency power flow. Afterwards, the value of the line flow acquired from equation (3.28) is compared its limits and the prevention is executed if the limit is violated.

Similarly, the line outage distribution factor is used to determine the line overloads when the line outage happens in the system. The line outage distribution factor is defined as:

$$d_{li} = \frac{\Delta f_l}{f_i^0} \tag{3.29}$$

where d_{li} is the line outage distribution factor when monitoring l^{th} line after an outage of ith, Δf_l is the change in MW flow on l^{th} line and f_i^0 is the pre-contingency line flow on the ith line.

The new power flow on each line is given below.

$$\hat{f}_l = f_l^0 + d_{li} f_i^0 \tag{3.30}$$

where f_l^0 and f_i^0 are the pre-contingency or pre-outage flows on lines l and i respectively and $\hat{f}_l$ is the power flow on l^{th} line with i^{th} line out.

3.5 IDENTIFICATION OF SENSITIVE LINE AND GENERATOR CONTINGENCY ANALYSIS

Identification of sensitive line and generator is important to perform contingency analysis to a power system since the result can be used to notify the power system operators for any potential occurrence of system violation due to any contingency. In this case, multi-contingencies are considered during the optimization for the next chapter. The selections of components outages are based on the most severe generator and line in the system to maximize the performance of the system. They are normally ranked based on their severity so that the lines or generators, which give high influence to the system stability, could be identified. The objective is to identify the list or contingencies which can occur in the system that would generate violations in the system operating states. The severe generators and lines are ranked based on the *SVSI* index.

Line outage ranking analysis was conducted by executing the load flow while removing one line at a time consecutively. On the other hand, generator outage ranking analysis was conducted by removing one generator at a time followed by evaluation of *SVSI* for each line in the system. The ranking process is determined by sorting the highest *SVSI* values for each outage in descending order to rank the severity of each generator and line outage. Hence, the generator and line outage which give significant impact to the system stability can be identified with respect to a particular loading condition.

3.5.1 Algorithm for Sensitive Line used for Contingency Analysis

Once the line outages have been ranked according to their severities, the critical line outage can be identified with respect to a particular loading condition. Critical line outage is the line that may cause voltage instability condition in the system which is signified by its high *SVSI* value and be able to be used to identify the contingencies that disrupt the system stability and may lead to voltage collapse in the system [26]. This algorithm is incorporated the line outage simulation and voltage stability analysis together. For any line outage simulated which leads to non-convergence of the load flow, the proposed techniques will assign an *SVSI* value of unity for the outage. This would indicate the voltage collapse that has occurred in the system due to the outage. The line outage selections are implemented according to the following procedures:-

i. Select a load bus and the maximum loadability.

ii. Set a loading factor, λ for the load bus. (below λ_{max})

iii. Set maximum counter, μ = total line number

iv. Set a line counter ($k = 1$)

v. Read system data

vi. Remove line (k)

vii. Run Newton-Raphson load flow analysis.

viii. Calculate *SVSI* values for all remaining lines, i.e.; for line 1 to ($\mu - 1$)

ix. Reinsert the removed line (k)

x. Test counter,

if $k \geq \mu$, repeat step (v) to (ix) for $k = k + 1$.; otherwise

xi. Sort all *SVSI* in descending order for line outage (k) for 1 to μ.

xii. Ranking process will consider the most severe condition caused by line and generator outages.

xiii. Selection of line outages for the next optimization process considering multi-contingency in power transmission system for the next chapter.

The steps of the whole process can be represented in the flowchart as shown in Figure 3.7 [26].

3.5.2 Algorithm for Sensitive Generator used for Contingency Analysis

Instead of line outage contingency, contingency analysis caused by generator outage has been recognized as another issue towards voltage instability. The failure of generator caused by generator outage may interrupt system delivery and can cause the power system to become unstable. In this study, generator outages are simulated in order to identify the probability of generator outage contingencies, which can cause the system to become unstable. The results acquired from the load flow program are utilized to calculate *SVSI* values and the highest *SVSI* value is recorded. The process is repeated for all generators in the system. Hence, the *SVSI* values for each generator outage are sorting in descending order with the aim of generator outage contingency ranking. The generator outage selections are implemented according to the following procedures:-

i. Initialize system parameters

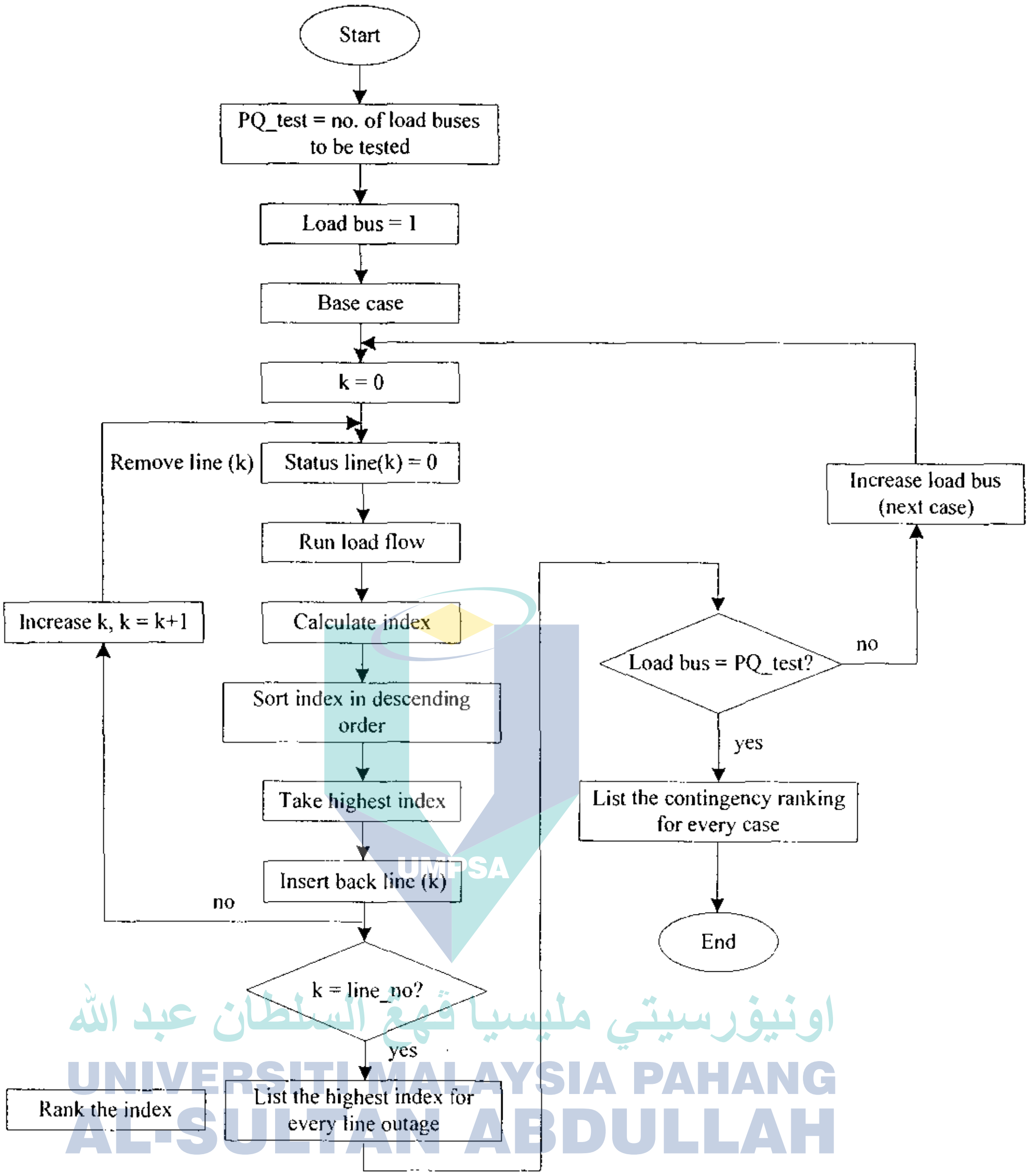

Figure 3.7: Flowchart for line outage contingency analysis

ii. Identify the generator buses in the system
iii. Set maximum counter; num = no. of generator
iv. Set counter; k=1
v. Read system data; bus data and line data
vi. Convert generator bus code to load bus code i.e. PV to PQ code
vii. Convert parameters for generator (k) = 0; this is to simulate generator outage
viii. Run load flow
ix. Compute *SVSI*
x. Identify the highest *SVSI* and the corresponding line
xi. Create highest *SVSI* array
xii. Repeat step (v) to (xi) for the nest generator until k = num
xiii. Identify the results for generator buses
xiv. Rank *SVSI* in descending order
xv. Ranking process considering the most severe condition caused by generator outage.
xvi. Selection of generator outages for the next optimization process considering multi-contingency in power transmission system for the next chapter.

The steps of the whole process can be represented in the flowchart as shown in Figure 3.8.

3.6 RESULTS AND DISCUSSION

The results are divided into three main sections. Results on weak and secure bus identifications are firstly presented. It was conducted through maximum loadability identifications using *SVSI* as the indicators. Subsequently, results on the contingency analysis caused by line outages; whilst the last section presents the results on contingency analysis caused by generator outages. The effect of line and generator outages to the voltage profile at a particular loaded bus is also monitored. The developed algorithms for line and generator outage contingency analysis and ranking have been tested on the IEEE 30-bus RTS and IEEE 118-bus RTS.

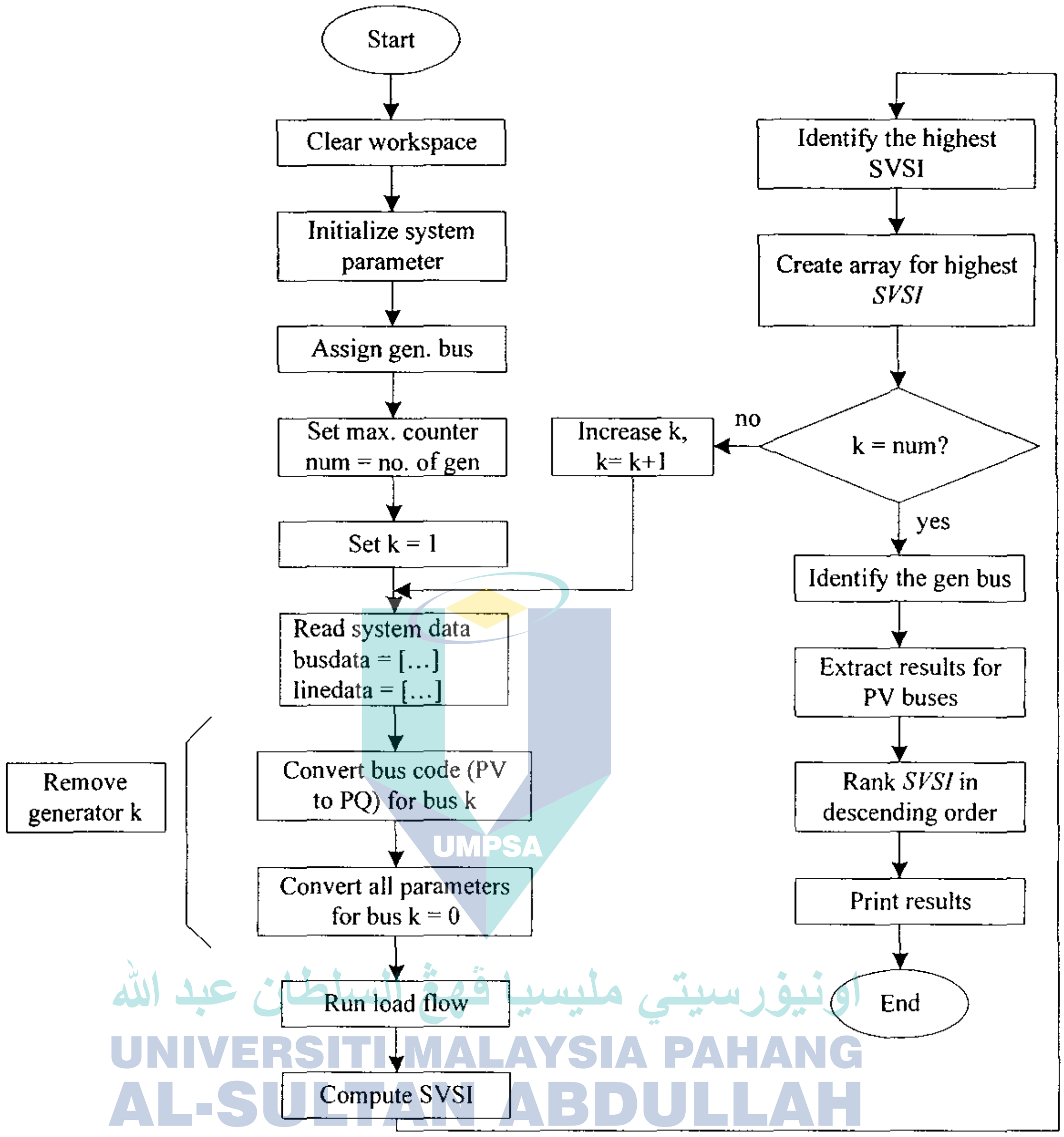

Figure 3.8: Flowchart for generator outage contingencies analysis

3.6.1 Weak and Secure Bus Identification

The determination of maximum loadability, Q_{max} is based on the maximum *SVSI* value for each load increment. Maximum loadability of a load bus is estimated by increasing the reactive power loading at the respective load bus. At the same time, the *SVSI* value is evaluated for all lines in the system. The maximum loadability was identified as the reactive power loading at which the *SVSI* value reaches 0.9. Maximum loadability of a load bus is estimated by increasing the reactive power loading at the respective load bus. The loading factor is gradually increased until the system reaches its instability point during contingency, where the maximum reactive power loading for the selected buses are identified. *SVSI* can be used to identify voltage stability weak bus and secure bus [28]. All participating buses are tested individually and the maximum loadability is extracted and sorted in ascending order.

3.6.1.1 Weak and Secure Bus Identification for IEEE 30-bus RTS

Five load buses were randomly chosen for this analysis namely buses 14, 25, 26, 29 and 30 in the IEEE 30-bus RTS. The maximum loadability for these buses are tabulated in Table 3.1. Results are recorded at the highest possible computable *SVSI* value prior to the divergence of load flow. From the table, the maximum reactive power loading at bus 26 is 3.2. This implies that the maximum loadability (Q_{max}) for bus 26 is 32 MVAr. On the other hand, the λ_{max} for bus 29 is 3.7 ; bus 25 is 7.0; bus 29 is 3.7; bus 30 is 3.5 while for bus 14, the λ_{max} value is 7. Bus 26 is ranked as the lowest indicating that it is the weakest bus since its maximum loadability is the lowest. Therefore, it can only sustain a reactive power loading up to 3.2 before voltage collapse may occur in the system. Therefore, bus 26 is selected as the test bus in the power system. From this observation, bus 30 is chosen as the second weak bus. On the other hand, bus 14 is ranked as the highest indicating as a secure bus due to large maximum loadability value. These buses are chosen for the test so as to ensure that the proposed technique works well in many cases i.e. weak and secure buses.

Table 3.1: Maximum loadability for each bus in IEEE 30-bus RTS (Base Case)

Bus No.	λ_{max}	Voltage (V)	*SVSI*	Loss (MW)
14	9.0	0.8036	0.5045	21.56
25	7.0	0.6490	0.7225	35.31
29	3.7	0.5876	0.6689	29.48
30	3.5	0.5916	0.7200	28.65
26	3.2	0.6358	0.6431	28.94

where Q = λr, r = 10 MVAr, λ is the loading factor

3.6.1.2 Weak and Secure Bus Identifications for IEEE 118-bus RTS

The maximum loadability identification was further tested in the IEEE 118-bus RTS. Three load buses were chosen for this analysis namely buses 22, 53 and 78. From Table 3.2, it is observed that the reactive power loading for bus 22 is 10, while the λ value for bus 53 and bus 78 is 14 and 100 respectively. Thus, bus 22 is ranked the highest indicating it is the weakest bus since its estimated maximum loadability is the lowest. Therefore, it can only sustain the reactive power loading up to 10 before voltage collapse occurs in the system. Then, bus 26 is selected as one of the buses in the system. Since bus 53 has λ_{max} = 14, therefore it is ranked the second in the group. In contrast, bus 78 is ranked the fifth indicating it as a secure bus with large value. Bus 22 is therefore chosen as the weak bus while bus 78 is chosen as the secure bus. In the next chapter, buses 22 and 78 are used as the test buses to perform for the study and comparisons are made for those buses in the system.

Table 3.2: Maximum loadability for each bus in IEEE 118-bus RTS (Base case)

Bus No.	λ_{max}	Voltage (V)	*SVSI*	Loss (MW)
22	10.8	0.8230	0.8539	138.2
53	14	0.8139	0.8034	140.17
20	22	0.6560	0.9402	158.51
81	79	0.8741	0.8244	139.40
78	100	0.8806	0.4382	176.44

where Q = λr, r = 10 MVAr, λ is the loading factor

3.6.2 Sensitive Line Identification

The results of line outage contingency analysis are discussed in 2 sub-sections. The first part will discuss the line outage contingency ranking for the IEEE 30-bus RTS followed by the line outage contingency ranking for the IEEE 118-bus RTS. The results will be used to select the multi-contingencies (*N-m*) consist of several line outages to be implemented into the power system with generator outage applied for the next chapter. The selections of outages are based on the most severe line in the system to maximize the performance of the system.

3.6.2.1 Line Outage Ranking for IEEE 30-bus RTS

Table 3.3 and Figure 3.9 (a) present the results for contingency analysis caused by line outages in the IEEE 30-bus RTS. The base conditions are chosen for the line outage contingency analysis to see the effect to line outage severity. The highest *SVSI* values obtained from every line outage are sorted in descending order. The result for the line outage contingency ranking given in Table 3.3 shows that line outage at line 1 is ranked the highest. The *SVSI* values for other line outages are far lower than 1.00 indicating that the system is still in its stability region. Referring to the line data of the IEEE 30-bus RTS at Appendix A, line 1 is connecting two generators namely bus 1 and bus 2. The

Table 3.3: Results for line outage contingency ranking in IEEE 30-Bus RTS (Base case)

Rank	Line Outage No.	*SVSI* (p.u)
1	1	0.5008
2	9	0.2436
3	7	0.2012
4	6	0.1995
5	8	0.1977
6	2	0.1954
7	4	0.1946
8	5	0.1935
9	15	0.1877
10	11	0.1869
11	3	0.1852
12	14	0.1768
13	18	0.1698
14	19	0.1696
15	16	0.1695
16	13	0.1694
17	22	0.1694
18	30	0.1694
19	10	0.1694
20	21	0.1694
21	30	0.1694
22	38	0.1694
23	23	0.1693
24	27	0.1693
25	32	0.1693
26	37	0.1693
27	39	0.1693
28	40	0.1693
29	20	0.1692
30	28	0.1692
31	29	0.1692
32	31	0.1692
33	33	0.1692
34	36	0.1692
35	24	0.1691
36	25	0.1691
37	35	0.1691
38	41	0.1691
39	26	0.169
40	12	0.1688
41	34	0.1683

removal of line 1 will cause the generator at bus 1 and bus 2 to be floating that can give direct impact to entire system stability.

However, outage at line 9 is ranked the second in the list because this line is connected through a transformer at bus 6. Removal of this line will cause high impact to the system stability. The high impact is normally experienced on the line connected through a transformer or close to a generator. This happens to lines 7, 6 and 8. This can be observed by the high *SVSI* value evaluated for the outages at these lines. The impact of line connecting two load buses is less severe; because practically, the outage of such line does not disturb system stability. This can be referred to line 34; where it is ranked the lowest. This is due to the fact that this line is connecting bus 25 and bus 26 which may not give significant impact when this line is experiencing outage. Three line outages are considered during the process applied for the next chapter. Therefore lines 1, 9, 7 were selected to be outage during the contingencies analysis in constrained power planning (CPP).

3.6.2.2 Line Outage Contingency Ranking for IEEE 118-bus RTS

Appendix C and Figure 3.9 (b) present the results for contingency analysis caused by line outages in the IEEE 118-bus RTS. The result for the line outage contingency ranking given in this table shows that outage at line 9 is ranked the highest. The *SVSI* values for other line outages are far lower than 1.00 indicating that the system is still in its stability region. Referring to the line data of the IEEE 118-bus RTS in Appendix B, line 9 is connecting a generator at bus 10 and a load at bus 9. The removal of line 9 will cause the generator at bus 10 to be floating that can give direct impact to entire system stability. The ranking is followed by outage at lines 7, 96, 51, 67, 66, 38, 31, 8 and 41; these are the top ten outages, which are considered to be critical. From the single diagram of IEEE 118-bus RTS given in Figure 3.2 and line data given in Appendix B, it can be seen that lines are connected either through a transformer or a generator. The high impact is normally experienced on the line connected through a transformer or

(a)

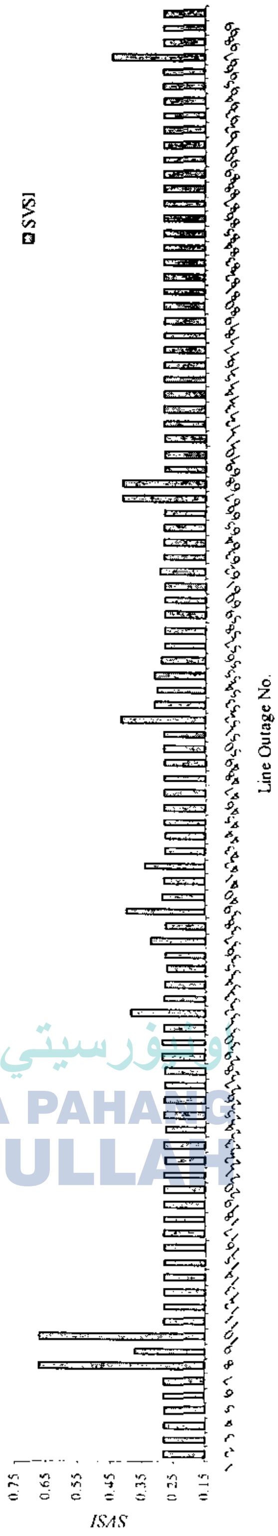

(b)

Figure 3.9 (a) Line outage contingency ranking in the IEEE 30-bus RTS

(b) Line outage contingency ranking in the IEEE 118-bus RTS close to a generator. This can be observed by the high *SVSI* value evaluated for the outages at these lines. The impact of line connecting two load buses is less severe; because practically, the outage of such line does not disturb system stability. Five line outages are considered during the process applied for the next chapter. Therefore lines 7, 9, 51, 67, 96 were selected to be outage during the contingencies analysis in constrained power planning (CPP).

3.6.3 Identification of Sensitive Generator

The results for the generator outage contingency analysis are discussed in two sub-sections. The first part will discuss the line outage contingency ranking for IEEE 30-bus RTS followed by the line outage contingency ranking for IEEE 118-bus RTS. The results will be used to select the multi-contingencies (*N-m*) consist of several generator outages to be implemented into the power system with line outage applied for the next chapter. The selections of outages are based on the most severe generator in the system to maximize the performance of the system.

3.6.3.1 Generator Outage Ranking for IEEE 30-bus RTS

The IEEE 30-bus RTS system has 6 generator buses and 24 load buses with 41 interconnected lines. In this study, all generators are removed consecutively one at a time except for generator at bus 1, since this generator is taken as the swing bus or reference bus. The maximum *SVSI* values evaluated for all load variation on every generator outage are sorted in descending order in order to identify the critical generator ranking. The results are tabulated in Table 3.4. From the table, it is observed that generator 13 is ranked the highest with *SVSI* value 0.1695 followed by generator 11 with *SVSI* value 0.1694. Referring to Appendix A, generators 13 and 11 is connecting with transformer tap changer. From the first until fourth ranked, the highest *SVSI* value was evaluated at line 5, which is connecting bus 2 to bus 5. However, when generator 5 was on outage; the highest *SVSI* value was obtained at line 15, which connects buses 4 and

12. Two generator outages are considered during the process applied for the next chapter. Therefore generator 11 and 13 were selected to be disconnected during the contingencies analysis in CPP.

Table 3.4: Generator outage rank based *SVSI* in the IEEE 30-Bus RTS (Base case)

Rank	Gen Outage No.	Line No.	*SVSI*
1	13	5	0.1695
2	11	5	0.1694
3	2	5	0.1634
4	8	5	0.1611
5	5	15	0.1463

3.6.3.2 Generator Outage Ranking for IEEE 118-bus RTS

The IEEE 118-bus RTS system has 54 generator buses and 64 load buses with 186 interconnected lines. In this study, all generators are removed consecutively one at a time except for generator at bus 69, since this generator is taken as the swing bus or reference bus. Table 3.5 tabulates the results for the generator outage ranking based on their severities most indicated by the respective *SVSI* value. It is observed that generator 12 is ranked the highest with *SVSI* value 0.2813 followed by generator 65 with *SVSI* = 0.2797, generator 49 with *SVSI* = 0.2792, generator 61 with *SVSI* = 0.2792 and generator 70 with *SVSI* = 0.2791. At the first ranking, the highest *SVSI* was obtained at line 67 which connects buses 42 and 49. Subsequently, from rank 2 until 5, the highest *SVSI* values were obtained at line 33 which connects buses 25 and 27. Five generator outages are considered during the process applied for the next chapter. Therefore generators 12, 49, 61, 65, 70 were selected to be outage during the contingencies analysis in CPP.

Table 3.5: Generator outage rank based *SVSI* in the IEEE 118-Bus RTS (Base case)

Rank	Gen Outage No.	Line No.	*SVSI*
1	12	67	0.2813
2	65	33	0.2797
3	49	33	0.2792
4	61	33	0.2792
5	70	33	0.2791

3.7 SUMMARY

The application of *SVSI* as an indicator to identify maximum loadability, weak and secure bus; and multi-contingencies component analysis have been presented in this chapter. The developed algorithms have been successfully tested on the IEEE 30-bus RTS and IEEE 118-bus RTS. Maximum loadability was identified by performing the VSA to the system. Results showed the application of maximum loadability in identifying the weak and secure bus in the system. Hence, two algorithms have been implemented separately in order to simulate the contingency analysis and ranking caused by line and generator outages. Results obtained from the studies indicated that the contingencies cause by line and generator outages listed in the top rank of the outage contingency ranking would affect the stability of a system. This information could be useful to the power system operator to perform continuous monitoring on the power system behavior and remedial action can be prepared in order to avoid insecure condition to the system.

CHAPTER 4
COMPUTATIONAL INTELLIGENCE CONSTRAINED POWER PLANNING TECHNIQUE FOR VOLTAGE STABILITY IMPROVEMENT AND LOSS MINIMIZATION CONSIDERING INSTALLATION COST

4.1 INTRODUCTION

This chapter presents a new approach for constrained power planning based on EP optimization technique considering multi-contingencies *(N-m)* that may occur in power system. The proposed technique will determine the optimum Constrained Reactive Power Control (CRPC), Constrained Active Power Scheduling (CAPS) and Constrained Hybrid Power Scheduling (CHPS) by the generators along with installation cost calculation in order to improve voltage stability condition of a system. Two objective functions were considered separately for the CPP namely improving voltage stability condition indicated by reduction in *SVSI* and transmission loss minimization (TLM) in the system. The cases are grouped into two separate objective functions. In each objective function; three cases involved namely the optimal CRPC, optimal CAPS and optimal CHPS. In the beginning, *SVSI* was taken as the fitness for determining the optimum values of reactive and/or real power for CRPC, followed by the CAPS and ending with CHPS. The optimization was then repeated for transmission loss minimization as the fitness function. A computer program was written in MATLAB and the proposed techniques were tested on the IEEE 30-bus RTS and IEEE 118-bus RTS. In this chapter, EP based optimization technique is proposed in order to determine the optimum active and/or reactive power compensation level for improving the voltage stability condition in the system. Subsequently, comparative studies are conducted by comparing the results with Artificial Immune System (AIS).

4.2 CONSTRAINED POWER PLANNING

CPP is identified as one method that can improve voltage stability condition as a result transmission losses can also be minimized. The study was first involved in determining the optimum CRPC for improving the voltage stability condition in the system along with installation cost calculation, followed by determination of the optimum CAPS. Finally, the optimum CHPS is implemented in order to improve the voltage stability condition in the system. The study will identify the best approach in terms of voltage stability improvement.

4.2.1 Problem Formulation

In constrained power planning; the objective function selected for optimization are minimization of *SVSI* hence the voltage stability is improved and minimization of transmission power losses in power system. The aim for the CPP is to optimize a certain objective subject to different sets of equality and inequality constraints. The equality constraints are the nodal power balance equations, while the inequality constraints are the limits of all control or state variables. The control variables are switchable shunt capacitor banks and real power settings in generator. The problem can be formulated as follows:

4.2.1.1 Voltage Stability Improvement as Objective Function

The concept of the voltage stability problem is demonstrated through a very simple two-bus system. The line voltage stability index derived by L. Qi [23] termed as *SVSI* is used as the fitness function. It is used to evaluate the voltage stability condition in the system. The mathematical equation for *SVSI* was formulated from a line model of two-bus system as shown in equation (3.24). The range of accepted *SVSI* values is between 0 and 1 in order to maintain stability in the system.

4.2.1.2 Transmission Loss Minimization as Objective Function

The objective function of the proposed method is to minimize the active power loss subject to a set of equality and inequality constraints in the system. Generators have maximum and minimum output powers and reactive powers which add inequality constraints. Furthermore, to maintain the quality of electrical service and system security, bus voltages usually have maximum and minimum magnitudes. These limits again require the addition of inequality constraints. This objective function is mathematically stated as follows [115];

$$\begin{aligned} \min f_p &= \sum_{k \in N_E} P_{k_{Loss}}(V,\theta) \\ &= \sum_{\substack{k \in N_E \\ k=(i,j)}} g_k\left(V_i^2 + V_j^2 - 2V_iV_j\cos\theta_{ij}\right) \end{aligned}$$

s.t. (4.1)

$$h_{Qi} = Q_{Gi} - Q_{Di} - V_i \sum_{j \in N_i} V_j\left(G_{ij}\sin\theta_{ij} - B_{ij}\cos\theta_{ij}\right) = 0, i \in N_{PQ}$$

$$V_{i\,min} \le V_i \le V_{i\,max}\ , i \in N_B$$

$$Q_{Gi\,min} \le Q_{Gi} \le Q_{Gi\,max}\ , i \in \{N_{PV}, n_s\}$$

Subject to the constraint of equality in reactive and active power balance

$$\begin{aligned} &Q_i - Q_{Gi} + Q_{Di} = 0 \\ &Q_i = Q_{Gi} - Q_{Di} - V_i \sum_{j \in N_i} V_j\left(G_{ij}\sin\theta_{ij} - B_{ij}\cos\theta_{ij}\right) = 0, \quad i \in N_{PQ} \\ &P_i - P_{Gi} + P_{Di} = 0 \\ &P_i = P_{Gi} - P_{Di} - V_i \sum_{j \in N_i} V_j\left(G_{ij}\cos\theta_{ij} - B_{ij}\sin\theta_{ij}\right) = 0, \quad i \in N_{B-1} \end{aligned} \tag{4.2}$$

Hence, inequality constraints on control variable limits; generator reactive power capability limits, generator active power capability limits, and voltage constraints are given by equation (4.3);

$$
\begin{aligned}
&Q_{Gi_{\min}} \le Q_{Gi} \le Q_{Gi_{\max}} \qquad i \in N_G \\
&Q_{ci_{\min}} \le Q_{ci} \le Q_{ci_{\max}} \qquad i \in N_c \\
&P_{Gi_{\min}} \le P_{Gi} \le P_{Gi_{\max}}, \qquad i \in Slackbus \\
&V_{i_{\min}} \le V_i \le V_{i_{\max}} \qquad i \in N_B
\end{aligned}
\tag{4.3}
$$

where, g_k is the conductance of branch k, n_s is the slack (reference) bus number; N_{PQ} is PQ bus number, N_{PV} is PV bus number, N_B is the total number of buses, N_{B-1} is the total buses excluding slack bus, N_c is the possible reactive power source installation buses number, N_E is the branch number, N_i is the numbers of buses adjacent to bus i including bus i, θ_{ij} is voltage angle different between bus i and bus j(rad), Q_i and Q_j are the reactive power on the sending and receiving buses; Q_G is the generated reactive power, V_i and V_j are the voltage magnitude at the sending and receiving buses , G_{ij} and B_{ij} is the mutual conductance and susceptance between bus i and bus j and $P_{K_{Loss}}$ is the total active power loss in the system. The equation (4.1) can be simplified to generalize objective function as:

$$
\min f_p = \sum_{k \in N_E} P_{k_{Loss}}(V, \theta) + \sum_{k \in NVPQ_{\lim}} \lambda_{Vi}\left(V_i - V_i^{\lim}\right)^2 + \sum_{k \in NQg_{\lim}} \lambda_{Qg\lim}\left(Q_{gi} + Q_{gi}^{\lim}\right)^2 \tag{4.4}
$$

s.t.

$$
Q_{Gi} - Q_{Di} - V_i \sum_{k \in N_E} V_j \left(G_{ij} \sin\theta_{ij} - B_{ij} \cos\theta_{ij}\right) = 0, \quad i \in N_{PQ} \tag{4.5}
$$

$$
P_{Gi} - P_{Di} - V_i \sum_{k \in N_E} V_j \left(G_{ij} \cos\theta_{ij} - B_{ij} \sin\theta_{ij}\right) = 0, \quad i \in N_{B-1} \tag{4.6}
$$

where λ_{Vi} and λ_{Qgi} indicate the penalty factor which can increase the optimization procedure, $N_{VPQ_{\lim}}$ is the number of PQ bus at which the voltage violates the limits and $N_{Qg_{\lim}}$ denotes the number of buses at which the reactive power generation violates the limits.

$$
V_i^{\lim} = \begin{cases} V_i^{\min} & \text{if } V_i < V_i^{\min} \\ V_i^{\max} & \text{if } V_i < V_i^{\max} \end{cases}
$$
$$
Q_{g_i}^{\lim} = \begin{cases} Q_{g_i}^{\min} & \text{if } Q_{gi} < Q_{g_i}^{\min} \\ Q_{gi}^{\max} & \text{if } Q_{gi} < Q_{gi}^{\max} \end{cases} \tag{4.7}
$$

4.2.1.3 Installations Cost

The cost of reactive power injected to the system comprises two equations. The first equation represents the total cost of energy loss as follows [115]:

$$
\begin{aligned}
W_C &= h \sum_{l \in N_l} d_l P_{loss}^l \\
&= h \sum_{l \in N_l} d_l \left[\sum_{\substack{k \in N_E \\ k=(i,j)}} g_k \left(V_i^2 + V_j^2 - 2V_i V_j \cos\theta_{ij} \right) \right]^l
\end{aligned} \tag{4.8}
$$

where h is the per unit energy cost (£/p.u.Wh, with S_B = 100 MVA), d_l is the duration of load level (h) and P_{loss}^l is the active power loss during the period of load level l.

The equation (4.9) represents the cost of reactive power source installation which consists of the fixed installation cost and the purchase cost.

$$
I_C = \sum_{l \in N_C} \left(e_i + C_{ci} |Q_{ci}| \right) \tag{4.9}
$$

where Q_{ci} is the amount of reactive power either positive (reactance) or negative (capacitance) installation, e_i is the fixed reactive power source installation cost at bus (£), C_{ci} is the per unit reactive power source purchase cost at bus i (£/p.u.VAr, S_B =100 MVA)

4.3 OPTIMIZATION TECHNIQUE USING EVOLUTIONARY PROGRAMMING

In this chapter, EP based optimization technique is proposed in order to determine the optimum active/reactive power compensation level for improving the voltage stability condition in power system. The merit of the proposed EP technique in solving power system optimization problems can be highlighted as an important contribution in voltage stability improvement technique.

4.3.1 Application of Evolutionary Programming in Constrained Power Planning

In this study, EP was used to optimize the active or/and reactive power to be scheduled by the generator buses in order to improve voltage stability condition in a power system. The optimization processes in EP evolved by applying the evolutionary programming operators such as initialization, mutation, combination and selection. The flowchart for the implementation of EP technique is shown in Figure 4.1. However, the details are described in the subsequent sections.

4.3.1.1 Initial Population Generation

The first population called the initial population of N (population size) individuals is generated and used as the parent population of the first iteration or generation. The random numbers will be assigned as the active power required to be scheduled by the generators. The size of population (N) is chosen to be 20. The population is initialized randomly. It generates parent individual, x_i within their feasible range as indicated at equation (4.6) and equation (4.7). For the system without contingency, the number of variable depends on the number of generator buses excluding slack bus. For the system with contingencies, two generator buses are selected to be outage. The number of variable depends on the number of generator buses excluding slack bus and outage generators.

The parent, x_i is;

For optimal CRPC

$$x_{im} = \lfloor Q_{g_{2i}}, Q_{g_{5i}} Q_{g_{8i}} \rfloor \text{for IEEE 30-bus RTS} \tag{4.10}$$

$$x_{im} = \lfloor Q_{g_{1i}}, Q_{g_{15i}}, Q_{g_{18i}}, Q_{g_{19i}}, Q_{g_{31i}} \rfloor \text{ for IEEE 118-bus RTS}$$

For optimal CAPS

$$x_{im} = \lfloor P_{g_{2i}}, P_{g_{5i}} P_{g_{8i}} \rfloor \text{ for IEEE 30-bus RTS} \tag{4.11}$$

$$x_{im} = \lfloor P_{g_{1i}}, P_{g_{15i}}, P_{g_{18i}}, P_{g_{19i}}, P_{g_{31i}} \rfloor \text{ for IEEE 118-bus RTS}$$

For optimal CHPS

$$x_{im} = \lfloor Q_{g_{2i}}, Q_{g_{5i}} Q_{g_{8i}}, P_{g_{2i}}, P_{g_{5i}}, P_{g_{8i}} \rfloor \text{ for IEEE 30-bus RTS} \tag{4.12}$$

$$x_{im} = \lfloor Q_{g_{1i}}, Q_{g_{15i}}, Q_{g_{18i}}, Q_{g_{19i}}, Q_{g_{31i}}, P_{g_{1i}}, P_{g_{15i}}, P_{g_{18i}}, P_{g_{19i}}, P_{g_{31i}} \rfloor \text{ for IEEE 118-bus RTS}$$

where i= 1,2,3,4,...m. The variable, m indicated the population size from a set of random distributions ranging from Q_{min} to Q_{max} or P_{min} to P_{max}. It represents the initial values of active power to be scheduled by the generator buses. The initial parent should satisfy the constraints which is the fitness function in the system.

4.3.1.2 Mutation

Mutation is a process to produce offspring. New individual (offspring) is produced by mutating the existing individual (parents). During mutation, the Gaussian mutation operator is performed to generate new population (offspring) to the selected

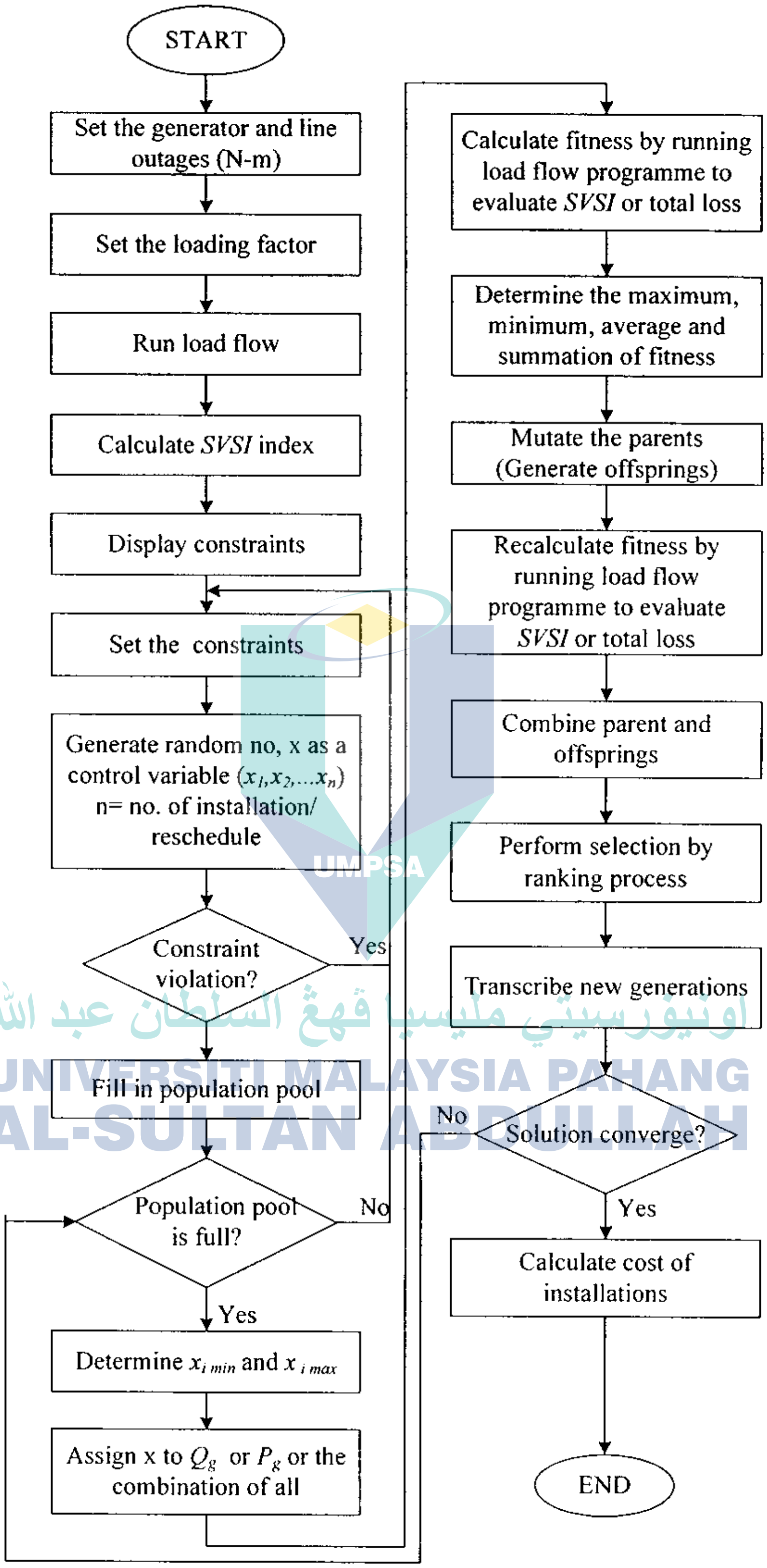

Figure 4.1: Flowchart for the CPP using EP.

individual, $x_{i,j}$ randomly by using a standard deviation, σ which is the square root of the variance. The standard deviation decides the features of offspring produced related to its parent. Let p_j' be the new individual produced from old individual p_i according to:

$$x_{i+m,j} = x_{i,j} + N\left(0, \sigma_{i,j}^2\right) \tag{4.13}$$

where $x_{i+m,j}$ and $x_{i,j}$ are the value of j^{th} element in p_j' and p_j respectively and $N\left(0, \sigma_{i,j}^2\right)$ is Gaussian random number with a mean of zero and a standard deviation of $\sigma_{i,j}$. The standard deviation decides the features of offspring produced related to its parent. The expression for $\sigma_{i,j}$ is:

$$\sigma_{i,j} = \beta\left(x_{j\max} - x_{j\min}\right)\left(\frac{f_i}{f_{\max}}\right) \tag{4.14}$$

where f_i is the fitness of individual i; f_{max} is the maximum fitness within the population, $x_{j\,max}$, $x_{j\,min}$ denote the maximum and minimum random number of variable j and β is the mutation scale ($0 < \beta < 1$). The mutation scale, β determines the convergence speed and iteration which can be manually adjusted to achieve better convergence. The larger value of β will cause slow convergence caused by large search step and vice versa [41].

4.3.1.3 Combination

It is a process which combines the parents and offsprings in cascode mode after the implementation of mutation.

4.3.1.4 Tournament Selection

The offspring produces from the mutation process are combined with the clone parent to undergo a selection process in order to identify the candidates that have the chance to be transcribed into the next generation. From all the individuals of the offspring population, the best N individuals are selected according to a selection scheme to form the parent population for the next generation. The selection technique used here is the tournament scheme. In this case, the populations of individuals with better fitness function are sorted in ascending order to imply *SVSI* minimization and loss minimization. The first half or the population would be retained as the new individuals or parent for the next generation and the others will be removed from the pool. The process is continued until a convergence is reached.

4.3.1.5 Convergence criterion

The convergence criterion is defined as the difference between the maximum and minimum fitness of the objective function. The optimal solution is achieved when there is no significant changed between the new generation and the last generation. If $fitness_{max}$ and $fitness_{min}$ represent the maximum and minimum values of the objective functions inside a given parent generation, the convergence criterion process will be achieved if:

$$SVSI_{max} - SVSI_{min} \leq 0.0001 \qquad \text{for VSI} \tag{4.15}$$

$$loss_{max} - loss_{min} \leq 0.0001 \qquad \text{for TLM} \tag{4.16}$$

If the criterion is not reached, the process will be repeated.

4.4 CONSTRAINED POWER PLANNING FOR VOLTAGE STABILITY IMPROVEMENT AND TRANSMISSION LOSS MINIMIZATION

At the beginning, the multi-contingencies (*N-m*) consist of several outages namely line outages and generator outages are implemented into the power system. The selections of outages are based on the most severe generator and line in the system to maximize the performance of the system. In IEEE 30-bus RTS system, two generator outages and three line outages are considered during the process. By referring to Table 3.3 and Table 3.4 in Chapter 3, generator buses 13, 11 and lines 1, 9, 7 were selected to be outage during the contingencies analysis in CPP. Two load buses were chosen randomly for this analysis namely buses 14 and 26. From Table 3.3, it shows that bus 26 is the weakest bus and bus 14 is the secure bus in the system. On the other hand, five generator outages and five line outages are considered during the process for IEEE 118-bus RTS system. Generator buses 12, 49, 61, 65, 70 and lines 7, 9, 51, 67, 96 were selected to be outage in this test. Two load buses were chosen for this analysis namely buses 22 and 14. From Appendix C and Table 3.5 in Chapter 3, it is observed that bus 22 is the weak bus in the system and bus 78 is the secure bus. This is based on *SVSI* value.

4.4.1 Constrained Reactive Power Control

CRPC was implemented to the system by using *SVSI* and transmission loss as the objective function. In order to improve the voltage stability condition of the test system, the variable namely the reactive powers were injected on the generator buses. In this technique, EP was used to determine the optimum reactive power to be controlled and dispatched by the chosen generator buses. Several outages namely line outages and generator outages were subjected into the system. The selections of outages are based on the most severe generator and line in the system to maximize the performance of the system. For the IEEE 30-bus RTS, two generator outages and five line outages were subjected into the system i.e., generator buses 11, 13 and lines 1, 4, 8, 9, 7. Furthermore, five generator outages and five line outages were subjected into the IEEE 118-bus RTS system, i.e., generator buses 12, 49, 61, 65, 70 and lines 7, 9, 51, 67, 96. In this optimization process, the random number represents the injected reactive power of the generator buses in the system. The number of variables depends on the number of generator buses in a system excluding the slack bus and generator outage.

For the IEEE 30- bus RTS, three variables namely x_1, x_2 and x_3 were generated to represent the reactive power to be injected to generator buses 2, 5 and 8. On the other hand, five variables namely x_1, x_2, x_3, x_4 and x_5 were generated to represent the reactive power to be dispatched by generator buses 1, 15, 19, 18 and 31 in IEEE 118-bus RTS. These variables are assigned as the reactive load (Q_d) with negative sign (or loaded negatively) representing the reactive power injected or generated at the particular generator buses. Then, the sign of active power loading was also modified to negative sign to indicate the active power to be scheduled in the system. Furthermore, the generator bus (PV bus) was modified to load bus (PQ bus) code with negatively loaded reactive power to indicate reactive power dispatch. These settings were implemented in the system data of the load flow program before being used to calculate the *SVSI* as the fitness.

Several constraints were set in order for EP to generate only a random numbers that satisfy some constraints violations. The constraints implemented during the initialization for *SVSI* as the objective function are the *SVSI* value must be less than *SVSI*_set and the bus voltage must be higher than *V_set*. As for transmission loss minimization, the constraints are the transmission loss value must be less than *loss_set* and the bus voltage limit must be higher than V_*set*. The constraints were set in such way in so that the fitness can be improved; otherwise the *SVSI*, the transmission loss and VSI may not be improved although the solution is converged. *SVSI_set* is the *SVSI* value, *loss_set* is the transmission loss value, *V_set* is the voltage at the loaded bus before the optimal CRPC is implemented. Refer to Figure 4.1, the following procedures present the implementation of EP for the optimization process:-

i. Set the multi-contingencies *(N-m)* in the system i.e. generator and line outages.
    - two generator outages and five line outages are set into the IEEE 30-bus RTS system i.e., generator buses 11, 13 and lines 1, 4, 8, 9, 7.
    - five generator outages and five line outages are set into the IEEE 118-bus RTS system, i.e., generator buses 12, 49, 61, 65, 70 and lines 7, 9, 51, 67, 96.

ii. Set the loading factor, λ.

iii. Set the CRPC constraints i.e. $SVSI \leq SVSI\_set$ and $V_m\ (bus) \leq V\_set$ for voltage stability improvement as objective function. $total\ loss \leq loss\_set$ and $V_m\ (bus) \leq V\_set$ are set for transmission loss minimization as objective function.

iv. Generate random number i.e. three random numbers namely x_1, x_2 and x_3 are generate for IEEE 30-bus system and x_1, x_2, x_3, x_4 and x_5 for 118-bus RTS system.

v. Check for constraint violations. If constraints violated, go to step iv, otherwise go to step vi.

vi. Fill in population pool. Repeat step (iv) if pool was not full, otherwise continue to step (vii).

vii. Determine *x_min* and *x_max* from the process data.

viii. Assign x_1, x_2 and x_3 to Q_{g1}, Q_{g2} and Q_{g3} in the IEEE 30-bus system data and x_1, x_2, x_3, x_4 and x_5 to Q_{g1}, Q_{g2}, Q_{g3}, Q_{g4} and Q_{g5} in the IEEE 118-bus system data.

ix. Calculate fitness by running load flow program to evaluate *SVSI* values and transmission loss values.

x. Determine *SVSI_min, SVSI_max, SVSI_avg* and *SVSI_sum* for statistical evaluation for VSI as objective function. *loss_min, loss_max, loss_avg* and *loss_sum* when TLM as objective function.

xi. Mutate the parents i.e. x_1, x_2 and x_3 for IEEE 30-bus or x_1, x_2, x_3, x_4 and x_5 for IEEE 118-bus to generate offsprings.

xii. Recalculate fitness using the offspring by running the load flow program.

xiii. Combine parents and offsprings (combination process).

xiv. Perform selection by tournament selection process from combination data.

xv. Identify and transcribe new generations.

xvi. If solution is not converged, repeat step (vii) to (xv), otherwise go to step xvii.

xvii. Calculate installation cost.

xviii. End.

4.4.2 Constrained Active Power Scheduling

CAPS was scheduled with the aim of improving the voltage stability condition of the test system by minimizing the *SVSI* value and minimizing the transmission loss in a system. Active powers were taken as the variables in order to improve stability condition in the system. For the IEEE 30- bus RTS, three variables namely x_1, x_2 and x_3 were generated to represent the active power to be scheduled for generator buses 2, 5 and 8. Five variables namely x_1, x_2, x_3, x_4 and x_5 were generated to represent the active power to be scheduled to generator buses 1, 15, 19, 18 and 31 in IEEE 118-bus RTS. In this case, similar constraints as in section 4.5.1 are required in EP optimization process. The participating parameters are the active power at generator. Once *SVSI* has been optimized, the active values are the optimized values that can be used to improve the voltage stability in the system. Refer to Figure 4.1, the following procedures indicate the development of EP program for CAPS optimization:-

i. Set the multi-contingencies *(N-m)* in the system i.e. generator and line outages.
   - two generator outages and five line outages are set into the IEEE 30-bus RTS system i.e., generator buses 11, 13 and lines 1, 4, 8, 9, 7.
   - five generator outages and five line outages are set into the IEEE 118-bus RTS system, i.e., generator buses 12, 49, 61, 65, 70 and lines 7, 9, 51, 67, 96.

ii. Set the loading factor, λ.

iii. Set the CAPS constraints i.e. $SVSI \leq SVSI\_set$ and $V_m\ (bus) \leq V\_set$ for voltage stability improvement as objective function. $total\ loss \leq loss\_set$ and $V_m\ (bus) \leq V\_set$ are set for transmission loss minimization as objective function.

iv. Generate random number i.e. three random numbers namely x_1, x_2 and x_3 are generate for IEEE 30-bus system and x_1, x_2, x_3, x_4 and x_5 for 118-bus RTS system.

v. Check for constraint violations. If constraints violated, go to step iv, otherwise go to step (vi).

vi. Fill in population pool. Repeat step (iv) if pool was not full, otherwise continue to step (vii).

vii. Determine x_min and x_max from the process data.

viii. Assign x_1, x_2 and x_3 to P_{g1}, P_{g2} and P_{g3} in the IEEE 30-bus system data and x_1, x_2, x_3, x_4 and x_5 to P_{g1}, P_{g2}, P_{g3}, P_{g4} and P_{g5} in the IEEE 118-bus system data.

ix. Calculate fitness by running load flow program to evaluate *SVSI* values and transmission loss values.

x. Determine *SVSI_min, SVSI_max, SVSI_avg* and *SVSI_sum* for statistical evaluation for VSI as objective function. *loss_min, loss_max, loss_avg* and *loss_sum* when TLM as objective function.

xi. Mutate the parents i.e. x_1, x_2 and x_3 for IEEE 30-bus or x_1, x_2, x_3, x_4 and x_5 for IEEE 118-bus to generate offsprings.

xii. Recalculate fitness using the offspring by running the load flow program.

xiii. Combine parents and offsprings (combination process).

xiv. Perform selection by tournament selection process from combination data.

xv. Identify and transcribe new generations.

xvi. If solution is not converged, repeat step (vii) to (xv), otherwise go to step (xvii).

xvii. End

4.4.3 Constrained Hybrid Power Scheduling

In the third part of the study, both CRPC and CAPS are considered and termed as hybrid in order to determine the optimized values for the injected reactive powers together with the active power scheduled for improving the voltage stability. This scheme is termed as CHPS. The voltage control variables would be the injected reactive powers and active powers. Since the IEEE 30-bus RTS and IEEE 118-bus system were chosen as the test systems, therefore the variables involve in the optimization process will be six and ten variables. For IEEE 30-bus RTS, the variables represent the three generated reactive powers and three active powers on the generator buses. On the other hand, the ten variables represent the five reactive and five active powers on the generator buses in IEEE 118-bus RTS. Refer to Figure 4.1, the following procedures indicate the development of EP program for the hybrid power scheduling optimization:-

i. Set the multi-contingencies *(N-m)* in the system i.e. generator and line outages.

- two generator outages and five line outages are set into the IEEE 30-bus RTS system i.e., generator buses 11, 13 and lines 1, 4, 8, 9, 7.

- five generator outages and five line outages are set into the IEEE 118-bus RTS system, i.e., generator buses 12, 49, 61, 65, 70 and lines 7, 9, 51, 67, 96.

ii. Set the loading factor, λ.

iii. Set the CHPS constraints i.e. $SVSI \leq SVSI\_set$ and $V_m\ (bus) \leq V\_set$ for voltage stability improvement as objective function. $total\ loss \leq loss\_set$ and $V_m\ (bus) \leq V\_set$ are set for transmission loss minimization as objective function.

iv. Generate random number i.e. six random numbers namely x_1, x_2, x_3, x_4, x_5 and x_6 are generate for IEEE 30-bus system and x_1, x_2, x_3, x_4, x_5, x_6, x_7, x_8, x_9 and x_{10} for 118-bus RTS system.

v. Check for constraint violations. If constraints violated, go to step (iv), otherwise go to step (vi).

vi. Fill in population pool. Repeat step (iv) if pool was not full, otherwise continue to step (vii).

vii. Determine x_min and x_max from the process data.

viii. Assign x_1, x_2, x_3, x_4, x_5 and x_6 to Q_{g1}, Q_{g2}, Q_{g3}, P_{g1}, P_{g2} and P_{g3} in the IEEE 30-bus system data and x_1, x_2, x_3, x_4 until x_{10} to Q_{g1}, Q_{g2}, Q_{g3}, Q_{g4}, Q_{g5}, P_{g1}, P_{g2}, P_{g3}, P_{g4} and P_{g5} in the IEEE 118-bus system data.

ix. Calculate fitness by running load flow program to evaluate *SVSI* values and transmission loss values.

x. Determine *SVSI_min*, *SVSI_max*, *SVSI_avg* and *SVSI_sum* for statistical evaluation for VSI as objective function. *loss_min*, *loss_max*, *loss_avg* and *loss_sum* when TLM as objective function.

xi. Mutate the parents i.e x_1, x_2, x_3, x_4, x_5 and x_6 for IEEE 30-bus or x_1, x_2, x_3, x_4, x_5, x_6, x_7, x_8, x_9 and x_{10} for IEEE 118-bus to generate offsprings.

xii. Recalculate fitness using the offspring by running the load flow program.

xiii. Combine parents and offsprings (combination process).

xiv. Perform selection by tournament selection process from combination data.

xv. Identify and transcribe new generations.

xvi. If solution is not converged, repeat step (vii) to (xv), otherwise go to step (xvii).

xvii. Calculate installation cost.

xviii. End.

4.5 RESULTS AND DISCUSSION

The results are divided in two sub-sections. The first part presents the results for CPP with VSI and TLM as the objective function and the second part presents the results for the comparative studies implemented between EP and AIS for both objective functions. In each objective, three procedures implemented namely the optimal CRPC, optimal CAPS and lastly optimal CHPS. Algorithms for CRPC, CAPS and CHPS engine have been developed for the implementation in the IEEE 30-bus RTS and IEEE 118-bus RTS. The optimization engine is executed with variation in loading conditions at the respective load bus so that the *SVSI*, voltage profiles, transmission loss variations and installation cost can be monitored.

4.5.1 Constrained Power Planning for Voltage Stability Improvement and Transmission Loss Minimization

The analysis was conducted at various loading conditions to see the effect to the *SVSI*, transmission loss and voltage at the loaded bus. There were two constraints assigned before the CRPC and CAPS are optimized. VSI is chosen as the first objective function with *SVSI* taken as the fitness, while the second objective function is the TLM.

4.5.1.1 Constrained Reactive Power Control

CRPC was implemented as the CPP technique in order to improve the voltage stability condition and transmission loss in a system. Similar test systems are considered for this case. The results for IEEE 30-bus RTS are tabulated in Table 4.1 and Table 4.2 while Table 4.3 and Table 4.4 tabulate the results for IEEE 118-bus RTS.

(a) Results for CRPC in the IEEE 30-bus RTS

In this study CRPC is performed to the system with bus 26 and bus 14 subjected to load variation. Table 4.1 and Table 4.2 tabulate the effect of loading factor (λ) increment to *SVSI*, transmission losses, voltage profile and installation cost for those buses. From the tables, both buses were subjected to variation of loading conditions in order to observe the effect of the implementations of CRPC.

As tabulated in Table 4.1, it is observed that all the *SVSI* values reduce as compared with pre-CRPC with respect to λ variation for both objective functions. It implies that the voltage stability has been improved. In addition, voltage profiles in the system are also improved and transmission losses are minimized as a result of the implementation of CRPC. For VSI as the objective function, it can be seen that at λ= 2.3, the *SVSI* value is improved from 0.6888 to 0.1952 while the transmission loss is reduced from 111.38 MW to 13.16 MW. In addition, the voltage has been improved from 0.5571 p.u. to 1.0053 p.u.. The cost of CRPC installation is £1,217,583.16. The results for other loading factor are indicated in the same table. The performances of the optimization technique for loss minimization as the objective function are tabulated in the same table. By referring to the results of λ = 2.3, it is observed that the *SVSI* value is reduced from 0.6888 to 0.1888. This implies improvement in voltage stability condition has been achieved. It has also reduced the transmission loss in the system from 111.38 MW to 13.06 MW and at the same time voltage profile has been improved from 0.557 p.u. to 0.977 p.u.. The cost of installation is £999,073.31.

Table 4.1: Results for CRPC when bus 26 was reactively loaded: IEEE 30-bus RTS.

	Pre-CRPC			Objective Function							
				VSI				TLM			
λ	*SVSI*	Trans. Loss (MW)	V_m (p.u)	*SVSI*	Trans. Loss (MW)	V_m (p.u)	Cost (£)	*SVSI*	Trans. Loss (MW)	V_m (p.u)	Cost (£)
1.0	0.5969	82.74	0.824	0.1933	11.34	1.116	782,159.26	0.1888	11.43	1.126	836,250.12
1.5	0.6126	87.26	0.758	0.1825	11.84	1.085	996,639.16	0.186	11.76	1.070	836,605.42
2.0	0.6409	95.94	0.667	0.1807	12.44	1.021	997,921.52	0.1807	12.44	1.021	996,045.69
2.3	0.6888	111.38	0.557	0.1952	13.16	1.005	1,217,583.16	0.2067	13.06	0.977	999,073.31

Table 4.2 tabulates the results for CRPC performed to the system with load variation at bus 14 since this bus is one of the secure buses in the system. Loading factor, λ is increased gradually in order to observe the similar properties as that for bus 26. λ was increased up to 3.5 which is its maximum loadability. The application for *SVSI* minimization and transmission losses as the objective function using EP has significantly reduced the *SVSI* values and losses as while increasing the voltage profile value at the loaded bus. It is noticed that the *SVSI* and transmission losses value decreased accordingly and the voltage profiles for post-CRPC are higher with the increment in the loading factor. This implies that with the implementation of CRPC optimization, voltage has been improved, while *SVSI* and transmission losses have been reduced indicating voltage stability improvement. As shown in the table, at loading condition of 3.5 the *SVSI* has been decreased from 0.7371 to 0.1869 for VSI and 0.1866 for TLM as the objective function. Similarly, the transmission loss has been reduced from 121.19 MW to 13.034 MW for VSI and 12.63 MW for TLM, respectively. Furthermore, the voltage profile also increased from 0.6849 p.u. to 1.0854 p.u. for VSI and 1.0378 p.u. for TLM as the objective function. The cost of installation is £1,753,849.19 and £1,198,628.18, respectively as highlighted in the table. The results for other loading factor are indicated in the same table.

Table 4.2: Results for CRPC when bus 14 was reactively loaded: IEEE 30-bus RTS.

	Pre-CRPC			Objective Function							
				VSI				TLM			
λ	*SVSI*	Trans. Loss (MW)	V_m (p.u)	*SVSI*	Trans. Loss (MW)	V_m (p.u)	Cost (£)	*SVSI*	Trans. Loss (MW)	V_m (p.u)	Cost (£)
1.0	0.5977	82.48	0.8882	0.1869	11.26	1.1691	837,483.15	0.1866	11.26	1.1689	836,038.27
1.5	0.6093	85.26	0.8631	0.1841	11.38	1.1547	996,107.94	0.1855	11.29	1.1396	836,021.49
2.0	0.6232	88.77	0.8355	0.1792	11.46	1.1242	997,168.57	0.1904	11.44	1.1081	836,216.32
2.5	0.6409	93.39	0.8043	0.1841	11.68	1.0913	996,635.90	0.1841	11.68	1.0911	995,218.72
3.0	0.6647	99.91	0.7673	0.1865	12.41	1.1116	1,533,568.44	0.1897	12.06	1.0552	997,962.74
3.5	0.7371	121.19	0.6849	0.1917	13.03	1.0854	1,753,849.19	0.2177	12.63	1.0378	1,198,628.18

The value for Q_{g2}, Q_{g5} and Q_{g8} identified by the CRPC scheme is also shown in Table 4.3. Those values are the optimized reactive power to be controlled by the generators in order to improve the voltage stability condition and transmission losses in the system.

Table 4.3: CRPC sizing when bus 26 and bus 14 was reactively loaded: IEEE 30-bus RTS

Test Bus	λ	Q_g	Sizing		
			pre-CRPC	VSI	TLM
			MVAr		
26	2.3	Q_{g2}	246.960	9.719	14.446
		Q_{g5}	30.458	6.986	1.110
		Q_{g8}	98.209	23.281	17.151
14	3.5	Q_{g2}	278.274	26.799	12.645
		Q_{g5}	30.458	4.577	11.719
		Q_{g8}	103.567	26.491	15.011

(b) Results for CRPC in the IEEE 118-bus RTS

CRPC has also been performed to the IEEE 118-bus RTS with bus 22 and bus 78 are reactively loaded. *Results* for CRPC when bus 22 is subjected to load variation are tabulated in Table 4.4. λ is gradually increased in order to observe the effect of *SVSI*, transmission losses, voltage profile and cost of installation. With the implementation of CRPC for both objective functions, all the *SVSI* values are smaller before its implementation. It implies that the voltage stability has been improved. Voltage profile in the system is also improved and transmission losses are minimized as a result of the implementation of CRPC. It can be seen that at λ = 10, the *SVSI* value is improved from 0.9819 to 0.5607 while the transmission loss is reduced from 305.3 MW to 155.18 MW resulted from VSI as the objective function. Additionally, the voltage has been improved from 0.8198 p.u. to 0.9426 p.u.. The cost of CRPC installation is £5,661,641.20. The results for other loading factor are indicated in the same table. Similar patterns can be observed when TLM as the objective function was implemented to the system. For instance, the transmission loss decreases from 305.3 MW to 158.79 MW at loading factor of 10. Subsequently, the CRPC manage to improve the *SVSI* value from 0.9819 to 0.5819 and increase the voltage at bus 22 with the increment from 0.8198 p.u. to 0.8511 p.u.. The installation cost is £5,185,169.43.

Table 4.4: Results for CRPC when bus 22 was reactively loaded: IEEE 118-bus RTS.

	Pre-CRPC			Objective Function							
				VSI				TLM			
λ	*SVSI*	Trans. Loss (MW)	V_m (p.u)	*SVSI*	Trans. Loss (MW)	V_m (p.u)	Cost (£)	*SVSI*	Trans. Loss (MW)	V_m (p.u)	Cost (£)
2	0.9741	298.46	0.9373	0.5261	154.74	0.9691	5,654,048.63	0.5261	154.74	0.9691	5,139,090.65
4	0.9753	299.37	0.911	0.5264	155.24	0.9424	5,662,054.56	0.5264	155.18	0.9426	5,145,353.17
6	0.977	300.73	0.883	0.5268	156.01	0.9142	5,151,122.87	0.5268	155.95	0.9144	5,156,254.01
8	0.9791	302.66	0.8528	0.5275	157.18	0.8839	5,163,051.56	0.5275	157.12	0.8841	5,168,140.27
10	0.9819	305.30	0.8198	0.5264	155.18	0.9426	5,661,641.20	0.5819	158.79	0.8511	5,185,169.43

Table 4.5 tabulates the effect of λ increment to *SVSI*, voltage profiles, transmission losses and installation cost for load subjected to a secure bus namely bus 78 for both objective functions. Referring to the table for both objective functions, it is observed that the same phenomenon can be observed for this case. The *SVSI* values, transmission losses and the voltage profile are improved with the reduction in *SVSI* value and transmission losses as well as improvement in voltage profile with respect to λ variation. At λ = 100, the *SVSI* value has been reduced from 0.983 to 0.5313 for both objective functions. As well as the transmission losses, it has been reduced from 343.80 MW to 198.92 MW. Furthermore, small increments are indicated for voltage profile in both

Table 4.5: Results for CRPC when bus 78 was reactively loaded: IEEE 118-bus RTS.

	Pre-CRPC			Objective Function							
				VSI				TLM			
λ	*SVSI*	Trans. Loss (MW)	V_m (p.u)	*SVSI*	Trans. Loss (MW)	V_m (p.u)	Cost (£)	*SVSI*	Trans. Loss (MW)	V_m (p.u)	Cost (£)
5	0.9734	298.10	1.0006	0.5259	154.66	1.0007	5,654,424.05	0.5259	154.66	1.0007	5,142,199.73
10	0.9734	298.37	0.995	0.5259	154.92	0.9951	5,657,116.63	0.5259	154.92	0.9951	5,144,892.31
20	0.9736	299.48	0.9837	0.526	156.00	0.9838	5,668,063.42	0.526	156.00	0.9838	5,155,839.09
30	0.974	301.39	0.972	0.5262	157.85	0.9721	5,686,881.90	0.5262	157.85	0.9721	5,174,657.56
40	0.9746	304.16	0.9601	0.5265	160.54	0.9602	5,714,184.52	0.5265	160.54	0.9602	5,201,960.18
50	0.9753	307.87	0.9478	0.527	164.13	0.9479	5,750,671.11	0.527	164.13	0.9479	5,238,446.74
100	0.983	343.80	0.8803	0.5313	198.92	0.8804	6,104,250.73	0.5313	198.92	0.8804	5,592,026.25

objective functions from 0.8803 p.u. to 0.8804 p.u., respectively. The cost of installation for VSI was £6,104,250.73 which was higher than TLM by £512,224.48. The results for other loading factor are indicated in the same table.

Table 4.6 tabulates the sizing for CRPC at all generators namely Q_{g1}, Q_{g15}, Q_{g18}, Q_{g19} and Q_{g31}. It also summarizes the sizing of all Q_g values for VSI and TLM schemes when loads subjected to buses 22 and 78. These results can be used as reference to power system operators to perform CRPC.

Table 4.6: CRPC sizing when bus 22 and bus 78 was reactively loaded: IEEE 118-bus RTS

Test Bus	λ	Q_g	Sizing		
			pre-CRPC	VSI	TLM
			MVAr		
22	10	Q_{g1}	15.489	9.237	9.246
		Q_{g15}	40.589	16.259	16.281
		Q_{g18}	38.704	42.425	42.462
		Q_{g19}	41.356	22.383	22.400
		Q_{g31}	37.694	28.373	28.497
78	100	Q_{g1}	15.516	8.756	9.237
		Q_{g15}	40.300	25.398	16.256
		Q_{g18}	38.385	31.585	42.426
		Q_{g19}	-4.916	21.471	22.384
		Q_{g31}	37.555	48.684	28.357

4.5.1.2 Constrained Active Power Scheduling

CAPS was implemented in the system as one of the CPP techniques in order to improve the voltage stability condition and transmission loss in a system. Similar test systems are considered so that comparison can later be conducted accordingly. The results for IEEE 30-bus RTS are tabulated in Table 4.7 and Table 4.8 while the results for IEEE 118-bus RTS are tabulated in Table 4.9 and Table 4.10.

(a) Results for CAPS in the IEEE 30-bus RTS

Table 4.7 tabulates the results for CAPS performed to the system with load variation subjected to bus 26. The loading factor is gradually increased until the system reaches its instability point during contingency. Increment of λ values reduces the voltage profile while increases the *SVSI* value. With the implementation of CAPS, the transmission losses are minimized while *SVSI* profiles are reduced indicating voltage stability improvement. For instance at λ= 2.3 implemented for VSI as the objective function, it is observed that the *SVSI* value is reduced from 0.6888 to 0.3306. This implies improvement in voltage stability condition. It has also reduced the transmission loss in the system from 111.38 MW to 34 MW and at the same time voltage profile has been improved from 0.5571 p.u. to 0.9546 p.u.. The active power setting that should be scheduled to generator buses 2, 5 and 8 as depicted in Table 4.9 are 39.108 MW, 1.250 MW and 41.976 MW as highlighted in the table. Similar observation for other loading factor can also be referred in the same table. A small increment are indicated for *SVSI* in TLM as the objective function where the *SVSI* value only can reduce from 0.6888 to 0.6629 as compared to VSI. However, the TLM is able to outperformed VSI in terms of transmission loss and voltage profile which able to reduce the value to 17.54 MW and 1.2096 p.u.. Similar observation for other loading factor can also be referred in the same table.

Table 4.7: Results for CAPS when bus 26 was reactively loaded: IEEE 30-bus RTS.

	Pre-CAPS			Objective Function					
				VSI			TLM		
λ	*SVSI*	Trans. Loss (MW)	V_m (p.u)	*SVSI*	Trans. Loss (MW)	V_m (p.u)	*SVSI*	Trans. Loss (MW)	V_m (p.u)
1.0	0.5969	82.74	0.8235	0.3736	37.34	1.0783	0.5849	21.44	1.263
1.5	0.6126	87.26	0.7584	0.3211	37.77	1.0175	0.6116	19.68	1.2343
2.0	0.6409	95.94	0.6671	0.3259	38.88	0.9425	0.6337	18.18	1.2175
2.3	0.6888	111.38	0.5571	0.3306	34.00	0.9546	0.6629	17.54	1.2096

Table 4.8 tabulates the results for CAPS performed to the system with load variation at secure bus namely bus 14. For instance, at $\lambda = 3.5$ taking VSI as the objective function, it is observed that the *SVSI* value is reduced from 0.7371 to 0.2843 which implies a significant voltage stability improvement. Transmission loss has been reduced from 121.19 MW to 31.35 MW, while voltage has been improved from 0.6849 p.u. to 1.013 p.u.. Similar observation for other λ values can be referred to the same table.

As for the TLM as objective function; at $\lambda = 3.5$, *SVSI* value is reduced from 0.7371 to 0.5732 while the transmission loss is reduced from 111.38 MW to 16.01 MW. Voltage profile has been improved from 0.6849 p.u. to 1.2445 p.u..

Table 4.8: Results for CAPS when bus 14 was reactively loaded: IEEE 30-bus RTS.

	Pre-CAPS			Objective Function					
				VSI			TLM		
λ	*SVSI*	Trans. Loss (MW)	V_m (p.u)	*SVSI*	Trans. Loss (MW)	V_m (p.u)	*SVSI*	Trans. Loss (MW)	V_m (p.u)
1.0	0.5977	82.48	0.8882	0.3717	37.23	1.1149	0.5797	21.32	1.2881
1.5	0.6093	85.26	0.8631	0.3204	37.32	1.0832	0.6088	19.43	1.2847
2.0	0.6232	88.77	0.8355	0.323	37.64	1.0479	0.6084	18.06	1.2793
2.5	0.6409	93.39	0.8043	0.3288	32.56	1.0644	0.616	16.92	1.2735
3.0	0.6647	99.91	0.7673	0.2912	32.91	1.0269	0.5943	16.34	1.2591
3.5	0.7371	121.19	0.6849	0.2843	31.35	1.013	0.5732	16.01	1.2445

The values for P_{g2}, P_{g5} and P_{g8} for both buses identified by the CAPS technique are tabulated in Table 4.9 are the optimized active power to be scheduled by the generators in order to improve the voltage stability condition and transmission losses in the system.

Table 4.9: CAPS sizing when bus 26 and bus 14was reactively loaded: IEEE 30-bus RTS

Test Bus	λ	P_g	Sizing		
			pre-CAPS	VSI	TLM
			MW		
26	2.3	P_{g2}	40.000	39.108	50.350
		P_{g5}	0.000	1.250	95.581
		P_{g8}	0.000	41.976	75.081
14	3.5	P_{g2}	40.000	34.331	59.242
		P_{g5}	0.000	18.903	93.055
		P_{g8}	0.000	32.426	84.702

(b) Results for CAPS in the IEEE 118-bus RTS

CAPS has also been performed on the IEEE 118-bus RTS with bus 22 and bus 78 are reactively loaded. Results for bus 22 are tabulated in Table 4.10 with load variation subjected to this bus. λ is increased gradually in order to observe the effect of *SVSI*, transmission losses, voltage profile and cost of installation. With the implementation of CAPS for both objective functions, all the *SVSI* values are lower which implies voltage stability improvement. This process has improved the voltage profile and minimized the transmission losses. For instance at $\lambda = 10$, the *SVSI* value is improved from 0.9819 to 0.6481 while the transmission loss is reduced from 305.3 MW to 186.95 MW resulted from VSI as the objective function. Furthermore, the voltage has been improved from 0.8198 p.u. to 0.8546 p.u.. This phenomenon indicates a significant voltage stability improvement. Results for other loading factor are indicated in the same table. Similar observations are experienced in the system with TLM as the objective function.

Table 4.10: Results for CAPS when bus 22 was reactively loaded: IEEE 118-bus RTS.

	Pre-CAPS			Objective Function					
				VSI			TLM		
λ	*SVSI*	Trans. Loss (MW)	V_m (p.u)	*SVSI*	Trans. Loss (MW)	V_m (p.u)	*SVSI*	Trans. Loss (MW)	V_m (p.u)
2	0.9741	298.46	0.9373	0.6478	183.43	0.9716	0.5261	154.74	0.9722
4	0.9753	299.37	0.911	0.6456	183.36	0.9458	0.5264	155.18	0.9458
6	0.977	300.73	0.883	0.6462	184.10	0.9177	0.5268	155.95	0.9177
8	0.9791	302.66	0.8528	0.647	185.25	0.8875	0.5275	157.12	0.8875
10	0.9819	305.30	0.8198	0.6481	186.95	0.8546	0.5819	158.79	0.8546

Table 4.11 tabulates the effect of λ increment to *SVSI*, voltage profiles and transmission losses for load subjected to bus 78 for both objective functions. From the table, it is observed that the same phenomenon can be observed for this case. The *SVSI* value, transmission losses and the voltage profile are improved with the reduction in *SVSI* and transmission losses as well as improvement in voltage profile with respect to λ variation. At λ = 100, the *SVSI* has been reduced from 0.983 to 0.5313 for both objective functions. As well as the transmission losses, it has been reduced from 343.80 MW to 164.13MW. Furthermore, a small increment is indicated for voltage profile in both objective functions from 0.8803 p.u. to 0.8804 p.u., respectively. The results for other loading factor are indicated in the same table.

Table 4.11: Results for CAPS when bus 78 was reactively loaded: IEEE 118-bus RTS.

	Pre-CAPS			Objective Function					
				VSI			TLM		
λ	*SVSI*	Trans. Loss (MW)	V_m (p.u)	*SVSI*	Trans. Loss (MW)	V_m (p.u)	*SVSI*	Trans. Loss (MW)	V_m (p.u)
5	0.9734	298.10	1.0006	0.645	182.94	1.0006	0.6449	182.91	1.0006
10	0.9734	298.37	0.995	0.6451	183.20	0.9951	0.645	183.17	0.9951
20	0.9736	299.48	0.9837	0.6452	184.29	0.9837	0.6451	184.26	0.9837
30	0.974	301.39	0.972	0.6454	186.16	0.9721	0.6453	186.13	0.9721
40	0.9746	304.16	0.9601	0.6458	188.87	0.9602	0.6457	188.84	0.9602
50	0.9753	307.87	0.9478	0.6463	192.50	0.9479	0.6462	192.47	0.9479
100	0.983	343.80	0.8803	0.6513	227.64	0.8804	0.6512	227.62	0.8804

The results for CAPS sizing at the maximum λ value for both buses are tabulated in Table 4.12. As in Table 4.12, it can be seen that the values for P_{g1}, P_{g15}, P_{g18}, P_{g19} and P_{g31} are the optimized active power values to be scheduled at generator buses 1, 15, 18, 19 and 31 determined by the EP in order to improve the voltage stability condition and transmission losses when reactive load is subjected to bus 22 and bus 78.

Table 4.12: CAPS sizing when bus 22 and bus 78 was reactively loaded: IEEE 118-bus RTS

Test Bus	λ	P_g	Sizing		
			pre-CAPS	VSI	TLM
			MW		
22	10	P_{g1}	0.000	98.708	98.727
		P_{g15}	0.000	29.623	29.642
		P_{g18}	0.000	85.257	85.276
		P_{g19}	0.000	95.468	95.487
		P_{g31}	0.000	57.946	57.967
78	100	P_{g1}	0.000	98.708	98.727
		P_{g15}	0.000	29.623	29.642
		P_{g18}	0.000	85.257	85.276
		P_{g19}	0.000	95.468	95.487
		P_{g31}	0.000	57.946	57.967

4.5.1.3 Constrained Hybrid Power Scheduling

This scheme was implemented to the system to assess the same properties i.e. voltage stability, voltage profile, transmission loss and cost of the installation. EP optimizing technique was used to determine the optimal reactive power to be dispatched and optimal active power to be scheduled by the generators. Similar test bus and loading condition as previous test were used to access the proposed technique. Results for IEEE 30-bus RTS are tabulated in Table 4.13, Table 4.14 and Table 4.15 while the results for IEEE 118-bus RTS are tabulated in Table 4.16, Table 4.17 and Table 4.18.

(a) Results for CHPS in the IEEE 30-bus RTS

This scheme has been implemented in the IEEE 30-bus RTS with similar test buses i.e. the bus 26 and bus 14 are reactively loaded. Results are tabulated in Table 4.13, Table 4.14 and Table 4.15. From Table 4.13, it is observed that all the *SVSI* values are decreased accordingly with the increment of λ for both objective functions. It implies that the voltage stability has been improved. Additionally, voltage profiles in the system are also improved and transmission losses are minimized after the implementation of HPS. For VSI as the objective function, it can be seen that at λ = 2.3, the *SVSI* value is improved from 0.6888 to 0.1876 while the transmission loss is reduced from 111.38 MW to 8.90 MW. This has also improved the voltage from 0.5571 p.u. to 1.0257 p.u.. The cost for the CHPS scheme is £1,250,940.83. Results for other λ values are indicated in the same table. The performances of the optimization technique for loss minimization as the objective function are indicated in the same table. For instance, at λ = 2.3, it is observed that the *SVSI* value is reduced from 0.6888 to 0.1877 which implies a significant voltage stability condition improvement. It has also reduced the transmission loss in the system from 111.38 MW to 8.89 MW and at the same time voltage profile has been improved from 0.5571 p.u. to 1.0255 p.u.. The cost of installation is £1,249,494.30.

Table 4.14 tabulates the results for CHPS performed to the system with load variation subjected to bus 14. Effect of λ increment to *SVSI* value, voltage profile and transmission losses are also assessed. λ was increased up to 3.5 for this purpose. Its significant reduction in *SVSI* value and transmission losses have been experienced by the

Table 4.13: Results for CHPS when bus 26 was reactively loaded: IEEE 30-bus RTS.

	Pre-CRPC			Objective Function							
				VSI				TLM			
λ	*SVSI*	Trans. Loss (MW)	V_m (p.u)	*SVSI*	Trans. Loss (MW)	V_m (p.u)	Cost (£)	*SVSI*	Trans. Loss (MW)	V_m (p.u)	Cost (£)
1.0	0.5969	82.74	0.8235	0.1793	10.07	1.0715	994,758.39	0.2859	8.32	1.173	1,248,909.40
1.5	0.6126	87.26	0.7584	0.1593	11.72	1.0098	1,215,501.18	0.2483	8.31	1.1222	1,248,829.40
2.0	0.6409	95.94	0.6671	0.1788	12.03	0.9851	1,519,784.00	0.2089	8.56	1.0647	1,249,185.87
2.3	0.6888	111.38	0.5571	0.1876	8.90	1.0257	1,250,940.83	0.1877	8.89	1.0255	1,249,494.30

system at all λ values. This happens to both objective functions. Voltage level for each λ value has also been improved in both objective functions. For instance, at $\lambda = 3.5$ the *SVSI* value is reduced from 0.7371 to 0.1616 for VSI and 0.1615 for TLM as the objective function. Transmission loss has been reduced from 121.19 MW to 7.87 MW for VSI and 7.86 MW for TLM, respectively. Voltage has been increased from 0.6849 p.u. to 1.0642 p.u. for VSI and 1.0642 p.u. when TLM as the objective function. The cost of installation is £1,249,070.88 and £1,248,421.62, respectively. These results indicate a significant benefit to the power system operators if any remedial action is to be taken to improve systems performance.

Table 4.14: Results for CHPS when bus 14 was reactively loaded: IEEE 30-bus RTS.

	Pre-CRPC			Objective Function							
				VSI				TLM			
λ	*SVSI*	Trans. Loss (MW)	V_m (p.u)	*SVSI*	Trans. Loss (MW)	V_m (p.u)	Cost (£)	*SVSI*	Trans. Loss (MW)	V_m (p.u)	Cost (£)
1.0	0.5977	82.48	0.8882	0.178	9.83	1.1171	994,486.84	0.283	8.15	1.212	1,248,724.23
1.5	0.6093	85.26	0.8631	0.1598	9.76	1.0872	994,770.28	0.2489	7.91	1.1861	1,248,400.64
2.0	0.6232	88.77	0.8355	0.1457	11.22	1.0542	1,216,364.40	0.2152	7.75	1.1587	1,248,222.78
2.5	0.6409	93.39	0.8043	0.1504	11.48	1.0178	1,216,374.03	0.1817	7.67	1.1295	1,248,260.07
3.0	0.6647	99.91	0.7673	0.1561	11.96	0.9767	1,217,155.68	0.159	7.70	1.0982	1,248,187.07
3.5	0.7371	121.19	0.6849	0.1616	7.87	1.0642	1,249,070.88	0.1615	7.86	1.0642	1,248,421.62

Table 4.15 tabulates the values for Q_{g2}, Q_{g5}, Q_{g8}, P_{g1}, P_{g5}, and P_{g8} identified by the CHPS for voltage stability improvement and transmission loss minimization to the system.

Table 4.15: CHPS sizing when bus 26 and bus 14 was reactively loaded: IEEE 30-bus RTS

Test Bus	λ	Q_g /P_g	Sizing		
			pre	VSI	TLM
			MVAr/MW		
26	2.3	Q_{g2}	246.960	5.969	5.952
		Q_{g5}	30.458	9.547	9.531
		Q_{g8}	98.209	25.744	25.729
		P_{g2}	40.000	97.715	97.662
		P_{g5}	0.000	79.658	79.627
		P_{g8}	0.000	69.903	69.859
14	3.5	Q_{g2}	278.274	5.960	5.953
		Q_{g5}	30.458	9.541	9.532
		Q_{g8}	103.567	25.741	25.730
		P_{g2}	40.000	97.690	97.666
		P_{g5}	0.000	79.619	79.629
		P_{g8}	0.000	69.884	69.862

(b) Results for CHPS in the IEEE 118-bus RTS

The test was also conducted to the IEEE 118-bus RTS with bus 22 and bus 78 subjected reactively loaded. The results for bus 22 are tabulated in Table 4.16. Similar properties are to be assessed in this case. With the implementation of CHPS for both objective functions, all the *SVSI* values at all λ values are lower as compared to the pre-CHPS. Voltage profile in the system is also improved and transmission losses are minimized through this implementation. It can be seen that at λ = 10, the *SVSI* value is improved from 0.9819 to 0.5607 while the transmission loss is reduced from 305.3 MW to 164.76 MW resulted from VSI as the objective function. Additionally, the voltage has been improved from 0.8198 p.u. to 0.6542 p.u.. The cost of CHPS installation is £10,785,469.32. The results for other λ values are indicated in the same table. Same scenario can be observed when TLM as the objective function. The transmission loss is reduced from 305.3 MW to 192.11 MW as shown in the table. *SVSI* is reduced from

Table 4.16: Results for CHPS when bus 22 was reactively loaded: IEEE 118-bus RTS.

	Pre-CRPC			Objective Function							
				VSI				TLM			
λ	*SVSI*	Trans. Loss (MW)	V_m (p.u)	*SVSI*	Trans. Loss (MW)	V_m (p.u)	Cost (£)	*SVSI*	Trans. Loss (MW)	V_m (p.u)	Cost (£)
2	0.9741	298.46	0.9373	0.6477	187.36	0.9619	10,736,455.86	0.6476	187.34	0.9619	10,738,058.76
4	0.9753	299.37	0.911	0.6482	187.91	0.9352	742,024.97	0.6481	187.89	0.9352	10,743,626.51
6	0.977	300.73	0.883	0.6489	188.82	0.9066	10,751,329.05	0.6488	188.80	0.9066	10,752,928.90
8	0.9791	302.66	0.8528	0.6498	190.19	0.8759	10,765,219.24	0.6497	190.17	0.8759	10,766,816.97
10	0.9819	305.30	0.8198	0.6542	192.13	0.8424	10,785,469.32	0.6541	192.11	0.8424	10,786,527.69

0.9819 to 0.6541 and voltage at bus 22 has been increased from 0.8198 p.u. to 0.8424 p.u.. The installation cost is £10,786,527.69 as highlighted in the table.

Table 4.17 tabulates the effect of λ increment to *SVSI*, voltage profiles, transmission losses and installation cost for load subjected to bus 78 for both objective functions. At λ = 100, the *SVSI* value is improved from 0.983 to 0.6537 for VSI and 0.6536 for TLM as the objective function. Transmission loss has been reduced from 343.80 MW to 231.93 MW for VSI and 231.91 MW for TLM. A small increment is indicated for voltage profile in both objective functions from 0.8803 p.u. to 0.8804 p.u., respectively. The cost of installation for VSI is £11,189,420.39 and £11,191,021.29 for TLM as highlighted in the table. The results for other loading factor are indicated in the same table.

Table 4.17: Results for CHPS when bus 78 was reactively loaded: IEEE 118-bus RTS.

	Pre-CRPC			Objective Function							
				VSI				TLM			
λ	*SVSI*	Trans. Loss (MW)	V_m (p.u)	*SVSI*	Trans. Loss (MW)	V_m (p.u)	Cost (£)	*SVSI*	Trans. Loss (MW)	V_m (p.u)	Cost (£)
5	0.9734	298.10	1.0006	0.6474	187.22	1.0006	10,735,015.96	0.6474	187.20	1.0006	10,736,619.70
10	0.9734	298.37	0.995	0.6432	183.75	0.9951	4,901,862.81	0.6474	187.46	0.9951	10,739,331.06
20	0.9736	299.48	0.9837	0.6475	187.48	0.9951	10,737,727.33	0.6475	188.55	0.9837	10,750,374.11
30	0.974	301.39	0.972	0.6478	190.44	0.9721	10,767,768.36	0.6477	190.42	0.9721	10,769,371.92
40	0.9746	304.16	0.9601	0.6482	193.15	0.9602	10,795,340.04	0.6481	193.13	0.9602	10,796,943.44
50	0.9753	307.87	0.9478	0.6487	196.78	0.9479	10,832,192.76	0.6486	196.76	0.9479	10,833,795.93
100	0.983	343.80	0.8803	0.6537	231.93	0.8804	11,189,420.39	0.6536	231.91	0.8804	11,191,021.29

As tabulated in Table 4.18, the values for Q_{g2}, Q_{g15}, Q_{g18}, Q_{g19}, Q_{g31}, P_{g2}, P_{g15}, P_{g18}, P_{g19} and P_{g31} are the optimized reactive and active powers need to be injected and scheduled to generator in order to improve the voltage stability condition and transmission losses in the system.

Table 4.18: CHPS sizing when bus 22 and bus 78 was reactively loaded: IEEE 118-bus RTS

Test Bus	λ	Location	Sizing		
			pre	VSI	TLM
			MVAr/MW		
22	10	Q_{g1}	15.489	9.853	9.858
		Q_{g15}	40.589	20.975	20.980
		Q_{g18}	38.704	41.402	41.410
		Q_{g19}	41.356	11.102	11.105
		Q_{g31}	37.694	210.938	210.960
		P_{g1}	0.000	98.706	98.727
		P_{g15}	0.000	29.615	29.642
		P_{g18}	0.000	85.264	85.276
		P_{g19}	0.000	95.482	95.487
		P_{g31}	0.000	57.936	57.967
78	100	Q_{g1}	15.516	9.856	9.858
		Q_{g15}	40.300	20.977	20.980
		Q_{g18}	38.385	41.404	41.410
		Q_{g19}	-4.916	11.101	11.105
		Q_{g31}	37.555	210.915	210.960
		P_{g1}	0.000	98.703	98.727
		P_{g15}	0.000	29.627	29.642
		P_{g18}	0.000	85.270	85.276
		P_{g19}	0.000	95.478	95.487
		P_{g31}	0.000	57.944	57.967

4.5.2 Comparative Studies of Constrained Power Planning between Evolutionary Programming and Artificial Immune System

A comparative study is performed by implementing similar studies using AIS. The comparisons are made in terms of *SVSI*, transmission loss, voltage profile and installation cost.

4.5.2.1 Constrained Reactive Power Control

The results obtained from the implementation of CRPC for each objective function are compared between EP and AIS for each participating bus. The comparisons are made in terms of voltage stability improvement, transmission loss reduction, voltage profile and cost of installation.

(a) Results for CRPC in the IEEE 30-bus RTS

The result for CRPC performed at all selected load buses using EP and AIS are tabulated in Table 4.19 and Table 4.20. Table 4.19 tabulates the results of comparative studies using EP and AIS for VSI and TLM as the objective functions when bus 26 was loaded. From the table, it is observed that when EP was used to optimize the CRPC, it gives better results as compared to AIS in terms of *SVSI* value and installation cost. The comparison was made in terms of VSI where EP technique successfully reduces the *SVSI* value from 0.6888 to 0.1952 as compared to 0.4758 performed using AIS which indicates that EP gives better results than AIS. However, it is observed that EP and AIS method managed to improve the same amount of transmission loss in the system from 111.38 MW to 13.06 MW. As for the voltage profile, when AIS was used to optimize the CRPC, it gives better results as compared to EP. AIS has improved the voltage profile from 0.5571 p.u. to 1.1268 p.u. but for the EP, voltage profile is only increased to 1.0053 p.u.. In contrast, an installation cost of £1,217,583.16 will be required to perform the reactive power support scheme optimized by EP while AIS gives £3,163,592.67. Similar patterns are observed when TLM as the objective function except for the transmission loss. EP has improved the transmission loss from 111.38 MW to 13.06 MW while AIS only manage to reduce to 18.32 MW.

Table 4.19: Comparison results for CRPC between EP and AIS when bus 26 was loaded: IEEE 30-bus RTS.

Criteria	Pre-CRPC	Post-CRPC at $\lambda = 2.3$			
		EP		AIS	
		VSI	TLM	VSI	TLM
SVSI	0.6888	0.1952	0.2067	0.4758	0.4758
Trans. loss (MW)	111.38	13.16	13.06	13.16	18.32
Voltage (p.u.)	0.5571	1.0053	0.9766	1.1268	1.1268
Cost of Installation (£)		1, 217,583.16	999,073.31	3,163,592.67	3,163,592.67

Table 4.20 tabulates the comparison results of CRPC using EP and AIS for both objective functions for bus 14 in the IEEE 30-bus system. Firstly, the comparison was made in terms of VSI. From the table, it shows that EP has outperformed AIS in all criteria except the voltage profile. It shows that EP is better than AIS since EP managed to reduce *SVSI* value and the largest transmission loss reduction in the system. For instance, at λ= 3.5, EP method has reduced the transmission loss from 121.19 MW to 13.03 MW while AIS managed to reduce the transmission loss value to 16.77 MW. In contrast, AIS outperformed EP in terms of voltage profile with the increment from 0.6849 p.u. to 1.1651 p.u. as compared to EP which is only able to increase the voltage up to 1.0854 p.u.. On the other hand, the installation cost of CRPC required using EP technique is £1,753,849.19 which is lower as compared to AIS. The installation cost for AIS is £3,161,827.97. Secondly, similar patterns are observed when TLM as the objective function. It is observed that, EP outperformed AIS in terms of *SVSI* reduction, transmission loss reduction and cost of installation except voltage profile. This reveals the strength of EP as compared to AIS.

Table 4.20: Comparison results for CRPC between EP and AIS when bus 14 was loaded: IEEE 30-bus RTS.

Criteria	Pre-CRPC	Post-CRPC at λ= 3.5			
		EP		AIS	
		VSI	TLM	VSI	TLM
SVSI	0.7371	0.1917	0.2177	0.388	0.388
Trans. loss (MW)	121.19	13.03	12.63	16.77	16.77
Voltage (p.u.)	0.6849	1.0854	1.0378	1.1651	1.1651
Cost of Installation (£)		1,753,849.19	1,198,628.18	3,161,827.97	3,161,852.43

(b) Results for CRPC in the IEEE 118-bus RTS

The result for CRPC performed at all selected load buses using EP and AIS are tabulated in Table 4.21 and Table 4.22. Table 4.21 tabulate the results of comparative studies using EP and AIS for VSI and TLM as the objective functions at bus 22 when λ =10 From the table, EP managed to reduce *SVSI* value and improved voltage profile value as compared to AIS for both objective function. This reveals the strength of EP in improving voltage stability condition. In addition, EP also reduces the transmission losses as compared to AIS. On the other hand, AIS outperformed EP in terms of installation cost when the VSI is taken as the objective function.

Table 4.21: Comparison results for CRPC between EP and AIS when bus 22 was loaded: IEEE 118-bus RTS.

Criteria	Pre-CRPC	Post-CRPC at λ = 10			
		EP		AIS	
		VSI	TLM	VSI	TLM
SVSI	0.9819	0.5264	0.5819	0.6459	0.5856
Trans. loss (MW)	305.30	155.18	158.79	160.08	168.35
Voltage (p.u.)	0.8198	0.9426	0.8511	0.8433	0.8505
Cost of Installation (£)		5,661,641.2	5,185,169.43	4,619,436.58	12,297,457.12

Table 4.22 tabulates the results of comparative studies using EP and AIS for VSI and TLM as the objective functions when bus 78 was loaded. From the table, it is observed that when EP was used to optimize the CRPC, it gives better results as compared to AIS in terms of *SVSI* value, transmission loss and installation cost. In terms of VSI, EP technique successfully reduces the *SVSI* value from 0.983 to 0.5313 as compared to 0.5351 performed using AIS which indicates that the voltage stability improvement is better. As for the transmission loss reduction, EP also gives better results as compared to AIS. EP has improved the transmission loss from 343.80 MW to 198.92 MW but for the AIS, transmission loss is only reduced to 208.40 MW. However, it is observed that EP and AIS method managed to improve the same amount of voltage profile in the system from 0.8803 p.u. to 0.8804 p.u., respectively. In contrast, an installation cost equal to

Table 4.22: Comparison results for CRPC between EP and AIS when bus 78 was loaded: IEEE 118-bus RTS.

Criteria	Pre-CRPC	Post-CRPC at $\lambda = 100$			
		EP		AIS	
		VSI	TLM	VSI	TLM
SVSI	0.983	0.5313	0.5313	0.5351	0.5351
Trans. loss (MW)	343.80	198.92	198.92	208.40	208.40
Voltage (p.u.)	0.8803	0.8804	0.8804	0.8804	0.8804
Cost of Installation (£)		6,104,250.73	5,592,026.25	12,704,443.4	12,704,652.84

£6,104,250.73 is obtained by EP, while AIS gives £12,704,443.4 which is higher while the reduction of transmission losses is lower than EP. Similar patterns are observed when TLM as the objective function except for the cost of installation.

4.5.2.2 Constrained Active Power Scheduling

The results obtained from the implementation of CAPS for each objective function are compared between EP and AIS for each participating bus. The comparisons are made in terms of voltage stability improvement, transmission loss reduction, voltage profile and cost of installation.

(a) Results for CAPS in the IEEE 30-bus RTS

The comparisons are made in terms of *SVSI* minimization, transmission loss minimization, voltage profile improvement and cost of installation. The results for comparative studies when load was subjected to bus 26 are tabulated in Table 4.23. From the tables, it is observed that when EP was used to optimize the CAPS, it gives better results as compared to AIS in terms of *SVSI* value. For instance, at $\lambda = 2.3$, with the implementation of VSI as the objective function, EP method managed to reduce the *SVSI* value from 0.6888 to 0.3306, while AIS only managed to reduce *SVSI* value to 0.6863. On the other hand, AIS outperformed EP in terms of transmission loss and voltage profile. It has decreased the transmission loss in the system from 111.37 MW to

17.58 MW, while it is 34 MW given by EP. Furthermore, the voltages for both optimization techniques increased from 0.5571 p.u. to 0.9546 p.u. using EP and 1.2178 p.u. using AIS. It reveals that AIS outperformed EP indicated by bigger voltage profile at the selected loading condition. For the TLM as the objective function, it is observed that the results given by EP are better than AIS in terms of transmission loss and voltage profile however not for *SVSI* value. This revealed the merit of EP as compared to AIS optimization technique.

Table 4.23: Comparison results for CAPS between EP and AIS when bus 26 was loaded: IEEE 30-bus RTS.

Criteria	Pr- CAPS	Post-CAPS at $\lambda = 2.3$			
		EP		AIS	
		VSI	TLM	VSI	TLM
SVSI	0.6888	0.3306	0.6629	0.6863	0.2477
Trans. loss (MW)	111.38	34.00	17.54	17.58	40.34
Voltage (p.u.)	0.5571	0.9546	1.2096	1.2178	0.8848

The results for bus 14 when the λ= 3.5 are tabulated in Table 4.24. Similar patterns are observed for this case as that for bus 26 for both objective functions. From the table, the implementation of CAPS optimization for each objective function has improved the voltage profile while *SVSI* and transmission losses are reduced. It can be seen that for VSI, AIS outperformed EP in all criteria in terms of loss minimization and voltage profile improvement except for the *SVSI* profile. The optimum active power implemented by EP techniques manages to improve the *SVSI* from 0.7371 to 0.2843 while AIS only manages to improve the *SVSI* to 0.6316. In contrast, AIS performed better than EP by reducing the transmission loss from 121.19 MW to 16.89 MW and increase the voltage at bus 26 indicated by its increment from 0.6849 p.u. to 1.2617 p.u.. As compared to EP, this optimization technique is only able to decrease the transmission loss to 31.35 MW and increase the voltage up to 1.013 p.u. only.

On the other hand, the implementation of TLM as the objective function tabulated in Table 4.24 shows that EP has outperformed AIS in loss minimization and voltage profile improvement except for *SVSI* profile. EP managed to reduce the largest transmission loss and increase the voltage profile in the system. For instance, at $\lambda = 2.3$, EP has improved the transmission loss value from 121.19 MW to 16.01 MW while AIS only manages to improve the transmission loss value to 41.10 MW. EP has also outperformed AIS in terms of voltage profile with the increment from 0.6849 p.u. to 1.2445 p.u. as compared to AIS which is only able to increase the voltage up to 0.9017 p.u.. In terms of *SVSI*, the value obtained using EP is higher than AIS.

Table 4.24: Comparison results for CAPS between EP and AIS when bus 14 was loaded: IEEE 30-bus RTS.

Criteria	Pre-CAPS	Post-CAPS at $\lambda = 3.5$			
		EP		AIS	
		VSI	TLM	VSI	TLM
SVSI	0.7371	0.2843	0.5732	0.6316	0.3623
Trans. loss (MW)	121.19	31.35	16.01	16.89	41.10
Voltage (p.u.)	0.6849	1.013	1.2445	1.2617	0.9017

(b) Results for CAPS in the IEEE 118-bus RTS

The result for CAPS performed at all selected load buses using EP and AIS are tabulated in Table 4.25 and Table 4.26. Table 4.25 tabulates the results of comparative studies using EP and AIS for VSI and TLM as the objective functions at bus 22 when λ=10. From the table, EP managed to reduce *SVSI* and increase voltage profile value as compared to AIS for both objective functions. This reveals the strength of EP in improving voltage stability condition. In addition, EP has reduced the transmission loss profile by reducing the largest transmission loss as compared to AIS. This observation highlights the strength of EP over AIS technique.

Table 4.25: Comparison results for CAPS between EP and AIS when bus 22 was loaded: IEEE 118-bus RTS.

Criteria	Pre-CAPS	Post-CAPS at $\lambda = 10$			
		EP		AIS	
		VSI	TLM	VSI	TLM
SVSI	0.9819	0.6481	0.5819	0.8108	0.809
Trans. loss (MW)	305.30	186.95	158.79	242.47	243.430
Voltage (p.u.)	0.8198	0.8546	0.8546	0.8392	0.839

Table 4.26 tabulates the results of comparative studies using EP and AIS for both objective functions when bus 78 was loaded. From the table, it is observed that when EP was used to optimize the CAPS, it gives better results as compared to AIS in terms of *SVSI* and transmission loss. In terms of VSI, EP technique successfully reduces the *SVSI* value from 0.983 to 0.6513 as compared to 0.8131 performed using AIS which indicates that the voltage stability improvement is better. As for the transmission loss, EP also gives better results as compared to AIS. EP has improved the transmission loss from 343.80 MW to 227.64 MW but for the AIS, transmission loss is only reduced to 282.22 MW. However, it is observed that EP and AIS method managed to improve the same amount voltage profile in the system from 0.8803 p.u. to 0.8804 p.u., respectively. This shows that voltage profile is an issue when load is subjected to a secure bus. Similar patterns are observed when TLM as the objective function where EP outperformed AIS in terms of *SVSI* value and transmission loss. This has again showed the merit of EP over AIS.

Table 4.26: Comparison results for CAPS between EP and AIS when bus 78 was loaded: IEEE 118-bus RTS.

Criteria	Pre-CAPS	Post-CAPS at $\lambda = 100$			
		EP		AIS	
		VSI	TLM	VSI	TLM
SVSI	0.983	0.6513	0.6512	0.8131	0.8113
Trans. loss (MW)	343.80	227.64	227.62	282.22	283.17
Voltage (p.u.)	0.8803	0.8804	0.8804	0.8804	0.8804

4.5.2.3 Constrained Hybrid Power Scheduling

The results obtained from the implementation of CHPS for each objective function are compared between EP and AIS for each participating bus. The comparisons are made in terms of voltage stability improvement, transmission loss reduction, voltage profile and cost of installation.

(a) Results for CHPS in the IEEE 30-bus RTS

The result for the CHPS performed at all selected load buses using EP and AIS are tabulated in Table 4.27 and Table 4.28. Table 4.27 tabulates the results of comparative studies using EP and AIS both objective functions when bus 26 was reactively loaded. From the table, it is observed that when EP was used to optimize the CHPS, it gives better results as compared to AIS in terms of *SVSI* value, transmission loss and installation cost. The comparison was made in terms of VSI where EP technique successfully reduces the *SVSI* value from 0.6888 to 0.1876 as compared to 0.3689 performed using AIS which indicates that the voltage stability improvement is better. In addition, it is observed that EP method has reduced the transmission loss value from 111.38 MW to 8.9 MW while AIS only manages to reduce the transmission loss value to 13.47 MW. As for the voltage profile, when AIS was used to optimize the CHPS, it outperformed EP by improving the voltage profile from 0.5571 p.u. to 1.1069 p.u. This improvement is very significant. However, EP only managed to increase the voltage profile to 1.0053 p.u.. In contrast, an installation cost of £1,217,583.16 is obtained by EP which is lower than AIS. Similar patterns are observed when TLM as the objective function except transmission loss value. EP has outperformed AIS in all criteria. EP has reduced the transmission loss value from 111.38 MW to 13.06 MW while AIS only manage to reduce to 18.32 MW. This reveals that the superiority of EP over AIS.

Table 4.27: Comparison results for CHPS using EP and AIS when bus 26 was loaded: IEEE 30-bus RTS.

Criteria	Pre-CHPS	Post-CHPS at λ = 2.3			
		EP		AIS	
		VSI	TLM	VSI	TLM
SVSI	0.6888	0.1876	0.1877	0.3689	0.338
Trans. loss (MW)	111.38	8.90	8.89	13.47	31.09
Voltage (p.u.)	0.5571	1.0257	1.0255	1.1069	0.758
Cost of Installation (£)		1,217,583.16	1,249,494.30	3,163,592.67	2,199,503.91

Table 4.28 tabulate the comparison results between EP and AIS for the CHPS for both objective functions when load variation is subjected to bus 14. The comparison was

made in terms of VSI. From the table, it shows that EP has outperformed AIS in all criteria except the voltage profile. It is discovered that EP is better than AIS since EP managed to reduce *SVSI* value and the largest transmission loss in the system. For instance, at $\lambda = 3.5$, EP method has reduced the transmission loss value from 121.19 MW to 7.87 MW while AIS manage to reduce the transmission loss value to 11.93 MW. Additionally, EP technique successfully reduces the *SVSI* value from 0.7371 to 0.1616 as compared to 0.2638 performed using AIS which indicates that the voltage stability improvement. AIS outperformed EP in terms of voltage profile with its increment from 0.6849 p.u. to 1.141 p.u. as compared to EP which is only able to increase the voltage up to 1.0642 p.u.. On the other hand, the installation cost of CHPS given by EP is £1,753,849.19 which is lower as compared to AIS. The installation cost for AIS is £2,310,598.32. Secondly, similar patterns are observed when TLM as the objective function. It is observed that, the comparison was made in terms of TLM. EP outperformed AIS in all criteria namely *SVSI*, transmission loss, voltage profile and cost of installation. This reveals the strength of EP as compared to AIS.

Table 4.28: Comparison results for CHPS using EP and AIS when bus 14 was loaded: IEEE 30-bus RTS.

Criteria	Pre-CHPS	Post-CHPS at $\lambda = 3.5$			
		EP		AIS	
		VSI	TLM	VSI	TLM
SVSI	0.7371	0.1616	0.1615	0.2638	0.3989
Trans. loss (MW)	121.19	7.87	7.86	11.93	33.01
Voltage (p.u.)	0.6849	1.0642	1.064	1.141	0.7792
Cost of Installation (£)		1,753,849.19	1,248,421.62	2,310,598.32	2,201,642.33

(b) Results for CHPS in the IEEE 118-bus RTS

The result for the CHPS performed at all selected load buses using EP and AIS are tabulated in Table 4.29 and Table 4.30. Table 4.29 tabulates the results of comparative studies using EP and AIS for both objective functions at bus 22. At λ=10, EP managed to reduce *SVSI* value and transmission loss as compared to AIS for both objective functions. In addition, EP also outperformed AIS by reducing the largest transmission loss as compared to AIS. The cost of installation required by EP also lowers than AIS for both objective functions. This reveals the superiority of EP over AIS.

Table 4.29: Comparison results for CHPS between EP and AIS when bus 22 was loaded: IEEE 118-bus RTS.

Criteria	Pre-CHPS	Post-CHPS at $\lambda = 10$			
		EP		AIS	
		VSI	TLM	VSI	TLM
SVSI	0.9819	0.6542	0.6541	0.8741	0.8741
Trans. loss (MW)	305.30	192.13	192.11	273.25	273.25
Voltage (p.u.)	0.8198	0.8424	0.8424	0.8218	0.8218
Cost of Installation (£)		10,785,469.32	10,786,527.69	12,302,173.13	12,303,299.94

Table 4.30 tabulates the results of comparative studies using EP and AIS for both objective functions when bus 78 was reactively loaded. From the table, it is observed that when EP was used to optimize the CHPS, it gives better results as compared to AIS in all criteria. In terms of VSI, EP technique successfully reduces the *SVSI* value from 0.983 to 0.6537 as compared to 0.8751 performed using AIS which indicates the voltage stability improvement. EP has reduced the transmission loss from 343.80 MW to 231.93 MW instead to 311.46 MW for AIS. In addition, it also observed that EP managed to improve a small amount of voltage profile from 0.8803 p.u. to 0.8804 p.u. as compare to AIS. AIS technique failed to improve the voltage profile in the system. On the other

Table 4.30: Comparison results for CHPS between EP and AIS when bus 78 was loaded: IEEE 118-bus RTS.

Criteria	Pre-CHPS	Post-CHPS at $\lambda = 100$			
		EP		AIS	
		VSI	TLM	VSI	TLM
SVSI	0.983	0.6537	0.6536	0.8751	0.8751
Trans. loss (MW)	343.80	231.93	231.91	311.46	311.46
Voltage (p.u.)	0.8803	0.8804	0.8804	0.8803	0.8803
Cost of Installation (£)		11,189,420.39	11,191,021.29	12,704,443.40	12,691,607.89

hand, the installation cost of CHPS required using EP technique is £11,189,420.39 which is lower as compared to AIS. The installation cost for AIS is £12,704,443.40.

Similar patterns are observed for TLM as the objective function where EP outperformed AIS in all criteria.

4.6 SUMMARY

This chapter has presented the application of evolutionary programming optimization technique in the CPP for the voltage stability improvement and transmission losses minimization in a system under *(N-m)* contingencies. The studies proposed the CRPC, CAPS and CHPS as three CPP techniques. For each technique, two separate objective functions were implemented namely voltage stability improvement with *SVSI* value as the fitness function and transmission loss minimization with the transmission loss in the system as the fitness function. In optimizing the CRPC, the EP has given a solution for reactive power to be dispatched by the generator buses in order to improve the voltage stability condition of to minimize the transmission loss in the system. The next CPP technique was the CAPS optimization, where the EP identified the optimal active power to be scheduled by the generator buses for improving the voltage stability condition or loss minimization in the system. In the case of CHPS as a CPP technique, the EP has given a solution for reactive power to be controlled and active power to be scheduled by the generator buses in order to improve the voltage stability condition or to minimize the transmission loss in the system. Finally, results obtained from the EP techniques were compared with AIS and it was found that EP outperformed AIS for 32 cases out of 44 cases for VSI and 38 cases out of 44 cases for TLM.

CHAPTER 5
COMPUTATIONAL INTELLIGENCE TECHNIQUE FOR FACTS DEVICES INSTALLATION

5.1 INTRODUCTION

Voltage stability improvement in power system is an important consideration in power system operation when involving heavily stressed system with large amount of real and reactive power demand and low voltage condition. The electrical energy demand increases continuously from time to time. This increase should be monitored because few problems could appear with the power flows through the existing electric transmission networks. If this situation fails to be controlled, some lines located on the particular paths might become overloaded [2]. Due to the overloaded conditions of the transmission lines, the system will have to be driven close to or even beyond their transfer capacities.

This chapter presents a new approach for installation of FACTS based on EP optimization technique considering multi-contingencies *(N-m)* occurrence in the system. The proposed technique determines the optimum sizing of Static VAR Compensator (SVC), Thyristor Controlled Series Compensator (TCSC) and Unified Power Flow Controller (UPFC) in order to reduce the total transmission loss in the system. *SVSI* is used as the tool to indicate the FACTSs location to be installed into the power system network. Transmission loss minimization (TLM) was used as the objective function in the system. A computer program was written in MATLAB and the proposed techniques were tested on the IEEE 30-bus RTS and IEEE 118-bus RTS. Subsequently, comparative studies were conducted by comparing the results with Artificial Immune System (AIS).

5.2 MATHEMATICAL MODEL OF FACTS DEVICES

In optimization of FACTS devices, the objective function selected for optimization is minimization of total transmission losses in the system. The process involve several equation and constraint; equality constraint and inequality constraint. The equality constraints are the nodal power balance equations, while the inequality constraints are the limits of all control or state variables. The different types of FACTS device have been applied and the parameter of the selected devices is optimized in order to control the power flows in the system. The line reactance can be changed by using TCSC and SVC can be utilized to control the reactive power at the bus. Subsequently, UPFC is the most and versatile device, which controls the line reactance. In this work, three different types of FACTS devices have been selected namely SVC, TCSC and UPFC. The mathematical models of SVC, TCSC and UPFC are incorporated into the transmission line model as shown in Figure 5.1. It shows the parameters of a transmission line which are connected between bus i and bus j.

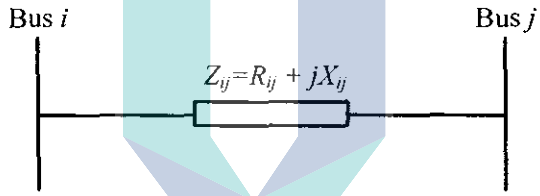

Figure 5.1: Transmission line model

The real and reactive power flows between bus i and bus j are given in equation (5.1).

$$
\begin{aligned}
P_{ij} &= V_i^2 G_{ij} - V_i V_j \times \left[G_{ij}\cos\delta_{ij} + B_{ij}\sin\delta_{ij}\right] \\
Q_{ij} &= -V_i^2\left[B_{ij} + B_{sh}\right] - V_i V_j \times \left[G_{ij}\sin\delta_{ij} - B_{ij}\cos\delta_{ij}\right]
\end{aligned}
\tag{5.1}
$$

Then, the real and reactive power flows between buses j and i are given below.

$$
\begin{aligned}
P_{ji} &= V_j^2 G_{ij} - V_i V_j \times \left[G_{ij}\cos\delta_{ij} - B_{ij}\sin\delta_{ij}\right] \\
Q_{ji} &= -V_j^2\left[B_{ij} + B_{sh}\right] + V_i V_j \times \left[G_{ij}\sin\delta_{ij} + B_{ij}\cos\delta_{ij}\right]
\end{aligned}
\tag{5.2}
$$

where

$$
\begin{aligned}
G_{ij} &= R_{ij} / \left(R_{ij}^2 + X_{ij}^2\right), \\
B_{ij} &= X_{ij} / \left(R_{ij}^2 + X_{ij}^2\right)
\end{aligned}
\tag{5.3}
$$

$\delta_{ij} = \delta_i - \delta_j$,V_i, δ_i and V_j, δ_j are the voltages and angles at bus i and j, respectively as highlighted in the table.

5.2.1 Modeling of Static VAR Compensator

SVC can provide a fast-acting reactive support in power system. The SVC can be operated as both inductive and capacitive compensation which can control bus voltage by absorbing or injecting reactive power [170]. The SVC is modelled as a shunt variable susceptance added at both ends of the line. The model of SVC considered in this study is shown in Figure 5.2.

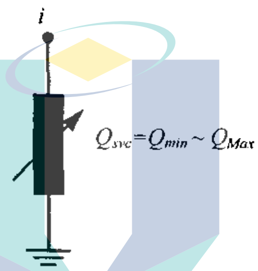

Figure 5.2: SVC model

Hence, it is modelled as ideal reactive power injections to perform the steady-state condition at bus i. The absorbed or injected power at bus i in the system is represented by Q_{svc}. Consequently, the SVC device constraint limit is given in equation (5.4).

$$\begin{gathered} Q_{\min} \le Q_{SVC} \le Q_{\max} \\ -200MVAr \le Q_{SVC} \le 200MVAr \end{gathered} \tag{5.4}$$

5.2.2 Modeling of Thyristor Controlled Series Compensator

In this work, TCSC can be represented as the inductive or capacitive compensation by decreasing or increasing the reactance of the transmission line branch. Its value is function of the reactance of the line X_L where the TCSC is located [209]. The mathematical models of TCSC, is shown in Figure 5.3. In this figure, the series reactance of TCSC as been assumed to be connected between buses *i* and *j*.

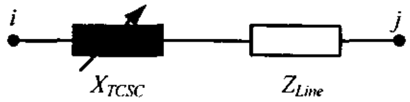

Figure 5.3: TCSC model

$$Z_{ij} = Z_L + jX_{TCSC}, X_{TCSC} = r_{TCSC} .X_L \tag{5.5}$$

where Z_L is the impedance of the transmission line, X_{TCSC} is the reactance of the line where TCSC is located and r_{TCSC} is the coefficient which represents the compensation degree of TCSC. The TCSC device constraint limit is given by [210],

$$-0.8X_L \leq X_{TCSC} \leq 0.2X_L \tag{5.6}$$

5.2.3 Modeling of Unified Power Flow Controller

UPFC model is illustrated in Figure 5.4. It consists of two voltage-source converters, which is connected back to back through a DC capacitor [210].

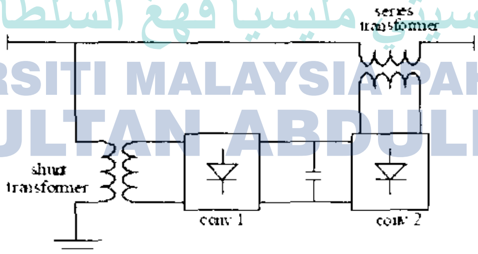

Figure 5.4: UPFC model

In this work, the UPFC is modeled by the simultaneous presence of several FACTS devices in the same power transmission line [210]. In this research, TCSC is installed in the line while SVC installed at a bus in an adjacent branch and both incorporated as an UPFC. The elements characteristics used to represent this device are the same as above for the SVC and TCSC. Hence, the UPFC device constraint limit is given by [210],

$$-0.8X_L \leq X_{TCSC} \leq 0.2X_L \tag{5.7}$$

$$-200MVAR \leq Q_{SVC} \leq 200MVAR \tag{5.8}$$

5.2.4 FACTS Devices Installations Cost

The cost of installation of FACTS devices namely SVC, TCSC and UPFC are mathematically formulated and given by [158];

$$IC = C_{FACTS} \times S \times 1000 \tag{5.9}$$

where IC is the installation cost of SVC devices in US$ and C_{FACTS} is the cost of FACTS devices in US$/KVAr.

Installation cost includes the sum of installation cost of all the devices and it can be calculated using the cost function given by [158];

$$C_{SVC} = 0.0003S^2 - 0.3051S + 127.38(US\$/KVAr) \tag{5.10}$$

$$C_{TCSC} = 0.0015S^2 - 0.7130S + 153.75(US\$/KVAr) \tag{5.11}$$

$$C_{UPFC} = 0.0003S^2 - 0.2691S + 188.22(US\$/KVAr) \tag{5.12}$$

$$S = |Q_2 - Q_1| \tag{5.13}$$

where,

S = operating range of FACTS devices in MVAr

Q_1 = reactive power flow through the branch before FACTS installation

Q_2 = reactive power flow through the branch after FACTS installation

5.3 FACTS DEVICES INSTALLATION

Firstly, the placement of the FACTS devices installation in the network must be determined and then, the setting of the control parameters of FACTS is optimized by controlling the device parameters. Locations of FACTS devices in the system are obtained based on the performance using the voltage stability index measured each line for the same operating conditions. FACTSs are installed on the weak buses and heavily loaded areas to reduce stressed condition in the system. The *SVSI* technique was applied as the tool to indicate the FACTSs location into the network. When the load flow program was run, stability indices are calculated for FACTS placed in every line one at a time for the same operating conditions and the system identified the line with the highest *SVSI* for the purpose of installing the FACTS. The EP optimization technique is then used to determine the optimal sizing of the FACTS devices namely SVC, TCSC and UPFC. The concept of the *SVSI* is demonstrated through a simple two-bus system model as shown in section 3.2 of Chapter 3. The mathematical formulation for *SVSI* [23] is given as in equation (3.24).

5.4 TOTAL LOSS MINIMIZATION AS OBJECTIVE FUNCTION

The objective function of the proposed method is to minimize the active power loss subject to a set of equality and inequality constraints in the system. Generators have maximum and minimum output powers and reactive powers which add inequality constraints. Furthermore, to maintain the quality of electrical service and system security, bus voltages usually have maximum and minimum magnitudes. These limits again require the addition of inequality constraints. The objective function is mathematically stated as follows [114];

$$\min f_p = \sum_{k \in N_E} P_{k_{Loss}}(V,\theta)$$
$$= \sum_{\substack{k \in N_E \\ k=(i,j)}} g_k\left(V_i^2 + V_j^2 - 2V_iV_j\cos\theta_{ij}\right)$$

Subject to:- (5.14)

$$h_{Qi} = Q_{Gi} - Q_{Di} - V_i \sum_{j \in N_i} V_j\left(G_{ij}\sin\theta_{ij} - B_{ij}\cos\theta_{ij}\right) = 0, i \in N_{PQ}$$

$$V_{i\,min} \le V_i \le V_{i\,max}\ ,\ i \in N_B$$

$$Q_{Gi\,min} \le Q_{Gi} \le Q_{Gi\,max}\ ,\ i \in \{N_{PV}, n_s\}$$

Subject to the constraint of equality in reactive and active power balance

$$Q_i - Q_{Gi} + Q_{Di} = 0$$
$$Q_i = Q_{Gi} - Q_{Di} - V_i \sum_{j \in N_i} V_j\left(G_{ij}\sin\theta_{ij} - B_{ij}\cos\theta_{ij}\right) = 0, \quad i \in N_{PQ}$$
$$P_i - P_{Gi} + P_{Di} = 0 \qquad (5.15)$$
$$P_i = P_{Gi} - P_{Di} - V_i \sum_{j \in N_i} V_j\left(G_{ij}\cos\theta_{ij} - B_{ij}\sin\theta_{ij}\right) = 0, \quad i \in N_{B-1}$$

Hence, inequality constraints on control variable limits; generator power reactive capability limits, generator power active capability limits, and voltage constraints are given by;

$$Q_{Gi_{min}} \le Q_{Gi} \le Q_{Gi_{max}} \quad i \in N_G$$
$$Q_{ci_{min}} \le Q_{ci} \le Q_{ci_{max}} \quad i \in N_c$$
$$P_{Gi_{min}} \le P_{Gi} \le P_{Gi_{max}}, \quad i \in Slackbus \qquad (5.16)$$
$$V_{i_{min}} \le V_i \le V_{i_{max}} \quad i \in N_B$$

where, g_k is the conductance of branch k, n_s is the slack (reference) bus number; N_{PQ} is PQ bus number, N_{PV} is PV bus number, N_B is the total number of buses, N_{B-1} is the total buses excluding slack bus, N_c is the possible reactive power source installation buses number, N_E is the branch number, N_i is the numbers of buses adjacent to bus i including bus i, θ_{ij} is voltage angle different between bus i and bus j(rad), Q_i and Q_j are the reactive power on the sending and receiving buses; Q_G is the generated reactive power, V_i and V_j are the voltage magnitude at the sending and receiving buses , G_{ij} and B_{ij} is the mutual conductance and subceptance between bus i and bus j and $P_{K_{Loss}}$ is the total active power loss in the system. The equation (5.14) can be simplified to generalize objective function as:

$$\min f_p = \sum_{k \in N_E} P_{k_{Loss}}(V,\theta) + \sum_{k \in NVPQ_{\lim}} \lambda_{Vi}\left(V_i - V_i^{\lim}\right)^2 + \sum_{k \in NQg_{\lim}} \lambda_{Qg\lim}\left(Q_{gi} + Q_{gi}^{\lim}\right)^2 \quad (5.17)$$

Subject to:-

$$Q_{Gi} - Q_{Di} - V_i \sum_{k \in N_E} V_j\left(G_{ij}\sin\theta_{ij} - B_{ij}\cos\theta_{ij}\right) = 0, \quad i \in N_{PQ} \quad (5.18)$$

$$P_{Gi} - P_{Di} - V_i \sum_{k \in N_E} V_j\left(G_{ij}\cos\theta_{ij} - B_{ij}\sin\theta_{ij}\right) = 0, \quad i \in N_{B-1} \quad (5.19)$$

where λ_{Vi} and λ_{Qgi} indicate the penalty factor which can increase the optimization procedure, $N_{VPQ_{\lim}}$ is the number of PQ bus at which the voltage violates the limits and $N_{Qg_{\lim}}$ denotes the number of buses at which the reactive power generation violates the limits.

$$V_i^{\lim} = \begin{cases} V_i^{\min} & \text{if } V_i < V_i^{\min} \\ V_i^{\max} & \text{if } V_i < V_i^{\max} \end{cases}$$
$$Q_{g_i}^{\lim} = \begin{cases} Q_{g_i}^{\min} & \text{if } Q_{gi} < Q_{g_i}^{\min} \\ Q_{gi}^{\max} & \text{if } Q_{gi} < Q_{gi}^{\max} \end{cases} \quad (5.20)$$

5.5 APPLICATION OF EVOLUTIONARY PROGRAMMING IN FACTS INSTALLATION

In this analysis, EP was used to optimize the FACTS devices namely SVC, TCSC and UPFC in order to improve transmission loss in the system. EP involved initialization, mutation, combination and selection. The detailed background of EP algorithm has already been discussed in Chapter 4. Therefore, this section will only concentrate on the development of EP for optimizing the SVC, TCSC and UPFC. Transmission loss minimization was chosen as the objective function for the optimization process. The general flow chart for the implementation of EP optimization technique is shown in Figure 5.5. However, the details procedures are explained in the next section.

5.6 OPTIMIZATION OF FACTS FOR TRANSMISSION LOSS MINIMIZATION

The following procedures present the implementation of EP for the optimization process considering multi-contingencies *(N-m)* occur in the system:-

i. Set the multi-contingencies *(N-m)* in the system i.e. generator and line outages.
   - two generator outages and five line outages are set into the IEEE 30-bus RTS system i.e., generator buses 11, 13 and lines 1, 4, 8, 9, 7.
   - five generator outages and five line outages are set into the IEEE 118-bus RTS system, i.e., generator buses 12, 49, 61, 65, 70 and lines 7, 9, 51, 67, 96.

ii. Set the loading factor, λ.

iii. Run the load flow analysis.

iv. Calculate *SVSI* values for all lines and sort all *SVSI* in descending order.

v. Extract the highest *SVSI* and select the highest *SVSI* for FACTS constraint.

vi. Set the FACTS constraints i.e. $total\ loss \leq loss\_set$ and $V_m\ (bus) \leq V\_set$.

vii. Generate random numbers i.e. five random numbers namely x_1, x_2, x_3, x_4 and x_5 are generate for IEEE 30-bus system and x_1, x_2, x_3, x_4, x_5, x_6, x_7, x_8, x_9 and x_{10} for 118-bus RTS system.

viii. Check for constraint violations. If constraints violated, go to step (iv), otherwise go to step (vi).

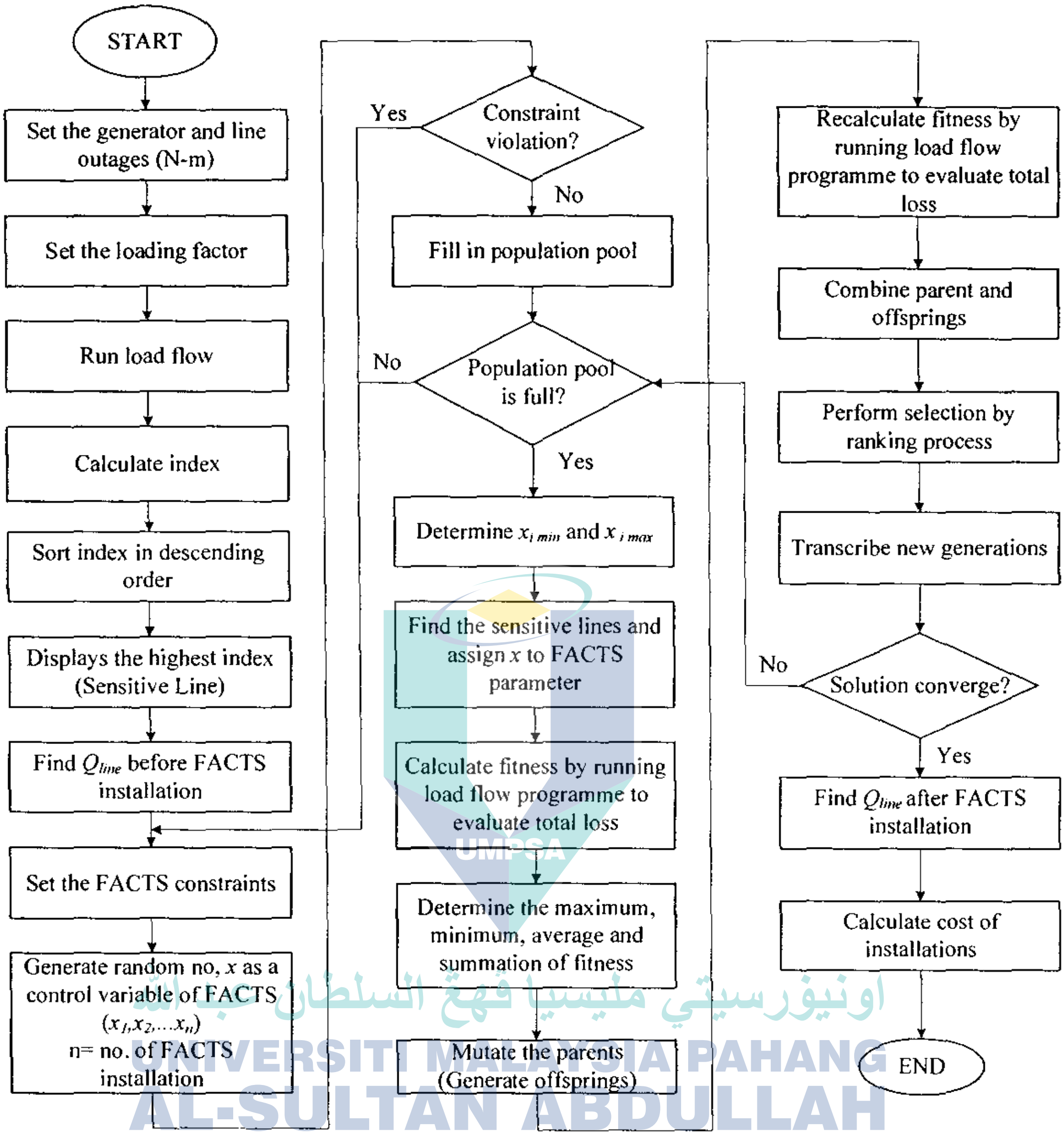

Figure 5.5: Flowchart for optimization of FACTS using EP.

ix. Fill in population pool. Repeat step (iv) if pool was not full, otherwise continue to step vii.

x. Determine *x_min* and *x_max* from the process data.

xi. Assign x_1, x_2 until x_5 to FACTS variables in the IEEE 30-bus system data and x_1, x_2, and x_{10} to FACTS variable in the IEEE 118-bus system data.

xii. Calculate fitness by running the load flow program to evaluate the transmission loss values.

xiii. Determine *loss_min, loss_max, loss_avg* and *loss_sum* for statistical evaluation.

xiv. Mutate the parents i.e. x_1, x_2 and x_3 for IEEE 30-bus or x_1, x_2, x_3, x_4 and x_5 for IEEE 118-bus and generate offsprings.

xv. Recalculate fitness using the offsprings by running the load flow program.

xvi. Combine parents and offsprings (combination process).

xvii. Perform selection by tournament selection process from the combined data.

xviii. Identify and transcribe new generations.

xix. If solution is not converged, repeat step (vii) to (xv), otherwise go to step (xvii).

xx. Calculate installation cost.

xxi. End.

5.7 RESULTS AND DISCUSSION

The results are divided in two sub-sections. The first part presents the results for FACTS optimization with transmission loss minimization as the objective function and the second part presents the results for the comparative studies implemented between EP and AIS. In this process, three types of FACTS devices are implemented namely the optimal CSVC, optimal CTCSC and lastly optimal CUPFC. The test was conducted on the IEEE 30-bus RTS and IEEE 118-bus RTS with several buses were reactively loaded. The optimization engine is executed with variation in loading conditions at the respective load bus so that the voltage profiles, transmission loss variations and installation cost can be observed.

5.7.1 Constrained Static VAR Compensator for Transmission Loss Minimization

The analysis was conducted at various loading conditions to observe the impact to the transmission loss, voltage profile and installation cost at the loaded bus. There were two constraints assigned before the CSVC is optimized namely *total loss* $\leq$ *loss_set* and V_m *(bus)* $\leq$ *V_set.* The results for IEEE 30-bus RTS are tabulated in Table 5.1 and Table 5.2 while Table 5.3 and Table 5.4 tabulate the results for IEEE 118-bus RTS.

(a) CSVC in the IEEE 30-bus RTS

The test was conducted on the IEEE 30-bus RTS with the weak bus and secure bus namely bus 26 and bus 14 are reactively loaded. Table 5.1 and Table 5.2 tabulate the effect of loading factor, λ variation to transmission losses, voltage profile and installation cost for those buses. The five locations of SVCs installation in the network are also identified by using *SVSI* technique and shown in Table 5.3. Different loading condition shows a different location for the SVCs placement in the system as it depends on which buses are the weakest when subjected to λ variation.

As tabulated in Table 5.1, it is observed that all the transmission loss values reduce with respect to λ variation. At λ = 2.3, the transmission loss is reduced from 111.38 MW to 59.2 MW MW with the 46.8% lower than before the installment of SVCs. In addition,

Table 5.1: Results for CSVC when bus 26 was reactively loaded: IEEE 30-bus RTS.

λ factor	Analysis CSVC	Transmission loss (MW)	ΔLoss (%)	V_m (p.u)	Cost (US$)
1.0	Pre	82.74	33.3	0.8235	44,091.35
	Post	55.20		0.8459	
1.5	Pre	87.26	29.8	0.7584	53,998.39
	Post	61.22		0.9489	
2.0	Pre	95.94	38.1	0.6671	70,055.27
	Post	59.42		1.1093	
2.3	Pre	111.38	46.8	0.5571	97,227.54
	Post	59.22		1.0789	

voltage profiles are also improved from 0.5571 p.u. to 1.0789 p.u. as a result of the implementation of CSVC. The cost of SVC installation is US$ 97,227.54. The results for other λ value are indicated in the same table.

Table 5.2 tabulates the results for CSVC scheme performed to the system with load variation at a secure bus namely bus 14. λ was increased up to 3.7. EP has significantly reduced the transmission losses as well as increased the voltage profile value at the loaded bus. It is observed that the transmission losses value decreased accordingly and the voltage profiles for post-CSVC are higher with respect to λ. At $\lambda = 3.7$ the transmission losses have been reduced from 121.19 MW to 60.39 MW with the reduction of 50.2%. In addition, the range of transmission losses reduction for all loading conditions is in between 33.6% to 50.2% as indicated in the table. It is also obvious that with the implementation of CSVC installation it has significantly improved the voltage profile at all λ factors. It is found that the installations of the CSVCs in the system can help to minimize the losses and improve the voltage profile for the system. The cost of SVC installation is US$ 118,165.25. The results for other λ values are indicated in the same table.

Table 5.2: Results for CSVC when bus 14 was reactively loaded: IEEE 30-bus RTS.

λ	Analysis CSVC	*SVSI* (p.u.)	Transmission loss (MW)	ΔLoss (%)	V_m (p.u)	Cost (US$)
1.0	Pre	0.5977	82.48	33.6	0.8882	44,414.33
	Post	0.586	54.75		1.0957	
2.0	Pre	0.6232	88.77	36.4	0.8355	56,737.81
	Post	0.5792	56.44		1.0546	
3.0	Pre	0.6647	99.91	43.0	0.7673	77,954.69
	Post	0.5637	56.97		0.8174	
3.7	Pre	0.7371	121.19	50.2	0.6849	118,165.25
	Post	0.4413	60.39		1.033	

The value and location for SVC installation identified by the EP technique is shown in Table 5.3. Those values are the optimized SVC sizing to be installed into the system in order to improve transmission losses in the system.

Table 5.3: SVC sizing and location when bus 26 and bus 14 were reactively loaded: IEEE 30-bus RTS

Test Bus	λ	Location (Line No.)	Sizing (MVAr)
26	2.3	1	-42.902
		31	-21.285
		2	-9.789
		5	-44.989
		37	-88.403
14	3.7	1	-163.829
		2	178.775
		5	-170.770
		37	0.115
		12	-46.468

(b) CSVC in the IEEE 118-bus RTS

The test was conducted on the IEEE 118-bus RTS with buses namely bus 22 and bus 78 are reactively loaded. The results for a weak bus namely bus 22 are tabulated in Table 5.4. From the table, bus 22 was subjected to variation of loading conditions. λ is gradually increased in order to observe the effect of transmission losses, voltage profile and cost of installation. With the implementation of CSVC scheme, all the transmission loss values are smaller before its implementation. It implies that the transmission loss has been reduced. Voltage profile in the system is also improved as a result of the implementation of CSVC. It can be seen that at $\lambda = 10$, the transmission loss is reduced from 305.3 MW to 297.7 MW. Additionally, the voltage is improved from 0.8198 p.u. to 0.8489 p.u.. The cost of SVC installation is US$19,347.53. The results for other λ values are indicated in the same table.

Table 5.4: Results for CSVC when bus 22 was reactively loaded: IEEE 118-bus RTS.

λ	Analysis CSVC	*SVSI* (p.u.)	Transmission loss (MW)	ΔLoss (%)	V_m (p.u.)	Cost (US$)
2	Pre	0.9741	298.46	2.2	0.9373	18,470.44
	Post	0.7407	291.92		0.9377	
4	Pre	0.9753	299.37	2.2	0.9110	17,012.09
	Post	0.758	292.86		0.9115	
6	Pre	0.977	300.73	2.3	0.8830	16,498.30
	Post	0.7846	293.76		0.9067	
8	Pre	0.9791	302.66	2.4	0.8528	17,057.57
	Post	0.7715	295.27		0.8699	
10	Pre	0.9819	305.30	2.5	0.8198	19,347.53
	Post	0.8775	297.70		0.8489	

Table 5.5 tabulates the effect of λ variation to voltage profiles, transmission losses and installation cost for load subjected to a secure bus namely bus 78. Similar patterns as that for bus 22 are observed, where the transmission losses and the voltage profile were improved with the reduction of transmission losses as well as increment in voltage profile with respect to λ variation. For instance, $\lambda = 100$, the transmission loss has been reduced from 343.8 MW to 337.71 MW with the reduction of 1.8 % only. On the other hand, the voltage profile values were remained unchanged for each λ implemented using EP for a secure bus in IEEE 118-bus RTS. The cost of SVC installation is US$ 18,178.09. The results for other λ values are indicated in the same table.

Table 5.5: Results for CSVC when bus 78 was reactively loaded: IEEE 118-bus RTS.

λ	Analysis CSVC	*SVSI* (p.u.)	Transmission loss (MW)	ΔLoss (%)	V_m (p.u)	Cost ($US)
10	Pre	0.9734	298.37	2.1	0.9950	19,332.18
	Post	0.7550	292.12		0.9950	
30	Pre	0.9740	301.39	2.1	0.9720	19,341.57
	Post	0.7554	295.13		0.9720	
50	Pre	0.9753	307.87	2.0	0.9478	19,363.40
	Post	0.7564	301.59		0.9478	
100	Pre	0.9830	343.80	1.8	0.8803	18,178.09
	Post	0.7639	337.71		0.8803	

As tabulated in Table 5.6, it is observed that the sizing values for SVC are the optimized SVC values determined by the EP in order to improve the transmission losses when λ is subjected to bus 22 and bus 78. Some locations may require an inductive compensation and in some other locations will require a capacitive compensation in order to minimize the transmission loss for the whole system.

Table 5.6: SVC sizing when bus 22 and bus 78 were reactively loaded: IEEE 118-bus RTS

Test Bus	λ	Location (Line No.)	Sizing (MVAr)
22	10	101	-114.486
		100	86.168
		27	-147.616
		92	-163.413
		104	-89.904
		94	-89.904
		64	-198.498
		63	-34.022
		102	-188.905
		31	84.307
78	100	101	-114.699
		100	86.068
		92	-147.767
		104	-163.381
		120	-89.909
		94	-89.909
		102	-198.537
		64	-34.174
		63	-189.128
		103	84.095

5.7.2 Constrained Thyristor Controlled Series Compensator for Transmission Loss Minimization

CTCSC scheme was implemented in the system in order to improve the voltage stability condition and transmission loss in a system. Similar test systems are considered so that comparison can later be conducted accordingly. The results for IEEE 30-bus RTS are tabulated in Table 5.7 and Table 5.8 while Table 5.9 and Table 5.10 tabulate the results for the IEEE 118-bus RTS.

(a) CTCSC in the IEEE 30-bus RTS

Table 5.7 tabulates the results for CTCSC scheme performed to the system with load variation at weak bus namely bus 26. The λ is gradually increased until the system reaches its instability point during contingency. With the implementation of CTCSC scheme, the transmission losses are reduced while voltage profiles are higher indicating that the total transmission loss in the system is improved. For instance at λ= 2.3, it is observed that the transmission loss value is reduced from 95.94 MW to 84.28 MW. It has also improved the voltage profile in the system from 0.5571 p.u. to 0.6578 p.u.. These improvements are significant. The TCSC sizing that should be installed to lines 1, 31, 2, 5 and 37 as highlighted in Table 5.9 are 0.1867 p.u., 0.1544 p.u., 0.0228 p.u., - 0.0230 p.u. and - 0.1136 p.u.. The cost of TCSC installation is US$ 58,359.27. Similar observation for other λ values can be referred to the same table.

Table 5.7: Results for CTCSC when bus 26 was reactively loaded: IEEE 30-bus RTS.

λ	Analysis CTCSC	*SVSI* (p.u.)	Transmission loss (MW)	ΔLoss (%)	V_m (p.u.)	Cost (US$)
1	Pre	0.5969	82.74	8.5	0.8235	28,787.82
	Post	0.4795	75.71		0.8459	
1.5	Pre	0.6126	87.26	9.7	0.7584	32,338.90
	Post	0.4888	78.80		0.7840	
2	Pre	0.6409	95.94	12.2	0.6671	35,864.73
	Post	0.5155	84.28		0.7160	
2.3	Pre	0.6888	111.38	19.6	0.5571	58,359.27
	Post	0.5304	89.59		0.6578	

Table 5.8 tabulates the results for CTCSC scheme performed in the system with λ variation at secure bus namely bus 14. Similarly with the weak bus, the transmission losses reduce accordingly, while voltage profile increases as the load factor increases. For instance at λ = 3.7, it is observed that a reduction in transmission loss in the system is observed from 121.19 MW to 91.78 MW and at the same time voltage profile is improved from 0.6849 p.u. to 0.7576 p.u.. The cost of TCSC installation is US$ 83,657.24. Similar observation for other λ values can also be referred to the same table.

Table 5.8: Results for CTCSC when bus 14 was reactively loaded: IEEE 30-bus RTS.

λ	Analysis CTCSC	*SVSI* (p.u.)	Transmission loss (MW)	ΔLoss (%)	V_m (p.u)	Cost (US$)
1.0	Pre	0.5977	82.48	8.6	0.8882	28,971.39
	Post	0.4798	75.35		0.9143	
2.0	Pre	0.6232	88.77	11.0	0.8355	36,898.58
	Post	0.4926	78.99		0.8708	
3.0	Pre	0.6647	99.91	15.3	0.7673	50,255.19
	Post	0.5121	84.67		0.8174	
3.7	Pre	0.7371	121.19	24.3	0.6849	83,657.24
	Post	0.5344	91.78		0.7576	

Table 5.9 tabulates the sizing values for TCSC with the implementation of CTCSC optimization using EP in order to improve the transmission losses when λ variation is subjected to buses 14 and 26.

Table 5.9: TCSC sizing when bus 26 and bus 14 were reactively loaded: IEEE 30-bus RTS

Test Bus	λ	Location (Line No.)	Sizing (p.u.)
26	2.3	1	0.1867
		31	0.1544
		2	0.0228
		5	-0.0230
		37	-0.1136
14	3.7	1	0.1867
		2	0.1544
		5	0.0228
		37	-0.0230
		12	-0.1136

(b) CTCSC in the IEEE 118-bus RTS

The test was conducted on the IEEE 118-bus RTS with bus 22 and bus 78 are reactively loaded. The results for transmission loss, voltage profile, SVSI and installation cost with respect to λ variation are tabulated in Table 5.10. With the implementation of CTCSC scheme, the voltage profile in the system is improved and transmission losses are minimized. It can be seen that at λ = 10, the transmission loss is

Table 5.10: Results for CTCSC when bus 22 was reactively loaded: IEEE 118-bus RTS.

λ	Analysis CTCSC	*SVSI* (p.u.)	Transmission loss (MW)	ΔLoss (%)	V_m (p.u)	Cost (US$)
2	Pre	0.9741	298.46	11.0	0.9373	50,466.80
	Post	0.9695	265.71		0.9392	
4	Pre	0.9753	299.37	10.9	0.9110	51,092.88
	Post	0.9737	266.74		0.9135	
6	Pre	0.9770	300.73	9.8	0.8830	47,934.75
	Post	1.0369	271.26		0.8867	
8	Pre	0.9791	302.66	11.0	0.8528	37,474.93
	Post	1.0108	269.37		0.8550	
10	Pre	0.9819	305.30	10.2	0.8198	46,549.36
	Post	1.0782	274.22		0.8378	

reduced from 305.3 MW to 274.22 MW and the voltage is improved from 0.8198 p.u. to 0.8378 p.u.. The installation cost for TCSC is US$ 46,549.36. The results for other λ values are indicated in the same table.

Consequently, a similar pattern can be observed in Table 5.11 for λ variation subjected to a secure bus namely bus 78 as the test bus, where the transmission losses and the voltage profile were also improved with the reduction of transmission losses as well as increment in voltage profile with respect to λ variation. For instance, the total transmission loss decreases from 343.8 MW to 314.58 MW or 8.5% decrement at λ = 10. Furthermore, the CTCSC scheme manages to increase the voltage profile with the

Table 5.11: Results for CTCSC when bus 78 was reactively loaded: IEEE 118-bus RTS.

λ	Analysis CTCSC	*SVSI* (p.u.)	Transmission loss (MW)	ΔLoss (%)	V_m (p.u)	Cost (US$)
10	Pre	0.9734	298.37	8.2	0.9950	34,822.51
	Post	1.0266	273.76		0.9950	
30	Pre	0.9740	301.39	8.2	0.9720	34,844.10
	Post	1.0271	276.75		0.9720	
50	Pre	0.9753	307.87	8.0	0.9478	34,894.60
	Post	1.0285	283.18		0.9478	
100	Pre	0.9830	343.80	8.5	0.8803	32,141.45
	Post	0.9566	314.58		0.8812	

increment from 0.8803 p.u. to 0.8812 p.u.. The cost of installation for TCSC is US$ 32, 141.45. The results for other λ values are indicated in the same table.

As tabulated in Table 5.12, it observed that the sizing value for both buses are the optimized TCSC values to be installed at the respective line determined by the *SVSI* in order to reduce the transmission losses when reactive load is subjected to bus 22 and bus 78.

Table 5.12: TCSC sizing when bus 22 and bus 78 were reactively loaded: IEEE 118-bus RTS

Test Bus	λ	Location (Line No.)	Sizing (p.u.)
22	10	101	-0.5192
		100	-0.7888
		27	0.1829
		92	0.1988
		104	-0.1320
		94	-0.1320
		64	-0.3729
		63	-0.5549
		102	0.0674
		31	0.0544
78	100	101	-0.0636
		100	-0.7243
		92	0.1747
		104	0.0510
		120	0.0506
		94	0.0506
		102	0.1680
		64	-0.1710
		63	-0.4539
		103	-0.2556

5.7.3 Constrained Unified Power Flow Controller for Transmission Loss Minimization

The next FACTS devices namely UPFC was implemented in order to reduce the total transmission loss in multi-contingencies system. Similar test bus and loading condition as previous test were used to access the proposed technique. The results for

IEEE 30-bus RTS are tabulated in Table 5.13, Table 5.14 and Table 5.15 while Table 5.16, Table 5.17 and Table 5.18 tabulate the results for the IEEE 118-bus RTS.

(a) CUPFC in the IEEE 30-bus RTS

The test was conducted on the IEEE 30-bus RTS with the weak bus and secure bus namely bus 26 and bus 14 are reactively loaded. In this test, the UPFC is modeled by the simultaneous presence of several FACTS devices in the same power transmission line. The five variables required in the CUPFC are combined with the five variables making total of ten variables for this scheme. λ value at bus 26 was increased gradually and the optimum values of UPFC were determined in order to reduce the total transmission loss in the system. The results are tabulated in Table 5.13, Table 5.14 and Table 5.15.

As tabulated in Table 5.13, it is observed that all the voltage profiles in the system are improved and transmission losses are minimized with the implementation of the CUPFC scheme. At $\lambda = 2.3$, it is observed that the transmission loss value is reduced from 111.38 MW to 58.45 MW which indicates 47.5 % reduction. It has also improved the voltage profile in the system from 0.5571 p.u. to 0.9132 p.u.. The cost of installation is US$ 113, 471.41.

Table 5.13: Results for CUPFC when bus 26 was reactively loaded: IEEE 30-bus RTS.

λ	Analysis CUPFC	Transmission loss (MW)	ΔLoss (%)	V_m (p.u)	Cost (US$)
1.0	Pre	82.74	32.4	0.8235	67,895.67
	Post	55.95		1.0264	
1.5	Pre	87.26	33.2	0.7584	94,829.49
	Post	58.27		1.1438	
2.0	Pre	95.94	32.9	0.6671	112,342.98
	Post	64.34		1.3173	
2.3	Pre	111.38	47.5	0.5571	113,471.41
	Post	58.45		0.9132	

Table 5.14: Results for CUPFC when bus 14 was reactively loaded: IEEE 30-bus RTS.

λ	Analysis CUPFC	Transmission loss (MW)	ΔLoss (%)	V_m (p.u)	Cost (US$)
1	Pre	82.48	32.7	0.8882	68,369.93
	Post	55.51		1.104	
2	Pre	88.77	32.0	0.8355	59,741.60
	Post	60.40		1.0021	
3	Pre	99.91	43.6	0.7673	106,161.29
	Post	56.39		1.0197	
3.7	Pre	121.19	50.9	0.6849	147,444.23
	Post	59.51		1.0053	

Table 5.14 tabulates the results for the CUPFC scheme performed to the system with load variation at a secure bus namely bus 14. λ value is gradually increased in order to observe the effect of voltage profile and transmission losses when the UPFC is injected in the system. λ value was increased up to 3.7. The implementation of CUPFC using EP has significantly reduced the transmission losses as well as increased the voltage profile value at the loaded bus. At $\lambda = 3.7$, the transmission losses have been reduced from 121.19 MW to 59.51 MW. Furthermore, the voltage profile is increased from 0.6849 p.u. to 1.0053 p.u.. The cost of installation is US$ 147, 444.23. The results for other λ values are indicated in the same table.

Table 5.15: UPFC sizing when bus 26 and bus 14 was reactively loaded: IEEE 30-bus RTS

Test Bus	λ	Location (Line No.)	Sizing	
			p.u.	MVAr
26	2.3	1	-0.4230	-142.7868
		31	-0.4178	-8.9658
		2	-0.1129	83.2543
		5	-0.6789	-104.9522
		37	-0.7235	-43.7493
14	3.7	1	-0.4228	-142.7962
		2	-0.4177	-9.1345
		5	-0.1127	83.2366
		37	-0.6790	-104.9983
		12	-0.7239	-43.7391

Table 5.15 tabulates the sizing values for UPFC with the implementation of CUPFC optimization using EP in order to reduce the transmission losses when λ variation is subjected to bus 14 and bus 26.

(b) CUPFC in the IEEE 118-bus RTS

The test was conducted on the IEEE 118-bus RTS with buses namely bus 22 and bus 78 are reactively loaded. The results for a weak bus namely bus 22 are tabulated in Table 5.16. From the table, bus 22 was subjected to variation of loading conditions indicated by; where λ is increased gradually in order to observe the effect of transmission losses, voltage profile and cost of installation. With the implementation of CUPFC, the voltage profile in the system is improved and transmission losses are minimized. It can be seen that at $\lambda = 10$, the transmission loss is reduced from 305.3 MW to 269.63 MW which implies 11.7% reduction. Furthermore, the voltage profile is also improved from 0.8198 p.u. to 0.8496 p.u.. The cost of UPFC installation is US$3,818.55. The results for other λ values are indicated in the same table.

Table 5.16: Results for CUPFC when bus 22 was reactively loaded: IEEE 118-bus RTS.

λ	Analysis CUPFC	Transmission loss (MW)	ΔLoss (%)	V_m (p.u)	Cost (US$)
2	Pre	298.46	4.5	0.9373	55,453.80
	Post	284.94		0.9400	
4	Pre	299.37	5.5	0.9110	55,462.98
	Post	282.84		0.9128	
6	Pre	300.73	5.6	0.8830	32,955.00
	Post	283.96		0.8955	
8	Pre	302.66	5.9	0.8528	53,361.09
	Post	284.67		0.8554	
10	Pre	305.30	11.7	0.8198	53,818.55
	Post	269.63		0.8496	

Table 5.17 tabulates the effect of λ increment to voltage profiles, transmission losses and installation cost for load subjected to a secure bus namely bus 78 considering transmission loss minimization as an objective function. Referring to the table, it is

Table 5.17: Results for CUPFC when bus 78 was reactively loaded: IEEE 118-bus RTS.

λ	Analysis CUPFC	Transmission loss (MW)	ΔLoss (%)	V_m (p.u)	Cost (US$)
10	Pre	298.37	7.7	0.995	55,085.66
	Post	275.29		0.995	
30	Pre	301.39	7.7	0.972	55,114.26
	Post	278.28		0.972	
50	Pre	307.87	7.5	0.9478	55,181.94
	Post	284.71		0.9479	
100	Pre	343.80	8.1	0.8803	27,307.49
	Post	315.93		0.8822	

observed that at λ = 100, the transmission loss has been reduced from 343.80 MW to 315.93 MW which implies 8.1 % reduction. A small increment is indicated for voltage profile from 0.8803 p.u. to 0.8822 p.u.. The cost of installation for UPFC is $US 27,307.49. The results for other λ values are indicated in the same table.

Table 5.18: TCSC sizing when bus 22 and bus 78 was reactively loaded: IEEE 118-bus RTS

Test Bus	λ	Location (Line No.)	Sizing	
			p.u.	MVAr
22	10	101	0.1545	25.8409
		100	-0.7534	-91.9935
		27	-0.1088	-134.6647
		92	0.0751	-108.7890
		104	-0.2544	-15.9539
		94	-0.2243	-136.7844
		64	-0.5825	-135.6302
		63	0.1679	62.9839
		102	0.0606	171.1220
		31	-0.2838	48.2739
78	100	101	-0.3095	25.8409
		100	-0.7442	-91.9935
		92	0.1733	-134.6647
		104	-0.6548	-108.7890
		120	0.1045	-15.9539
		94	-0.7151	-136.7844
		102	-0.2402	-135.6302
		64	-0.5737	62.9839
		63	-0.5188	171.1220
		103	-0.0380	48.2739

As stated in Table 5.18, it can be seen that the sizing values for CUPFC are the optimized UPFC values determined by the EP for the transmission losses minimization in the system when λ variation is subjected to bus 22 and 78. Some locations may be required an inductive compensation and in some location will be required a capacitive compensation in order to minimize the transmission loss for the whole system.

5.8 COMPARATIVE STUDIES OF FACTS OPTIMIZATION BETWEEN EVOLUTIONARY PROGRAMMING AND ARTIFICIAL IMMUNE SYSTEM

A comparative study is performed by implementing similar scheme, using artificial immune system. The comparisons are made in terms of transmission losses, voltage profile and installation cost.

5.8.1 Constrained Static VAR Compensator

The results obtained from the implementation of CSVC scheme are compared between EP and AIS for each participating bus. The comparisons are made in terms transmission loss reduction, voltage profile and cost of installation.

(a) Comparison of CSVC in the IEEE 30-bus RTS

The result for CSVC scheme performed at all the selected load buses namely bus 26 amd bus 14 using EP and AIS are tabulated in Table 5.19 and Table 5.20. Table 5.19 tabulates the results of comparative studies using EP and AIS for transmission loss minimization (TLM) as the objective function when bus 26 was loaded. From the table, it is observed that when EP was used to optimize the SVC, it gives better results as compared to AIS in terms of transmission losses reduction. However, it is noticed that AIS outperformed EP in term of voltage profile and installation cost. For instance, at λ = 3.2 , EP has reduced the transmission loss from 111.38 MW to 59.22 MW which implies

46.89% as compared to AIS which only managed to reduce to 67.59 MW which implies 39.3% . On the other hand, AIS has improved the voltage profile from 0.5571 p.u. to 1.2586 p.u. but for the EP, voltage profile has only been increased to 1.0789 p.u.. In addition, installation cost of five SVC devices equal to US$ 90, 629.36 is obtained by AIS technique, while for the same number of SVC devices; the installation cost obtained by EP technique is US$ 97, 227.54 which is higher than AIS.

Table 5.19: Comparison results for CSVC between EP and AIS when bus 26 was loaded: IEEE 30-bus RTS.

λ	Pre-CSVC		Post-CSVC							
			EP				AIS			
	Voltage (V)	Loss (MW)	Voltage (V)	Loss (MW)	ΔLoss (%)	Cost (US$)	Voltage (V)	Loss (MW)	ΔLoss (%)	Cost (US$)
2.0	0.8235	82.74	0.8459	55.20	33.3	44,091.35	0.8235	63.29	23.5	39,393.91
2.5	0.7584	87.26	0.9489	61.22	29.8	53,998.39	1.0246	71.55	18.0	48,614.89
3.0	0.6671	95.94	1.1093	59.42	38.1	70,055.27	1.3022	69.29	27.8	66,863.44
3.2	0.5571	111.38	1.0789	59.22	46.8	97,227.54	1.2586	67.59	39.3	90,629.36

Table 5.20 tabulates the comparison of results between EP and AIS for a secure bus in the system namely bus 14. It is observed that EP outperformed AIS in terms of transmission losses only. For instance, at $\lambda = 3.2$, EP has reduced the total transmission loss value from 111.38 MW to 59.22 MW while AIS only manages to reduce to 67.59 MW only. In contrast, AIS outperformed EP in terms of voltage profile with the improvement from 0.6849 p.u. to 1.3611 p.u. as compared to EP which is only able to increase the voltage up to 1.033 p.u.. Then again, the installation cost of CSVC

Table 5.20: Comparison results for CSVC between EP and AIS when bus 14 was loaded: IEEE 30-bus RTS.

λ	Pre-CSVC		Post-CSVC							
			EP				AIS			
	Voltage (V)	Loss (MW)	Voltage (V)	Loss (MW)	ΔLoss (%)	Cost (US$)	Voltage (V)	Loss (MW)	ΔLoss (%)	Cost (US$)
1.0	0.8882	82.48	1.0957	54.75	33.6	44,414.33	0.9394	70.16	14.9	31,359.95
2.0	0.8355	88.77	1.0546	56.44	36.4	56,737.81	1.1381	64.94	26.8	26,453.66
3.0	0.7673	99.91	0.8174	56.97	43.0	77,954.69	1.103	64.40	35.5	50,206.81
3.7	0.6849	121.19	1.033	60.39	50.2	118,165.25	1.3611	90.26	25.5	117,614.22

optimized using AIS technique is US$ 117, 614.22 which is lower as compared to EP. The installation cost optimized using EP is US$ 118, 165.25.

(b) Comparison of CSVC in the IEEE 118-bus RTS

The result for CSVC scheme performed at all similar selected load buses using EP and AIS are tabulated in Table 5.21 and Table 5.22. Table 5.21 tabulates the results of comparative studies using EP and AIS at bus 22 as the weak bus. From the table, EP managed to improve the voltage profile value as compared to AIS with the implementation of CSVC optimization. EP demonstrates significant transmission loss reduction as compared to AIS for each λ value. However, AIS outperformed EP in terms of cost of installation for most λ values except for λ = 4 and 6.

Table 5.21: Comparison results for CSVC between EP and AIS when bus 22 was loaded: IEEE 118-bus RTS.

λ	Pre-CSVC		Post-CSVC							
			EP				AIS			
	Voltage (V)	Loss (MW)	Voltage (V)	Loss (MW)	ΔLoss (%)	Cost (US$)	Voltage (V)	Loss (MW)	ΔLoss (%)	Cost (US$)
2	0.9373	298.46	0.9377	291.92	2.2	18,470.44	0.9372	295.24	1.1	12,018.16
4	0.9110	299.37	0.9115	292.86	2.2	17,012.09	0.9112	293.62	1.9	17,164.79
6	0.8830	300.73	0.9067	293.76	2.3	16,498.30	0.9054	296.68	1.3	18,119.16
8	0.8528	302.66	0.8699	295.27	2.4	17,057.57	0.8609	298.90	1.2	8,046.90
10	0.8198	305.30	0.8489	297.70	2.5	19,347.53	0.8303	300.73	1.5	12,878.88

Table 5.22 tabulates the results of comparative studies using EP and AIS when λ variation is subjected to bus 78. From the table, it is observed that when EP was used to optimize the SVC, it gives better results as compared to AIS in terms of transmission loss reduction. At λ=100, EP has reduced the transmission loss from 343.80 MW to 337.71 MW as compared to AIS which slightly reduced to 338.04 MW. However, it is observed that both methods were unsuccessful to improve the voltage profile for all λ in the system. In contrast, an installation cost of ten SVC devices is equal to US$ 15, 991.23 is obtained by AIS technique, while for the same number of SVC devices the installation cost obtained by EP technique is US$ 19, 335.44 which is higher than AIS.

Table 5.22: Comparison results for CSVC between EP and AIS when bus 78 was loaded: IEEE 118-bus RTS.

λ	Pre-CSVC		Post-CSVC							
			EP				AIS			
	Voltage (V)	Loss (MW)	Voltage (V)	Loss (MW)	ΔLoss (%)	Cost (US$)	Voltage (V)	Loss (MW)	ΔLoss (%)	Cost (US$)
10	0.9950	298.37	0.9950	292.12	2.1	19,332.18	0.9950	295.15	1.1	12,011.95
30	0.9720	301.39	0.9720	295.13	2.1	19,341.57	0.9720	298.16	1.1	12,016.31
50	0.9478	307.87	0.9478	301.59	2.0	19,363.40	0.9478	304.63	1.1	12,026.67
100	0.8803	343.80	0.8803	337.71	1.8	19,335.44	0.8803	338.04	1.7	15,991.23

5.8.2 Constrained Thyristor Controlled Static Compensator

The results obtained from the implementation of CTCSC scheme are compared between EP and AIS for each participating bus. The comparisons are made in terms of transmission loss reduction, voltage profile and cost of installation.

(a) Comparison of CTCSC in the IEEE 30-bus RTS

The results for comparative studies when load was subjected at bus 26 are tabulated in Table 5.23. From the table, it is observed that when EP was used to optimize the CTCSC, it gives better results as compared to AIS in terms of transmission loss value. For instance, at $\lambda = 2.3$, EP method manages to reduce the transmission loss value from 111.38 MW to 89.59 MW while AIS only managed to reduce its value to 97.12 MW. This indicates that EP outperformed AIS in terms of loss reduction. On the other hand, AIS outperformed EP in terms of voltage profile and installation cost. It has increased the voltage profile in the system from 0.5571 p.u. to 0.6792 p.u., while its value is 0.6578 p.u. obtained using EP. Furthermore, the installation cost for five TCSC devices using EP is US$ 58,359.27 and while the cost is US$ 42,550.94 using AIS. It reveals that AIS outperformed EP indicated by lower installation cost shown in the table.

Table 5.23: Comparison results for CTCSC between EP and AIS when bus 26 was loaded: IEEE 30-bus RTS.

λ	Pre-CTCSC		Post-CTCSC							
			EP				AIS			
	Voltage (V)	Loss (MW)	Voltage (V)	Loss (MW)	ΔLoss (%)	Cost (US$)	Voltage (V)	Loss (MW)	ΔLoss (%)	Cost (US$)
1.0	0.8235	82.74	0.8459	75.71	8.5	28,787.82	0.8277	81.70	1.3	6,075.74
1.5	0.7584	87.26	0.784	78.80	9.7	32,338.90	0.7628	82.00	6.0	18,794.71
2.0	0.6671	95.94	0.716	84.28	12.2	35,864.73	0.7345	91.00	5.2	21,163.98
2.3	0.5571	111.38	0.6578	89.59	19.6	58,359.27	0.6792	97.12	12.8	42,550.94

The results for comparative studies performed using EP and AIS at all λ variation subjected to bus 14 are tabulated in Table 5.24. From the table, at λ =3.7 it can be seen that EP has outperformed AIS in terms of loss minimization. The CTCSC scheme implemented using EP techniques managed to reduce the transmission loss from 121.19 MW to 91.78 MW as compared to AIS which only able to reduce the value to 115.95 MW. This indicates a significant difference between EP and AIS. On the other hand, it is observed that both methods share the same increment in terms of voltage profile value where the voltage profile is improve from 0.6849 p.u. to 0.7576 p.u., respectively as highlighted in the table. The installation cost using AIS is US$ 16, 983.59 lower than the cost optimized using EP (US$ 83, 657.24).

Table 5.24: Comparison results for CTCSC between EP and AIS when bus 14 was loaded: IEEE 30-bus RTS.

λ	Pre-CTCSC		Post-CTCSC							
			EP				AIS			
	Voltage (V)	Loss (MW)	Voltage (V)	Loss (MW)	ΔLoss (%)	Cost (US$)	Voltage (V)	Loss (MW)	ΔLoss (%)	Cost (US$)
1.0	0.8882	82.48	0.9143	75.35	8.6	28,971.39	0.9143	77.20	6.4	22,395.30
2.0	0.8355	88.77	0.8708	78.99	11.0	36,898.58	0.8708	81.36	8.3	28,411.43
3.0	0.7673	99.91	0.8174	84.67	15.3	50,255.19	0.8174	87.88	12.0	40,230.00
3.7	0.6849	121.19	0.7576	91.78	24.3	83,657.24	0.7576	115.95	4.3	16,983.59

(b) Comparison of CTCSC in the IEEE 118-bus RTS

The result of comparative studies for CTCSC scheme performed at all selected load buses using EP and AIS are tabulated in Table 5.25 and Table 5.26. Table 5.25 tabulates the results of comparative studies using EP and AIS. At λ=10, EP manages to reduce the transmission loss and increase the voltage profile value as compared to AIS. This observation highlights the strength of EP over AIS technique. Additionally, EP also outperformed AIS in terms of installation cost at certain λ value; λ =2 and λ = 10.

Table 5.25: Comparison results for CTCSC between EP and AIS when bus 22 was loaded: IEEE 118-bus RTS.

λ	Pre-CTCSC		Post-CTCSC							
			EP				AIS			
	Voltage (V)	Loss (MW)	Voltage (V)	Loss (MW)	ΔLoss (%)	Cost (US$)	Voltage (V)	Loss (MW)	ΔLoss (%)	Cost (US$)
2	0.9373	298.4641	0.9392	265.71	11.0	50,466.80	0.9397	276.17	7.5	53,591.75
4	0.911	299.3705	0.9135	266.74	10.9	51,092.88	0.9118	291.20	2.7	23,185.02
6	0.883	300.7335	0.8867	271.26	9.8	47,934.75	0.8914	294.17	2.2	39,830.38
8	0.8528	302.6591	0.855	269.37	11.0	37,474.93	0.8535	283.44	6.3	31,184.87
10	0.8198	305.3025	0.8378	274.22	10.2	46,549.36	0.8287	297.44	2.6	49,136.00

Table 5.26 tabulates the results of comparative studies using EP and AIS when bus 78 was reactively loaded shown by the variation in λ value. From the table, it is observed that when EP was used to optimize the CTCSC, it gives better results as compared to AIS in terms of transmission loss reduction. At λ = 100, EP technique successfully reduces the transmission loss from 343.80 MW to 314.58 MW but for the AIS, transmission loss is only reduced to 318.6 MW. However, EP and AIS give close values in terms of voltage profile in all λ value. The installation cost for EP and AIS at λ =100 is US$ 32,141.45 and US$ 48,970.97, respectively as highlighted in the table. This implies the superiority of EP over AIS.

Table 5.26: Comparison results for CTCSC between EP and AIS when bus 78 was loaded: IEEE 118-bus RTS.

λ	Pre-CTCSC		Post-CTCSC							
			EP				AIS			
	Voltage (V)	Loss (MW)	Voltage (V)	Loss (MW)	ΔLoss (%)	Cost (US$)	Voltage (V)	Loss (MW)	ΔLoss (%)	Cost (US$)
10	0.9950	298.37	0.9950	273.76	8.2	34,822.51	0.9950	289.96	2.8	22,402.11
30	0.9720	301.39	0.9720	276.75	8.2	34,844.10	0.9721	292.96	2.8	22,422.28
50	0.9478	307.87	0.9478	283.18	8.0	34,894.60	0.9479	299.40	2.8	22,468.21
100	0.8803	343.80	0.8812	314.58	8.5	32,141.45	0.8814	318.60	7.3	48,970.97

5.8.3 Constrained Unified Power Flow Controlled

The results obtained from the implementation of CUPFC scheme are compared between EP and AIS for each participating bus. The comparisons are made in terms of transmission loss reduction, voltage profile and cost of installation.

(a) Comparison of CUPFC in the IEEE 118-bus RTS

The result for the comparative studies of CUPFC performed at all selected load buses using EP and AIS are tabulated in Table 5.27 and Table 5.28. Table 5.27 tabulates the results of comparative studies using EP and AIS when bus 26 was reactively loaded indicated in the variation of λ value. From the table, it is observed that when EP was used to optimize the CUPC, it gives better results as compared to AIS in terms of transmission loss reduction and voltage profile improvement. At λ = 2.3, EP method has successfully reduced the transmission loss value from 111.38 MW to 58.45 MW while AIS only manages to reduce to 71.33 MW. As for the voltage profile, EP outperformed AIS by improving the voltage profile from 0.5571 p.u. to 0.9132 p.u. as compared to AIS which only managed to increase the voltage profile to 0.7736 p.u.. In addition, an installation cost of US$ 125,540.87 is obtained using EP technique which is lower than AIS technique. This reveals the superiority of EP with respect to AIS.

Table 5.27: Comparison results for CUPFC between EP and AIS when bus 26 was loaded: IEEE 30-bus RTS.

λ	Pre-CUPFC		Post-CUPFC							
			EP				AIS			
	Voltage (V)	Loss (MW)	Voltage (V)	Loss (MW)	ΔLoss (%)	Cost (US$)	Voltage (V)	Loss (MW)	ΔLoss (%)	Cost (US$)
1.0	0.8235	82.74	1.0264	55.95	32.4	67,895.67	0.8325	74.83	9.6	32,682.20
1.5	0.7584	87.26	1.1438	58.27	33.2	94,829.49	0.7822	61.33	29.7	76,017.33
2.0	0.6671	95.94	1.3173	64.34	32.9	112,342.98	0.6789	74.61	22.2	62,569.61
2.3	0.5571	111.38	0.9132	58.45	47.5	113,471.41	0.7736	71.33	36.0	125,540.87

Table 5.28 tabulates the comparison results between EP and AIS for a secure bus namely bus 14 in the system. From the table, it is discovered that EP performed better than AIS since EP managed to reduce the largest transmission loss in the system. For instance, at λ = 3.7, EP method has reduced the transmission loss value from 121.19 MW to 59.51 MW while AIS only managed to reduce the transmission loss value to 62.79 MW. In contrast, AIS outperformed EP in terms of voltage profile with the increment from 0.6849 p.u. to 1.2384 p.u. as compared to EP which is only able to increase the voltage up to 1.0053 p.u.. However, EP outperforms AIS at other λ values. Additionally, the installation cost for EP and AIS at λ = 3.7 is US$ 147, 444.23 and US$ 135, 371.14, respectively as highlighted in the table.

Table 5.28: Comparison results for CUPFC between EP and AIS when bus 14 was loaded: IEEE 30-bus RTS.

λ	Pre-CUPFC		Post-CUPFC							
			EP				AIS			
	Voltage (V)	Loss (MW)	Voltage (V)	Loss (MW)	ΔLoss (%)	Cost (US$)	Voltage (V)	Loss (MW)	ΔLoss (%)	Cost (US$)
1.0	0.8882	82.48	1.104	55.51	32.7	68,369.93	1.0071	63.10	23.5	68,257.26
2.0	0.8355	88.77	1.0021	60.40	32.0	59,741.60	0.9293	64.69	27.1	46,719.96
3.0	0.7673	99.91	1.0197	56.39	43.6	106,161.29	0.8253	75.98	24.0	73,077.95
3.7	0.6849	121.19	1.0053	59.51	50.9	147,444.23	1.2384	62.79	48.2	135,371.14

(b) Comparison of CUPFC in the IEEE 118-bus RTS

The result for the CUPFC scheme performed at all selected load buses using EP and AIS are tabulated in Table 5.29 and Table 5.30. Table 5.29 tabulates the results of comparative studies using EP and AIS when load variation (λ) is subjected to bus 22. At $\lambda = 10$, EP managed to reduce the largest amount of transmission loss as compared to AIS. In addition, EP also improves the voltage profile value as compared to AIS at this λ value ($\lambda = 10$). This reveals the superiority of EP with respect to AIS. In contrast, the cost of installation required by EP is higher than AIS at this λ value

Table 5.29: Comparison results for CUPFC between EP and AIS when bus 22 was loaded: IEEE 118-bus RTS.

λ	Pre-CUPFC		Post-CUPFC							
			EP				AIS			
	Voltage (V)	Loss (MW)	Voltage (V)	Loss (MW)	ΔLoss (%)	Cost (US$)	Voltage (V)	Loss (MW)	ΔLoss (%)	Cost (US$)
2	0.9373	298.46	0.94	284.94	4.5	55,453.80	0.9395	287.23	3.8	44,179.04
4	0.9110	299.37	0.9128	282.84	5.5	55,462.98	0.9116	293.49	2.0	82,061.61
6	0.8830	300.73	0.8955	283.96	5.6	32,955.00	0.9018	292.29	2.8	95,717.90
8	0.8528	302.66	0.8554	284.67	5.9	53,361.09	0.8605	293.90	2.9	95,828.74
10	0.8198	305.30	0.8496	269.63	11.7	53,818.55	0.8236	284.95	6.7	42,300.08

Table 5.30 tabulates the results of comparative studies using EP and AIS when bus 78 was subjected to load variation indicated by λ value. From the table, it is observed that EP gives better results as compared to AIS in all criteria except for voltage profile. At λ=100, EP technique successfully reduces the transmission loss value from 343.8 MW to 315.93 MW as compared to 321.21 MW performed using AIS.

As for the voltage profile, both methods failed to improve the voltage profile except at λ=100. AIS gives better results as compared to EP. AIS managed to improve a small amount of voltage profile in the system from 0.8803 p.u. to 0.8841 p.u. as compared to EP with the amount of 0.8822 p.u.. On the other hand, the installation cost for the CUPFC using EP is US$ 27, 307.49 which is lower then the cost optimized using AIS. The installation cost for AIS is US$ 86, 875.74 shown in the table.

Table 5.30: Comparison results for CUPFC between EP and AIS when bus 78 was loaded: IEEE 118-bus RTS.

λ	Pre-CUPFC		Post-CUPFC							
			EP				AIS			
	Voltage (V)	Loss (MW)	Voltage (V)	Loss (MW)	ΔLoss (%)	Cost (US$)	Voltage (V)	Loss (MW)	ΔLoss (%)	Cost (US$)
10	0.995	298.37	0.995	275.29	7.7	55,085.66	0.995	284.79	4.6	62,294.19
30	0.972	301.39	0.972	278.29	7.7	55,114.26	0.972	287.78	4.5	62,319.08
50	0.9478	307.87	0.9478	284.71	7.5	55,181.94	0.9478	294.22	4.4	62,377.18
100	0.8803	343.80	0.8822	315.93	8.1	27,307.49	0.8841	321.21	6.6	86,875.74

5.9 SUMMARY

This chapter has presented the application of evolutionary programming optimization technique implemented for FACTS in order to minimize the total transmission losses in a system under *(N-m)* contingencies. The studies proposed the CSVC, CTCSC and CUPFC as three constrained FACTS schemes. For each scheme, transmission loss minimization as the objective function was implemented with the transmission loss in the system as the fitness function.

The *SVSI* technique was applied as the tool to identify the FACTSs location in the system. When the load flow program was run, stability indices are calculated for FACTS placed in every line one at a time for the same operating conditions and the system identified the lines with the highest *SVSI* for the purpose of installing the FACTS. The EP optimization technique is then used to determine the suitable sizing value of the FACTS devices namely SVC, TCSC and UPFC to be installed in order to minimize the total transmission loss in the system.

Finally, results obtained from the EP techniques were compared with AIS. From the study, EP outperformed AIS for 84 cases out 153 cases for TLM therefore EP gives better results in transmission loss minimization in the system as compared to AIS technique.

CHAPTER 6
OPERATING GENERATOR SCHEDULING (OGS) FOR INTELLIGENT REACTIVE POWER CONTROL

6.1 INTRODUCTION

This chapter presents a new approach for operating generator scheduling (OGS) to be applied on reactive power control based on Evolutionary Programming optimization technique in power system. The proposed technique determines the best combination of generator that should be dispatched by the reactive power in the system based on *SVSI*, total transmission loss and installation cost in order to improve voltage stability condition of a system. Two objective functions were considered separately for the OGS namely improving voltage stability condition indicated by reduction in *SVSI* and TLM in the system. In the beginning, *SVSI* was taken as the fitness to determine the optimum values of RPC and then the optimization was repeated for total transmission loss minimization as the fitness function. The operating generator scheduling is developed to assist the system operator in scheduling the generator units in an economic way or as required by the utility company. In this study, an assumption is made, i.e. the technique is not a unit commitment based approach. A computer program was written in MATLAB and the proposed techniques were tested on the IEEE 30-bus RTS. A novel technique to schedule the generator units that should be dispatched the reactive power to power system network is introduced.

6.2 APPLICATION OF EVOLUTIONARY PROGRAMMING FOR OPERATING GENERATOR SCHEDULING

Operating generator scheduling involves selecting the combination of generator that should dispatch the reactive power compensator support to the system thus improving the power system security by considering the voltage stability index, total transmission loss and installation cost. This will assist the power system operator in the decisions making process which is required by the utility companies. For economic allocation of reactive power by generator to meet system demand, a suitable decision making tool is required. The development of operating generator scheduling algorithm is important to help the system operator in choosing the right solution for improving the power system required by utility companies. In practice, system operators optimize the system such that the total transmission loss is minimized while the system operates within the security region. The balance between the cost of improving and maintaining the power system stability is a main factor in electricity market.

6.2.1 Algorithm for Operating Generator Scheduling

Figure 6.1 illustrates the general algorithm for OGS. The following procedures present the implementation of OGS in order to identify the best combination of generators that should be dispatched the reactive power to the system.

i. Set the combination of operating generator for the RPC scheme which includes i.e. G_2, G_5, G_8, G_{11} and G_{13} appointed to the generators.
ii. Determine *SVSI* value, total transmission loss, voltage profile and installation cost by running the RPC optimization technique process using for both objective function namely VSI and TLM. [The flowchart for the RPC optimization using EP is shown in Figure 6.2. The details procedures can be referred in section 4.3]
iii. Check for the combination of operating generator. If combination is completed go to step (iv), otherwise go to step (i).
iv. Identify the operating generator by listing and ranking the generator based on *SVSI*, total transmission loss and installation cost.
v. End

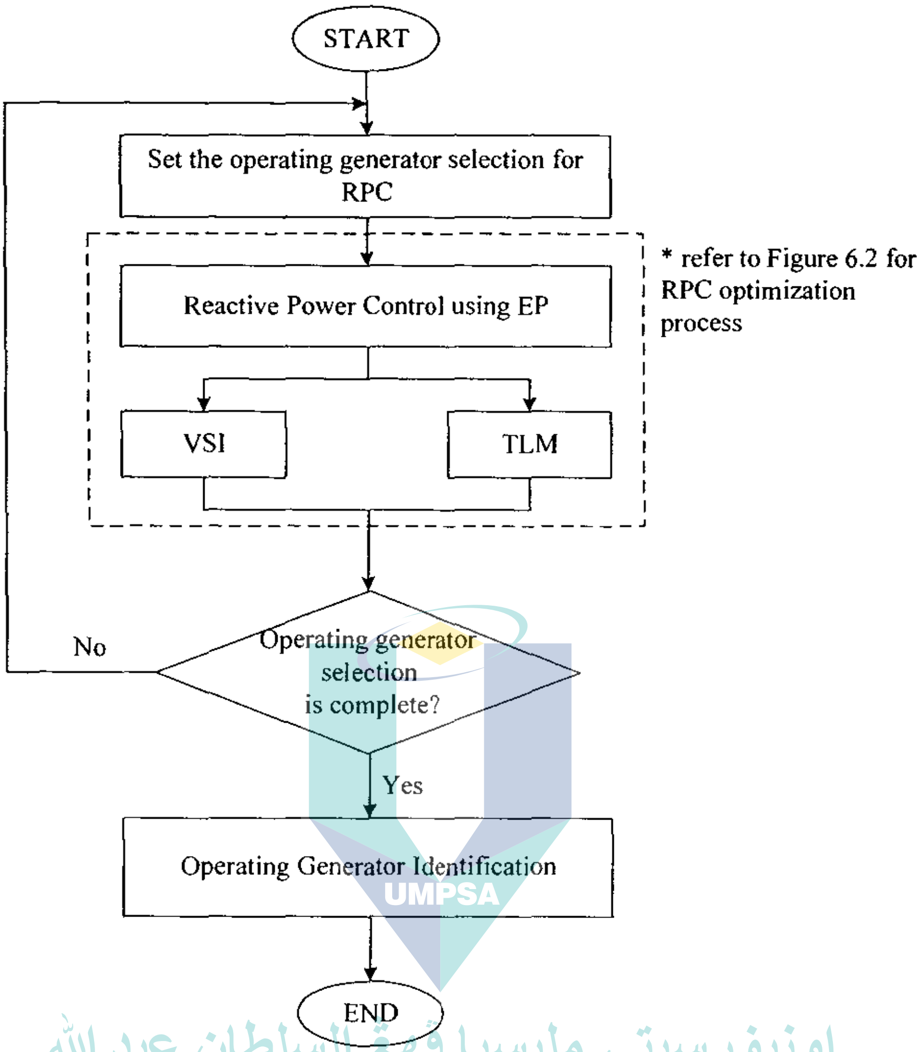

Figure 6.1: OGS block diagram

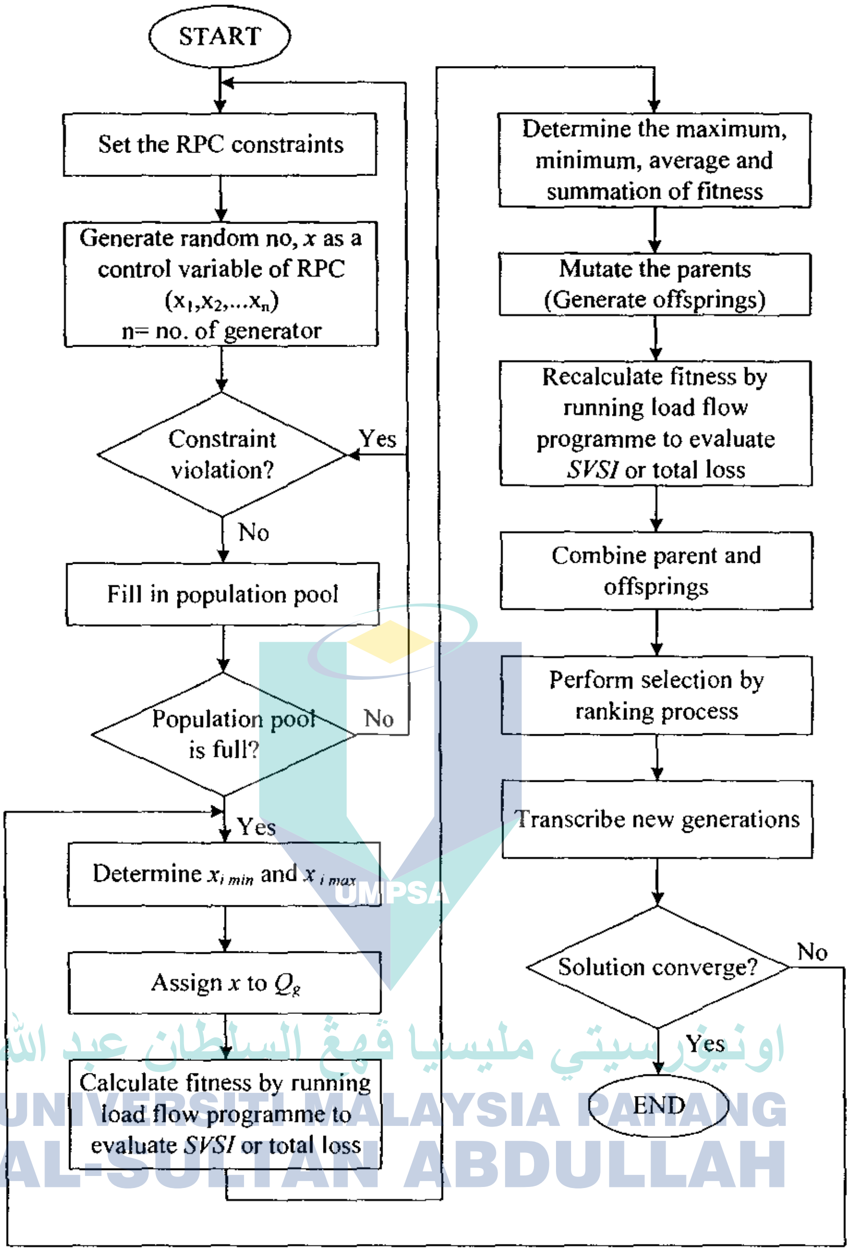

Figure 6.2: Flowchart for the RPC using EP

6.3 RESULTS AND DISCUSSION

The results are divided in two sub-sections. The first part presents the results for combination of generator applied for RPC with VSI as the objective function and the second part presents the results applied for RPC with TLM as the objective function.

The optimization engine is executed at the maximum loadability point at the respective load bus so that the *SVSI*, voltage profiles, total transmission loss variations and installation cost can be monitored.

6.3.1 Results for Operating Generator Scheduling using Evolutionary Programming Technique

The analysis was conducted at various combinations of generators to see the effect to the *SVSI*, total transmission loss and installation cost. There were two constraints assigned in each combination of generator before the RPC is implemented with EP. Similar test systems are considered for this case. The results for VSI as the objective function are tabulated in Table 6.1, Table 6.2 and Table 6.3 while Table 6.4, Table 6.5 and Table 6.6 tabulate the TLM as the object function. The test system parameters values for pre-RPC are shown below.

Bus No = 26

$\lambda = 3.2$

Population = 20

SVSI = 0.588

Total Transmission Loss = 28.82 MW

Voltage = 0.6511 p.u.

Q_{g2} = 65.578 MVAr

Q_{g5} = 39.350 MVAr

Q_{g8} = 61.693 MVAr

Q_{g11} = 23.741 MVAr

Q_{g13} = 20.544 MVAr

6.3.1.1 Voltage Stability Improvement as the Objective Function

In this study, EP with VSI as the objective function is performed to the system with bus 26 subjected to maximum loadability with various combinations of generator applied for RPC. Table 6.1, Table 6.2 and Table 6.3 tabulate the effect of generator variation to *SVSI*, total transmission losses, voltage profile and installation cost, respectively. Each table is ranked based on *SVSI* value, total transmission loss and installation cost in order to observe the effect of generator combination in the system.

SVSI has a value between 0 and 1, in which 0 represents the no-load condition and 1 represents unstable condition. Therefore, to obtain stability in the system, *SVSI* has to be maintained far below 1.

Each combination require single run of EP; therefore for the whole generator combinations 31 EP optimization processes are implemented. As tabulated in Table 6.1, there are 31 possible combinations for performing the optimal RPC process. It is

Table 6.1-*SVSI* ranking of operating generator scheduling for RPC : VSI as the objective function

Operating Generator					*SVSI*	Trans. Loss (MW)	Voltage (p.u.)	Q_{g2}	Q_{g5}	Q_{g8}	Qg_{11}	Q_{g13}	Cost (£)
G_2	G_5	G_8	G_{11}	G_{13}				MVAr					
1	1	1	1	1	0.3188	11.69	0.9137	33.032	17.213	28.336	21.930	18.525	£3,589,368.97
1	1	1	0	1	0.3842	11.96	0.8280	34.719	34.853	25.546		17.926	£3,408,919.87
1	1	1	1	0	0.3884	11.92	0.8231	34.719	34.853	25.546	17.926		£3,408,877.63
0	1	1	1	1	0.4080	11.19	0.8017		27.838	34.853	15.474	17.927	£2,899,477.64
1	1	1	0	0	0.4266	12.19	0.7825	29.849	37.275	33.994			£3,050,433.38
1	0	1	1	1	0.4361	17.13	0.7730	34.720		34.853	15.474	17.927	£3,112,713.72
0	1	1	0	1	0.4515	11.69	0.7585		23.960	37.278		20.457	£2,467,137.95
0	1	1	1	0	0.4524	11.57	0.7576		23.960	37.278	20.457		£2,467,000.20
0	0	1	1	1	0.4679	18.99	0.7436			23.961	22.394	20.457	£2,028,985.50
1	0	1	0	1	0.4775	17.71	0.7352	29.847		37.278		20.457	£2,650,616.75
1	1	0	1	1	0.4792	14.92	0.7338	17.071	25.665		18.393	23.790	£2,568,566.44
1	0	1	1	0	0.4800	17.62	0.7330	29.849		37.278	20.457		£2,650,602.28
0	1	1	0	0	0.4856	12.18	0.7283		30.494	39.643			£2,119,960.20
0	0	1	0	1	0.5032	19.73	0.7138			37.281		20.457	£1,756,586.57
0	0	1	1	0	0.5038	19.62	0.7132			37.281	20.457		£1,756,501.92
0	1	0	1	1	0.5071	14.88	0.7106		23.960		22.395	20.457	£2,024,273.95
1	1	0	0	1	0.5079	15.70	0.7100	34.254	27.481			22.494	£2,547,727.74
1	0	1	0	0	0.5123	18.27	0.7065	38.050		39.645			£2,353,654.00
1	1	0	1	0	0.5129	15.57	0.7060	34.254	27.481		22.494		£2,547,581.38
1	0	0	1	1	0.5270	24.58	0.6951	29.847			22.395	20.457	£2,211,936.87
0	1	0	0	1	0.5334	15.55	0.6902		30.490			23.791	£1,648,136.23
1	1	0	0	0	0.5358	16.41	0.6884	38.055	39.641				£2,351,582.06
0	0	0	1	1	0.5361	27.18	0.6882				22.396	20.457	£1,318,543.45
0	0	1	0	0	0.5369	20.29	0.6876			37.449			£1,147,578.32
0	1	0	1	0	0.5372	15.56	0.6873		35.995		21.909		£1,756,842.19
1	0	0	0	1	0.5519	25.23	0.6765	38.052				23.791	£1,886,011.42
1	0	0	1	0	0.5553	25.16	0.6741	38.052			23.791		£1,885,925.54
0	1	0	0	0	0.5612	16.09	0.6698		37.443				£1,142,594.87
0	0	0	0	1	0.5634	27.85	0.6683					22.496	£707,578.17
0	0	0	1	0	0.5652	27.77	0.6671				22.496		£707,490.51
1	0	0	0	0	0.5799	25.80	0.6569	46.787					£1,433,987.08

observed that the minimum *SVSI* is obtained when generator 2, 5, 8, 11 and 13 are dispatching the reactive power into the power system. As highlighted in the table, the *SVSI* value is improved from 0.588 to 0.3188 while the total transmission loss is reduced from 28.82 MW to 11.69 MW. In addition, the voltage has been improved from 0.6511 p.u. to 0.9137 p.u.. The cost of capacitor installation is £3,589,368.97. On the other

Table 6.2 - Transmission loss ranking of operating generator scheduling for RPC : VSI as the objective function

Operating Generator					*SVSI*	Trans. Loss (MW)	Voltage (p.u.)	Q_{g2}	Q_{g5}	Q_{g8}	Q_{g11}	Q_{g13}	Cost (£)
G_2	G_5	G_8	G_{11}	G_{13}				MVAr					
0	1	1	1	1	0.4080	11.19	0.8017		27.838	34.853	15.474	17.927	£2,899,477.64
0	1	1	1	0	0.4524	11.57	0.7576		23.960	37.278	20.457		£2,467,000.20
0	1	1	0	1	0.4515	11.69	0.7585		23.960	37.278		20.457	£2,467,137.95
1	1	1	1	1	0.3188	11.69	0.9137	33.032	17.213	28.336	21.930	18.525	£3,589,368.97
1	1	1	1	0	0.3884	11.92	0.8231	34.719	34.853	25.546	17.926		£3,408,877.63
1	1	1	0	1	0.3842	11.96	0.8280	34.719	34.853	25.546		17.926	£3,408,919.87
0	1	1	0	0	0.4856	12.18	0.7283		30.494	39.643			£2,119,960.20
1	1	1	0	0	0.4266	12.19	0.7825	29.849	37.275	33.994			£3,050,433.38
0	1	0	1	1	0.5071	14.88	0.7106		23.960		22.395	20.457	£2,024,273.95
1	1	0	1	1	0.4792	14.92	0.7338	17.071	25.665		18.393	23.790	£2,568,566.44
0	1	0	0	1	0.5334	15.55	0.6902		30.490			23.791	£1,648,136.23
0	1	0	1	0	0.5372	15.56	0.6873		35.995		21.909		£1,756,842.19
1	1	0	1	0	0.5129	15.57	0.7060	34.254	27.481		22.494		£2,547,581.38
1	1	0	0	1	0.5079	15.70	0.7100	34.254	27.481			22.494	£2,547,727.74
0	1	0	0	0	0.5612	16.09	0.6698		37.443				£1,142,594.87
1	1	0	0	0	0.5358	16.41	0.6884	38.055	39.641				£2,351,582.06
1	0	1	1	1	0.4361	17.13	0.7730	34.720		34.853	15.474	17.927	£3,112,713.72
1	0	1	1	0	0.4800	17.62	0.7330	29.849		37.278	20.457		£2,650,602.28
1	0	1	0	1	0.4775	17.71	0.7352	29.847		37.278		20.457	£2,650,616.75
1	0	1	0	0	0.5123	18.27	0.7065	38.050		39.645			£2,353,654.00
0	0	1	1	1	0.4679	18.99	0.7436			23.961	22.394	20.457	£2,028,985.50
0	0	1	1	0	0.5038	19.62	0.7132			37.281	20.457		£1,756,501.92
0	0	1	0	1	0.5032	19.73	0.7138			37.281		20.457	£1,756,586.57
0	0	1	0	0	0.5369	20.29	0.6876			37.449			£1,147,578.32
1	0	0	1	1	0.5270	24.58	0.6951	29.847			22.395	20.457	£2,211,936.87
1	0	0	1	0	0.5553	25.16	0.6741	38.052			23.791		£1,885,925.54
1	0	0	0	1	0.5519	25.23	0.6765	38.052				23.791	£1,886,011.42
1	0	0	0	0	0.5799	25.80	0.6569	46.787					£1,433,987.08
0	0	0	1	1	0.5361	27.18	0.6882				22.396	20.457	£1,318,543.45
0	0	0	1	0	0.5652	27.77	0.6671				22.496		£707,490.51
0	0	0	0	1	0.5634	27.85	0.6683					22.496	£707,578.17

hand, the maximum *SVSI* is accomplished if only generator 2 operates in dispatching the reactive power into the system. It is observed that the *SVSI* value is slightly reduced from 0.588 to 0.5799. It has also reduced the total transmission loss in the system from 28.82 MW to 25.80 MW and at the same time voltage profile has been improved from 0.6511 p.u. to 0.6569 p.u.. The cost of installation is £1,433,987.08.

The performances of the generator combination ranked based on total transmission loss are tabulated in Table 6.2. It is observed that the lowest total transmission loss is obtained when generator 5, 8, 11 and 13 are dispatching the reactive power into the power system network. The total transmission loss is reduced from 28.82 MW to 11.19 MW while the *SVSI* value is improved from 0.588 to 0.4080. In addition, the voltage has been improved from 0.6511 p.u. to 0.8017p.u.. The cost of RPC installation is £2,899,477.64. In contrast, the highest total transmission loss is obtained if only generator 13 operates in dispatching the reactive power into the system. It is observed that the total transmission loss is slightly reduced from 28.82 MW to 27.85 MW. It has also reduced the *SVSI* value in the system from 0.588 to 0.5634 and at the same time voltage profile has been improved from 0.6511 p.u. to 0.6683 p.u.. The cost of installation is £707,578.17.

The performances of the generator combination ranked based on installation cost are tabulated in Table 6.3.It is observed that the smallest installation cost is obtained when generator 5 is dispatching the reactive power to power system. The cost of RPC installation is £707,490.51. The total transmission loss is reduced from 28.82 MW to 27.77 MW while the *SVSI* value is improved from 0.588 to 0.5652. Additionally, the voltage has been improved from 0.6511 p.u. to 0.6671 p.u.. In contrast, the biggest installation cost is obtained if all generators operate in dispatching the reactive power into the system. It is observed that the cost of installation is £3,589,368.97. The total transmission loss is significantly reduced from 28.82 MW to 11.69 MW. It has also improved the *SVSI* value in the system from 0.588 to 0.3188 and at the same time voltage profile has been improved from 0.6511 p.u. to 0.9137 p.u..

Table 6.3 - Installation cost ranking of operating generator scheduling for RPC : VSI as the objective function

Operating Generator					*SVSI*	Trans. Loss (MW)	Voltage (p.u.)	Q_{g2}	Q_{g5}	Q_{g8}	Qg_{11}	Q_{g13}	Cost (£)
G_2	G_5	G_8	G_{11}	G_{13}				MVAr					
0	0	0	1	0	0.5652	27.77	0.6671				22.496		£707,490.51
0	0	0	0	1	0.5634	27.85	0.6683					22.496	£707,578.17
0	1	0	0	0	0.5612	16.09	0.6698		37.443				£1,142,594.87
0	0	1	0	0	0.5369	20.29	0.6876			37.449			£1,147,578.32
0	0	0	1	1	0.5361	27.18	0.6882				22.396	20.457	£1,318,543.45
1	0	0	0	0	0.5799	25.80	0.6569	46.787					£1,433,987.08
0	1	0	0	1	0.5334	15.55	0.6902		30.490			23.791	£1,648,136.23
0	0	1	1	0	0.5038	19.62	0.7132			37.281	20.457		£1,756,501.92
0	0	1	0	1	0.5032	19.73	0.7138			37.281		20.457	£1,756,586.57
0	1	0	1	0	0.5372	15.56	0.6873		35.995		21.909		£1,756,842.19
1	0	0	1	0	0.5553	25.16	0.6741	38.052			23.791		£1,885,925.54
1	0	0	0	1	0.5519	25.23	0.6765	38.052				23.791	£1,886,011.42
0	1	0	1	1	0.5071	14.88	0.7106		23.960		22.395	20.457	£2,024,273.95
0	0	1	1	1	0.4679	18.99	0.7436			23.961	22.394	20.457	£2,028,985.50
0	1	1	0	0	0.4856	12.18	0.7283		30.494	39.643			£2,119,960.20
1	0	0	1	1	0.5270	24.58	0.6951	29.847			22.395	20.457	£2,211,936.87
1	1	0	0	0	0.5358	16.41	0.6884	38.055	39.641				£2,351,582.06
1	0	1	0	0	0.5123	18.27	0.7065	38.050		39.645			£2,353,654.00
0	1	1	1	0	0.4524	11.57	0.7576		23.960	37.278	20.457		£2,467,000.20
0	1	1	0	1	0.4515	11.69	0.7585		23.960	37.278		20.457	£2,467,137.95
1	1	0	1	0	0.5129	15.57	0.7060	34.254	27.481		22.494		£2,547,581.38
1	1	0	0	1	0.5079	15.70	0.7100	34.254	27.481			22.494	£2,547,727.74
1	1	0	1	1	0.4792	14.92	0.7338	17.071	25.665		18.393	23.790	£2,568,566.44
1	0	1	1	0	0.4800	17.62	0.7330	29.849		37.278	20.457		£2,650,602.28
1	0	1	0	1	0.4775	17.71	0.7352	29.847		37.278		20.457	£2,650,616.75
0	1	1	1	1	0.4080	11.19	0.8017		27.838	34.853	15.474	17.927	£2,899,477.64
1	1	1	0	0	0.4266	12.19	0.7825	29.849	37.275	33.994			£3,050,433.38
1	0	1	1	1	0.4361	17.13	0.7730	34.720		34.853	15.474	17.927	£3,112,713.72
1	1	1	1	0	0.3884	11.92	0.8231	34.719	34.853	25.546	17.926		£3,408,877.63
1	1	1	0	1	0.3842	11.96	0.8280	34.719	34.853	25.546		17.926	£3,408,919.87
1	1	1	1	1	0.3188	11.69	0.9137	33.032	17.213	28.336	21.930	18.525	£3,589,368.97

6.3.1.2 Transmission Loss Minimization as the Objective Function

In this study, EP with TLM as the objective function is performed to the system with bus 26 subjected to maximum loadability with various combination of generator applied for RPC. Table 6.4, Table 6.5 and Table 6.6 tabulate the effect of generator variation to *SVSI*, total transmission losses, voltage profile and installation cost, respectively. Each table presents the results based on the ranking in *SVSI* value, total transmission loss and installation cost for all the generator combinations. 31 generators combinations are implemented for this case; thus EP optimization engine is run for 31 times to come out with all the results.

As tabulated in Table 6.4, it is observed that the minimum *SVSI* is obtained when generator 2, 5, 8, 11 and 13 are dispatching the reactive power into power system

Table 6.4 - *SVSI* ranking of operating generator scheduling for RPC : TLM as the objective function

Operating Generator					*SVSI*	Trans. Loss (MW)	Voltage (p.u.)	Q_{g2}	Q_{g5}	Q_{g8}	Q_{g11}	Q_{g13}	Cost (£)
G_2	G_5	G_8	G_{11}	G_{13}				MVAr					
1	1	1	1	1	0.3159	12.06	0.9181	8.713	38.838	38.320	12.157	19.403	£3,541,684.69
1	1	1	0	1	0.4098	11.23	0.7997	4.257	17.270	27.769		14.539	£1,931,827.39
1	1	1	1	0	0.4162	11.09	0.7930	9.738	6.995	23.295	19.455		£1,801,115.98
0	1	1	1	1	0.4194	10.95	0.7898		7.492	19.973	21.645	21.911	£2,147,101.98
1	0	1	1	1	0.4386	16.96	0.7706	17.081		25.671	18.397	23.793	£2,571,595.25
1	1	1	0	0	0.4415	11.66	0.7679	9.130	19.953	35.991			£1,968,470.15
0	1	1	0	1	0.4601	11.63	0.7506		10.631	39.317		17.620	£2,043,271.06
0	1	1	1	0	0.4603	11.51	0.7504		10.633	39.317	17.620		£2,043,191.28
0	0	1	1	1	0.4679	18.99	0.7436			23.970	22.400	20.462	£2,029,588.51
1	0	1	1	0	0.4800	17.62	0.7330	29.855		37.284	20.461		£2,651,075.88
0	1	1	0	0	0.4856	12.18	0.7283		30.479	39.636			£2,119,314.00
1	0	1	0	1	0.4862	17.71	0.7278	13.100		39.319		17.620	£2,124,363.15
1	1	0	1	1	0.4870	14.66	0.7271	18.874	10.614		23.587	17.607	£2,141,159.26
0	0	1	0	1	0.5031	19.72	0.7138			37.287		20.461	£1,756,889.44
0	0	1	1	0	0.5038	19.62	0.7132			37.285	20.461		£1,756,725.03
1	0	1	0	0	0.5123	18.27	0.7065	38.061		39.649			£2,354,095.59
0	1	0	1	1	0.5138	14.81	0.7053		10.631		23.597	17.620	£1,575,300.47
1	1	0	1	0	0.5213	15.17	0.6994	9.128	19.948		21.633		£1,541,553.32
1	0	0	1	1	0.5269	24.58	0.6951	29.855			22.400	20.461	£2,212,478.53
0	0	0	1	1	0.5345	27.15	0.6894				21.646	21.911	£1,339,639.73
0	0	1	0	0	0.5369	20.29	0.6876			37.451			£1,147,625.14
1	1	0	0	1	0.5389	15.26	0.6861	2.692	3.081			13.181	£588,982.88
0	1	0	0	1	0.5500	15.49	0.6779		2.844			17.928	£642,803.20
0	1	0	1	0	0.5504	15.39	0.6776		2.844		17.928		£642,686.63
1	0	0	0	1	0.5519	25.23	0.6765	38.049				23.791	£1,885,927.28
1	1	0	0	0	0.5540	15.49	0.6750	2.675	3.068				£191,918.57
1	0	0	1	0	0.5553	25.16	0.6741	38.052			23.792		£1,885,962.63
0	0	0	0	1	0.5634	27.85	0.6683					22.497	£707,632.02
0	0	0	1	0	0.5651	27.77	0.6671				22.497		£707,544.88
0	1	0	0	0	0.5686	15.80	0.6647		4.576				£156,272.27
1	0	0	0	0	0.5840	25.75	0.6541	21.453					£673,894.29

network. The *SVSI* value is improved from 0.588 to 0.3159 while the total transmission loss is reduced from 28.82 MW to 12.06 MW. In addition, the voltage has been improved from 0.6511 p.u. to 0.9181 p.u.. The cost of RPC installation is £3,541,684.69. On the other hand, the maximum *SVSI* is accomplished if only generator 2 operates in dispatching the reactive power into the system. It is observed that the *SVSI* value is slightly reduced from 0.588 to 0.584. It has also reduced the total transmission loss in the system from 28.82 MW to 25.75 MW and at the same time voltage profile has been improved from 0.6511 p.u. to 0.6541 p.u.. The cost of installation is £673,894.29.

The performances of the generator combination ranked based on the total transmission loss ranking are tabulated in Table 6.5. It is observed that the lowest total transmission loss is obtained when generator 5, 8, 11 and 13 dispatching the reactive power to power system. The total transmission loss is reduced from 28.82 MW to 10.95 MW while the *SVSI* value is improved from 0.588 to 0.4194. In addition, the voltage has been improved from 0.6511 p.u. to 0.7898 p.u.. The cost of RPC installation is £2,147,101.98. In contrast, the lowest total transmission loss is obtained if only generator 13 operates in dispatching the reactive power into the system. It is observed that the total transmission loss is slightly reduced from 28.82 MW to 27.85 MW. It has also reduced the *SVSI* value in the system from 0.588 to 0.5634 and at the same time voltage profile has been improved from 0.6511 p.u. to 0.6683 p.u.. The cost of installation is £707,632.02.

Table 6.5 - Transmission loss ranking of operating generator scheduling for RPC : TLM as the objective function

Operating Generator					*SVSI*	Trans. Loss (MW)	Voltage (p.u.)	Q_{g2}	Q_{g5}	Q_{g8}	Q_{g11}	Q_{g13}	Cost (£)
G_2	G_5	G_8	G_{11}	G_{13}				MVAr					
0	1	1	1	1	0.4194	10.95	0.7898		7.492	19.973	21.645	21.911	£2,147,101.98
1	1	1	1	0	0.4162	11.09	0.7930	9.738	6.995	23.295	19.455		£1,801,115.98
1	1	1	0	1	0.4098	11.23	0.7997	4.257	17.270	27.769		14.539	£1,931,827.39
0	1	1	1	0	0.4603	11.51	0.7504		10.633	39.317	17.620		£2,043,191.28
0	1	1	0	1	0.4601	11.63	0.7506		10.631	39.317		17.620	£2,043,271.06
1	1	1	0	0	0.4415	11.66	0.7679	9.130	19.953	35.991			£1,968,470.15
1	1	1	1	1	0.3159	12.06	0.9181	8.713	38.838	38.320	12.157	19.403	£3,541,684.69
0	1	1	0	0	0.4856	12.18	0.7283		30.479	39.636			£2,119,314.00
1	1	0	1	1	0.4870	14.66	0.7271	18.874	10.614		23.587	17.607	£2,141,159.26
0	1	0	1	1	0.5138	14.81	0.7053		10.631		23.597	17.620	£1,575,300.47
1	1	0	1	0	0.5213	15.17	0.6994	9.128	19.948		21.633		£1,541,553.32
1	1	0	0	1	0.5389	15.26	0.6861	2.692	3.081			13.181	£588,982.88
0	1	0	1	0	0.5504	15.39	0.6776		2.844		17.928		£642,686.63
1	1	0	0	0	0.5540	15.49	0.6750	2.675	3.068				£191,918.57
0	1	0	0	1	0.5500	15.49	0.6779		2.844			17.928	£642,803.20
0	1	0	0	0	0.5686	15.80	0.6647		4.576				£156,272.27
1	0	1	1	1	0.4386	16.96	0.7706	17.081		25.671	18.397	23.793	£2,571,595.25
1	0	1	1	0	0.4800	17.62	0.7330	29.855		37.284	20.461		£2,651,075.88
1	0	1	0	1	0.4862	17.71	0.7278	13.100		39.319		17.620	£2,124,363.15
1	0	1	0	0	0.5123	18.27	0.7065	38.061		39.649			£2,354,095.59
0	0	1	1	1	0.4679	18.99	0.7436			23.970	22.400	20.462	£2,029,588.51
0	0	1	1	0	0.5038	19.62	0.7132			37.285	20.461		£1,756,725.03
0	0	1	0	1	0.5031	19.72	0.7138			37.287		20.461	£1,756,889.44
0	0	1	0	0	0.5369	20.29	0.6876			37.451			£1,147,625.14
1	0	0	1	1	0.5269	24.58	0.6951	29.855			22.400	20.461	£2,212,478.53
1	0	0	1	0	0.5553	25.16	0.6741	38.052			23.792		£1,885,962.63
1	0	0	0	1	0.5519	25.23	0.6765	38.049				23.791	£1,885,927.28
1	0	0	0	0	0.5840	25.75	0.6541	21.453					£673,894.29
0	0	0	1	1	0.5345	27.15	0.6894				21.646	21.911	£1,339,639.73
0	0	0	1	0	0.5651	27.77	0.6671				22.497		£707,544.88
0	0	0	0	1	0.5634	27.85	0.6683					22.497	£707,632.02

The performances of the generator combination based on the installation cost ranking are tabulated in Table 6.6. It is observed that the smallest installation cost is obtained when generator 5 is dispatching the reactive power to the system. The cost of RPC installation is £156,272.27. The total transmission loss is reduced from 28.82 MW to 15.80 MW while the *SVSI* value is improved from 0.588 to 0.5686. Additionally, the voltage has been improved from 0.6511 p.u. to 0.6647 p.u.. In contrast, the largest installation cost is obtained if all generators operate in dispatching the reactive power into the system. It is observed that the cost of installation is £3,541,684.69. The total transmission loss is significantly reduced from 28.82 MW to 12.06 MW. It has also improved the *SVSI* value in the system from 0.588 to 0.3159 and at the same time voltage profile has been improved from 0.6511 p.u. to 0.9181 p.u..

Table 6.6 - Installation cost ranking of operating generator scheduling for RPC : TLM as the objective function

Operating Generator					*SVSI*	Trans. Loss (MW)	Voltage (p.u.)	Q_{g2}	Q_{g5}	Q_{g8}	Qg_{11}	Q_{g13}	Cost (£)
G_2	G_5	G_8	G_{11}	G_{13}				MVAr					
0	1	0	0	0	0.5686	15.80	0.6647		4.576				£156,272.27
1	1	0	0	0	0.5540	15.49	0.6750	2.675	3.068				£191,918.57
1	1	0	0	1	0.5389	15.26	0.6861	2.692	3.081			13.181	£588,982.88
0	1	0	1	0	0.5504	15.39	0.6776		2.844		17.928		£642,686.63
0	1	0	0	1	0.5500	15.49	0.6779		2.844			17.928	£642,803.20
1	0	0	0	0	0.5840	25.75	0.6541	21.453					£673,894.29
0	0	0	1	0	0.5651	27.77	0.6671				22.497		£707,544.88
0	0	0	0	1	0.5634	27.85	0.6683					22.497	£707,632.02
0	0	1	0	0	0.5369	20.29	0.6876			37.451			£1,147,625.14
0	0	0	1	1	0.5345	27.15	0.6894				21.646	21.911	£1,339,639.73
1	1	0	1	0	0.5213	15.17	0.6994	9.128	19.948		21.633		£1,541,553.32
0	1	0	1	1	0.5138	14.81	0.7053		10.631		23.597	17.620	£1,575,300.47
0	0	1	1	0	0.5038	19.62	0.7132			37.285	20.461		£1,756,725.03
0	0	1	0	1	0.5031	19.72	0.7138			37.287		20.461	£1,756,889.44
1	1	1	1	0	0.4162	11.09	0.7930	9.738	6.995	23.295	19.455		£1,801,115.98
1	0	0	0	1	0.5519	25.23	0.6765	38.049				23.791	£1,885,927.28
1	0	0	1	0	0.5553	25.16	0.6741	38.052			23.792		£1,885,962.63
1	1	1	0	1	0.4098	11.23	0.7997	4.257	17.270	27.769		14.539	£1,931,827.39
1	1	1	0	0	0.4415	11.66	0.7679	9.130	19.953	35.991			£1,968,470.15
0	0	1	1	1	0.4679	18.99	0.7436			23.970	22.400	20.462	£2,029,588.51
0	1	1	1	0	0.4603	11.51	0.7504		10.633	39.317	17.620		£2,043,191.28
0	1	1	0	1	0.4601	11.63	0.7506		10.631	39.317		17.620	£2,043,271.06
0	1	1	0	0	0.4856	12.18	0.7283		30.479	39.636			£2,119,314.00
1	0	1	0	1	0.4862	17.71	0.7278	13.100		39.319		17.620	£2,124,363.15
1	1	0	1	1	0.4870	14.66	0.7271	18.874	10.614		23.587	17.607	£2,141,159.26
0	1	1	1	1	0.4194	10.95	0.7898		7.492	19.973	21.645	21.911	£2,147,101.98
1	0	0	1	1	0.5269	24.58	0.6951	29.855			22.400	20.461	£2,212,478.53
1	0	1	0	0	0.5123	18.27	0.7065	38.061		39.649			£2,354,095.59
1	0	1	1	1	0.4386	16.96	0.7706	17.081		25.671	18.397	23.793	£2,571,595.25
1	0	1	1	0	0.4800	17.62	0.7330	29.855		37.284	20.461		£2,651,075.88
1	1	1	1	1	0.3159	12.06	0.9181	8.713	38.838	38.320	12.157	19.403	£3,541,684.69

6.4 SUMMARY

This chapter has presented the application of OGS to be applied on reactive power control based on EP optimization technique in power system. The OGS is developed to assist the system operator in scheduling the generator units in an economic way or as required by the utility company. In this technique, two separate objective functions were implemented namely the VSI with *SVSI* value as the fitness function and TLM with the total transmission loss in the system as the fitness function. Each combination of generators for each objective function is ranked based on *SVSI* value, total transmission loss and installation cost in order to observed the effect of generator combination in the system. The results obtained from the study can be used by the power system operators to achieve minimal VSI, total transmission loss or minimal installation cost. In addition, information on generator scheduling can also be identified.

CHAPTER 7
CONSTRAINED REACTIVE POWER CONTROL BASED MULTI-OBJECIVE OPTIMIZATION UNDER MULTI-CONTINGENCIES *(N-m)*

7.1 INTRODUCTION

This chapter presents a new approach for constrained power planning based on Multi-Objective Evolutionary Programming (MOEP) optimization technique considering multi-contingencies *(N-m)* that may occur in power system. The proposed technique determines the optimum Constrained Reactive Power Control (CRPC), by the generators in order to improve voltage stability condition of a system. The multi objective of constrained reactive power control problems has been implemented by considering two combinations of objective functions namely voltage stability improvement and transmission loss minimization. *SVSI* and transmission loss were taken as the fitness for determining the optimum values of CRPC. This study was initiated as those in Chapter 4; where CPP is conducted using single objective function. In this chapter, CPP is implemented using multi-objective in order to avoid inconsistencies of both objective function experienced by single objective. A computer program was written in MATLAB and the proposed technique was tested on the IEEE 30-bus RTS. Finally, comparative studies are conducted by comparing the results with Multi-Objective Artificial Immune System (MOAIS). An algorithm to apply such multi-objective optimization has been formulated based on the same non-dominated sorting concept implemented in non-dominated sorting genetic algorithm (NSGA-II). In addition, a program is also developed to obtain best compromise solution in a power system.

7.2 MULTI-OBJECTIVE OPTIMIZATION

Multi-objective optimization is a process to find the value of the variables that minimize the objective function namely *SVSI* and transmission loss while the system is operating within its constraint limit. Multi-objective problems are more difficult to solve compared to single objective since there is no unique solution. Instead of one optimal solution, the implementation of multi-objective can give a set of optimal solutions. These optimal solutions are known as *Pareto-optimal solutions*. A Pareto optimal solution cannot be improved with respect to any objective without worsening at least one other objective. The set of all feasible non-dominated solution is referred to as the *Pareto optimal set*, and for a given Pareto optimal set, the corresponding objective function values in the objective space is called the *Pareto front*. In this study, a multi-objective optimization problem consists of two objectives to be optimized simultaneously and it is associated with a number of equality and inequality constraints are implemented. The multi-objective problem can be formulated as follows:

Min	$F(x) = [f_1(x), f_2(x)]$	(7.1)
Subjected to	$g_j(x, u) \leq 0$	(7.2)
	$h_k(x, u) = 0$	(7.3)

where F is the objective vector, $f_1(x)$ and $f_2(x)$ are the two objective functions, x is the vector of dependent variable, u is the vector of control variables, g is the equality constraints and h is the inequality constraint. The details information related to objective functions namely *SVSI* and transmission loss have been described in Chapter 4.

7.3 MULTI-OBJECTIVE OPTIMIZATION USING EVOLUTIONARY PROGRAMMING AND ARTIFICIAL IMMUNE SYSTEM

The procedure for MOEP and MOAIS is represented in flowchart as shown in Figure 7.1 and Figure 7.2. Several inequality constraints are set in this study so as to achieve the optimal solution. In this study, CRPC was implemented to the system by using *SVSI* and transmission loss as the objective function. In order to improve the voltage stability condition of the test system, the variable namely the reactive powers were injected on the generator buses. In this technique, MOEP and MOAIS were used to determine the optimum reactive power to be controlled and dispatched by the chosen generator buses. Several outages namely line outages and generator outages were subjected into the system. The selections of outages are based on the most severe generator and line in the system to maximize the performance of the system. Two generator outages and five line outages were subjected to the system i.e., generators: 11 and 13 and lines: 1, 4, 8, 9 and 7.

Several constraints were set simultaneously in order for MOEP and MOAIS to generate only random numbers that satisfy some constraints violations. The constraints implemented during the initialization for *SVSI* as the objective function are the *SVSI* value less than *SVSI*_set and the transmission loss value less than *loss_set*. The following procedures are presented in the implementation of MOEP for the optimization process.

i. Set the multi-contingencies *(N-m)* in the system i.e. generator and line outages.
   - two generator outages and five line outages are set into the IEEE 30-bus RTS system.

ii. Set the loading factor, λ.

iii. Set the CRPC constraints i.e. $SVSI \leq SVSI\_set$ and $total\ loss \leq loss\_set$ as objective functions.

iv. Generate random number i.e. x_1, x_2 and x_3. Check for constraint violations. If constraints violated, go to step (iii), otherwise go to step (v).

v. Fill in population pool. Repeat step (iv) if pool was not full, otherwise continue to step (vi).

vi. Calculate the non-dominated solution for each individual in the population.

vii. Sort the entire population using front.

viii. Calculate the crowding distance for each front

ix. Mutate the parents x_1, x_2 and x_3 to generate offsprings.

x. Assign x_1, x_2 and x_3 to Q_{g1}, Q_{g2} and Q_{d3} in the bus system data

xi. Calculate fitness by running load flow program to evaluate *SVSI* values and transmission loss values.

xii. Combine parents and offsprings (combination process).

xiii. Perform selection by tournament selection process from the combinated data.

xiv. Identify and transcribe new generations.

xv. If solution is not converged, repeat step (v) to (xiv), otherwise go to step (xvi).

xvi. Sort the Pareto optimal front.

xvii. Find the best compromise solution.

xviii. Plot the Pareto optimal front=1 and the best compromise solution into graph.

xix. End

The concept of MOAIS is based on the same non-dominated sorting concept implemented in NSGA-II. The algorithms required a number of parameters. MOAIS method involves several operators which have similarities with the MOEP methods such as fitness function, initialization and mutation. However in MOAIS, the combination between offspring and parents do not occur in this process. In addition, the major dissimilarity between MOEP and MOAIS is the application of cloning process over the parents. The following are procedures presented the implementation of MOAIS for the optimization process.

i. Set the multi-contingencies *(N-m)* in the system i.e. generator and line outages.

- two generator outages and five line outages are set into the IEEE 30-bus RTS system.

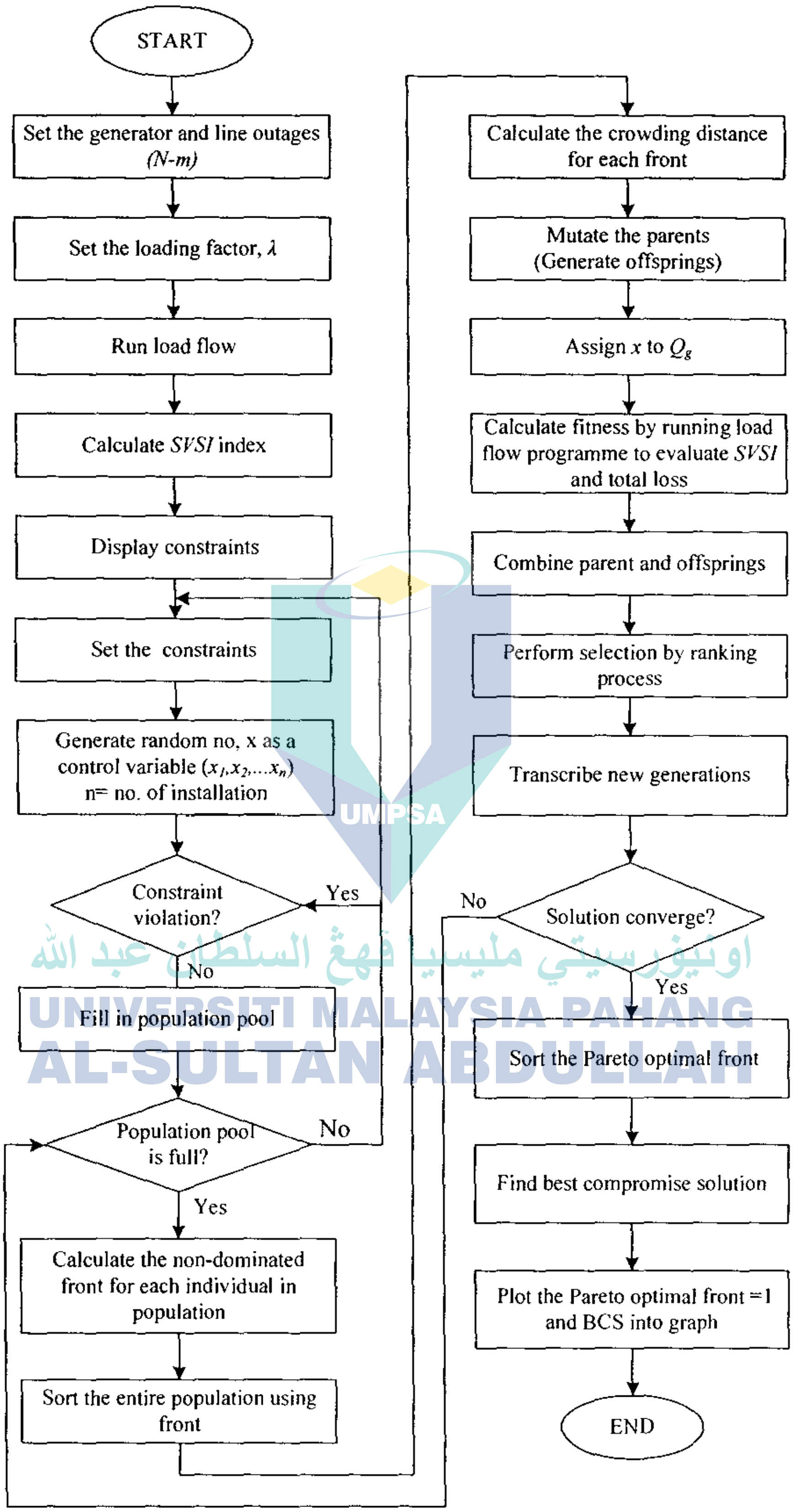

Figure 7.1: Flowchart for CRPC using MOEP.

ii. Set the loading factor, λ.

iii. Set the CRPC constraints i.e. $SVSI \leq SVSI\_set$ and $total\ loss \leq loss\_set$ as objective functions.

iv. Generate random number i.e. x_1, x_2 and x_3. Check for constraint violations. If constraints violated, go to step (iii), otherwise go to step (v).

v. Fill in population pool. Repeat step (iv) if pool was not full, otherwise continue to step (vi).

vi. Clone the parents.

vii. Assign x_1, x_2 and x_3 to Q_{g1}, Q_{g2} and Q_{g3} in the bus system data

viii. Calculate fitness by running load flow program to evaluate *SVSI* values and transmission loss values.

ix. Calculate the non-dominated solution for each individual in the population.

x. Sort the entire population using front.

xi. Calculate the crowding distance for each front

xii. Mutate the parents x_1, x_2 and x_3 to generate offsprings.

xiii. Recalculate fitness using the offspring by running the load flow program.

xiv. Perform selection by tournament selection process.

xv. Identify and transcribe new generations.

xvi. If solution is not converged, repeat step (vi) to (xv), otherwise go to step (xvii).

xvii. Sort the Pareto optimal front.

xviii. Find the best compromise solution.

xix. Plot the Pareto optimal front=1 and the best compromise solution into graph

xx. End

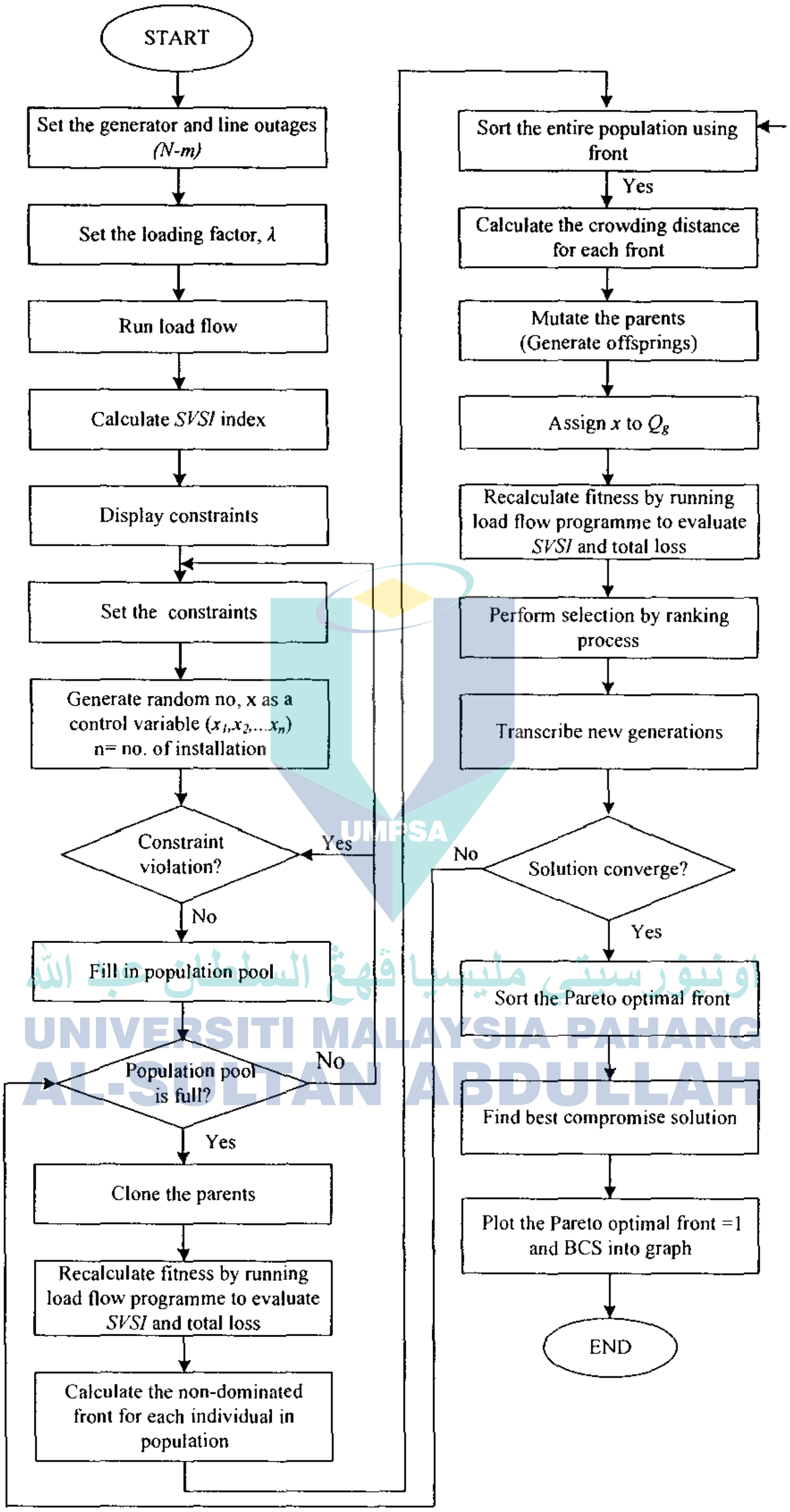

Figure 7.2: Flowchart for CRPC using MOAIS.

7.3.1 Non-domination Sorting and Pareto Optimality

After the initialization, the population is sorted based on non-domination sorting where two solutions are compared whether one solution dominates the other solution or not. If a feasible solution is not dominated by any other feasible solutions of the problem, this solution is called non-dominated solution. In addition, solution $x^{(1)}$ dominates $x^{(2)}$ if $x^{(1)}$ no worse than $x^{(2)}$ in all objectives and $x^{(1)}$ is strictly better than $x^{(2)}$ in at least one objective. Solution $x^{(1)}$ is said to dominate $x^{(2)}$ or $x^{(1)}$ is said to be non-dominated by $x^{(2)}$ if both above conditions are true [193]. The solutions that are non-dominated within the entire search region are represented as Pareto-optimal.

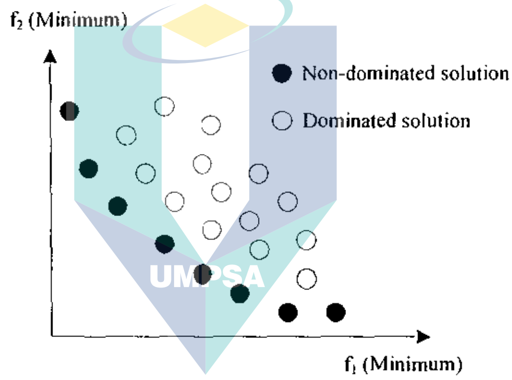

Figure 7.3: All solutions of objective functions for multi-objective optimization

Figure 7.3 shows a set of solutions of two objective functions where $f_1(x)$ and $f_2(x)$ are minimized. The set of non-dominated solution is referred as Pareto optimal front. Pareto optimal point in Figure 7.4 shows different Pareto optimal solutions sets for different combinations of objective functions.

7.3.2 Crowding Distance

Crowding distance is assigned to the population after the non-dominated sorting is completed. The purpose of crowding distance is to provide the diversity in the

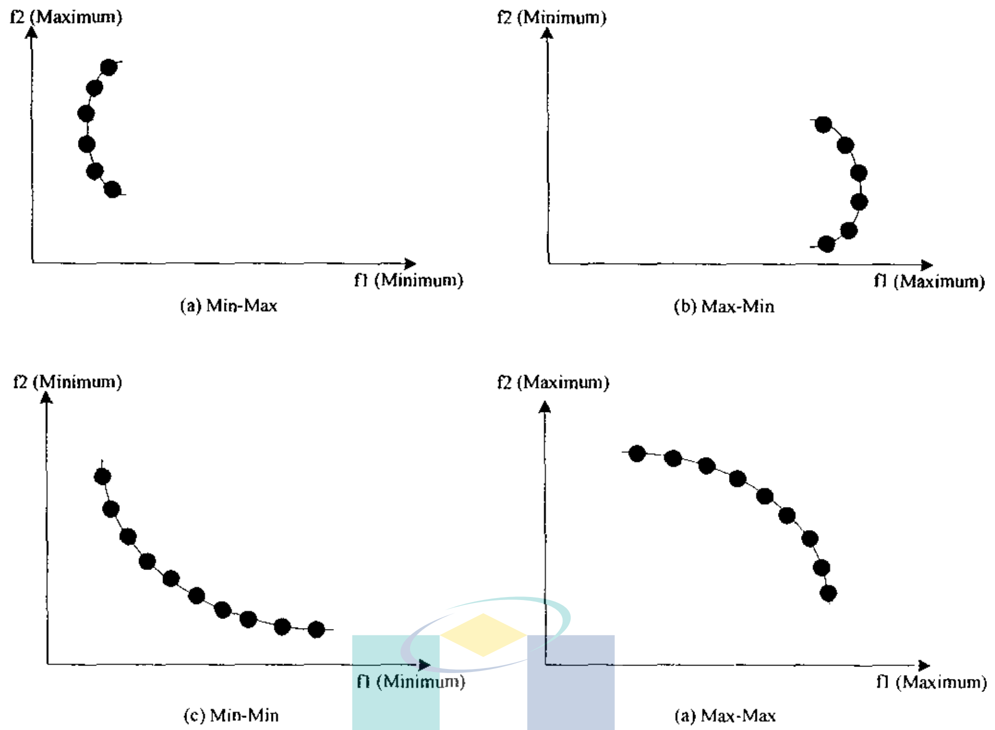

Figure 7.4: Pareto optimal front for difference type objective functions

population. Then, the individual solutions are sorted in descending order based on the magnitude of the crowding distance values calculated as follows [211].

$$d_{I_j^m} = d_{I_j^m} + \frac{f_m^{\left(I_{j+1}^m\right)} - f_m^{\left(I_{j+1}^m\right)}}{f_m^{\max} - f_m^{\min}} \tag{7.4}$$

where $m = 1,2,\ldots, M$, M is the number of objective function, I_j is the solution index of the j^{th} in the sorted list, f^{max} is the maximum population and f^{min} is the minimum population.

7.3.3 Cloning

Cloning is the process in which the control variables were copied in order to increase the population. During cloning, the size of each parent is expanded for producing offspring. This creates the same number of clones for each individual. The basic immune models and algorithm in AIS are; Bone Marrow models, negative selection algorithm, clonal selection algorithm and immune network models.

7.3.4 Mutation

Mutation is a process to produce offspring. New individual (offspring) is produced by mutating the existing individual (parents). The polynomial mutation operators are selected in this process and the equation is described as follows [211].

$$c_k = p_k + \left(p_k^u - p_k^l\right)\delta_k \tag{7.5}$$

where

c_k = offspring

p_k = parent

p_k^u = upper bound on the parent component

p_k^l = lower bound on the parent component

δ_k = variation from polynomial distribution

The variation from polynomial distribution is calculated using the following equations;

$$\delta_k = \left(2r_k\right)^{\frac{1}{(\eta+1)}} - 1 \qquad \text{if } r_k < 0.5 \tag{7.6}$$

$$\delta_k = 1 - \left[\left(2\left(1 - r_k\right)\right)\right]^{\frac{1}{(\eta+1)}} - 1 \qquad \text{if } r_k \geq 0.5 \tag{7.7}$$

where r_k is a uniformly sampled random number between 0 to 1 and η is the mutation distribution index.

7.3.5 Combination and Selection

The parent populations and offsprings population is combined in cascode mode and tournament selection is applied after the implementation of mutation in order to generate individual for the next generation. The details have been described in Chapter 4. Then, the populations are sorted based on the non-dominated sorting again.

7.3.6 Best Compromise Solution (BCS)

BCS is defines as the most suitable solution to multi-objective optimization process [211]. Optimization of multi-objective using EP produces a set of Pareto optimal solution by which one objective cannot be improved without sacrificing other objective. However, one solution must be selected by the decision maker for practical applications. The solution is called best compromise solution. The equation for best compromise solution is given below [211]:

$$\beta_i = \frac{\sum_{k=1}^{M} u_i^k}{\sum_{i=1}^{N_{obj}} \sum_{k=1}^{M} u_i^k} \tag{7.8}$$

The variation for u_i^k is determined using

$$u_i^k = 1 \qquad \text{if } \left(F_i^k > F_{\max}^k\right) \tag{7.9}$$

$$u_i^k = \frac{F_{\max}^k - F_i^k}{F_{\max}^k - F_{\min}^k} \qquad \text{if } \left(F_{\min}^k \le F_i^k \le F_{\max}^k\right) \tag{7.10}$$

$$u_i^k = 0 \qquad \text{If } \left(F_i^k < F_{\min}^k\right) \tag{7.11}$$

where M is the number of objective function, N_{obj} is the number of non-dominated solution, F_i^k is the fitness value of i^{th} solution of k^{th} objective, $F_{\max}^k$ is the maximum fitness value of k^{th} objective function and β_i is the normalize membership function. The

β_i provides the fuzzy of the non-dominated solution. The maximum membership β_i in fuzzy set can be considered as the best compromise solution.

7.4 RESULTS AND DISCUSSION

The results have been obtained from the developed algorithm for multi-objective reactive power control based on NSGA-II. The developed algorithm has been tested on the IEEE 30-Bus RTS whose data are given in Appendix A. The multi-objective power control problem has been formed with considering multi-contingencies *(N-m);* stress, lines and generator outages have been occurred in the system which are formulated with objective of minimizing the static voltage stability index (*SVSI*) and real power loss respectively. For the studies, the following parameters are used:

- Population size = 200
- Mutation probability= 0.1
- Distribution index for mutation= 20

Population size of 200 was chosen based on exhaustive experiment on various population sizes ranging from 20 to 200.

7.4.1 Multi-Objective Evolutionary Programming for Constrained Reactive Power Control

In this study, MOEP algorithm has been applied where both *SVSI* and transmission loss were optimized simultaneously. The developed algorithm has been tested with bus 26 and bus 14 subjected to maximum loadability in the IEEE 30-bus RTS. The simulation results are tabulated in Table 7.1 and Table 7.2 for both cases. The Pareto optimal fronts set are shown in Figure 7.5 and Figure 7.6 respectively. The diversity of the Pareto-optimal set over the trade-off surface for bus 26 is shown in Figure 7.5. It is observed that the proposed approach produce 200 Pareto-optimal solutions. Out of the solutions obtained, two non-dominated solutions that represent the best *SVSI* value and best transmission loss are given in Table 7.1. The best compromise solution of this method is also given in this table. It is observed that the *SVSI* and transmission loss values reduce with respect to λ after the implementation of MOEP in the system. It implies that the voltage stability has been improved. The best *SVSI* value is 0.1867 while the best transmission loss is 13.02 MW. The best compromise solution is 0.1919 for *SVSI* and 13.12 MW for transmission loss.

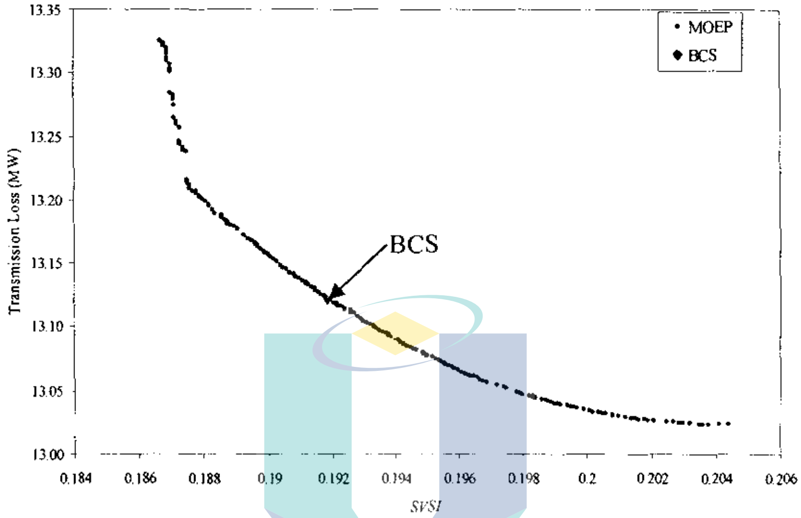

Figure 7.5: Pareto front for *SVSI* and transmission loss minimization obtained using MOEP for CRPC at bus 26.

Table 7.1: Results for MOEP when bus 26 was reactively loaded for $\lambda = 2.3$

Units (in MVAr)	pre-CRPC	MOEP		
		Solution at minimum *SVSI*	Solution at minimum Transmission Loss	Best Compromise Solution
Q_{g2}	246.960	11.206	27.467	28.893
Q_{g5}	30.458	5.543	-10.070	-7.530
Q_{g8}	98.209	29.222	16.773	21.075
SVSI	0.6888	0.1867	0.2044	0.1919
Transmission Loss (in MW)	111.38	13.32	13.02	13.12

The diversity of the Pareto-optimal set over the trade-off surface for load subjected to bus 14 is shown in Figure 7.6. It is observed that the proposed approach produces 200 Pareto-optimal solutions. Out of the solutions obtained, two non-dominated solutions that represent the best *SVSI* value and best transmission loss are given in Table 7.2. The

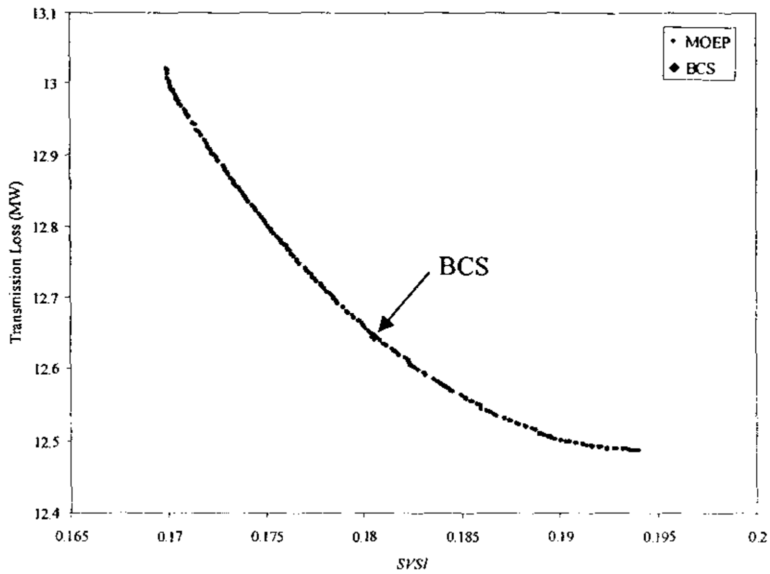

Figure 7.6: Pareto front for *SVSI* and Transmission Loss minimization obtained using MOEP for CRPC at bus 14.

Table 7.2: Results for MOEP when bus 14 was reactively loaded for $\lambda = 3.5$

Units (in MVAr)	pre-CRPC	MOEP		
		Solution at minimum *SVSI*	Solution at minimum Transmission Loss	Best Compromise Solution
Q_{g2}	278.274	9.305	38.127	18.175
Q_{g5}	30.458	-10.550	-9.948	-5.402
Q_{g8}	103.567	38.544	13.739	27.827
SVSI	0.7371	0.1699	0.1940	0.1806
Transmission Loss (in MW)	121.19	13.02	12.49	12.65

best compromise solution of this method is also given in this table. It is observed that the *SVSI* and transmission loss have been reduced with the implementation of MOEP. It implies that the voltage stability has been improved. The best *SVSI* value is 0.1699 while the best transmission loss is 12.49 MW. The best compromise solution is 0.1806 for *SVSI* and 12.65 MW for transmission loss.

7.4.2 Multi-Objective Artificial Immune System for Constrained Reactive Power Control

In this study, MOAIS algorithm has been applied where both *SVSI* and transmission loss were optimized simultaneously. The aim is to perform comparative study with respect to MOEP. The developed algorithm has been tested to the system with load subjected to bus 26 and bus 14 in the IEEE 30-bus RTS. The simulation results are tabulated in Table 7.3 and Table 7.4 for both buses. The optimal Pareto fronts set are shown in Figure 7.7 and Figure 7.8 respectively.

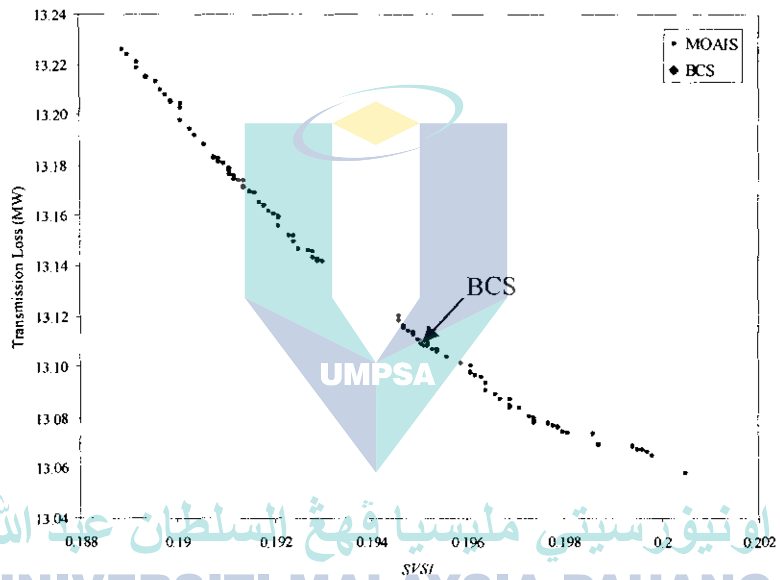

Figure 7.7: Pareto front for *SVSI* and Transmission Loss minimization obtained using MOAIS for CRPC at bus 26.

The diversity of the Pareto-optimal set over the trade-off surface for load subjected to bus 26 is shown in Figure 7.7. It is observed that the proposed approach produces 115 Pareto-optimal solutions. Out of the solutions obtained, two non-dominated solutions that represent the best *SVSI* value and best transmission loss are given in Table 7.3. The best compromise solution of this method is also given in this table. It is observed that the *SVSI* and transmission loss value reduce after the implementation of MOAIS in the system. It implies that the voltage stability has been improved. The best *SVSI* value is

Table 7.3: Results for MOAIS when bus 26 was reactively loaded for $\lambda = 2.3$

Units (in MVAr)	pre-CRPC	MOAIS		
		Solution at minimum *SVSI*	Solution at minimum Transmission Loss	Best Compromise Solution
Q_{g2}	246.960	17.923	17.973	17.727
Q_{g5}	30.458	2.945	-0.444	0.108
Q_{g8}	98.209	23.782	18.949	22.151
SVSI	0.6888	0.1889	0.2005	0.1951
Transmission Loss (in MW)	111.38	13.23	13.06	13.11

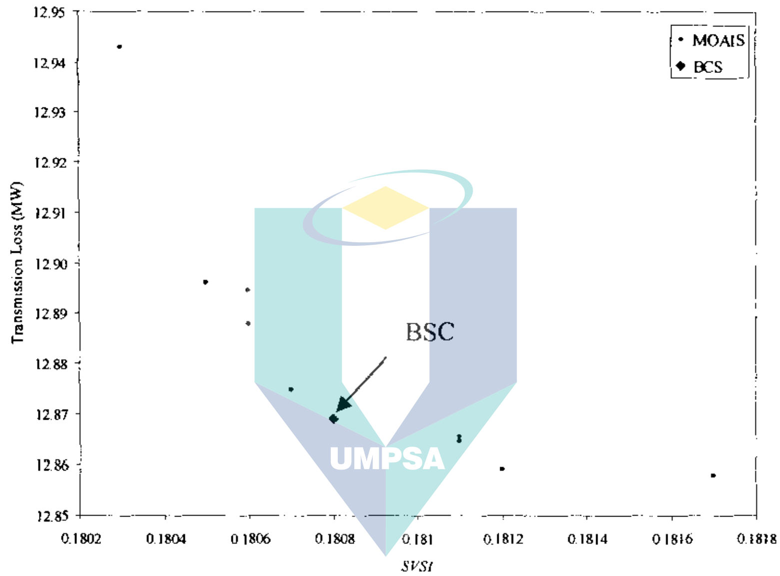

Figure 7.8: Pareto front for *SVSI* and Transmission Loss minimization obtained using MOAIS for CRPC at bus 14.

0.1889 while the best transmission loss is 13.06 MW. The best compromise solution is 0.1951 for *SVSI* and 13.11 MW for transmission loss.

The diversity of the Pareto-optimal set over the trade-off surface for load subjected to bus 14 is shown in Figure 7.8. It is observed that the proposed approach produces only 10 Pareto-optimal solutions. Out of the solutions obtained, two non-dominated solutions that represent the best *SVSI* value and best transmission loss are given in Table 7.4. The best compromise solution of this method is also given in this table. It is observed that the *SVSI* and transmission loss value reduce with the implementation of MOAIS in the system. It implies that the voltage stability has been improved. The best

Table 7.4: Results for MOAIS when bus 14 was reactively loaded for $\lambda = 3.5$

Units (in MVAr)	pre-CRPC	MOAIS		
		Solution at minimum *SVSI*	Solution at minimum Transmission Loss	Best Compromise Solution
Q_{g2}	278.274	20.356	21.039	19.605
Q_{g5}	30.458	-2.066	-1.755	-1.486
Q_{g8}	103.567	36.306	33.835	34.634
SVSI	0.7371	0.1803	0.1817	0.1808
Transmission Loss (in MW)	121.19	12.94	12.86	12.87

SVSI value is 0.1803 while the best transmission loss is 12.86 MW. The best compromise solution is 0.1808 for *SVSI* and 12.87 MW for transmission loss.

7.4.3 Comparative Studies

The comparison result for the best compromise solution for different optimization technique using MOEP and MOAIS for the implementation of CRPC is tabulated in Table 7.5. In this table, the results are verified from three aspects in terms of *SVSI* value, transmission loss and amount of non-dominated solutions. When load is subjected to bus 26, it shows that only 115 non dominated solutions distributed along Pareto Front using MOAIS. Nevertheless, the MOEP has presented 200 non-dominated solutions along the Pareto Front, in which it gives more choices of selection for CRPC to improve *SVSI* and reduce the transmission loss in the system. As highlighted in the table, it is observed that MOEP is better than MOAIS since MOEP managed to improve the *SVSI* value as compared to MOAIS in the system. However, MOAIS outperformed EP in terms of transmission loss. As for bus 14, MOEP outperformed MOAIS in all criteria as

Table 7.5: Best Compromise Solution for CRPC when bus 26 and bus 14 were reactively loaded.

Test Bus	Technique	Non dominated Solutions No.	*SVSI*	Transmission Loss (in MW)
26	MOEP	200	0.1919	13.121
	MOAIS	115	0.1951	13.109
14	MOEP	200	0.1806	12.645
	MOAIS	10	0.1808	12.869

highlighted in the table. The MOEP has obtained 200 non-dominated solutions along the Pareto Front, which gives more choices of selection for CRPC than MOAIS. MOAIS only able to get 10 non dominated solutions distributed along the Pareto Front.

7.5 SUMMARY

This chapter has presented multi-objective optimization techniques termed as MOEP and MOAIS in implementing the optimal CRPC scheme. The combination of *SVSI* and transmission loss minimization as objective function has been solved for the IEEE 30-bus RTS system with bus 26 and bus 14 subjected to loading condition. The Pareto-optimal front has been obtained in all schemes and the best compromise solution shows the promising results where MOEP and MOAIS successfully improved the *SVSI* value and reduced the transmission loss values in the system. Finally, results obtained from the MOEP techniques were compared with MOAIS and it was found that MOEP outperformed MOAIS in most cases.

CHAPTER 8
OVERALL CONCLUSION AND RECOMMENDATION

8.1 CONCLUSION

This thesis presents a novel computer-aided control for voltage stability assessment and improvement considering multi-contingencies occurs in power system. The system involved the implementation of voltage stability index referred to line, development of contingency analysis and ranking caused by line and generator outages, development of a constrained power planning optimization algorithm and FACTS based on evolutionary programming for voltage stability improvement, development of a novel operating generator scheduling and development of constrained reactive power control optimization algorithm based on MOEP for voltage stability improvement. The proposed techniques were verified by several IEEE Reliability Test System; IEEE 30-bus and IEEE 118-bus, and the results indicated that the proposed techniques are flexible and robust which can be implemented on other practical systems. Comparative studies were also conducted between the results obtained from the proposed techniques with others technique and an agreement were achieved among themselves.

In Chapter 3, a line voltage stability index was applied termed as *SVSI*. This index was developed from the quadratic voltage equation at the receiving end of a general 2-bus system. Voltage stability analysis was conducted to the test systems by gradually increasing the reactive power loading on a load bus and *SVSI* was evaluated for every line in the system as the indicator to voltage stability conditions. A line evaluated with *SVSI* value close to unity implies that the line has reached its voltage stability limits, beyond which voltage instability will occur leading to voltage collapse in the whole system. *SVSI* can be used as an indicator in order to identify the most sensitive line with respect to a particular load bus in the system [6]. The most sensitive line with respect to a load bus is the line having the highest *SVSI* value which is close to a unity. The application of the *SVSI* formulation was further extended for the use of contingency analysis and ranking processes. In this study, *SVSI* was utilized as the line outage severity indicator. An algorithm to simulate the line outage contingency analysis and ranking was developed. A computer program was written in MATLAB to run the whole process in one program. The developed line outage contingency analysis and ranking algorithm was successfully tested on several IEEE Reliability Test System (RTS) i.e. IEEE 30-bus RTS and IEEE 118-bus RTS. The results revealed that contingencies caused by line outage gave a direct impact to the system stability. The lines ranked in the top of the list were found to be the critical lines that would cause system instability if outages were to occur on these lines. In addition, contingencies caused by generator outage were also investigated. An algorithm has been developed in order to automatically simulate generator outage in the system. In this study, *SVSI* was applied as the generator outage severity indicator. The highest computed *SVSI* during the generator outage was evaluated on the line having direct connection to the heavily loaded bus.

In Chapter 4, the application of newly developed EP as an optimization technique was also presented for the voltage stability improvement considering multi-contingencies *(N-m)* have occurred in the system. The selection of outages namely line outage and generator outage are based on the contingencies analysis and ranking analysis in previous chapter. Three constrained power planning techniques namely CRPC, CAPS and CHPS were developed utilizing the EP for the optimization procedure. The applications of *SVSI* and transmission loss in the system were taken as two separate objective functions for the realization of the CPP techniques. In the implementation of CRPC, optimum reactive powers to be generated by the generators for improving voltage stability and minimizing transmission losses in the system were identified. The implementation of CAPS as the second CPP technique has utilized the EP to optimize the active power values for the voltage stability improvement and loss minimization in the system. The third CPP technique was to optimize the CHPS using the EP in order to improve the voltage stability condition of the system and also to minimize the system losses. Comparative studies were performed with AIS on the three CPP techniques implemented with subjected to two objective functions namely voltage stability improvement and also transmission loss minimization in the system. The result revealed that the application of EP as an optimization technique was found to be better than AIS technique in both objective functions namely voltage stability improvement and also transmission losses minimization in the system.

The application of newly developed EP as an optimization technique was also presented in Chapter 5 for FACTS in order to minimize the total transmission losses in a system under *(N-m)* contingencies. The selection of outages namely line outage and generator outage are based on the contingencies analysis and ranking analysis in Chapter 3. The studies proposed the CSVC, CTCSC and CUPFC as three constrained FACTS techniques. For each technique, one objective function was implemented namely transmission loss minimization with the transmission loss in the system as the fitness function. The *SVSI* technique was applied as the tool to indicate the FACTS location into the system network. When the load flow program was run, stability indices are calculated for FACTS placed in every line one at a time for the same operating conditions and the system identified the line buses with the highest *SVSI* for the purpose of installing the FACTS. The EP optimization technique is then used to determine the suitable sizing value of the FACTS devices namely SVC, TCSC and UPFC to be installed in order to minimize the total transmission loss in the system. Finally, results obtained from the EP techniques were compared with AIS. It was found at most of the results, EP gives better results in transmission loss minimization to the system than AIS technique.

In Chapter 6 also presented a novel technique for operating generator scheduling applied on reactive power control based on EP optimization technique. Hence, two separate objective functions were implemented namely voltage stability improvement with *SVSI* value as the fitness function and transmission loss minimization with the transmission loss in the system as the fitness function. Each combination of generators for each objective function is ranked based on *SVSI* value, transmission loss and installation cost in order to observed the effect of generator combination in the system. The results show that the OGS is able to assist the system operator in scheduling generator units in an economic way or as required by the utility company.

Finally, the application of newly developed multi-objective evolutionary programming as a multi-objective optimization technique was also presented for the voltage stability improvement in Chapter 7. CRPC was developed utilizing the EP for the optimization procedure. The applications of *SVSI* and transmission loss in the system were combined as objective functions for the realization of the CRPC techniques. In the implementation of CRPC, optimum reactive powers to be generated by the generators for improving voltage stability and minimizing transmission losses simultaneously in the system were identified. Comparative studies were performed with MOAIS with subjected to two objective functions namely voltage stability improvement and also transmission loss minimization in the system. The Pareto-optimal front has been obtained in all schemes and the best compromise solution shows the promising results where MOEP and MOAIS successfully improved the *SVSI* value and reduced the transmission loss value in the system. On the other hand, results obtained from the MOEP techniques were compared with MOAIS and it was found MOEP outperformed MOAIS in most cases.

8.2 RECOMMENDATIONS AND FUTURE WORK

This study has represented the EP technique used in voltage stability analysis studies which only considered the static voltage stability condition of a system. Therefore for future work, it is recommended that the EP technique is to be developed for the dynamic voltage stability condition of a system. It is also recommended to integrate the graphic user interface (GUI) with the developed technique so that the data of system could be easily collected by the power system operators.

REFERENCES

[1] D. T. Bansilal, K. Parthasarathy, "Optimal reactive power algorithm for voltage stability improvement", Journal of Electrical Power and Energy Systems, vol. 18, pp. 461-468, 1996.

[2] A. Kazemi, S. Jamali, M. Habibi and S. Ramezan-Jamaat , "Optimal Location of TCSCs in a power system by means of Genetic Algorithms considering loss reduction", in *First International Power and Energy Conference (PECon 2006)*, 2006, pp. 134-139.

[3] A. S. Quintela and C. A. Castro, "Improved branched-based voltage stability proximity indices Part II: Application in security analysis", in *Proceedings IEEE Large Power Engineering Systems Conference on Power Engineering*, 2002, pp. 115 – 119.

[4] G. Eugene Preston, L. Martin Baughman and W. M. Grady, "A new model for outaging transmission lines in large electric networks", *IEEE Transaction on Power Systems*, vol. 14, pp. 412 – 418, May 1999.

[5] Y. Y. Hsu and H. C. Kuo, "Fuzzy-Set Based Contingency Ranking", *IEEE Transaction on Power Systems*, vol. 7, pp. 1189 – 1196, August 1992.

[6] I. Musirin, "New technique for voltage stability assessment and improvement in power system", Ph.D thesis, University Teknologi Mara, Malaysia, 2003.

[7] A. El-Keib and X. Ma, "Application of Artificial Neural Networks in voltage stability assessment", *IEEE Transaction on Power System*, vol.10, pp. 1890 – 1896, November 1995.

[8] T. K. A. Rahman and G. B. Jasmon, "A new voltage stability index and load flow technique for power system analysis", *International Journal of Power and Energy System*, vol. 17, pp. 28 – 37, 1997.

[9] H. C. Nallan and P. Rastgoufard, "Computational voltage stability assessment of large-scale power systems", *Electric Power Systems Research,* vol.38, pp. 177 – 181, 1997.

[10] H. K. Nam, Y. K. Kim, K. S. Shim and K. Y. Lee, "A new eigen-sensitivity theory of Augmented Matrix and its applications to power system stability analysis", *IEEE Trans. on Power Systems*, vol. 15, pp. 363 – 369, February 2000.

[11] P. A. Lof, T. Smed, G. Anderson and J. Hill, "Fast calculation of voltage stability index", *IEEE Transaction on Power System*, vol. 7, pp. 54 – 64, February 1992.

[12] J. Su, Y. Yu, H. Jia, P. Li, N. He, Z. Tang and H. Fu, "Visualization of voltage stability region of bulk power system", in *Proceedings IEEE International Conference of Power System Technology (Powercon 2002),* vol. 3, 2002, pp. 1665 – 1668.

[13] IEEE Power System Engineering Committee, System Dynamic Performance Subcommittee: "Voltage stability of power systems: concepts, analytical tools and industry experience", *IEEE Special Publication* No. 90 THO 358-2 PWR.

[14] K. Visakha, D. Thukaram and L. Jenkins, "An Approach for real power scheduling to improve system stability margins under normal and networks contingencies", *Journal of Electric Power System Research*, vol. 71, pp. 109-117, October 2004.

[15] C. T. Su and C. T. Lin, "Fuzzy-Based Voltage/Reactive Power Scheduling for Voltage Security Improvement and Loss Reduction", *IEEE Transactions on Power Delivery,* Vol. 16, No.2, pp. 319-323, April 2001.

[16] J. F. Dopazo, O.A. Klitin, G.W. Stagg, and M. Watson, "An optimization technique for real and reactive power allocation", in *Proceedings of the IEEE*, vol. 55, 1967, pp. 1877-1885.

[17] A. Kumar, S.C. Srivastave, S.N. Singh, "A zonal congestion management approach using real and reactive power rescheduling", *IEEE Transactions on Power Systems*, vol. 19, pp. 554-562, February 2004.

[18] L. Goel, and C. Feng, "Well-being framework for composite generation and transmission system reliability evaluation", in *IEEE Proceedings on Generation, Transmission and Distribution*, vol. 146, 1999, pp. 528-534.

[19] A. Shaban, and A. Go, "A reliability and economic evaluation of a transmission system-i: using frequency and duration of failure method", in *Twenty-Fifth Southeastern Symposium on System Theory*, 1993, pp. 94-100.

[20] FERC Order No.888, Promotion of wholesale competition through open access non-discriminatory transmission services by public utilities and recovery of stranded costs by public utilities and transmitting utilities, Issued April 1996.

[21] B. D. Thukaram and K. Parthasarathy, 'Optimal reactive power algorithm for voltage stability improvement", *Journal of Electrical Power and Energy Systems*, Vol. 18, pp. 461-468, 1996.

[22] D. I. Eromon, J. Kueck and T. Rizy, "Distributed Energy Resource (DER) using FACTS, STATCOM, SVC and synchronous condensers for dynamic systems

control of VAR", *National Association of Industrial Technology (NAIT) Convention*, 2005, pp. 1-16.

[23] L. Qi, "AC system stability analysis and assessment for shipboard power systems", PH.D thesis, University of A & M Texas, 2004.

[24] IEEE Power System Engineering Committee, System Dynamic Performance Subcommittee: "Voltage stability of power systems: concepts, analytical tools and industry experience", *IEEE Special Publication* No. 90 THO 358-2 PWR.

[25] I. Musirin and T. K. A. Rahman, "Estimating maximum loadability for weak bus identification using FVSI", *IEEE Power Engineering Review*, vol. 22, pp. 50 – 52, 2002.

[26] I. Musirin and T. K. A. Rahman, "Simulation technique for voltage collapse prediction and contingency ranking in power system", in *Proceedings IEEE International Student Conference of Research and Development 2002 (SCOReD2002)*, 2002, pp. 188 – 191.

[27] I. Musirin and T. K. A. Rahman, "Novel Fast Voltage Stability Index (FVSI) for voltage stability analysis in power transmission system", in *Proceedings IEEE International Student Conference of Research and Development 2002 (SCOReD2002)*, 2002, pp. 265 – 268.

[28] I. Musirin and T. K. A. Rahman, "A Novel Fast Voltage Stability Index (FVSI) for voltage collapse prediction in power system", in *Proceedings 2nd World Engineering Congress*, 2002, pp. 79 - 84.

[29] D. Thukaram and A. Lomi, "Selection of Static VAR Compensator location and size for system voltage stability improvement", *International Journal of Electrical Power and Energy Systems*, vol. 54, pp. 139 – 150, May 2000.

[30] C. DeMarco and T. Overbye, "An energy based security measure for assessing vulnerability to voltage collapse", *IEEE Transaction on Power System*, vol. 5, pp. 419 – 427, May 1990.

[31] F. D. Galiana and Z. C. Cheng, "Analysis of the load behaviour near Jacobian Singularity," *IEEE Transaction on Power System*, vol. 7, pp. 1529 -1542, November 1992.

[32] M. Moghavemmi and F. M. Omar, "Technique for contingency monitoring and voltage collapse prediction", in *IEE Proceedings on Generation, Transmission and Distribution*, vol. 145, 1998, pp. 634 – 640.

[33] A. Mohamed, G. B. Jasmon and S. Yusoff, "A Static voltage collapse indicator using line stability factors", *Journal of Industrial Technology*, vol. 7, pp. 73 – 85, 1989.

[34] I. Musirin and T. K. A. Rahman, "Fast Voltage Stability Index (FVSI) for on-line stability monitoring in distribution system", presented at *International Conference of Transmission and Distribution CIRED*, August 2002. pp. PS2-4: 1-7.

[35] A. M. Chebbo, M. R. Irving and M. J. H. Sterling, "Voltage collapse proximity indicator: behaviour and implications", in *IEE Proceedings-C; Generation, Transmission and Distribution,* vol. 139, 1992, pp. 241 - 252.

[36] S. G. Johansson, J. E. Daalder, D. Popovic and D. J. Hill, "Avoiding voltage collapse by fast active power rescheduling", *International Journal of Electrical Power and Energy Systems*, vol. 19, pp. 501 – 509, November1997.

[37] M. Z. El-Sadek, G. A. Mahmoud, M. M. Dessouky and W. I. Rashed, "Optimum load shedding for avoiding steady-state voltage instability", *Electric Power System Research*, vol. 50, pp. 119 – 123, May 1999.

[38] R. S. Tare and P. R. Bijwe, "A new index for voltage stability monitoring and enhancement", *International Journal of Electrical Power and Energy Systems*, vol. 20, pp. 345 – 351, June 1998.

[39] G. B. Jasmon and L. H. C. C. Lee "Stability of loadflow techniques for distribution system voltage stability analysis", *IEE Proc.-C*, vol. 138, 1993, pp. 479 - 484.

[40] B. Strmenik and F. Gubina, "Voltage collapse proximity in case of radial network", in *Proceedings IEEE International Symposium of Circuits and Systems (ISCAS'96)*, vol. 1, pp. 446 – 449.

[41] R. Lind and D. Karlsson, "Distribution system modelling for voltage stability studies", *IEEE Transaction on Power Systems*, vol. 11, pp. 1677 – 1682, November 1996.

[42] D. Gan, Z. Qu and X. Wu, "Loadability of power systems with Steady-State and Dynamic Security Constraints", *Electrical Power and Energy Systems*, 2003, pp. 91-96.

[43] P. W. Sauer, R. J. Evans and M. A. Pai, "Maximum Unconstrained Loadability of power systems", in IEEE *International Symposium on Circuits and Systems*, vol. 3, 1990, pp. 1818 - 1821.

[44] A. C. G. Melo, S. Granville, J. C. O. Mello, A. M. Oliveira, C. R. R. Dornellas and J. O. Soto, "Assessment of maximum loadability in a probabilistic framework", in *Proceedings IEEE Power Engineering Society Winter Meeting,* 1999, pp. 263 - 268.

[45] I. A. Hiskens and R. J. Davy, "Exploring the power flow solution Space Boundary", *IEEE Transactions on Power Systems*, vol. 16, pp. 389-395, August 2001.

[46] T. V. Cutsem, C. Moisse and R. Mailhot, "Determination of secure operating limits with respect to voltage collapse", *IEEE Transaction on Power Systems*, vol. 14, pp. 327 – 335, February 1999.

[47] Y. Dai, J. D. McCalley and V. Vittal "Simplification, expansion and enhancement of Direct Interior Point algorithm for power system maximum loadability", *IEEE Transaction on Power Systems*, vol. 15, pp. 1014 – 1021, August 2000.

[48] J. Kubokawa, R. Inoue and H. Sasaki, "A solution of Optimal Power Flow with voltage stability constraints", in *Proceeding. International Conference of Power Systems Technology – PowerCon*, vol. 2, 2000, pp. 625 - 630.

[49] G. D. Irrisari, X. Wang, J. Tong and S. Mokhtari, "Maximum Loadability of power systems using Interior Point Non-Linear Optimization method", *IEEE Transaction on Power Systems*, vol. 12, pp. 162 –172, Feb. 1997.

[50] R. B. Prada and L. J. Souza, "Voltage Stability and Thermal Limit: Constraints on the maximum loading of electrical energy distribution feeders", in *IEE Proc. – Gener. Transm. Distrib.*, vol. 145, pp. 573 – 577, September 1998.

[51] K. A. Ellithy, A. Gastli, T. Al-Khusaibi and M. Irving, "Voltage stability margins assessment for Muscat power system", *International Journal of Electrical Power and Energy Systems*, vol. 24, pp. 665 – 671, October 2002.

[52] I. Musirin and T. K. A. Rahman, "Acceleration Search Technique Based on Evolutionary Programming for estimating Maximum Loadability in power ", in *Proceedings Artificial Intelligence Application in Industry Malaysia-Japan Seminar*, May 2003.

[53] I. Dobson and L. Lu, "New methods for computing a Closest Saddle Node Bifurcation and Worst Case Load Power Margin for voltage collapse", *IEEE Transactions on Power Systems*, vol. 8, pp. 905 – 913, August. 1993.

[54] D. Gan, Z. Qu and X. Wu, "Loadability of power systems with Steady-State and Dynamic Security Constraints", *International Journal of Electrical Power and Energy Systems*, pp. 91-96, 2003.

[55] A. C. G. Melo, S. Granville, J. C. O. Mello, A. M. Oliveira, C. R. R. Dornellas and J. O. Soto, "Assessment of Maximum Loadability in a Probabilistic

Framework", in *Proceedings IEEE Power Engineering Society Winter Meeting,* 1999, pp. 263 - 268.

[56] T. V. Cutsem, C. Moisse and R. Mailhot, "Determination of secure operating limits with respect to voltage collapse", *IEEE Transaction on Power Systems*, vol. 14, pp. 327 – 335, Feb. 1999.

[57] G. D. Irrisari, X. Wang, J. Tong and S. Mokhtari, "Maximum Loadability of power systems using Interior Point Non-Linear Optimization method", *IEEE Transaction on Power Systems*, vol. 12, pp. 162 – 172, February 1997.

[58] Y. H. Moon, B. K. Choi and B. H. Cho, "Estimation of Maximum Loadability in power systems by using Elliptic Properties of p-e Curve", *in Proceedings IEEE Power Engineering Society Winter Meeting*, vol. 1, 1999, pp. 677 - 682.

[59] Y. H Moon, B. K. Choi and B. H. Cho, "Improved method of Maximum Loadability estimation in power systems by transforming the distorted p-e Curve", in *Proceedings IEEE on Power Engineering Society Summer Meeting*, vol. 2, 2000, pp. 657 - 662.

[60] Z. Yao and S. Wennan, "Power system static voltage stability limit and the identification of weak bus", in *Proceedings IEEE TENCON*, 1993, pp. 157 – 160.

[61] F. Alvardo, I. Dobson and Y. Hu, "Computation of closest bifurcation in power systems", *IEEE Transaction on Power Systems*, vol. 9, pp. 918 – 928, May 1994.

[62] C. S. Chang and J. S. Huang, "Worst-Case Identification of reactive power margin and local weakness of power systems", *Electric Power System Research*, vol. 44, pp. 77 – 83, February 1998.

[63] D. E. Julian, R. P. Schulz, K. T. Vu, W. H. Quaintance, N. B. Bhatt and D. Novosel, "Quantifying Proximity to voltage collapse using the Voltage Instability Predictor (VIP)", in *Proceedings IEEE Power Engineering Society Meeting*, vol. 2, 2000, pp. 931 – 936.

[64] B. D. Thukaram and K. Parthasarathy, 'Optimal reactive power algorithm for voltage stability improvement", *Journal of Electrical Power and Energy Systems*, Vol. 18, pp. 461-468, 1996.

[65] S. Repo, "On-line voltage stability assessment of power system – An approach of Black-Box Modelling", Ph.D. dissertation, Tampere University of Technology, Finland, 2001.

[66] I. Dobson and L. Lu, "New methods for computing a Closest Saddle Node Bifurcation and Worst Case Load Power Margin for voltage collapse", *IEEE Transactions on Power Systems*, vol. 8, pp. 905 – 913, August. 1993.

[67] I. Dobson, H. Glavitsch, C. C. liu, Y. Tamura and K. Vu, "Voltage Collapse in power systems", *IEEE Transactions of Circuits and Devices*, pp. 40 – 45, May 1992.

[68] H. D. Chiang, I. Dobson and R. J. Thomas, "On voltage collapse in electric power systems", *IEEE Transactions on Power Systems*, vol. 5, pp. 601 – 611, May 1990.

[69] M. G. Lauby, "Evaluation of a local DC Load Flow Screening Method for branch contingency selection of overloads", *IEEE Transaction on Power Systems*, vol. 3, pp. 923 – 928, August 1988.

[70] J. Z. Zhu and G. Y. Xu, "Approach to automatic contingency selection by reactive type performance index", *in IEE Proceedings – C*, vol. 138, 1991, pp. 65 – 68.

[71] G. C. Ejebe, G. D. Irrisari, S. Mokhtari, O. Obadina, P. Ristanovic and J. Tong, "Methods for contingency screening and ranking for voltage stability analysis of power system", *IEEE Transaction on Power Systems*, vol. 11, pp. 350 – 356, February 1996.

[72] H. Mori, H. Tanaka and J. Kanno, "A preconditioned fast decoupled power flow method for contingency screening", *IEEE Transaction on Power Systems*, vol. 11, pp. 357 – 363, February 1996.

[73] A. O. Ekwue, A. M. Chebbo, M. E. Bradley and H. B.Wan, "Experience of Automatic Contingency Selection Algorithm on the NGC System", in *IEEE Power Engineering Review*, 1998, pp. 53 – 55.

[74] G. Kendall, "Power Outages during market deregulation", *IEEE Control System Magazine*, vol. 21, pp. 33-39, 2001.

[75] B. M. Zhang, S. Y. Wang, W. G. Zhu, and M. H. Pan, "A Security Analysis and Optimal Power Flow Package with Real-Time Implementation in Northeast China Power System", in *Proceedings IEE Conf. On Advances in Power System, Operation and Management*, vol. 2, 1993, pp. 816-821.

[76] J. R. Santos, A. G. Expostio and J. L. M. Ramos, "Distributed Contingency Analysis: practical issues", IEEE *Transaction on Power Systems*, vol. 14, pp. 1349 – 1354, November 1999.

[77] V. Brandwajn, "Efficient Bounding method for Linear Contingency Analysis", *IEEE Transaction on Power Systems*, vol. 3, pp. 38 – 43, February 1988.

[78] M. M. Begovic and R. Q. Mills, "Contingency Triggered voltage instability in power system", in *IEEE International Symposium on Circuits and Systems*, 1990, pp. 1827 – 1829.

[79] H. Mori and Y. Goto, "A Tabu Search based Approach to (N-K) Static Contingency Selection in power system", *in Proceedings IEEE International Conference on Systems, Man and Cybernatics,* vol. 3, 2001, pp. 1954 – 1959.

[80] P. R. Bijwe, J. Nanda and K. L. Puttabuddhi, "Ranking of line outages in an AC-DC system causing overload and voltage problems", in *IEE Proceedings-C,* vol. 138, 1991, pp. 207 – 212.

[81] F. M. El-Kady, "Contingency Analysis in the presence of series FACTS in power systems", in *Proceedings IEEE /PES Transmission and Distribution Conference and Exposition*, vol. 1, 2001, pp. 241 – 246.

[82] G. B. Jasmon and L. H. C. C. Lee, "New Contingency Ranking Technique incorporating a voltage stability criterion", in *IEE Proceedings – C*, vol. 140, 1993, pp. 87 – 90.

[83] G. C. Ejebe, G. D. Irrisari, S. Mokhtari, O. Obadina, P. Ristanovic and J. Tong, "Methods for Contingency Screening and Ranking for voltage stability analysis of power system", *IEEE Transaction on Power Systems*, vol. 11, pp. 350 – 356, February 1996.

[84] R. Napoli and F. Pigliane, "On-Line Security Assessment of power systems by a Progressive Learning Neural Network", in *Proceedings IEEE Mediterranean Electrotechnical Conference,* vol. 3, 1996, pp. 1435 –1438.

[85] S. Greene, I. Dobson and F. L. Alvarado, "Contingency Ranking for voltage collapse via sensitivities from a Single Nose Curve", *IEEE Transaction on Power Systems*, vol. 14, pp. 232 – 240, Feb. 1999.

[86] R. H. Chen, J. Gao, O. P. Malik, S. Y. Wang and N. Xiang, "Automatic Contingency Analysis and classification", in *Proceedings IEEE Conference on Power System Control and Management*, 1996, pp. 82 – 86.

[87] M. Moghavvemi and D. Faruque, "Real-Time Contingency Evaluation and Ranking Technique", in *IEE Proceedings Generation, Transmission and Distribution*, vol. 145, pp. 517 – 524, September 1998.

[88] R. B. Prada and J. O. R. dos Santos, "Fast Nodal Assessment of static voltage stability including contingency analysis", *Electric Power System Research*, vol. 51, pp. 55 – 59, July 1999.

[89] L. Wang and A. A. Girgis, "On-Line Detection of power system small disturbance voltage instability", *IEEE Transaction on Power Systems*, vol. 11, pp. 1304 – 1313, August 1996.

[90] M. Moghavvemi and M. O. Faruque, "Power System Security and Voltage Collapse: A line outage based indicator for prediction", *International Journal of Electrical Power and Energy Systems*, vol. 21, pp. 455 – 461, August 1999.

[91] L. D. Arya, S. C. Choube and D. P. Kothari, "Line Switching for alleviating overloads under line outage condition taking bus voltage limits into account", *International Journal of Electrical Power and Energy Systems*, vol. 22, pp. 213 – 221, March 2000.

[92] Z. Jia and B. Jeyasurya, "Contingecy Ranking for On-Line Voltage Stability Assessment", IEEE *Transaction on Power Systems*, vol. 15, pp. 1093 – 1097, August 2000.

[93] L. D. Arya, S. C. Choube and D. P. Kothari, "Line outage ranking for voltage limit violations with corrective rescheduling avoiding masking", *International Journal of Electrical Power and Energy Systems*, vol. 23, pp. 837 – 846, November 2001.

[94] A. S. Quientela and C. A. Castro, "Improved Branch-based Voltage Stability Proximity Indices Part II: Application in Security Analysis", in *Conference on Large Engineering Systems*, 2002, pp. 109 – 114.

[95] Y. Zhang and Z. Zhou, "Online Voltage Stability Contingency Selection using Improved RSI Method Based on ANN solution", in *Proceedings IEEE Power Society Meeting*, vol. 2, 2002, pp. 888 – 892.

[96] T. S. Chung and F. Ying, "An ANN-Based Network Equivalent approach for Power System On-Line Voltage Security Assessment", in *Proceedings IEEE International Conference on Power System Technology*, vol. 2, pp. 1504 – 1507, August 1998.

[97] J. Nahman and I. Skokljev, "Fuzzy Logic and Probability based Real Time Contingency Ranking", *International Journal of Electrical Power and Energy Systems*, vol. 22, pp. 223 – 229, March 2000. ,

[98] R. Caglar and A. Ozdemir, "Composite Electric Power System Adequacy Evaluation via transmission losses Based Contingency Selection Algorithm", in

Proceedings IEEE International Conference on Electric Power Engineering, 1999, p. 84.

[99] R. Caglar, A. Ozdemir and F. Mekic, "Contingency Selection based on real power transmission losses", in *Proceedings IEEE International Conference on Electric Power Engineering*, 1999, p. 117.

[100] A. A. Mohamed, H. Shaaban and A. Kahla, "A fast and efficient accurate technique for Circuit Contingency Evaluation", *Electric Power System Research*, vol. 45, pp. 181 – 189, June 1998.

[101] C. Fu and A. Bose, "Contingency Ranking Based on Severity Indices in Dynamic Security Analysis", *IEEE Transaction on Power Systems*, vol. 14, pp. 980 – 986, August 1999.

[102] C. M. M. Ferreira, J. A. Dias and F. P. M. Barbosa, "On-Line Security of an electric power system using a Transient Stability Contingency Screening and Ranking Technique", in *Proceedings IEEE MELECON*, 2002, pp. 331 – 335.

[103] D. Fourier, G. A. Hope, "Contingency Analysis Work Flow Diagram for Distribution Networks", in *Proceedings International Power Engineering Conference (IPEC)*, 2001, pp. 123 – 126.

[104] P. Kessel and H. Glavitsch, "Estimating the voltage stability of a power system", *IEEE Transactions on Power Delivery*, vol. 1, pp. 346-354, 1986.

[105] C. H. Lee and S. C. Hsieh, "Lessons learned from the power outages on 29 July and 21 September 1999 in Taiwan", *IEE Proceeding Generation, Transmission and Distribution*, vol. 149, pp. 543-549, September 2002.

[106] D. Chattopadhyay and B. B. Chakrabarti, "Voltage stability constrained var planning: model simplification using Statistical Approximation", *International Journal of Electrical Power and Energy Systems*, vol. 23, pp. 349 – 358, 2001.

[107] C. Hsu and M. S. Chen, "Reactive power planning and operating in deregulated power utilities", in *Proceedings IEEE International Conf. on Electric Utility Deregulation and Restructuring and Power Technologies (DRPT)*, 2000, pp. 72 – 77.

[108] N. Yorino, A. Funahashi, H. Sasaki and F. D. Galiana, "On reverse control action of On-Load Tap-Changers", *International Journal of Electrical Power and Energy Systems*, vol. 19, pp. 541 – 548, 1997.

[109] D. Gao, Q. Lu and J. Luo, "A new scheme for on-load tap-changer of transformers", in *Proceedings IEEE International Conference on Power System Technology*, vol. 2, 2002, pp. 1016 – 1020.

[110] M. Moghavvemi and M. O. Faruque, "Effects of FACTS devices on static voltage stability", in *Proceedings IEEE TENCON*, vol. 2, 2000, pp. 357 – 362.

[111] N. Yorino, E. E. El-Araby, H. Sasaki and S. Harada, "A new formulation for FACTS allocation for security enhancement against voltage collapse", *IEEE Transaction on Power Systems*, vol. 18, pp. 3 – 10, February 2003.

[112] C. A. Canizares and Z. T. Faur, "Analysis of SVC and TCSC controllers in voltage collapse", *IEEE Transaction on Power Systems*, vol. 14, pp. 158 – 165, February 1999.

[113] V. Ajjarapu, P. L. Lau and S. Battula, "An optimal reactive power planning strategy against voltage collapse", *IEEE Transaction on Power Systems*, vol. 9, pp. 906 – 917, May 1994.

[114] L. L. Lai and J. T. Ma, "Application of evolutionary programming to reactive power planning – Comparison with Nonlinear Programming Approach", *IEEE Transaction on Power Systems*, vol. 12, pp. 198 – 206, February 1997.

[115] J. T. Ma and L. L. Lai, "Evolutionary Programming approach to reactive power planning", in *IEE Proceedings – Gener. Trans. Distrib.*, vol. 143, 1996, pp. 365 – 370.

[116] H. T. Yong, Y. C. Huang and C. L. Huang, "Solution to capacitor placement in a radial distribution system using Tabu Search method", in *Proceedings IEEE International Conference on Energy Management and Power Delivery*, vol. 1, 1995, pp. 388 – 393.

[117] H. N. Ng, M. M. A. Salama and A. Y. Chikhani, "Classification of capacitor allocation techniques", *IEEE Transaction on Power Systems*, vol. 15, pp. 387 – 392, January 2000.

[118] S. J. Huang, "An Immune-based Optimization method to capacitor placement in a radial distribution system", *IEEE Transaction on Power Systems*, vol. 15, pp. 744 – 749, April 2000.

[119] P. Preedavichit and S. C. Srivastava, "Optimal Reactive Power Dispatch considering FACTS devices", in *Proceedings 4th International Conference on Advances in Power System Control, Operation and Management (APSCOM-97)*, 1997, pp. 620 – 625.

[120] Y. J. Cao and Q. H. Wu, "Optimal Reactive Power Dispatch using an Adaptive Genetic Algorithm", in *Proceedings Genetic Algorithms in Engineering Systems: Innovations and Applications*, 1997, pp. 117 –122.

[121] L. L. Lai and J. T. Ma, "Practical Application of Evolutionary Computing to reactive power planning", in *IEE Proceedings – Gener. Trans. Distrib.*, vol. 145, 1998, pp. 753 – 758.

[122] M. H. Haque, "Optimal locations of Shunt FACTS Devices in long transmission lines", in *IEE* Proc. *– Gener. Transm. Distrib.,* vol. 147, 2000, pp. 218 – 222.

[123] S. N. Singh, "Location of FACTS Devices for enhancing power system security", in *Proceedings IEEE Large Engineering System Conference on Power Engineering*, 2001, pp. 162 – 166.

[124] N. Amjady and M. Esmaili, "Voltage Security Assessment and Vulnerable Bus Ranking of power systems", *International Journal of Electrical Power and Energy Systems*, vol. 64, pp. 227 – 237, March 2003.

[125] F. Hamzaoglu and E. B. Makram, "Minimisation of series reactive power loss for the voltage instability problems", *Electric Power System Research*, vol. 50, pp. 175 – 181, June 1999.

[126] Y. L. Chen, "Weak Bus-Oriented Optimal Multi-Objective VAR Planning", *IEEE Transaction on Power Systems*, vol. 11, pp. 1885 – 1890, November 1996.

[127] B. H. Lee and K. Y. Lee, "Dynamic and Static Voltage Stability Enhancement of power systems", *IEEE Transaction on Power Systems*, vol. 8, pp. 231 – 238, Feb. 1993.

[128] C. T. Hsu, Y. H. Yan, C. S. Chen and S. L. Her, "Optimal Reactive Power Planning for distribution systems with Nonlinear Loads", in *Proceedings IEEE TENCON*, 1993, pp. 330 – 333.

[129] Bansilal, D. Thukaram and K. Parthasarathy, "An Expert System for Power System Voltage Stability Improvement", *International Journal of Electrical Power and Energy Systems*, vol. 19, No. 6, pp. 385 – 392, 1997.

[130] B. Kermanshahi, K. Takahashi, Y. Zhou, "Optimal Operation and Allocation of Reactive Power Resource considering static voltage stability", in *Proceedings IEEE International Conference on Power System Technology*, vol. 2, pp. 1473 – 1477, Aug. 1998.

[131] Z. Y. Dong, Y. Wang, D. J. Hill and Y. V. Makarov, "A new approach to power system VAR Planning aimed at Voltage Stability Enhancement with Feedback Control", in *Proceedings IEEE International Power Engineering Conference on Electric Power Engineering (PowerTech)*, Sept 1999, pp. 33.

[132] S. Osaka, Y. Kono, R. Fujiwara and A. Yamanishi, "Development of the Expert System for operation planning of power system", in *Proceedings IEEE International Workshop on Artificial Intelligence for Industrial Application*, 1998, pp. 545 – 663.

[133] T. Gomez, J. Lumbreras and V. M. Parra, "A Security-Constrained Decomposition approach to Optimal Reactive Power Planning", IEEE *Transaction on Power Systems*, vol. 6, No. 3, pp. 1069 – 1076, August 1991.

[134] Y. H. Yan, F. C. Chung and C. S. Chen, "Effect of Mutual Coupling to the reactive placement of power systems", in *Proceedings IEEE Conference TENCON*, 1992, pp. 381 – 385.

[135] K. Y. Lee, X. Bai and Y. M. Park, "Optimization method for reactive power planning by using a Modified Simple Genetic Algorithm", *IEEE Transaction on Power Systems*, vol. 10, pp. 1843 – 1850, November 1995.

[136] K. Iba, "Reactive power optimization", in *Proceedings IEEE Power Industry Computer Application Conference*, 1993, pp. 195 – 201.

[137] K. Iba, "Optimal VAR allocation by Genetic Algorithm", in *Proceedings IEEE Second International Forum on Application of Neural Networks to Power Systems (ANNPS'93)*, 1993, pp. 163 – 168.

[138] K. Iba, "Reactive power optimization by Genetic Algorithm", *IEEE Transaction on Power Systems*, vol. 9, pp. 685 – 692, May 1994.

[139] M. H. Haque, "Optimal locations of Shunt FACTS devices in long transmission lines", in *IEE Proc. – Gener. Transm. Distrib.*, vol. 147, 2000, pp. 218 – 222.

[140] W. N. Abdullah, H. Saibon, A. M. M. Zain and K. L. Lo, "Genetic Algorithm for Optimal Reactive Power Dispatch", in *Proceedings IEEE Energy Management and Power Delivery Conference*, vol. 1, 1998, pp. 160 –164.

[141] Q. H. Wu and J. T. Ma, "Genetic Search for Optimal Reactive Power Dispatch of Power Systems", in *Proceedings IEEE International Control Conference*, 1994, pp. 717 – 722.

[142] F. D. Galiana, K. Almeida, M. Toussaint, J. Griffin, D. Atanackovic, B. T. Ooi and D. T. McGillis, "Assessment and control of the impact of FACTS Devices on power system performance", *IEEE Transaction on Power Systems*, vol. 11, pp. 1931 – 1936, November. 1996.

[143] W. R. Thomas, R. M. Dunnett, A. M. Dizon, G. Schaff, D. T. Y. Cheng and J. D. Thorp, "Optimal Reactive Planning with security constraints", in *Proceedings IEEE Power Industry Computer Application Conference*, 1995, pp. 79 – 84.

[144] S. Granville and M. C. A. Lima, "Application of Decomposition Techniques to VAR planning methodological & computational aspects", *IEEE Transaction on Power Systems*, vol. 9, pp. 1780 –1787, November 1994.

[145] J. R. Gomes and O. R. Saavedra, "Optimal Reactive Power Dispatch Using Evolutionary Computation: Extended Algorithm", in *IEE Proceedings – Gener. Trans. Distrib.*, vol. 146, pp. 586 – 592, November 1999.

[146] Q. H. Wu and J. T. Ma, "Power system optimal reactive power dispatch using Evolutionary Programming", *IEEE Transaction on Power Systems*, vol. 10, pp. 1243 – 1249, August 1995.

[147] K. Y. Lee and F. F. Yang, "Optimal Reactive Power Planning Using Evolutionary Algorithms: A comparative study for Evolutionary Programming, Evolutionary Strategy, Genetic Algorithm, and Linear Programming", *IEEE Transaction on Power Systems*, vol. 13, pp. 101 – 108, February 1998.

[148] L. D. B. Terra and M. M. Gouvea Jr., "Fuzzy Goal Programming applied to the Optimal Reactive Power Flow problem", in *Proceedings IEEE International Conference on Electric Power Engineering (PowerTech),* 1999, p. 250.

[149] K. H. Abdul-Rahman and S. M. Shahidehpour, "Application of Fuzzy Sets to optimal reactive power planning with security constraints", *IEEE Transaction on Power Systems*, vol. 9, pp. 589 – 597, May 1994.

[150] K. H. Abdul-Rahman and S. M. Shahidehpour, "Application of Fuzzy Sets to optimal reactive power planning with security constraints", in *Proceedings IEEE Power Industry Computer Application Conference*, 1993, pp. 124 – 130.

[151] R. B. Prada, L. J. Souza and L. A. P. Sousa, "The need for a new constraint on Voltage/Reactive Power Studies to ensure proper voltage control", *International Journal of Electrical Power and Energy Systems*, vol. 24, pp. 535 – 540, October 2002.

[152] V. A. Levi and D. S. Popovic, "Integrated methodology for transmission and reactive power planning", in *Proceedings IEEE International Conference on Power Industry Computer Application*, pp. 284 – 289, May 1995.

[153] Z. E. Aygen, M. Bagriyanik, S. Seker and F. G. Bagriyanik, "An Artificial Neural Network Based Application to Reactive Power Dispatch problem", in *Proceedings IEEE Mediterranean Conference on Electrotechnical (MELECON)*, vol. 2, pp. 1080 – 1083, May 1998.

[154] M. E. Baran and F. F. Wu, "Optimal sizing of capacitors placed on a radial distribution system", *IEEE Transaction on Power Systems*, vol. 4, pp. 735 – 743, January 1989.

[155] X. Wong, Y. H. Song, Q. Lu and Y. Z. Sun, "Optimal allocation of transmission rights in systems with FACTS devices", in *IEE Proceedings – Gener. Transm. Distrib.*, vol. 149, pp. 359 – 366, May 2002.

[156] C. M. Affonso, L.C.P. da Silva, F.G. M. Lima, and S. Soares, "Optimal MW/MVAR dispatch and minimal load shedding strategy for improving voltage stability", *in IEEE Power Engineering Society General Meeting*, vol. 2, 2003 , pp. 890-895.

[157] C. M. Affonso, L.C. P. da Silva, F. G. M. Lima, and S. Soares, "MW and Mvar managemant on supply and demand side for meeting voltage stability margin criteria", *IEEE Transactions on Power Systems*, vol. 19, 2004, pp.1538-1545.

[158] G. Glanzmann and G. Andersson, "Using FACTS devices to resolve congestions in transmission grids", in *International Symposium CIGRE/IEEE PES 2005*, 2005, pp. 347 – 354.

[159] A. R. Messina, M. A. Perez and E. Hernandez, "Co-ordinated application of FACTS Devices to enhance steady-state voltage stability", *International Journal of Electrical Power and Energy Systems*, vol. 25, pp. 259 –267, May 2003.

[160] S. T. Jaya Christa, P. Venkatesh, "Optimal placement of Unified Power Flow Controllers: an approach to maximize the loadability of transmission lines", *Journal of Electrical Systems*, 2006, pp. 82-94.

[161] T.S. Chung, Y.Z. Li, "A Hybrid GA approach for OPF with consideration of FACTS Devices", *IEEE Power Engineering Review*, vol. 20, Issue 8, pp. 54–57, 2001.

[162] M. Eslami, H. Shareef, A. Mohamed, "Application of PSS and FACTS devices for intensification of power system stability", *International Review of Electrical Engineering (IREE)*, vol. 5, pp. 552-570, April 2010.

[163] P. Bhasaputra, W. Ongsakul, "Optimal Power Flow with Multi-Type of FACTS devices by Hybrid TS/SA approach", in *IEEE Proceedings on International Conference on Industrial Technology*, vol. 1, pp. 285–290, December 2002.

[164] R. Mohamad Idris, A. Khairuddin, M. W. Mustafa, A. Kalam, "Optimal allocation of Multi-Type FACTS Devices using BEE Algorithm for ATC enhancement in deregulated power system", *International Review of Electrical Engineering (IREE)*, vol. 5 n. 2, pp. 644 – 651, April 2010.

[165] K. P. Wang, J. Yurevich, A. Li, "Evolutionary Programming- Based Load Flow Algorithm for systems containing Unified Power Flow Controllers", *IEE Proceeding Generation Transmission Distribution,* vol. 150, pp. 441-446, July 2003.

[166] W. Ongsakul and P. Jirapong, "Optimal allocation of FACTS Devices to enhance Total Transfer Capability using Evolutionary Programming", in *IEEE International Symposium on Circuits and Systems*, vol. 5, 2005, pp.4175-4178.

[167] D. Radu, Y. Besanger, "A Multi-Objective Genetic Algorithm approach to optimal allocation of Multi-Type FACTS devices for power system security", *IEEE Power Engineering Society General Meeting*, June 2006, p. 8.

[168] L. Ippolito, P. Siano, "Selection of optimal number and location of Thyristor-Controlled Phase Shifters using Genetic Based Algorithms", *Proceeding Generation Transmission Distribution*, vol. 151, pp. 630-637, September 2004.

[169] H. I. Shaheen, G. I. Rashed, S. J. Cheng, "Optimal location and parameters setting of Unified Power Flow Controller based on Evolutionary Optimization Techniques", in *IEEE PES 2007 General Meeting*, 2007, pp. 1-8.

[170] M. Saravanan, S. M. R. Slochanal, P. Venkatesh, P. S. Abraham, "Application of PSO technique for optimal location of FACTS devices considering system loadability and cost of installation", in *Power Engineering Conference*, vol. 21, pp. 716 -721, 2005.

[171] D. J. Gotham and G. T. Heydt, "Power flow control and power flow studies for systems with FACTS devices", *IEEE Transaction on Power Systems*, vol. 13, pp. 60 – 65, February 1998.

[172] P. Bhasputra and W. Ongsakul, "Optimal power flow with multi-type of FACTS Devices by Hybrid TS/SA approach", in *Proceedings IEEE International Conference on Industrial Technology*, vol. 1, 2002, pp. 285 – 290.

[173] E. Barocio and A. R. Messina, "Analysis of Nonlinear Modal Interaction in stressed power systems with SVCs", in *Proceedings IEEE Power Engineering Society Winter Meeting*, vol. 1, pp. 1164 – 1169, January 2002.

[174] G. Chunlin, T. Luyuan and W. Zhonghong, "Stability control of TSCS between interconnected power networks", in *Proceedings IEEE International Conference on Power System Technology*, vol. 3, pp. 1943 – 1946, October 2002.

[175] J. Mahseredjian and G. Joos, "Solution methods for Varying Topology Networks", in *Proceedings IEEE Power Engineering Society Winter Meeting*, vol. 1, pp. 479 – 483, Jan 2002.

[176] K. N. Shubhanga and Anil M. Kulkarni, "Application of structure preserving energy margin sensitivity to determine the effectiveness of shunt and series FACTS devices", *IEEE Transactions on Power Systems*, vol. 17, pp. 730 – 738, August 2002.

[177] T. Orfanogianni and R. Bacher, "Steady-state optimization in power systems with series FACTS devices", *IEEE Transactions on Power Systems*, vol. 18, pp. 19 – 26, Feb. 2003.

[178] Y. Xiao, Y. H. Song and Y. Z. Sun, "Power Flow Control approach to power systems with embedded FACTS devices", *IEEE Transactions on Power Systems,* vol. 17, pp. 943 – 950, November 2002.

[179] N. D. M. Radzi, I. Musirin, M. K. Idris, A. R. Minhat, M. M. Othman, "Voltage control study using UPFC based on biological computing optimization technique", in *6th WSEAS Int. Conference on Computational Intelligence, Man-Machine Systems and Cybernetics*, 2007, pp. 186-191.

[180] Y. Lue and A. Abur, "Improving System Static Security via Optimal Placement of Thyristor Controlled Series Capacitors (TCSC), *IEEE Power Engineering Society Winter Meeting*, vol. 2 , pp. 516-521, 2001.

[181] S. O. Orero and M. R. Irving, "Scheduling of generators with a Hybrid Genetic Algorithm", in *First International Conference on Genetic Algorithms in Engineering Systems: Innovations and Application*, 1995, pp. 200 – 206.

[182] S. O. Orero and M. R. Irving, "A Genetic Algorithm for generator scheduling in power systems", *Journal of Electrical Power & Energy System*, vol. 18, No. 1, pp. 19 – 26, 1996.

[183] A. T. Lora, J. C. Riquelme, J. L. M. Ramos, J. M. R. Santos and A. G. Exposito, "Application of Evolutionary Computation Techniques to the Optimal Short-Term Scheduling of the electrical energy production", Lecturer Notes in Computer Science: Current Topics in Artificial Intelligence, Vol. 3040, 2004, pp. 656 – 665.

[184] J. S. Dhillon, J.S. Dhillon and D. P. Kothari, "Real Coded Genetic Algorithm for Stochastic Hydrothermal Generation Scheduling", *Journal of Systems Science and Systems Engineering*, 2011, pp. 087-109.

[185] D. Srinivasan, C. S. Chang and A. C. Liew, "Multiobjective Generation Scheduling using Fuzzy Optimal Search Technique", in *IEE Proceedings – Generation, Transmission and Distribution*, vol. 141, pp. 233 – 242, 1994.

[186] M. P. Walsh and M. J. O'Malley, "Augmented Hopfield Network for Constrained Generator Scheduling", *IEEE Transactions on Power Systems*, vol. 14, No. 2, pp. 765-771, 1999.

[187] K. P. Wong and Y. W. Wong, "Thermal Generator Scheduling using Hybrid Genetic/Simulated –Annealing Approach", in *IEE Proceeding- Generation, Transmission & Distribution*, vol. 142, No. 4, pp. 372 – 380, 1995.

[188] M. Mohatram and S. Kumar, "Application of Artificial Neural Network in Economic Generation Scheduling of Thermal Power Plants", Waljat Colleges of Applied Sciences, Muscat, Sultanate of Oman, with Birla Institute of Technology, Mesra (Ranchi), India.

[189] M. E. Flynn, "Generator resources and the scheduling problem", Ph.D Thesis, University College Dublin, 1999.

[190] L. L. Garver, "Power Generation Scheduling by Integer Programming-Development of Theory", *Journal of Power Apparatus and System*, vol. 81, pp. 730 – 734, 1962.

[191] K. P. Dahal, C. J. Aldridge and S. J. Galloway, "Evolutionary Hybrid approaches for generation scheduling in power systems", *European Journal of Operational Research*, vol. 177, pp. 2050-2068, 2007.

[192] P. A. Jeyanthy and D. Devaraj, "Multi-objective Genetic Algorithm for Reactive Power Optimization inclusing voltage stability", *International Journal of Engineering Science and Technology*, vol. 2 (7), pp. 2715-2729, 2010.

[193] K. Deb, S. Agrawal, A. Pratap, and T. Meyarivan, "A fast elitist non-dominated sorting genetic algorithm for multi-objective optimization: NSGA-II," in *Parallel Problem Solving from Nature PPSN VI. 6th International Conference. Proceedings (Lecture Notes in Computer Science Vol.1917)*, 2000, pp. 849-58.

[194] J. Horn, N. Nafpliotis, and D. E. Goldberg, "A niched Pareto genetic algorithm for multiobjective optimization," in *Proceedings of the First IEEE Conference on Evolutionary Computation. IEEE World Congress on Computational Intelligence*, 1994, pp. 82-87.

[195] Y. T. Hsaio, H. D. Chaing, C. C. Liu, and Y. L. Chen, "A Computer Package for Optimal Multi-objective VAR Planning in large scale power systems," *IEEE Trans. on Power Systems*, vol. 9, No. 2, pp. 668-676, 1994.

[196] K. Deb, A. Pratap, S. Agarwal, and T. Meyarivan, "A Fast and Elitist Multi-objective Genetic Algorithm: NSGA-II," *IEEE Trans. on Evolutionary Computation*, vol. 6, no. 2, pp. 182-197, Apr. 2002.

[197] Kalyanmoy Deb, "Multi-Objective Optimization using Evolutionary Algorithms", 1st Edition, John Wiley & Sons, Ltd., Singapore, (ISBN 9814-12-685-3)

[198] E. Zitzler, "Evolutionary algorithms for Multi-objective optimization: Methods and applications", Ph.D. dissertation, ETH 13398, Swiss Federal Institute of Technology (ETH), Zurich, Switzerland, 1999.

[199] J. Knowles and D. Corne, "The Pareto archived evolution strategy: A new baseline algorithm for multiobjective optimization," in *Proceedings of the 1999 Congress on Evolutionary Computation*, 1999, pp. 98–105.

[200] I. Marouani, T. Guesmi, H. Hadj Abdallah and A. Ouali, "Optimal Reactive Power Dispatch considering FACTS devices", *Leonardo Journal of Science (LJS),* 2011, pp. 97-114.

[201] A. A. A. El-Ela, R. A. Eo Sehiemy and A. A. M. Shaheen, "Multi-Objective Fuzzy Based procedure for Optimal Reactive Power Dispatch Problem", in *Proceedings of 14th International Middle East Power System Conference (MEPCON' 10),* 2010, pp. 941-946.

[202] Hsaio Y T, Chaing H D, Liu C C, Chen Y L., "A computer package for optimal multiobjective VAR planning in large scale power systems", *IEEE Trans. on Power Systems*, vol. 9, pp. 668-676, 1994.

[203] T. Back, D. Fogel and Z. Michalewicz, "Handbook of Evolutionary Computation. Oxford" U.K.: IOP Publishing Ltd. and Oxford University Press, 1997, vol.1.

[204] L. Chen, L. Mengshi, T. Wenjia and Q. H. Wu, "Multi-objective optimization of reactive power dispatch using a bacterial swarming algorithm", in *Proceedings of the 26th Chinese Control Conference*, 2007, pp. 460-464.

[205] C. Zhang, M. Chen and C. Luo, "A multi-objective optimization method for power system reactive power dispatch", in *Proceedings of the World Congress on Intelligent* Control and Automation, 2010, pp. 6-10.

[206] D. Donde, V. Lopez, B. Lesieutre, A. Pinar, Chao Yang and J. Meza, " Identification of severe multiple contingencies in electric power networks", in *Proceedings of the 37th Annual North American Power Symposium*, 2005, pp. 59 – 66.

[207] N. R. H. Abdullah, I. Musirin, M. M. Othman, Static VAR Compensator for Minimising Transmission Loss and Installation Cost Calculation, *Australian Journal of Basic and Applied Sciences(AJBAS)*, pp. 646-657, 2010.

[208] W. Ongskul, P. Jirapong, Optimal allocation of FACTS Devices to Enhance Total Transfer Capability using Evolutionary Programming, in *Proceedings on IEEE International Symposium on Circuits and Systems*, vol. 5, May 2005, pp.4175-4178.

[209] L. J. Cai, I. Erlich, "Optimal choice and allocation of facts devices using Genetic Algorithms", in *Proceedings on Twelfth Intelligent Systems Application to Power Systems Conference*, 2003, pp. 1–6.

[210] S. Gerbex, R. Cherkaoui and A. J. Germond, "Optimal location of FACTS devices to enhance power system security", in *Proceedings on IEEE Bologna PowerTech Conference*, vol. 3, 2003, pp.1-7.

[211] J. Dhillon, "Multi objective optimization of power dispatch problem using NSGA-II.", Master Thesis, Thapar University, Patiala, July 2009.

APPENDICES

APPENDIX A

IEEE 30-bus Reliability Test System (RTS) – Bus data

Bus No.	Type	Load		Generator		V (p.u)	B	Q_{max}	Q_{min}	P_{max}	P_{min}
		MW	MVAr	MW	MVAr			MVAr		MW	
1	Slack	0	0	260.2	-16.1	1.060	0	10	0	360.2	0
2	PV	21.7	12.7	40	50	1.043	0	50	-40	140	0
3	PQ	2.4	1.2	0	0	1.021	0	0	0	0	0
4	PQ	7.6	1.6	0	0	1.012	0	0	0	0	0
5	PV	94.2	19	0	37	1.010	0	40	-40	100	0
6	PQ	0	0	0	0	1.010	0	0	0	0	0
7	PQ	22.8	10.9	0	0	1.002	0	0	0	0	0
8	PV	30	30	0	37.3	1.010	0	40	-10	100	0
9	PQ	0	0	0	0	1.051	0	0	0	0	0
10	PQ	5.8	2	0	19	1.045	19	0	0	0	0
11	PV	0	0	0	16.2	1.082	0	24	-6	100	0
12	PQ	11.2	7.5	0	0	1.057	0	0	0	0	0
13	PV	0	0	0	10.6	1.071	0	24	-6	100	0
14	PQ	6.2	1.6	0	0	1.042	0	0	0	0	0
15	PQ	8.2	2.5	0	0	1.038	0	0	0	0	0
16	PQ	3.5	1.8	0	0	1.045	0	0	0	0	0
17	PQ	9	5.8	0	0	1.040	0	0	0	0	0
18	PQ	3.2	0.9	0	0	1.028	0	0	0	0	0
19	PQ	9.5	3.4	0	0	1.026	0	0	0	0	0
20	PQ	2.2	0.7	0	0	1.030	0	0	0	0	0
21	PQ	17.5	11.2	0	0	1.033	0	0	0	0	0
22	PQ	0	0	0	0	1.033	0	0	0	0	0
23	PQ	3.2	1.6	0	0	1.027	0	0	0	0	0
24	PQ	8.7	6.7	0	4.3	1.021	0	0	0	0	0
25	PQ	0	0	0	0	1.017	0	0	0	0	0
26	PQ	3.5	2.3	0	0	1.000	0	0	0	0	0
27	PQ	0	0	0	0	1.023	0	0	0	0	0
28	PQ	0	0	0	0	1.007	0	0	0	0	0
29	PQ	2.4	0.9	0	0	1.003	0	0	0	0	0
30	PQ	10.6	1.9	0	0	0.992	0	0	0	0	0

IEEE 30-bus Reliability Test System (RTS) – Line data

Line No.	From Bus	To Bus	R	X	B
			p.u.		
1	1	2	0.0192	0.0575	0.0528
2	1	3	0.0452	0.1652	0.0408
3	2	4	0.057	0.1737	0.0368
4	3	4	0.0132	0.0379	0.0084
5	2	5	0.0472	0.1983	0.0418
6	2	6	0.0581	0.1763	0.0374
7	4	6	0.0119	0.0414	0.009
8	5	7	0.046	0.116	0.0204
9	6	7	0.0267	0.082	0.017
10	6	8	0.012	0.042	0.009
11	6	9	0	0.208	0
12	6	10	0	0.556	0
13	9	11	0	0.208	0
14	9	10	0	0.11	0
15	4	12	0	0.256	0
16	12	13	0	0.14	0
17	12	14	0.1231	0.2559	0
18	12	15	0.0662	0.1304	0
19	12	16	0.0945	0.1987	0
20	14	15	0.221	0.1997	0
21	16	17	0.0524	0.1923	0
22	15	18	0.1073	0.2185	0
23	18	19	0.0639	0.1292	0
24	19	20	0.034	0.068	0
25	10	20	0.0936	0.209	0
26	10	17	0.0324	0.0845	0
27	10	21	0.0348	0.0749	0
28	10	22	0.0727	0.1499	0
29	21	22	0.0116	0.0236	0
30	15	23	0.1	0.202	0
31	22	24	0.115	0.179	0
32	23	24	0.132	0.27	0
33	24	25	0.1885	0.3292	0
34	25	26	0.2544	0.38	0

35	25	27	0.1093	0.2087	0
36	28	27	0	0.396	0
37	27	29	0.2198	0.4153	0
38	27	30	0.3202	0.6027	0
39	29	30	0.2399	0.4533	0
40	8	28	0.0636	0.2	0.0428
41	6	28	0.0169	0.0599	0.013

APPENDIX B

IEEE 118-bus Reliability Test System (RTS) – Bus data

Bus No.	Type	Load		Generator		V (p.u)	B	Q_{max}	Q_{min}	P_{max}	P_{min}
		MW	MVAr	MW	MVAr			MVAr		MW	
1	PV	51	27	0	0	0.955	0	15	-5	100	0
2	PQ	20	9	0	0	0.971	0	0	0	0	0
3	PQ	39	10	0	0	0.968	0	0	0	0	0
4	PV	39	12	0	0	0.998	0	300	-300	100	0
5	PQ	0	0	0	0	1.002	-40	0	0	0	0
6	PV	52	22	0	0	0.99	0	50	-13	100	0
7	PQ	19	2	0	0	0.989	0	0	0	0	0
8	PV	28	0	0	0	1.015	0	300	-300	100	0
9	PQ	0	0	0	0	1.043	0	0	0	0	0
10	PV	0	0	450	0	1.05	0	200	-147	550	0
11	PQ	70	23	0	0	0.985	0	0	0	0	0
12	PV	47	10	85	0	0.99	0	120	-35	185	0
13	PQ	34	16	0	0	0.968	0	0	0	0	0
14	PQ	14	1	0	0	0.984	0	0	0	0	0
15	PV	90	30	0	0	0.97	0	30	-10	100	0
16	PQ	25	10	0	0	0.984	0	0	0	0	0
17	PQ	11	3	0	0	0.995	0	0	0	0	0
18	PV	60	34	0	0	0.973	0	50	-16	100	0
19	PV	45	25	0	0	0.963	0	24	-8	100	0
20	PQ	18	3	0	0	0.958	0	0	0	0	0
21	PQ	14	8	0	0	0.959	0	0	0	0	0
22	PQ	10	5	0	0	0.97	0	0	0	0	0
23	PQ	7	3	0	0	1	0	0	0	0	0
24	PV	13	0	0	0	0.992	0	300	-300	100	0
25	PV	0	0	220	0	1.05	0	140	-47	320	0
26	PV	0	0	314	0	1.015	0	1000	-1000	414	0
27	PV	71	13	0	0	0.968	0	300	-300	100	0
28	PQ	17	7	0	0	0.962	0	0	0	0	0
29	PQ	24	4	0	0	0.963	0	0	0	0	0
30	PQ	0	0	0	0	0.968	0	0	0	0	0
31	PV	43	27	7	0	0.967	0	300	-300	107	0
32	PV	59	23	0	0	0.964	0	42	-14	100	0

33	PQ	23	9	0	0	0.972	0	0	0	0	0
34	PV	59	26	0	0	0.986	14	24	-8	100	0
35	PQ	33	9	0	0	0.981	0	0	0	0	0
36	PV	31	17	0	0	0.98	0	24	-8	100	0
37	PQ	0	0	0	0	0.992	-25	0	0	0	0
38	PQ	0	0	0	0	0.962	0	0	0	0	0
39	PQ	27	11	0	0	0.97	0	0	0	0	0
40	PV	66	23	0	0	0.97	0	300	-300	100	0
41	PQ	37	10	0	0	0.967	0	0	0	0	0
42	PV	96	23	0	0	0.985	0	300	-300	100	0
43	PQ	18	7	0	0	0.978	0	0	0	0	0
44	PQ	16	8	0	0	0.985	10	0	0	0	0
45	PQ	53	22	0	0	0.987	10	0	0	0	0
46	PV	28	10	19	0	1.005	10	100	-100	119	0
47	PQ	34	0	0	0	1.017	0	0	0	0	0
48	PQ	20	11	0	0	1.021	15	0	0	0	0
49	PV	87	30	204	0	1.025	0	210	-85	304	0
50	PQ	17	4	0	0	1.001	0	0	0	0	0
51	PQ	17	8	0	0	0.967	0	0	0	0	0
52	PQ	18	5	0	0	0.957	0	0	0	0	0
53	PQ	23	11	0	0	0.946	0	0	0	0	0
54	PV	113	32	48	0	0.955	0	300	-300	148	0
55	PV	63	22	0	0	0.952	0	23	-8	100	0
56	PV	84	18	0	0	0.954	0	15	-8	100	0
57	PQ	12	3	0	0	0.971	0	0	0	0	0
58	PQ	12	3	0	0	0.959	0	0	0	0	0
59	PV	277	113	155	0	0.985	0	180	-60	255	0
60	PQ	78	3	0	0	0.993	0	0	0	0	0
61	PV	0	0	160	0	0.995	0	300	-100	260	0
62	PV	77	14	0	0	0.998	0	20	-20	100	0
63	PQ	0	0	0	0	0.969	0	0	0	0	0
64	PQ	0	0	0	0	0.984	0	0	0	0	0
65	PV	0	0	391	0	1.005	0	200	-67	491	0
66	PV	39	18	392	0	1.05	0	200	-67	492	0
67	PQ	28	7	0	0	1.02	0	0	0	0	0
68	PQ	0	0	0	0	1.003	0	0	0	0	0
69	Slack	0	0	516.4	0	1.035	0	300	-300	805.2	0
70	PV	66	20	0	0	0.984	0	32	-10	100	0

71	PQ	0	0	0	0	0.987	0	0	0	0	0
72	PV	12	0	0	0	0.98	0	100	-100	100	0
73	PV	6	0	0	0	0.991	0	100	-100	100	0
74	PV	68	27	0	0	0.958	12	9	-6	100	0
75	PQ	47	11	0	0	0.967	0	0	0	0	0
76	PV	68	36	0	0	0.943	0	23	-8	100	0
77	PV	61	28	0	0	1.006	0	70	-20	100	0
78	PQ	71	26	0	0	1.003	0	0	0	0	0
79	PQ	39	32	0	0	1.009	20	0	0	0	0
80	PV	130	26	477	0	1.04	0	280	-165	577	0
81	PQ	0	0	0	0	0.997	0	0	0	0	0
82	PQ	54	27	0	0	0.989	20	0	0	0	0
83	PQ	20	10	0	0	0.985	10	0	0	0	0
84	PQ	11	7	0	0	0.98	0	0	0	0	0
85	PV	24	15	0	0	0.985	0	23	-8	100	0
86	PQ	21	10	0	0	0.987	0	0	0	0	0
87	PV	0	0	4	0	1.015	0	1000	-100	104	0
88	PQ	48	10	0	0	0.987	0	0	0	0	0
89	PV	0	0	607	0	1.005	0	300	-210	707	0
90	PV	163	42	0	0	0.985	0	300	-300	100	0
91	PV	10	0	0	0	0.98	0	100	-100	100	0
92	PV	65	10	0	0	0.993	0	9	-3	100	0
93	PQ	12	7	0	0	0.987	0	0	0	0	0
94	PQ	30	16	0	0	0.991	0	0	0	0	0
95	PQ	42	31	0	0	0.981	0	0	0	0	0
96	PQ	38	15	0	0	0.993	0	0	0	0	0
97	PQ	15	9	0	0	1.011	0	0	0	0	0
98	PQ	34	8	0	0	1.024	0	0	0	0	0
99	PV	42	0	0	0	1.01	0	100	-100	100	0
100	PV	37	18	252	0	1.017	0	155	-50	352	0
101	PQ	22	15	0	0	0.993	0	0	0	0	0
102	PQ	5	3	0	0	0.991	0	0	0	0	0
103	PV	23	16	40	0	1.001	0	40	-15	140	0
104	PV	38	25	0	0	0.971	0	23	-8	100	0
105	PV	31	26	0	0	0.965	20	23	-8	100	0
106	PQ	43	16	0	0	0.962	0	0	0	0	0
107	PV	50	12	0	0	0.952	6	200	-200	100	0
108	PQ	2	1	0	0	0.967	0	0	0	0	0

109	PQ	8	3	0	0	0.967	0	0	0	0	0
110	PV	39	30	0	0	0.973	6	23	-8	100	0
111	PV	0	0	36	0	0.98	0	1000	-100	136	0
112	PV	68	13	0	0	0.975	0	1000	-100	100	0
113	PV	6	0	0	0	0.993	0	200	-100	100	0
114	PQ	8	3	0	0	0.96	0	0	0	0	0
115	PQ	22	7	0	0	0.96	0	0	0	0	0
116	PV	184	0	0	0	1.005	0	1000	-1000	100	0
117	PQ	20	8	0	0	0.974	0	0	0	0	0
118	PQ	33	15	0	0	0.949	0	0	0	0	0

IEEE 118-bus Reliability Test System (RTS) – Line data

Line No.	From Bus	To Bus	R	X	B
				(p.u.)	
1	1	2	0.0303	0.0999	0.0254
2	1	3	0.0129	0.0424	0.0108
3	4	5	0.0018	0.008	0.0021
4	3	5	0.0241	0.108	0.0284
5	5	6	0.0119	0.054	0.0143
6	6	7	0.0046	0.0208	0.0055
7	8	9	0.0024	0.0305	1.162
8	8	5	0	0.0267	0
9	9	10	0.0026	0.0322	1.23
10	4	11	0.0209	0.0688	0.0175
11	5	11	0.0203	0.0682	0.0174
12	11	12	0.006	0.0196	0.005
13	2	12	0.0187	0.0616	0.0157
14	3	12	0.0484	0.16	0.0406
15	7	12	0.0086	0.034	0.0087
16	11	13	0.0222	0.0731	0.0188
17	12	14	0.0215	0.0707	0.0182
18	13	15	0.0744	0.2444	0.0627
19	14	15	0.0595	0.195	0.0502
20	12	16	0.0212	0.0834	0.0214
21	15	17	0.0132	0.0437	0.0444
22	16	17	0.0454	0.1801	0.0466
23	17	18	0.0123	0.0505	0.013

24	18	19	0.0112	0.0493	0.0114
25	19	20	0.0252	0.117	0.0298
26	15	19	0.012	0.0394	0.0101
27	20	21	0.0183	0.0849	0.0216
28	21	22	0.0209	0.097	0.0246
29	22	23	0.0342	0.159	0.0404
30	23	24	0.0135	0.0492	0.0498
31	23	25	0.0156	0.08	0.0864
32	26	25	0	0.0382	0
33	25	27	0.0318	0.163	0.1764
34	27	28	0.0191	0.0855	0.0216
35	28	29	0.0237	0.0943	0.0238
36	30	17	0	0.0388	0
37	8	30	0.0043	0.0504	0.514
38	26	30	0.008	0.086	0.908
39	17	31	0.0474	0.1563	0.0399
40	29	31	0.0108	0.0331	0.0083
41	23	32	0.0317	0.1153	0.1173
42	31	32	0.0298	0.0985	0.0251
43	27	32	0.0229	0.0755	0.0193
44	15	33	0.038	0.1244	0.0319
45	19	34	0.0752	0.247	0.0632
46	35	36	0.0022	0.0102	0.0027
47	35	37	0.011	0.0497	0.0132
48	33	37	0.0415	0.142	0.0366
49	34	36	0.0087	0.0268	0.0057
50	34	37	0.0026	0.0094	0.0098
51	38	37	0	0.0375	0
52	37	39	0.0321	0.106	0.027
53	37	40	0.0593	0.168	0.042
54	30	38	0.0046	0.054	0.422
55	39	40	0.0184	0.0605	0.0155
56	40	41	0.0145	0.0487	0.0122
57	40	42	0.0555	0.183	0.0466
58	41	42	0.041	0.135	0.0344
59	43	44	0.0608	0.2454	0.0607
60	34	43	0.0413	0.1681	0.0423
61	44	45	0.0224	0.0901	0.0224

62	45	46	0.04	0.1356	0.0332
63	46	47	0.038	0.127	0.0316
64	46	48	0.0601	0.189	0.0472
65	47	49	0.0191	0.0625	0.016
66	42	49	0.0715	0.323	0.086
67	42	49	0.0715	0.323	0.086
68	45	49	0.0684	0.186	0.0444
69	48	49	0.0179	0.0505	0.0126
70	49	50	0.0267	0.0752	0.0187
71	49	51	0.0486	0.137	0.0342
72	51	52	0.0203	0.0588	0.014
73	52	53	0.0405	0.1635	0.0406
74	53	54	0.0263	0.122	0.031
75	49	54	0.073	0.289	0.0738
76	49	54	0.0869	0.291	0.073
77	54	55	0.0169	0.0707	0.0202
78	54	56	0.0028	0.0096	0.0073
79	55	56	0.0049	0.0151	0.0037
80	56	57	0.0343	0.0966	0.0242
81	50	57	0.0474	0.134	0.0332
82	56	58	0.0343	0.0966	0.0242
83	51	58	0.0255	0.0719	0.0179
84	54	59	0.0503	0.2293	0.0598
85	56	59	0.0825	0.251	0.0569
86	56	59	0.0803	0.239	0.0536
87	55	59	0.0474	0.2158	0.0565
88	59	60	0.0317	0.145	0.0376
89	59	61	0.0328	0.15	0.0388
90	60	61	0.0026	0.0135	0.0146
91	60	62	0.0123	0.0561	0.0147
92	61	62	0.0082	0.0376	0.0098
93	63	59	0	0.0386	0
94	63	64	0.0017	0.02	0.216
95	64	61	0	0.0268	0
96	38	65	0.009	0.0986	1.046
97	64	65	0.0027	0.0302	0.38
98	49	66	0.018	0.0919	0.0248
99	49	66	0.018	0.0919	0.0248

100	62	66	0.0482	0.218	0.0578
101	62	67	0.0258	0.117	0.031
102	65	66	0	0.037	0
103	66	67	0.0224	0.1015	0.0268
104	65	68	0.0014	0.016	0.638
105	47	69	0.0844	0.2778	0.0709
106	49	69	0.0985	0.324	0.0828
107	68	69	0	0.037	0
108	69	70	0.03	0.127	0.122
109	24	70	0.0022	0.4115	0.102
110	70	71	0.0088	0.0355	0.0088
111	24	72	0.0488	0.196	0.0488
112	71	72	0.0446	0.18	0.0444
113	71	73	0.0087	0.0454	0.0118
114	70	74	0.0401	0.1323	0.0337
115	70	75	0.0428	0.141	0.036
116	69	75	0.0405	0.122	0.124
117	74	75	0.0123	0.0406	0.0103
118	76	77	0.0444	0.148	0.0368
119	69	77	0.0309	0.101	0.1038
120	75	77	0.0601	0.1999	0.0498
121	77	78	0.0038	0.0124	0.0126
122	78	79	0.0055	0.0244	0.0065
123	77	80	0.017	0.0485	0.0472
124	77	80	0.0294	0.105	0.0228
125	79	80	0.0156	0.0704	0.0187
126	68	81	0.0018	0.0202	0.808
127	81	80	0	0.037	0
128	77	82	0.0298	0.0853	0.0817
129	82	83	0.0112	0.0366	0.038
130	83	84	0.0625	0.132	0.0258
131	83	85	0.043	0.148	0.0348
132	84	85	0.0302	0.0641	0.0123
133	85	86	0.035	0.123	0.0276
134	86	87	0.0283	0.2074	0.0445
135	85	88	0.02	0.102	0.0276
136	85	89	0.0239	0.173	0.047
137	88	89	0.0139	0.0712	0.0193

138	89	90	0.0518	0.188	0.0528
139	89	90	0.0238	0.0997	0.106
140	90	91	0.0254	0.0836	0.0214
141	89	92	0.0099	0.0505	0.0548
142	89	92	0.0393	0.1581	0.0414
143	91	92	0.0387	0.1272	0.0327
144	92	93	0.0258	0.0848	0.0218
145	92	94	0.0481	0.158	0.0406
146	93	94	0.0223	0.0732	0.0188
147	94	95	0.0132	0.0434	0.0111
148	80	96	0.0356	0.182	0.0494
149	82	96	0.0162	0.053	0.0544
150	94	96	0.0269	0.0869	0.023
151	80	97	0.0183	0.0934	0.0254
152	80	98	0.0238	0.108	0.0286
153	80	99	0.0454	0.206	0.0546
154	92	100	0.0648	0.295	0.0472
155	94	100	0.0178	0.058	0.0604
156	95	96	0.0171	0.0547	0.0147
157	96	97	0.0173	0.0885	0.024
158	98	100	0.0397	0.179	0.0476
159	99	100	0.018	0.0813	0.0216
160	100	101	0.0277	0.1262	0.0328
161	92	102	0.0123	0.0559	0.0146
162	101	102	0.0246	0.112	0.0294
163	100	103	0.016	0.0525	0.0536
164	100	104	0.0451	0.204	0.0541
165	103	104	0.0466	0.1584	0.0407
166	103	105	0.0535	0.1625	0.0408
167	100	106	0.0605	0.229	0.062
168	104	105	0.0099	0.0378	0.0099
169	105	106	0.014	0.0547	0.0143
170	105	107	0.053	0.183	0.0472
171	105	108	0.0261	0.0703	0.0184
172	106	107	0.053	0.183	0.0472
173	108	109	0.0105	0.0288	0.0076
174	103	110	0.0391	0.1813	0.0461
175	109	110	0.0278	0.0762	0.0202

176	110	111	0.022	0.0755	0.02
177	110	112	0.0247	0.064	0.062
178	17	113	0.0091	0.0301	0.0077
179	32	113	0.0615	0.203	0.0518
180	32	114	0.0135	0.0612	0.0163
181	27	115	0.0164	0.0741	0.0197
182	114	115	0.0023	0.0104	0.0028
183	68	116	0.0003	0.004	0.164
184	12	117	0.0329	0.14	0.0358
185	75	118	0.0145	0.0481	0.012
186	76	118	0.0164	0.0544	0.0136

APPENDIX C

Results For Line Outage Contingency Ranking in IEEE 118-Bus RTS

Rank	Line Outage No.	*SVSI*
1	9	0.6709
2	7	0.6707
3	96	0.438
4	51	0.4151
5	67	0.4077
6	66	0.4077
7	38	0.3965
8	31	0.3842
9	8	0.3705
10	41	0.3406
11	36	0.3228
12	54	0.3103
13	52	0.3083
14	163	0.2998
15	53	0.2993
16	61	0.2905
17	55	0.2888
18	39	0.2847
19	29	0.2828
20	28	0.282
21	40	0.2816
22	56	0.2814
23	180	0.2812
24	27	0.2811
25	59	0.2805
26	108	0.2804
27	25	0.2798
28	16	0.2798
29	5	0.2797
30	3	0.2796
31	11	0.2795
32	48	0.2795
33	4	0.2795
34	178	0.2795
35	107	0.2794
36	10	0.2794
37	68	0.2794
38	17	0.2793
39	50	0.2792

40	20	0.2792
41	182	0.2792
42	6	0.2792
43	12	0.2792
44	105	0.2791
45	97	0.2791
46	106	0.2791
47	2	0.279
48	15	0.279
49	99	0.279
50	98	0.279
51	45	0.279
52	126	0.279
53	127	0.279
54	62	0.279
55	185	0.279
56	19	0.279
57	58	0.279
58	94	0.279
59	93	0.279
60	114	0.2789
61	63	0.2789
62	57	0.2789
63	113	0.2789
64	111	0.2789
65	69	0.2789
66	121	0.2789
67	186	0.2789
68	18	0.2789
69	87	0.2789
70	84	0.2789
71	86	0.2789
72	90	0.2789
73	85	0.2789
74	102	0.2789
75	47	0.2789
76	64	0.2789
77	176	0.2789
78	89	0.2789
79	141	0.2789
80	95	0.2789
81	88	0.2789
82	74	0.2789

83	159	0.2789
84	92	0.2789
85	161	0.2789
86	139	0.2789
87	162	0.2789
88	174	0.2789
89	154	0.2789
90	144	0.2789
91	142	0.2789
92	145	0.2789
93	146	0.2789
94	167	0.2789
95	160	0.2789
96	164	0.2789
97	134	0.2789
98	158	0.2789
99	138	0.2789
100	168	0.2789
101	170	0.2789
102	172	0.2789
103	156	0.2789
104	166	0.2789
105	171	0.2789
106	165	0.2789
107	173	0.2789
108	169	0.2789
109	140	0.2789
110	175	0.2789
111	155	0.2789
112	143	0.2789
113	77	0.2789
114	150	0.2789
115	91	0.2789
116	147	0.2789
117	130	0.2789
118	78	0.2789
119	115	0.2789
120	128	0.2789
121	132	0.2789
122	79	0.2789
123	157	0.2789
124	153	0.2789
125	131	0.2789

126	73	0.2789
127	135	0.2789
128	82	0.2789
129	133	0.2789
130	136	0.2789
131	149	0.2789
132	152	0.2789
133	148	0.2789
134	46	0.2789
135	137	0.2789
136	72	0.2789
137	101	0.2789
138	151	0.2789
139	100	0.2789
140	129	0.2789
141	83	0.2789
142	103	0.2789
143	119	0.2789
144	65	0.2789
145	80	0.2789
146	122	0.2789
147	75	0.2789
148	76	0.2789
149	81	0.2789
150	60	0.2789
151	177	0.2788
152	70	0.2788
153	49	0.2788
154	124	0.2788
155	71	0.2788
156	125	0.2788
157	14	0.2788
158	30	0.2788
159	123	0.2788
160	26	0.2788
161	120	0.2788
162	1	0.2787
163	13	0.2787
164	109	0.2787
165	104	0.2787
166	118	0.2787
167	183	0.2786
168	117	0.2786

169	112	0.2786
170	44	0.2786
171	110	0.2785
172	116	0.2784
173	184	0.2784
174	24	0.2784
175	22	0.2782
176	32	0.2781
177	179	0.2776
178	42	0.2773
179	23	0.2766
180	37	0.276
181	21	0.2751
182	43	0.2744
183	33	0.2744
184	35	0.274
185	181	0.2738
186	34	0.271